SYNTHESIS AND CHARACTERIZATION OF 1,2,3-TRIAZOLE LINKED CHEMO SENSORS USING Cu(I) CATALYZED ALKYNE-AZIDE CYCLOADDITION REACTION

Thesis Submitted for the Award of the Degree of

DOCTOR OF PHILOSOPHY (Ph.D.)

In

Chemistry

By

Parveen Saini
Registration number: 41800817

Supervised By

Dr. Harminder Singh (UID 11839)
Chemistry (Professor)
LPU Phagwara

Co-Supervised by

Dr. Jandeep Singh (UID 19394)
Chemistry (Assist. Professor)
LPU Phagwara

LOVELY PROFESSIONAL UNIVERSITY
PUNJAB
2023

DECLARATION

I, hereby declared that the presented work in the thesis entitled "**Synthesis and Characterization of 1,2,3-triazole linked chemo sensors using Cu(I) catalyzed alkyne-azide cycloaddition reaction**" in fulfillment of degree of **Doctor of Philosophy (Ph. D.)** is outcome of research work carried out by me under the supervision of **Prof.(Dr.) Harminder Singh**, working as **Professor in Chemistry** and **Dr. Jandeep Singh,** working as **Assistant Professor in Chemistry**, in the **School of Chemical Engineering and Physical Sciences** of Lovely Professional University, Punjab, India. In keeping with general practice of reporting scientific observations, due acknowledgements have been made whenever work described here has been based on findings of other investigator. This work has not been submitted in part or full to any other University or Institute for the award of any degree.

(Signature of Scholar)

Name of the scholar: **Parveen Saini**

Registration No.: **41800817**

Department/school: **School of Chemical Engineering and Physical Sciences**

Lovely Professional University, Punjab, India

CERTIFICATE

This is to certify that the work reported in the Ph. D. thesis entitled "**Synthesis and Characterization of 1,2,3-triazole linked chemo sensors using Cu(I) catalyzed alkyne-azide cycloaddition reaction**" submitted in fulfillment of the requirement for the reward of degree of **Doctor of Philosophy (Ph.D.)** in the **School of Chemical Engineering and Physical Sciences**, is a research work carried out by **Parveen Saini, Registration No. 41800817**, is bonafide record of her original work carried out under my supervision and that no part of thesis has been submitted for any other degree, diploma or equivalent course.

(Signature of Supervisor)	**(Signature of Co-Supervisor)**
Prof.(Dr.) Harminder Singh	Dr. Jandeep Singh
Prof. in Chemistry	Assist. Prof. in Chemistry

Department/school: School of Chemical Engineering and Physical Sciences

University: Lovely Professional University, Phagwara, Punjab-144001

ABSTRACT

Since 2001, 'Click Chemistry' has been of great interest among the researchers working in different areas, as it represents a family of wonderful linking reactions that are fast, easy to perform, wide in scope, generate less or inoffensive byproducts, high yielding, versatile and highly regio-specific. The reaction approach involves simple reaction conditions and benign solvents that can be easily separated and isolated from the product. Among the various types, the Huisgen 1,3-dipolar cycloaddition reaction involving cycloaddition of terminal alkyne and organic azide in the presence of Cu(I) as catalyst yielding 1,4-disustituted 1,2,3-triazole has gained worldwide popularity due to high stereoselectivity of reaction and purity of the product formed. The 1,2,3-triazole linked molecules formed as a result of this wonderful reaction are famous for their extensive applications in the areas, such as biomedical sciences, physical sciences, polymer chemistry, chemosensing etc. The utility of Cu(I)-catalyzed alkyne-azide cycloaddition (CuAAC) reaction to sew up a variety of structural units to prepare a library of molecules with huge number of applications suggested a way to choose this approach of organic syntheses to pursue this doctoral program. Thrust area of this research contribution was to generate various metal ion sensors through CuAAC reaction, whose sensing potential can be easily studied by techniques such as UV-Visible/Fluorescence spectroscopy. With the vast literature survey related to CuAAC reaction, the main objectives of the research work were as follows:

- To synthesize novel 1,2,3-triazole linked molecules using Cu(I)-catalyzed alkyne-azide cycloaddition (CuAAC) reaction.
- Characterization of newly synthesized compounds by spectroscopic tools like IR, NMR (^{1}H, ^{13}C), along with mass spectrometric studies.
- To study the chemosensing behavior of synthesized 1,2,3-triazole linkers for various ions using UV-Visible spectroscopy.

Thus, a total of eight novel 1,2,3-triazole linked molecules have been synthesized through Cu(I)-catalyzed click cycloaddition of novel terminal alkynes, synthesized during this

research work with the freshly prepared azides (azidomethylbenzene & azidomethylnaphthalene).

For the synthesis of terminal alkynes, the starting materials with good chromophoric units i.e., having absorption in UV-Visible region were searched and used. Each selected starting molecule was having hydroxyl group, whose hydrogen has been nucleophilically substituted by propynyl group from propargyl bromide using K_2CO_3 as base in suitable solvent, simply by stirring at room temperature. At the end, the product was isolated on treating the reaction mixture with ice-cold water followed by filtration, if solid or by solvent extraction method in case of liquid product. Thereafter, the newly synthesized alkynes were treated with different organic azides using Cu(I)-catalyst in order to generate designed 1,2,3-triazole linkers. All the synthesized molecules (terminal alkynes, azides and 1,2,3-triazole linkers) have been well characterized by IR, NMR (^1H, ^{13}C) along with mass spectrometric studies. Finally, the synthesized 1,2,3-triazole linkers were explored for their chemosensing nature through UV-Visible spectroscopy by performing their absorption titrations with various metal ions, like Na(I), K(I), Ba(II), Cr(III), Mn(II), Fe(II), Fe(III), Co(II), Ni(II), Zn(II), Cd(II), Hg(II), Pb(II) and Ce(III) in suitable solvent. The synthesized molecular assemblies are equipped with aromatic heterocyclic moiety with three nitrogen atoms constituted a perfect molecular framework to hold a specific metal ion. The specificity and selectivity of the probe towards a particular metal ion has been investigated through the UV-Visible results obtained during the addition of different metal ions separately into the solution of molecule under examination. The interaction of metal ion with receptor unit causes modulations in the absorption behavior of the receptor unit that helps in recognition of its chemosensing potential. The absorption responses recorded for various novel 1,2,3-triazole linkers, synthesized in this course are presented in this thesis in the form of various types of graphs and figures. The analytical calculations like minimum limit of detection (LOD), binding ratio and binding efficiency of different receptors towards specific metal ions has been done and presented in the text.

DEDICATED

TO

MY DEAR PARENTS

ACKNOWLEDGEMENTS

My first and foremost thanks to God, the Almighty, for providing me strength to start this program and showering his continuous blessings for the successful completion of my Ph.D. study. To achieve this milestone, the role of my esteemed supervisors **Dr. Harminder Singh** and **Dr. Jandeep Singh** is highly commendable. I would like to express my sincere gratitude to them for their constant support, guidance, motivation and immense knowledge. Their suggestions and personal attention helped me in all the time of research and writing of this thesis. It was a great privilege and honor to work under their advice.

I am very much grateful to my parents **Sh. Kundan Lal Saini** and **Smt. Ramesh Rani** for their unconditional love, support and encouragement that greatly helped me during my Ph.D. programme. I am also highly thankful to my family members, my husband **Mr. Shamsher Singh Saini**, my brothers **Mr. Paramjit Singh** and **Mr. Saravjit Singh** along with my sister in laws, **Mrs. Parveen** and **Mrs. Sonia,** ever-ready to help me throughout the journey of this research work. I would also like to express my specials thanks to kids of my family, my sweet daughter Oshin and son Ishan for their sacrifices and boosting me every time along with Shaina, Shivansh, Ranvir, Reet, Taksh and Vivan for their inspiring words and best wishes. A deep sense of gratitude to my parent-in-laws, **Late Sh. Ram Chand Saini** and **Smt. Bimla Devi** for their love and care for me in every situation. I have also been lucky to have a great and helpful research group including Gurleen Singh, Nancy George, Ridhima Singh from LPU and Ms. Kulwinder Kaur, Mr. Parth from GNDU, Amritsar that supported me a lot.

I am highly thankful to Mr. Manoj Kumar (Chemistry lab LPU) and Mr. Darshan Kumar (Chemistry lab, SDAM College Dinanagar) for their help in lab work. My heartfelt regards to all my friends and colleagues, who have supported me directly or indirectly to achieve this success.

Parveen Saini

TABLE OF CONTENTS

LIST OF FIGURES, SCHEMES AND TABLES

FIGURES

SCHEMES

TABLES

LIST OF ABBREVIATIONS

STANDARD UNITS

g	Gram(s)
h	Hour(s)
min	Minute(s)
°C	Degree Celsius
K	Kelvin
atm	Atmosphere
B.Pt.	Boiling point
equiv.	Equivalent(s)
M.Pt.	Melting point
Hz	Hertz
MHz	Mega hertz
mol	Mole(s)
mmol	Millimole(s)
ml	Milliliter(s)
ppm	Parts per million
cm	Centimeter
mm	Millimeter
nm	Nanometer
kcal/mol	Kilocalorie per mole
W	Watt

%	Percentage
Å	Angstrom
et al.	Latin words meaning “and others”

CHEMICALS

DMF	N,N-Dimethylformamide
MeOH	Methanol
AcOH	Acetic acid
DBU	1,8-Diazabicycloundec-7-ene
$CDCl_3$	Deuterated chloroform
DMSO-d_6	Deuterated dimethylsulphoxide
DCM	Dichloromethane
Et_3N/TEA	Triethylamine
THF	Tetrahydrofuran
DIPEA	Diisopropylethylamine
PMDETA	Pentamethyldiethyltriamine
HMTETA	Hexamethyltriethyltetraamine
tpy	Tripyridyl
dpy	Dipyridyl
TPMA	Tris(pyridylmethyl)amine
TBTA	Tris(benzyltriazolylmethyl)amine
THPTA	Tris(hydroxypropyltriazolylmethyl)amine
TTTA	Tris(t–butyltriazolylmethyl) amine

BTTAA	Bis(t–butyltriazolylmethyl) amino–methyltriazolylacetic acid
Et	Ethyl
Me	Methyl
Ph	Phenyl

OTHERS

MS	Mass spectrum
HRMS	High resolution mass spectrum
LCMS	Liquid chromatography mass spectrum
IR	Infrared
UV	Ultraviolet
stirr	Stirring
rt	Room temperature
M	Molecular mass
H	Hydrogen
µw	Microwave
λmax	Wavelength of maximum absorption
λex	Excitation wavelength
µM	Micro molar
ϵ_{max}	Molar absorptivity coefficient
NMR	Nuclear magnetic resonance
s	Singlet

d	Doublet
dd	Double doublet
t	Triplet
m	Multiplet
J	Coupling Constant
δ	Chemical shift
TLC	Thin layer chromatography
CuAAC	Copper catalyzed alkyne-azide cycloaddition
HSAB	Hard-Soft acid base
HOMO	Highest occupied molecular orbital
LUMO	Lowest unoccupied molecular orbital
v/v	Volume/Volume

Chapter 1

Introduction

This chapter of thesis represents literature survey carried out to perform research work. It lays out detailed motivational aspects especially methodology of synthesis and applications of titled molecules that inspired me to pursue research for Ph.D. program. This chapter lists out essential literature surveyed for successful completion of doctoral program, focused on detailed background of each portion of my research contribution.

1.1 Historical aspects of 'Click Chemistry'

K. B. Sharpless, Nobel prize winning American scientist introduced the concept of 'Click Chemistry' in 2001, that represents a family of linking reactions that are fast, easy to perform, wide in scope, generate less or inoffensive by products, high yielding, versatile and highly region-specific [1-5]. The reaction process involves simple reaction conditions and benign solvents that can be easily removed to make the isolation of product facile. These reactions proceed without any pre-treatment of reactants and involve combination of diverse structural units effectively [6-8]. The various categories of click chemistry reactions, as reported in literature include cycloadditions [9-12], thiol-ene, nucleophilic ring opening of strained heterocycles [13-15], photo click reactions etc. [16-19]. Among these categories, the cycloaddition reaction, especially Cu(I)-catalyzed Huisgen 1,3-dipolar cycloaddition reaction between organic azides and terminal alkynes results into the formation of 1,2,3-triazoles have gained immense importance. The preparation of 1,2,3-triazoles through 1,3-dipolar cycloaddition reaction was first reported by Rolf Huisgen, a German scientist, in 1960 [20-21], but this reaction gained worldwide importance with the introduction of Cu(I) as catalyst, leading to highly stereospecific product. The 'Click Chemistry' is hence not a new set of synthetic chemistry, but an advanced form of previously discovered reactions to be conducted under simple and ambient reaction conditions to get pure product with high yield [22-27].

1.2 1,3-Dipolar cycloaddition

The cycloaddition reaction between a 1,3-dipole and a dipolarophile (unsaturated molecule) to generate a five membered cyclic structure is termed as 1,3-dipolar cycloaddition graphically represented in Figure 1.1.

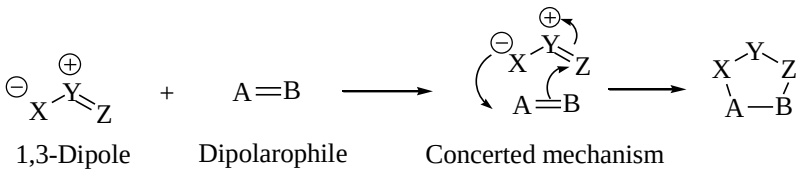

Figure 1.1: Mechanism of 1,3-dipolar cycloaddition reaction

The reactions involving 1,3-dipolar cycloaddition were discovered in late 19th century to early 20th century with the invention of various types of 1,3-dipoles [28-30]. The mechanism and application part of cycloaddition reaction was investigated in 1960s, primarily through the research contribution of Rolf Huisgen. 1,3-dipolar cycloaddition reaction has served as an important route for the formation of five membered heterocyclic rings. The reaction is highly stereoselective with respect to dipolarophile means cis-alkene gives syn-product and vice versa that supports concerted mechanism of cycloaddition [31-33].

1.3 Huisgen 1,3-dipolar cycloaddition reaction

Rolf Huisgen developed an uncatalyzed 1,3-dipolar cycloaddition reaction, which is also commonly referred to Huisgen reaction or Huisgen cycloaddition. The reaction has involved generation of 1,2,3-triazole as a mixture of 1,4 and 1,5-disubstituted adducts by 1,3-dipolar cycloaddition reaction between terminal alkynes as dipolarophile and organic azides as 1,3-dipole at 98 °C in 18 h, presented in Figure 1.2. The Huisgen reaction has involved the generation of a mixture of two isomers which suffered from the difficulty in separation from the mixture of regioisomers [34-35].

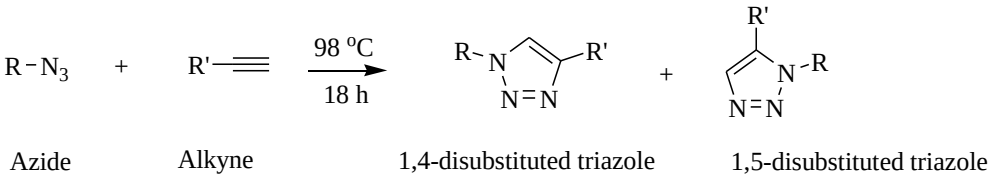

Figure 1.2: Rolf Huisgen reaction to produce two di-substituted 1,2,3-triazole products

In recent years, this reaction has gained extreme popularity when K. B. Sharpless introduced Cu(I) as catalyst in this cycloaddition reaction, making it exclusive for the formation of 1,4-disubstituted product and therefore, the Cu(I) catalyzed alkyne-azide cycloaddition (CuAAC) refers to the click synthesis of 1,2,3-triazoles. The generation of 1,4-disubstituted 1,2,3-triazole as only product of this

Cu(I)-catalyzed process has brought revolution in the synthetic organic chemistry [36].

1.4 CuAAC and Mechanism involving catalytic action of Cu(I)

The Cu(I)-catalyzed 1,3-dipolar cycloaddition reaction between terminal alkyne and azide, performed under relatively moderate reaction conditions with high stereoselectivity, is presented in Figure 1.3. The reaction process involves the fusion of terminal alkyne with organic azide in the presence of Cu(I) with stirring at room temperature using a variety of solvents like water, alcohol, tetrahydrofuran, acetonitrile etc. Another advanced technology to conduct this cycloaddition reaction involves the use of microwave radiations along with Cu(I) in a suitable solvent.

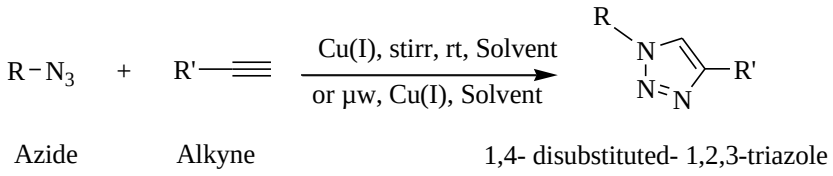

Figure 1.3: Scheme of Cu(I)-catalyzed alkyne-azide cycloaddition (CuAAC)

The addition of Cu(I) increases the rate as well as regulates the chemo or regioselectivity of cycloadditon reaction leading to 1,4-disubstituted isomer only [37-39]. For this reaction, only terminal alkynes can be used, because the reaction mechanism involves abstraction of terminal proton, which results into Cu-alkynyl intermediate. The binding of Cu(I) at one carbon, locked the stereochemistry to single position product. This intermediate binds with azide in next step to form six membered cyclic intermediate that rapidly change into stable triazole [40-42]. Sharpless and co-workers proposed a mechanism that involves a mononuclear Cu-alkynyl intermediate, as shown in Figure 1.4(a). These studies were later on supported by DFT studies in 2005, according to which, the use of Cu(I) cuts the activation energy barrier for the formation of intermediate from 14.9 kcal/mol to 24.7 kcal/mol in comparison to the reaction without catalyst. Thereafter, Fokin and Finn suggested the possibility of another mechanism that involved two Cu-centers in the transition state during whole process. It involves π-complexation of alkyne with a copper

species that decreases electron density on alkynyl carbon (sp-hybridized) and enhances the reactivity of alkynyl moiety towards deprotonation by second copper atom, thus facilitating the reaction of azide to produce bridged dicopper μ-alkenylidene intermediate, as shown in Figure 1.4(b). The intermediate formed in the mechanism involving two copper ions has been proved as thermally more stable than the ring strained intermediate formed as a result of mononuclear reaction mechanism [44-48].

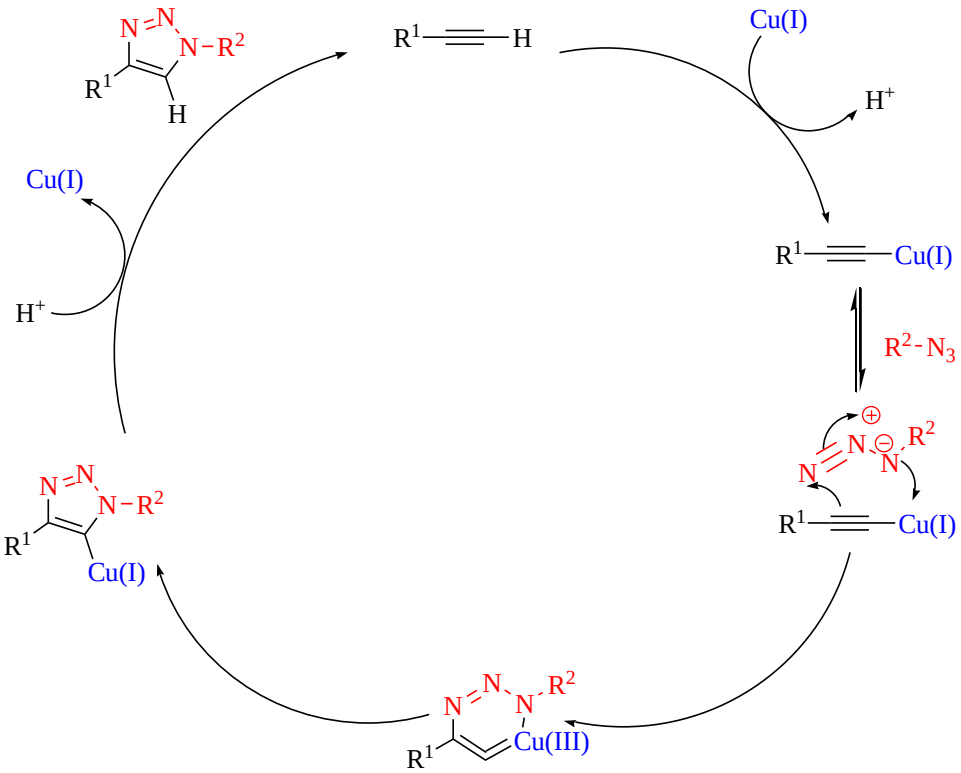

Figure 1.4(a): Mechanism proposed by Sharpless and his research group for Cu(I)-catalyzed alkyne-azide cycloaddition reaction

Since discovery, Cu(I)-catalyzed alkyne-azide cycloaddition has gained global popularity among the researchers from different disciplines due to formation of 1,2,3-triazole derivative, a heterocyclic compound which is aromatic, stable and chemically inert to different reaction conditions like hydrolysis, reduction and oxidation [49-50]. Alternative to the CuAAC, the cycloaddition of azides and terminal alkynes has also been reported through catalyzation by other transition metal ions such as Pt(II) [51], Ni(II) [51], Pd(II) [52], Ir(I) [53-54] as well as Ru(II) [55]. However, the

cycloaddition reaction catalyzed by Cu(I) is found to be superior over others in terms of reaction conditions, rate and yield of reaction as well as area of application [56].

More importantly, CuAAC follows the principles of green approach of organic synthesis. Alternately, several chemical methods have been reported which require strong reaction conditions and are accompanied by the formation of toxic by-products along with desired product that followed by certain techniques of purification [57-58]. Therefore, organic synthesis following click reaction approach is of great interest for both academic research as well as industrial applications.

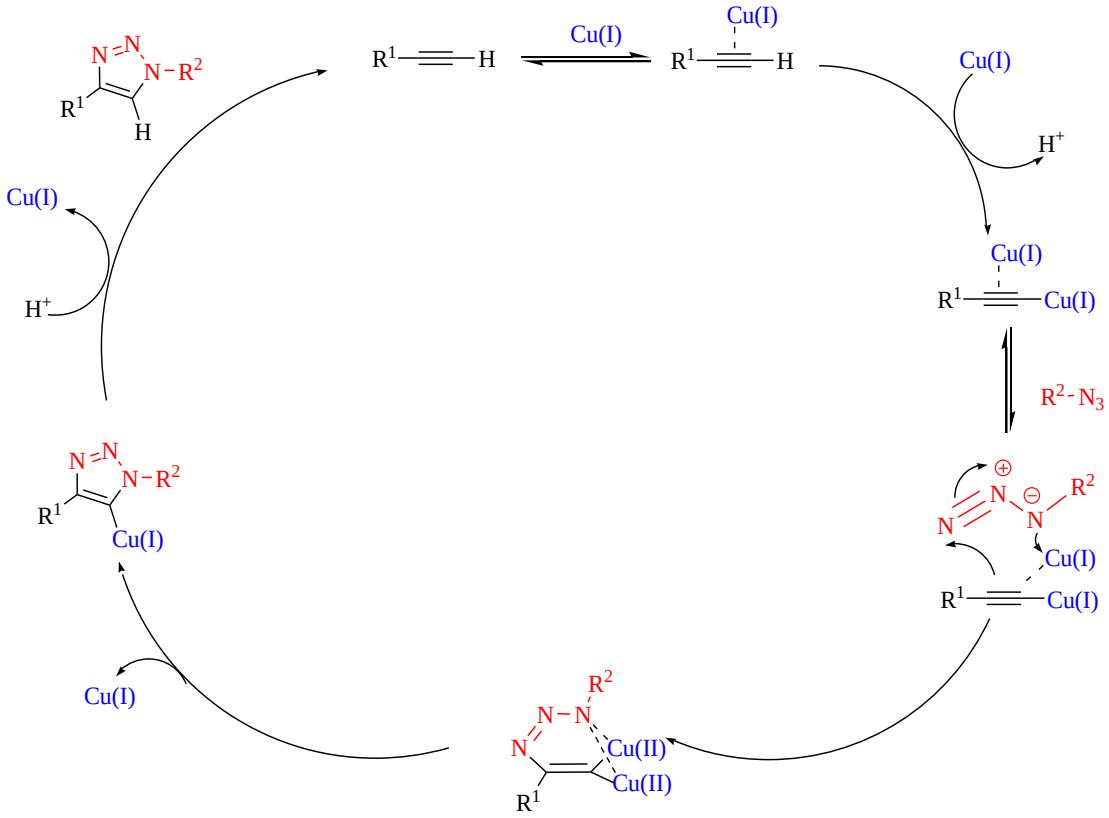

Figure 1.4(b): Mechanism proposed by Fokin and Finn for Cu(I)-catalyzed alkyne-azide cycloaddition reaction involving two copper centers

1.5 Catalytic systems as Cu(I) sources in CuAAC reaction

There are several types of Cu(I) sources found in literature that catalyze alkyne-azide cycloaddition reaction under particular reaction conditions. Depending

upon the kind of catalytic material, a variety of catalytic systems is introduced in the reports related to CuAAC reaction, a few are as follows:

- Cu(II) salts in combination with specific reducing agent [59-64]
- Cu(II) salts with reducing agent as well as phase transfer catalyst [65-68]
- Cu(II) salts with photoreduction conditions [69-72]
- Cu(I) salts/coordination complexes [73-75]
- Cu(I) ions anchored over dendrimers or solid supports [76-79]
- Ionic liquid crystals with Cu(I) immobilization [80-84]
- Copper nanoparticles [85-88]

1.6 Importance of 1,2,3-triazoles

1,2,3-triazoles are five membered heterocyclic molecules with little basic characteristics and consequently, operational under physiological pH without any protonation of molecules or loss of their identity. These are aromatic and are extremely stable to any chemical or metabolic degradation along with inertness to oxidizing, reducing and hydrolytic conditions, even at very high temperature. These distinctive features make them different from other heterocyclic compounds and therefore, 1,2,3-triazole linkers have great contribution in diverse research areas like environmental sciences, biochemical sciences, material sciences, polymer chemistry, medicinal chemistry with antimicrobial, anticancer, antiviral, antioxidant, anti-HIV and antitubercular activities [89-92].

One of the promising applications of synthetic 1,2,3-triazole linkers is chemosensing of ions (both cations and anions) [93]. The generation of 1,2,3-triazole linked molecules through CuAAC has been pursued for the synthesis of a variety of fluorescent ionophores [94]. The selective detection of metal ions by these chemosensors has attracted researcher's attention towards the human health and environment protection [95-96]. The contamination of heavy metal is a major environmental problem due to their strong toxicity that led to major health issues even at low concentration limits. The heavy metal ions like As(II), Pb(II), Cr(III), Hg(II), Cd(II) and Tl(I) form a major component of environmental contamination that severely affects living beings and cause serious health problems. Hence, these toxic

ions should be detected both qualitatively as well as quantitatively in order to treat them properly for environment safety [97-99].

1.7 Chemosensing

A chemosensor is a molecule that produces a detectable change on interaction with a specific analyte and is also called as molecular sensor. It exhibits molecular recognition characteristics or undergoes specific changes on binding with analyte that are then reflected in a signal [100]. A chemosensing device typically consists of following units:

- A receptor unit that selectively identifies a specific analyte and binds with that
- A transducer unit that converts the identification process into an optical signal
- A detector unit that detects and transforms the detected change into a readable output [101-104]

An interesting class of chemosensing material that meets all the above-mentioned features includes chromophoric or fluorophoric units in their molecules. These molecules can combine detection properties with optical transduction, i.e., change in absorption or fluorescence emission. The colorimetric reagents for the detection of various analytes based on complexation character have gained wide popularity. Past few decades have witnessed the growth in various analytical methods like voltammetry, atomic absorption spectroscopy and electrochemical methods etc. for the detection of ions. But due to expensive instruments, low selectivity, slow response time and complexity of methodology, their use has been limited for the utility as ion detection [105-106]. In recent years, there have been a growing need for the designing and construction of chemical sensors for fast, on-time and cost-effective monitoring of environmental samples. In contrast to the traditional analytical instruments, chemical sensors are transportable, easy to use and miniature in size. These features are ideal for the on-field measurements, therefore the errors caused by the sample transportation and storage can be reduced to large extent. Optical chemosensors having tendency to be used as indicators for heavy metal ions can provide simple and convenient procedures for on-site analysis. Therefore, the research and development in the area of chemosensing has expanded exponentially in terms of

financial investment, numbers of publications, and the number of active researchers worldwide. This research work focuses on the development of chromophoric chemical sensors using 'Click chemistry' approach to increase the applicability of final compounds.

The organic molecules having 1,2,3-triazole moiety have achieved great success in this field due to presence of nitrogen heteroatoms to coordinate with specific metal ions. Different kinds of such molecules have been reported as ion detectors and among them chemosensors based on luminescence properties have a set of merits: high selectivity (among the numerous kinds of ions, they detect only single ion), cost effectiveness, easy to use as well as biocompatibility [107-108]. For instance, the research group of Shainaz M. Landge synthesized a phenanthrene based triazole derivative **3** as fluorescent chemosensor for the detection of fluoride and copper ions by click reaction between 2-azidophenol **1** and 9-ethynylphenanthrene **2** using acetonitrile as solvent in round bottom flask with stirring at room temperature, as shown in Figure 1.5. 1,2,3-triazole moiety in final product **3** shows ligation with analyte ion and modulates fluorophoric behaviour of phenatharene unit that can be easily studied by UV-Visible and Fluorescence spectroscopic techniques [109].

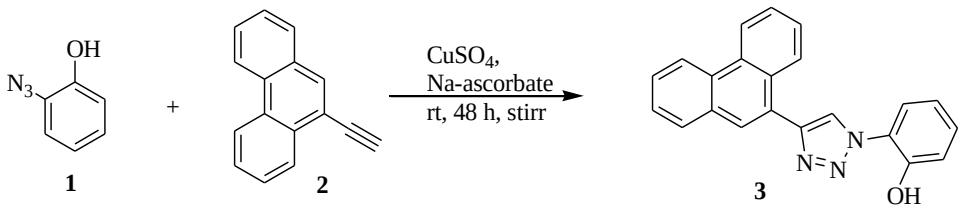

Figure 1.5: Synthesis of phenantharene based fluorescent chemosensor

Among the numerous kinds of luminescent chemosensors, the organic fluorescent materials are most widely used and studied because of their chemical structures. Their functional groups can be easily modified through various chemical processes to enhance their binding ability and fluorescence quantum yield. On binding with specific analytic ion, the changes in electronic distribution between the receptor unit and analyte cause modulations in their absorption or emission behavior that can be examined by UV-Visible or Fluorescence spectroscopy.

1.8 Mechanism of chemosensing

Chemosensing by molecular sensors is based upon the principle of host–guest relationship where target species (guest) binds non-covalently with receptor unit (host). The origin of molecular detection has his history back to macrocyclic compounds, capable of selective binding with alkali metal ions [110]. Crown ethers and metal chelators are the typical molecules of these types of hosts. Furthermore, the progress in chemosensing leads to the synthesis of more sophisticated organic species like cryptands, podants or calixarenes having oxygen, nitrogen and sulphur atoms as donor to interact with analyte based upon the principal of hard and soft acids and bases (HSAB) [111-112]. Hence, metals like Cs(I), Cu(I), Au(I), Ag(I), Hg(I), Pd(II), Cd(II) and Tl(I) categorized as soft acids prefer to bind with host molecules having sulphur donor atoms classified as soft bases, whereas the borderline acids like Fe(II), Co(II), Ni(II), Cu(II), Zn(II), Hg(II) and Pb(II) favorably interact with ligands carrying nitrogen donor atoms [113]. An effective chemical sensor must have following features:

- Should give an optical signal with high signal to noise ratio
- Should give an observable change on exposure to analyte
- Should be highly stable over sufficient time period on storage
- Should be non-toxic and be synthesized at adequate expenses

Fluorescent materials constitute a category of molecular sensors that fulfill these requirements to large extent, where target species gets bonded with receptor unit linked to the fluorescent unit (fluorophore) and results into changes in either position or intensity of emission band upon complexation [114-115].

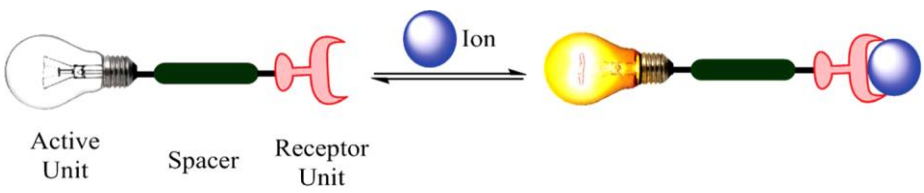

Figure 1.6: A typical design of fluorescent chemosensor [116]

The phenomenon of changes in the detectable signal of fluorescent chemosensor caused by interactions between the target ion and receptor unit is represented in Figure 1.6. This specific and selective nature of receptor unit imparts uniqueness to each chemosensor. In recent years, scientists have shown great interest in 'Click' variety of organic probes applicable as fluorescent chemosensors using a wide range of fluorescent alkynes and azides. UV-Visible and Fluorescence spectroscopic techniques are generally used in studying the chemosensing behavior [117-119].

1.9 UV-Visible and Fluorescence spectroscopy for chemosensing analysis

UV-Visible spectroscopy is an analytical tool used to determine various analytes such as biological molecules, transition metal ions, organic molecules etc. When UV-Visible radiations of range 200-800 nm fall on a molecule, broad band of specific intensity appears at a particular wavelength (wavelength absorbed by the molecule). There exists a change in absorption wavelength or intensity of absorbance, when that molecule gets bonded with an analyte thus resulting into chemosensing. The absorption spectra of molecules are also affected by solvent and pH changes. Similarly, modulations in fluorescence spectra can be observed on ligation of fluorescent chemosensor with an analyte [120]. Fluorescence takes place in the presence of UV-Visible electromagnetic radiations. It is a type of luminescence that involves excitation of molecule on absorption of light of particular wavelength and quickly return to the ground state by releasing photons of less energy or high wavelength, means the fluorescence can be monitored at a higher wavelength value. Generally, both of these methods are used in chemosensing, UV measures the absorption of light while fluorescence measures the light emitted by the sample, but the sensitivity of fluorometry is 10 to 100 times as much as that of UV-Visible absorption spectrometry. This high sensitivity makes fluorescence one of the best available methods for trace analysis [121-122].

1.10 Conclusion

The synthesis of sensing probes through Cu(I)-catalyzed alkyne-azide cycloaddition (CuAAC), a worldwide popular reaction of 'Click Chemistry', is

noticeable in terms of stereoselectivity of the reaction and the formation of almost pure product under benign reaction conditions. The versatility of CuAAC reaction to stitch a variety of terminal alkynes with organic azides under simple and ambient reaction conditions to produce 1,4-disubstituted 1,2,3-triazole derivatives having a wide range of applications in the areas, such as bio-medical sciences, environmental chemistry, polymer chemistry, physical sciences, catalysis and chemosensing, paved the way for the synthesis of 1,2,3-triazole derivatives to be used as metal ions sensors. Among the various techniques used to study the chemosensing behavior of molecular sensors, the UV-Visible and Fluoresence spectroscopy are the most simple and reliable techniques, if they are having absorption in UV-Visible region.

References:

1. H. C. Kolb, M. G. Finn, K. B. Sharpless, *Angew. Chem., Int. Ed.* **2001**, 40, 2004.
2. M. Meldal, C. W. Tornoe, *Chem. Rev.* **2008**, 108, 2952.
3. C. W. Tornoe, C. Christensen, M. Meldal, *J. Org. Chem.* **2002**, 67, 3057.
4. L. Zhang, X. Chen, P. Xue, H. H. Y. Sun, I. D. Williams, K. B. Sharpless, V. V. Fokin, G. Jia, *J. Am. Chem. Soc.* **2005**, 127,15998.
5. P. Wu, A. K. Feldman, A. K. Nugent, C. J. Hawker, B. Voit, J. Pyun, J. M. J. Frechet, K. B. Sharpless, V. V. Fokin, *Angew.Chem., Int. Ed.* **2004**, 43, 3928.
6. H. C. Kolb, K. B. Sharpless, *Drug Dis. Today.* **2003**, 8, 1128.
7. V. V. Rostovtsev, L. G. Green, V. V. Fokin, K. B. Sharpless, *Angew.Chem., Int. Ed.* **2002**, 41, 2596.
8. D. Dohler, P. Michael, W. H. Binder, *Acc. Chem. Res.* **2017**, 50, 2610.
9. Y. Laamari, A. Oubella, A. Bimoussa, A.E. Mansouri, E.M. Ketatni, O. Mentre, A. Auhmani, *Bioorg. Chem.* **2021**, 115, 105165.
10. N. Kaur, G. Singh, J. Singh, A. Singh, P. Satija, G. Kaur, J. Singh, *RSC Adv*. **2018**, 8, 36445.
11. C. E. Hoyle, A. B. Lowe, C. N. Bowman, *Chem. Soc. Rev.* **2010**, 39,1355.
12. G. Kim, B. Suh, C. Kim, *J. Mol. Struct*. **2022**, 1254, 132307.
13. A. B. Lowe, *Polym. Chem.* **2014**, 5, 4820.

14. S. Saha, S. Kamila, A. Chattopadhyay, P. Sahoo, *New J. Chem.* **2022**, 46, 4233.
15. G. T. Selvan, C. Varadaraju, R. T. Selvan, I. V. M. V. Enoch, P. M. Selvakumar, *ACS Omega*, **2018**, 3, 7985.
16. W. Song, Y. Wang, J. Qu, Q. Lin, *J. Am. Chem. Soc*. **2008**, 130, 9654.
17. R. J. Pounder, M. J. Stanford, P. Brooks, S. P. Richards, A. P. Dove, *Chem. Commun.* **2008**, 40, 5158.
18. M. J. Stanford, A. P. Dove, *Macromolecules*, **2009**, 42, 141.
19. G. Kaur, G. Singh, J. Singh, *Mat. Today Chem*. **2018**, 8, 56.
20. R. Huisgen, *Angew. Chem., Int. Ed.*, **1963**, 2, 565.
21. R. Huisgen, *Angew. Chem., Int. Ed.*, **1963**, 2, 633.
22. C. B. Kowollik, F. E. Du Prez, P. Espeel, C. J. Hawker, T. Junkers, H. Schlaad, *Angew. Chem. Int. Edit.* **2011**, 50, 60.
23. W. V. Camp, *Angew. Chem. Int. Edit.* **2011**, 50, 84.
24. F. Amblard, J. H. Cho, R. F. Schinazi, *Chem. Rev*. **2009**, 109, 4207.
25. "The Nobel Prize in Chemistry 2022". Nobel Prize.org. **2022.**
26. S. Bayindir, M. Toprak, *Spectrochim. Acta A: Mol. Biomol. Spectros.* **2019**, 13, 6.
27. C. Li, M. G. Finn, *J. Polym. Sci. Pol. Chem.* **2006**, 44, 5513.
28. R. Huisgen, *Org. Chem*. **1968**, 33, 2291.
29. R. Huisgen, A. Padwa, *Wiley-Interscience*. **1984**, 1, l.
30. A. Padwa, L. Fisera, K. F. Koehler, A. Rodriguez, G. S. K. Wong, J. *Org. Chem*. **1984**, 49, 276.
31. G. Roussi, J. Zhang, *Tetrahed. Lett.* **1988**, 29, 3481.
32. S. Takano, Y. Iwabuchi, K. Ogasawara, *J. Am. Chem. Soc.* **1987**, 109, 5523.
33. R. Huisgen, G. Szeimies, L. Mobius, *Chem. Ber*. **1967**, 100, 2494.
34. R. Huisgen, *J. Org. Chem.* **1976**, 41, 403.
35. R. Huisgen, *Pure Appl. Chem*. **1989**, 61, 613.
36. C. D. Hein, X. M. Liu, D. Wang, *Pharm. Res.* **2008**, 10, 2216.
37. N. V. Sokolova, V. G Nenajdenko, *RSC Adv.* **2013**, 3, 16212.
38. K. B. Sharpless, P. Wu, T. Vidar, J. G. Lindberg, *J. Chem. Educ.* **2005**, 82, 1751.

39. Y. Liu, D. D. Diaz, A. A. Accurso, K. B. Sharpless, V. V. Fokin, M. G. Finn, J. *Polym. Sci. Pol. Chem*. **2007**, 45, 5182.
40. H. Ben, E. Ayouchia, L. Bahsis, L. R. Domingo, S. Stiriba, *RSC Adv*. **2018**, 8, 7670.
41. W. H. Binder, R. Sachsenhofer, *Macromol. Rapid Commun.* **2008**, 29, 952.
42. V. O. Rodionov, V.I. Presolski, D.D. Diaz, V.V. Fokin, M.G. Finn, *J. Am. Chem. Soc.* **2007**,129, 12705.
43. J. E. Hein, V.V. Fokin, *Chem. Soc. Rev.* **2010**, 39, 1302.
44. J. F. Nierengarten, *Pure Appl. Chem.* **2012,** 84, 1027.
45. M. Ahlquist, V.V. Fokin, *Organometallics*, **2007**, 26, 4389.
46. B. F. Straub, *Chem. Commun.* **2007**, 37, 3868.
47. L. Li, Z. Zhang, *Molecules*, **2016**, 21, 1393.
48. K. Wang, X. Bi, S. Xing, P. Liao, X. Meng, *Green Chem*. **2011**, 13, 562.
49. C. Iacobucci, S. Reale, J. F. Gal, F. D. Angelis, *Angew. Chem. Int. Ed. Engl.* **2015**, 54, 3065.
50. B. R. Buckley, S. E. Dann, H. Heaney, *Chem. Eur. J.* **2010**, 16, 6278.
51. P. L. Golas, N. V. Tsarevsky, B. S. Sumerlin, K. Matyjaszewski, *Macromolecules*, **2006**, 39, 6451.
52. C. Chowdhury, S. B. Mandal, B. Achari, *Tetrahed. Lett.* **2005**, 46, 8531.
53. C. Wang, D. Ikhlef, S. Kahlal, J. Y. Saillard, D. Astruc, *Coord. Chem. Rev.* **2016**, 316, 1.
54. S. Ding, G. Jia, J. Sun, *Angew. Chem.* **2014**, 126, 1908.
55. S. Oppilliart, G. Mousseau, L. Zhang, G. Jia, P. Thuéry, B. Rousseau, *Tetrahedron*, **2007**, 63, 8094.
56. R. P. Johnson, J. V. John, I. Kim, *J. Eur. Polym.* **2013**, 49, 2925.
57. A. Marrocchi, A. Facchetti, D. Lanari, S. Santoro, L. Vaccaro, *Chem. Sci.* **2016**, 7, 6298.
58. N. Moini, M. J. Zohuriaan–Mehr, K. Kabiri, H. A. Khonakdar, *Appl. Surf. Sci.* **2019**, 487, 1131.
59. G. Acik, C. Altinkok, H. Olmez, M. A. Tasdelen, *Prog. Org. Coat*. **2018**, 125, 73.
60. T. R. Chan, R. Hilgraf, K. B. Sharpless, V. V. Fokin, *Org. Lett.* **2004**, 6, 2853.

61. A. J. Link, D. A. Tirrell, *J. Am. Chem. Soc.* **2003**, 125, 11164.
62. A. E. Speers, G. C. Adam, B. F. Cravatt, *J. Am. Chem. Soc.* **2003**,125, 4686.
63. S. Meunier, E. Strable, M. G. Finn, *Chem. Biol.* **2004**, 11, 319.
64. J. E. Hein, J. C. Tripp, L. B. Krasnova, K. B. Sharpless, V. V. Fokin, *Angew.Chem. Int. Ed.* **2009,** 48, 8018.
65. K. S. S. Praveena, E. V. V. S. Ramarao, Y. Poornachandra, C. G. Kumar, N. S. Babu, N. Y. S. Murthy, S. Pal, *Lett. Drug Des. Discov.* **2016**, 13, 210.
66. N. Kuntala, J. R. Telu, V. Banothu, S. Balasubramanian, J. S. Anireddy, S. Pal, *Mini Rev. Med. Chem.* **2018**, 18, 803.
67. J. Tan, N. Yasuda, *Org. Process Res. Dev.* **2015**, 19, 1731.
68. K. Maruoka, *Org. Process Res. Dev.* **2008**, 12, 679.
69. B. M. El-Zaatari, A. U. Shete, B. J. Adzima, C. J. Kloxin, *Phys. Chem. Chem. Phys.* **2016**, 18, 25504.
70. M. U. Kagveci, M. Ciftci, S. Evran, S. Timur, *Design. Mono. Polym.* **2015**, 18, 129.
71. M. Arslan, T. C. Bicak, B. A. Pulido, S. P. Nunes, Y. Yagci, *J. Eur. Polym.* **2018,** 100, 298.
72. M. A. Tasdelen, G. Yilmaz, B. Iskin, Y. Yagci, *Macromolecules*, **2012**, 45, 56.
73. K. Wang, X. Bi, S. Xing, P. Liao, Z. Fang, X. Meng, Q. Zhang, Q. Liu, Y. Ji, *Green Chem.* **2011**,13, 562.
74. F. Himo, T. Lovell, R. Hilgraf, V.V. Rostovtsev, L. Noodleman, K.B. Sharpless, V.V. Fokin, *J. Am. Chem. Soc.* **2005**, 127, 210.
75. M. Ahlquist, V.V. Fokin, *Organometallics*, **2007**, 26, 4389.
76. C. Deraedt, N. Pinaud, D. Astruc, *J. Am. Chem. Soc.* **2014**, 136,12092.
77. S. Sabaqian, F. Nemati, M. M. Heravi, H. T. Nahzomi, *Appl. Organomet. Chem.* **2017,** 31, 3660.
78. S. Shaabani, A. T. Tabatabaei, A. Shaabani, *Appl. Organomet. Chem.* **2017**, 31, 3559.
79. P. Shiri, J. Aboonajmi, *J. Org. Chem.* **2020,** 16, 551.
80. A. D. Sawant, D. G. Raut, N. B. Darvatkar, M. M. Salunkhe, *Green Chem. Lett. Rev.* **2011**, 4, 41.
81. Q. Zhang, H. Su, J. Luo, Y. Wei, *Green Chem.* **2012**, 14, 201.

82. A. Pourjavadi, N. Safaie, S. H. Hosseini, C. Bennett, *Appl. Organomet. Chem*. **2015**, 29, 601.
83. A. Pourjavadi, S. H. Hosseini, F. M. Moghaddam, S. E. Ayati, *RSC Adv.* **2015**, 5, 29609.
84. M. Tavassoli, A. L. Isfahani, M. Moghadam, S. Tangestaninejad, V. Mirkhani, I. M. Baltork, *Appl. Catal. A*, **2015**, 503, 186.
85. B. C. Ranu, R. Dey, T. Chatterjee and S. Ahmmed, *Chem. Sus.Chem*. **2012**, 5, 22.
86. T. Jin, M. Yan, Y. Yamamoto, *Chem. Cat. Chem*. **2012**, 4, 1217.
87. N. K. Devaraj, M. G. Finn, *Chem. Rev*. **2021**, 121, 6697.
88. N. N. Reddy, S. J. Hung, M. K. Swamy, A. Sanjeev, V. S. Rao, R. Rohini, A. K. Raju, K. Bhaskar, A. Hu, P. M. Reddy, *Molecules*, **2021**, 26, 1952.
89. K. S. S. Praveena, E. V. V. S. Ramarao, Y. Poornachandra, C. G. Kumar, N. S. Babu, N. Y. S. Murthy, S. Pal, *Lett. Drug Des. Discov*. **2016**, 13, 210.
90. N. Kuntala, J. R. Telu, V. Banothu, S. B. Nallapati, J. S. Anireddy, S. Pal, *Med. Chem. Commun.* **2015**, 6, 1612.
91. G. Singh, J. D. Kaur, Pawan, Priyanka, Mohit, A. Devi, S. Gupta, Y. Thakur, K. N. Singh, *Appl. Organomet. Chem*. **2022**, 36, 690.
92. L. D. Rodrigues, D. Sunil, D. Chaithra, P. Bhagavath, *J. Mole. Liquids*, **2019**, 18, 201.
93. Y. H. Lau, P. J. Rutledge, M. Watkinson, M. H. Todd, *Chem. Soc. Rev.* **2011**, 40, 2848.
94. L. Wang, J. Jin, L. Zhao, H. Shen, C. Shen, P. Zhang, *Carbohyd. Res.* **2016**, 18, 308.
95. F. Kolcu, D. Erdener, I. Kaya, *Synth. Meth*. **2021**, 272, 116668.
96. M. Saleem, K. H. Lee, *RSC Adv.* **2015**, 5, 72150.
97. G. Singh, Diksha, Mohit, Suman, Sushma, A. Devi, S. Gupta, C. Espinosa-Ruíz, M. A. Esteban, *Inorg. Chim. Acta*, **2022**, 537, 120926.
98. K. M. Lockhart, A. M. King, T. Harter, *J. Contam. Hydrol.* **2013**, 151, 140.
99. M. Schriks, M. B. Heringa, P. D. Voogt, A. P. Van Wezel, *Water Res.* **2010**, 44, 461.
100. G. R. Penzer, *J. Chem. Educ.* **1968**, 45, 692.

101. K. P. Carter, A. M. Young, A. E. Palmer, *Chem. Rev.* **2014**, 114, 4564.
102. A. P. de Silva, H. Q. N. Gunaratne, T. Gunnlaugsson, A. J. M. Huxley, C. P. McCoy, J. T. Rademacher, T. E. Rice, *Chem. Rev.* **1997**, 97, 1515.
103. W. Al Zoubi, N. Al Mohanna, *Spectrochim. Acta, Part A: Mol. Biomol. spectro.* **2014**, 132, 854.
104. S. Joo, R. B. Brown, *Chem. Rev.* **2008**, 108, 638.
105. J. R. Stetter, W. R. Panrose, S. Yao, *J. Electrochem. Soc.* **2003**, 150, 11.
106. H. H. Qazi, A. B. Mohammad, M. Akram, *Sensors*, **2012**, 12, 16522.
107. H. N. Kim, W. X. Ren, J. S. Kim, J. Yoon, *Chem. Soc. Rev.* **2013**, 41, 3210.
108. L. B. Desmonts, D. N. Reinhoudt, M. C. Calama, *Chem. Soc. Rev.* **2007**, 36, 993.
109. S. M. Landge, D. Y. Lazare, C. Freeman, J. Bunn, J. I. Cruz, D. Winder, C. Padgett, K. S Aiken, D. Ghosh, *Spectrochim. Acta, Part A: Mol. Biomol. spectro*. **2019**, 1, 8.
110. P. Buhlmann, E. Pretsch, E. Bakker, *Chem. Rev.* **1998**, 98, 1593.
111. F. P. Schmidtchen, M. Berger, *Chem. Rev.* **1997**, 97, 1609.
112. L. Rivera, D. Izquierdo, I. Garce, I. Salinas, J. Alonso, M. Puyol, *Sens. Actuators B.* **2009**, 137, 420.
113. R. G. Pearson, *J. Am. Chem. Soc.* **1963**, 265, 3533.
114. M. C. L. Yeung, V. W. W. Yam, *Chem. Soc. Rev.* **2015**, 44, 4192.
115. H. Wang, J. Lin, W. Huang, W. Wei, *Sens. Actuators B: Chem.* **2010**, 150, 798.
116. N. Kaur, G. Singh, J. Singh, A. Singh, P. Satija, G. Kaur, J. Singh, *RSC Adv.* **2018**, 8, 36445.
117. A. N. Kursunlu, E. Guler, *J. Molecular Str.* **2017**, 1134, 345.
118. A. N. Kursunlu, E. Guler, *Supramole. Chem.* **2013**, 25, 512.
119. Y. L. Liu, L. Yang, L. Li,Y. Q. Guo, X. X. Pang, P. Li, F. Ye, Y. Fu, *Molecules*, **2019,** 24, 3093.
120. R. Peng, Y. Xu, Q. Cao, *Chinese Chem. Lett.* **2018**, 29, 1465.
121. S. M. Barrett, P. S. Szalay, L. A. Zook-Gerdau, E. J. Schurter, *J. Chem. Educ.* **2020**, 97, 4097.
122. F. N. Arslan, G. A. Geyik, K. Koran, F. Ozen, D. Aydin, *J. Fluorescence*, **2020**, 30, 317.

Chapter 2

Review of literature

This chapter represents literature regarding the methodology adopted for the actual research work conducted during the doctoral program. It sketches out details of all the steps involved in the synthesis of titled molecules, survey of spectroscopic techniques for the characterization of synthesized molecules along with the literature related to chemosensing.

2.1 Introduction to heterocyclic compounds

Cyclic organic compounds with the ring structure made up of carbon atoms along with atoms like nitrogen, oxygen and sulfur are categorized as heterocyclic compounds. Furan, pyrrole and thiophene are the most common heterocyclic compounds with five membered cyclic rings containing only one heteroatom along with carbons. A large range of heterocyclic compounds are reported in literature having isolated or fused heterocyclic rings performing a variety of functions. Figure 2.1 shows few most commonly known heterocyclic compounds [1-3].

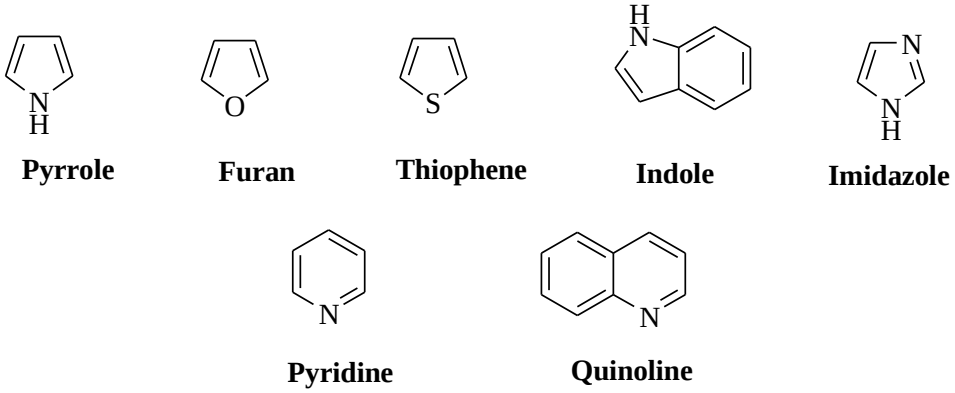

Figure 2.1: Five and six membered, simple and fused heterocyclic rings

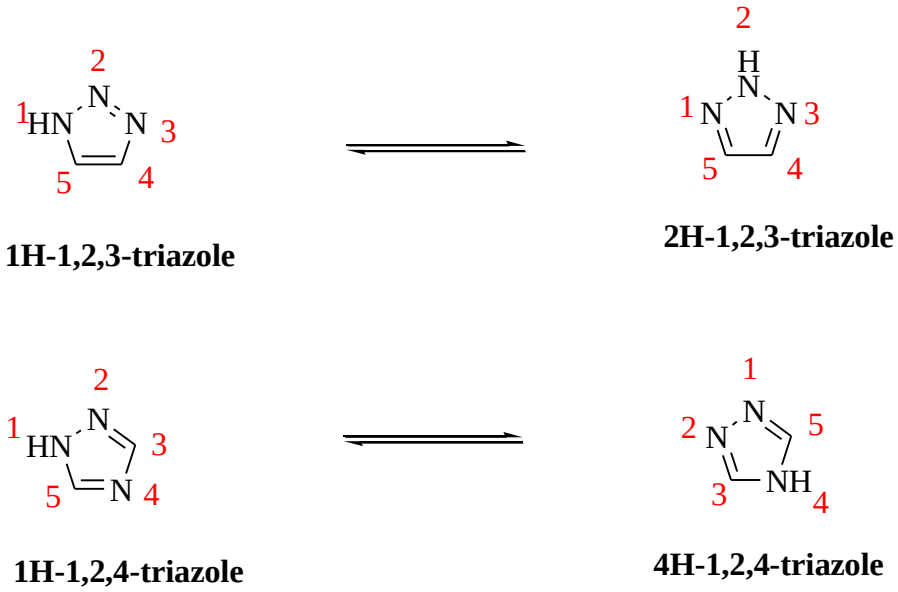

Figure 2.2: Tautomeric pairs of 1,2,3-triazole and 1,2,4-triazole molecules

The current research work involves the preparation of 1,2,3-triazole linked heterocyclic compounds through Cu(I) catalyzed cycloaddition reaction of terminal alkyne with organic azide. The triazole is a five membered heterocyclic compound with molecular formula $C_2H_3N_3$, containing three nitrogen and two carbon atoms in the ring. Based upon the position of nitrogen heteroatoms, triazoles are represented as 1,2,3-triazole and 1,2,4-triazole. In 1,2,3-triazole, all the three nitrogen atoms are adjacent to each other whereas in its isomer 1,2,4-triazole, one nitrogen atom is separated from other two by a carbon atom. These two isomeric molecules also exhibit tautomerism, a form of structural isomerism and conventionally classified into two pairs of tautomeric forms as shown in Figure 2.2. Two tautomers of each category differ by one hydrogen atom attached to nitrogen [4-6].

Triazole linked molecules are aromatic and thermally stable, so have multiple applications such as pharmacological significance, chemosensing, polymer chemistry and many more [7-11]. A wide array of medicinal drugs having triazole moiety as core component proves its biological as well as pharmacological significance such as antimalarial, antibacterial, anticancer, antitumor, antifungal etc. Another most encouraging field of application of triazole linked molecules is chemosensing. Presence of heteroatoms promotes their complexation with a range of metal ions that can further be sensed by various techniques based upon the nature of complete molecular assembly [12-17]. These distinctive attributes of the triazole ring have attracted the interest of budding researchers to generate novel triazole linkers. The objective of this research work was to synthesize and examine the chemosensing nature of novel 1,2,3-triazole linked molecules.

2.2 Preparation of 1,2,3-triazole linked molecules

The extensive literature survey hands us with various set of methodologies available for the generation of these five membered heterocyclic compounds, but in recent two decades, synthesis of 1,2,3-triazole linked molecules by Cu(I)-catalyzed 1,3-dipolar cycloaddition between terminal alkynes and organic azides have been in use due to mild reaction conditions and pure product formation. Based upon the nature of substituents on terminal alkynes and azides, a variety of these triazole

derivatives can be designed and synthesized in accordance with the field of application. The complete process involves following three steps:

- Synthesis of the terminal alkyne
- Synthesis of an organic azide
- Synthesis of 1,2,3-triazole linkers from cycloaddition of alkyne and azide

2.2.1 Synthesis of terminal alkynes

The extensive literature survey on the synthesis of terminal alkynes has reported various synthetic routes under different reaction conditions from various starting materials. In 1997, Bestmann and co-workers have reported a useful method of synthesis of terminal alkynes by reacting aldehydes with a phosphate derivative (Ohira-Bestmann reagent) in the presence of potassium carbonate and methanol as shown in Figure 2.3 [18].

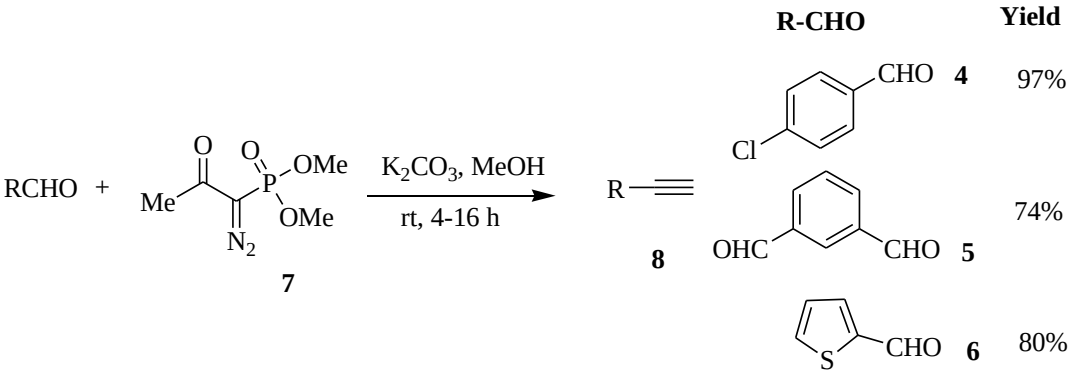

Figure 2.3: Conversion of aldehyde into terminal alkyne using Ohira-Bestmann Reagent

The synthesis of terminal alkynes from primary alcohols (benzylic, heterocyclic and propargylic alcohols) has also been reported in literature. It is a two-step process involving oxidation of alcohol into aldehyde using manganese dioxide as an oxidising agent followed by treatment with Ohira-Bestmann reagent [19].

C. Kuang *et al.* research group reported one pot microwave (200 W) assisted synthesis of alkynes **11, 12** using 2,3-dibromoalkanoic acids **10** in DMF and triethyl amine as shown in Figure 2.4 [20].

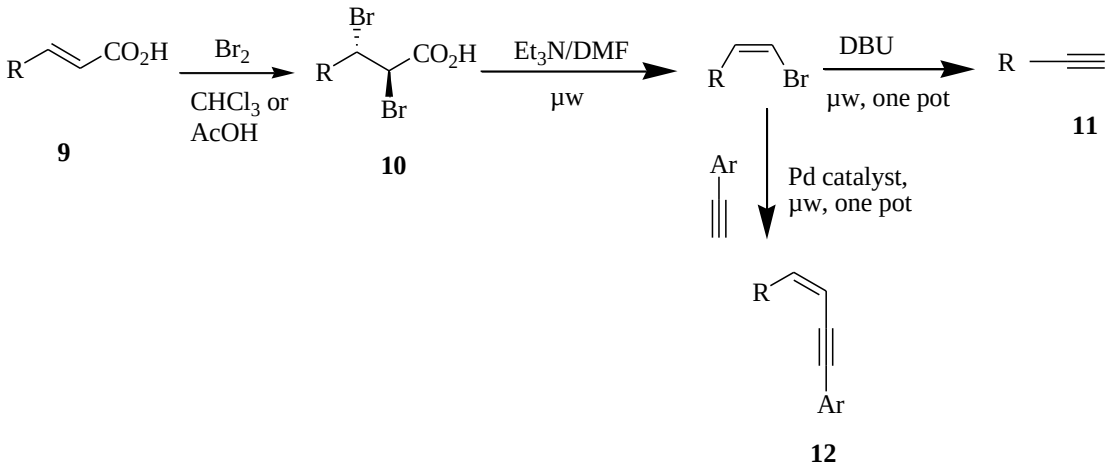

Figure 2.4: Microwave assisted synthesis of alkynes using 2,3-dibromoalkanoic acids

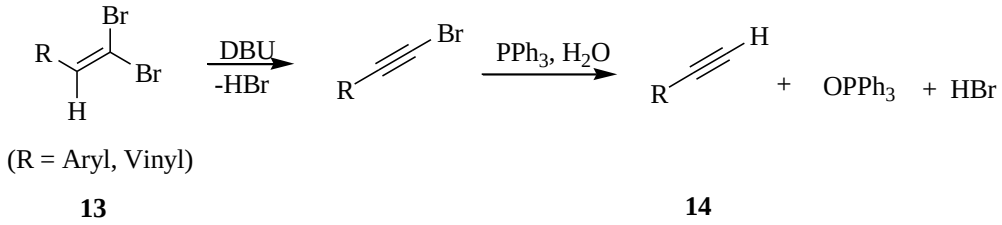

Figure 2.5: Synthesis of terminal alkyne from geminal-dibromoalkene

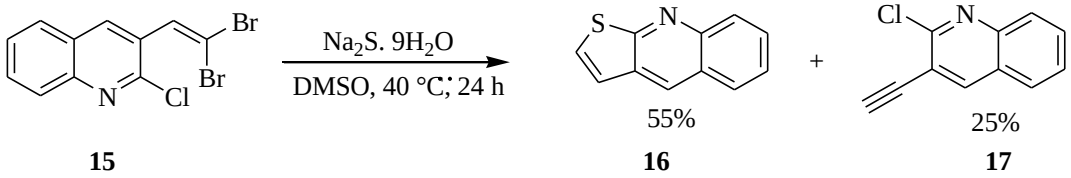

Figure 2.6: Na_2S mediated synthesis of alkyne from 2-chloro-3- (2,2-dibromoethenyl) quinoline

Doddi *et al.* described the synthesis of terminal alkynes **14** from geminal-dibromoalkenes **13** under ambient reaction conditions. The first step involves

dehydrohalogenation in the presence of DBU, followed by debromination on treatment with triphenylphosphine in aqueous medium as shown in Figure 2.5 and results into generation of terminal alkynes as 60-70% [21]. The work carried out by R.M. Singh and his research group describes Na_2S-mediated process involving alkyne **17** from germinal-dibromoalkene **15** at 30-40 °C in an open vessel, as shown in Figure 2.6 [22], whereas Yang *et al.* in 2011 used Cs_2CO_3 at 115 °C, Zhang (2015) conducted the same reaction in TBAF, TPP at 80 °C and Ramana *et al*. in 2015 in DBU at room temperature. Mild reaction conditions with inexpensive $Na_2S.\ 9H_2O$ under atmospheric air has significant advantages over other reaction conditions. The dehydration and dehydrogenation of alcohols using SO_2F_2 in the presence of K_2CO_3 in DMSO as solvent enabled a direct synthesis of alkynes under mild reaction conditions and the synthesized alkyne can be directly used in Cu(I)-catalyzed alkyne-azide cycloaddition [23].

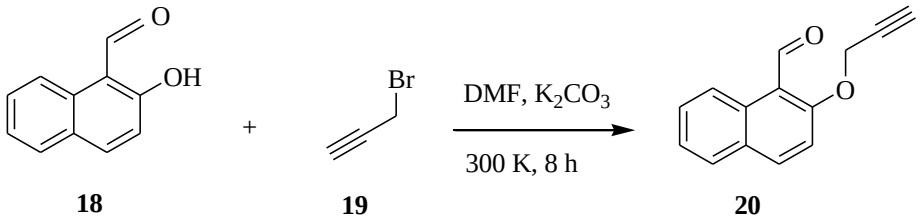

18 **19** **20**

Figure 2.7: Synthesis of alkyne by reacting 2-hydroxy-1-naphthaldehyde with propargyl bromide

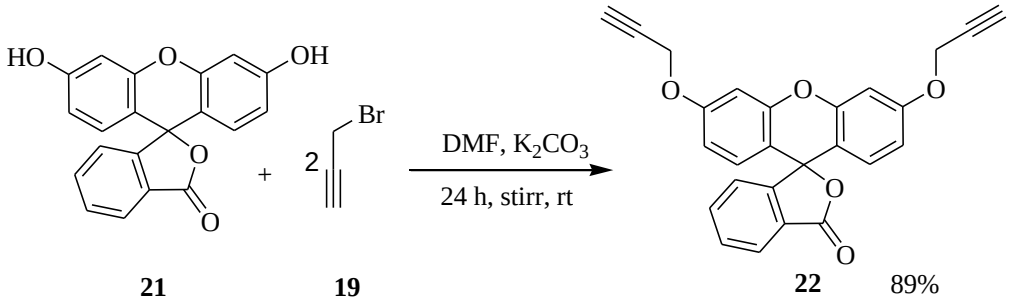

21 **19** **22** 89%

Figure 2.8: Terminal alkyne from Fluorescein dye using propargyl bromide with potassium carbonate

On the same note the reaction involving synthesis of terminal alkyne **20** by nucleophilic substitution on 2-hydroxy-1-naphthaldehyde **18** using propargyl bromide

19 under conditions, as shown in Figure 2.7, is also reported in literature [24]. In 2019, a research work has shown the synthesis of fluorescein based terminal alkyne **22** by stirring fluorescein dye **21** with propargyl bromide in DMF as solvent and potassium carbonate as base at room temperature with a good yield of 89% as shown in Figure 2.8 [25].

There are many publications involving synthesis of alkynes by nucleophilic substitution reaction on a large variety of compounds having functional groups –OH, $–NH_2$ etc. with propargyl bromide using solvents like N,N-dimethylformamide, acetonitrile and bases like potassium carbonate, sodium hydride etc. [26-31]. The reaction conditions vary with the type of solvent or base used, as the reaction with sodium hydride requires stirring under inert atmosphere at very low temperature, but with potassium carbonate, reaction can proceed at room temperature by stirring [32-38]. It means, this approach does not require strong reaction conditions and costly experimental setups, therefore, can be explored to synthesize novel terminal alkynes with excellent yield.

2.2.2 Preparation of organic azides

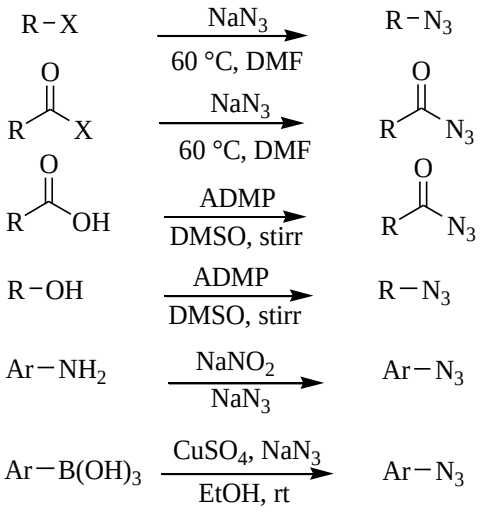

Figure 2.9: Some common methods of the synthesis of organic azides

Being highly reactive, the organic azides are in use since they were discovered more than 140 years ago. Earlier, these were synthesized using highly volatile, toxic

and explosive material like hydrogen azide, but these days different methods of azidation, (Figure 2.9) are being experienced that avoid use of such toxic materials [39]. Most of the methods involve nucleophilic substitution, S_N2-azidation of alkyl halides, acyl halides and aryl halides with sodium azide. To prepare azides from carboxylic acids, alcohols and amines, the diphenylphosphorylazide reagent is commonly used [40-41]. To replace hydroxyl group another more stable reagent 2-azido-1,3-dimethylimidazolinium hexafluorophosphate (ADMP) found to be a great reagent [42]. To synthesize aromatic azides, the process of diazotization of aromatic amines followed by nucleophilic substitution using sodium azide can be practiced.

2.2.3 Synthesis of 1,2,3-triazole from alkyne and azide (CuAAC)

The alkynes and azides, separately can give a variety of addition, cycloaddition and other types of reactions. Among the prominent reactions; electrophilic, nucleophilic and Diel's Alder type of cycloadditions are main categories of chemical processes shown by alkynes. Similarly, organic azides are too involved in various reactions. The structure of organic azide consists of three nitrogen atoms as shown in Figure 2.10, wherein the nitrogen at first position (N1) can work as a nucleophile (typical azidation Schmidt reaction) [43] and at third position (N3) shows reactivity as electrophile (electrophilic azidation straudinger reaction) [44].

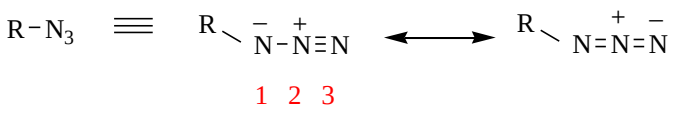

Figure 2.10: Structure and resonance forms of a typical organic azide.

The specific 1,3-dipolar character of organic azides takes part in [3+2] cycloaddition reaction with unsaturated compounds to produce triazoles and tetrazoles. From past few years, the cycloaddition reactions of different terminal alkynes with organic azides (Huisgen reaction shown in Figure 1.2) and the same in the presence of copper as catalyst (CuAAC mentioned in Figure 1.3) to form 1,2,3-triazoles have been a focus in various research areas. Copper as catalyst restricts the synthesis of only 1,4-disubstituted 1,2,3-triazoles instead of two isomers (1,4-adduct

and 1,5-adduct in Huisgen reaction) as shown in Figure 1.4(a) and 1.4(b). A library of alkyne-azide cycloaddition reactions using different catalytic systems as Cu(I) sources has been reported in literature.

2.2.3.1 CuAAC using Cu(II) salt along with reducing agent as catalytic system

Being more stable, Cu(II) salts are easily available and can be used as catalytic material in CuAAC reactions in the presence of suitable reducing agent. Most commonly used is $CuSO_4$. $5H_2O$, along with sodium ascorbate as reducing agent has been found in various research reports [45-49]. A reaction between substrates phenyl propargyl ether as terminal alkyne **23** and benzylazide **24** as shown in Figure 2.11, resulted into generation of very specific 1,4-disubstituted 1,2,3-triazole derivative **25** with a good yield of 91% using $CuSO_4.5H_2O$ and sodium ascorbate (1:5 mol%) as catalytic system upon stirring at room temperature in t-butanol:water (1:2) solvent mixture [50]. The generation and regiochemistry of the product of cycloaddition reaction was also supported by X-ray crystallographic data mentioned in the report.

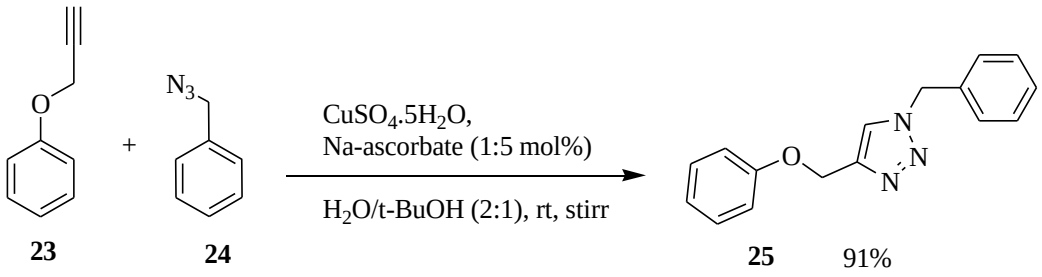

Figure 2.11: CuAAC reaction using Cu(II) salt along with reducing agent

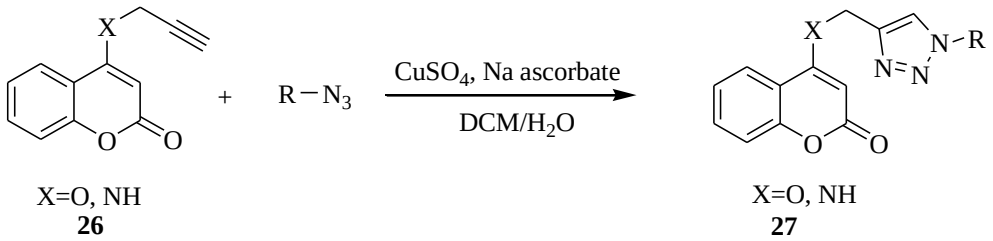

Figure 2.12: Formation of 1,2,3-triazole linked coumarin derivatives by CuAAC

In one of the research reports, the Cu(I)-catalyzed 1,3-dipolar cycloaddition reaction of O-propargylated and N-propargylated coumarins **26** with different organic azides to produce 1,4-disubstituted 1,2,3-triazole linked coumarin derivatives **27** has been presented, as shown in Figure 2.12. Cu(II) salt along with sodium ascorbate as reducing agent acts as Cu(I) source to catalyze the process. These two coumarin molecules were used to generate a group of triazole linked coumarins by varying substituents on the triazole moiety [51].

2.2.3.2 Photochemical reduction of Cu(II) and CuAAC

Besides the use of reducing agent in combination with Cu(II) to convert it into Cu(I), a different technique has been used for this reduction process is photo reduction, that involved conversion of Cu(II) to Cu(I) using UV-Visible radiations in the presence of a suitable photo-initiator in spite of reducing agent [52-55]. With this protocol, Yagci *et al.* group of researchers have made use of copper(II) chloride in combination with PMDETA ligand, which involved reduction of Cu(II) ions to Cu(I) through the electron transfer from π-system of the ligand by getting energy from ultraviolet light. Another way involved the use of molecules that are categorized as photo-initiators, that absorbs the UV light and produces high energy radicals that facilitates the reduction of Cu(II) to Cu(I), graphically shown in Figure 2.13 [56-57]. One of the typical reports on the light induced CuAAC involved use of Fullerene (C_{60}) attached with linear polystyrene as a photosensitizer and $CuSO_4.5H_2O$ as a source of copper. The alkyne-azide cycloaddition reaction got completed in 2 h in UV-Visible radiations and resulted into 96-97% of the product [58].

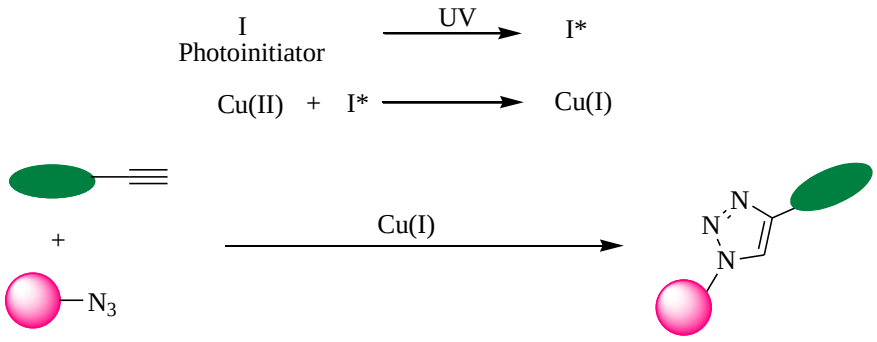

Figure 2.13: Graphical representation of light induced CuAAC

Another research group involved the use of [4-(2-hydroxyethoxy) phenyl-(2-hydroxy-2-propyl) ketone] **28** as a photo-initiator to generate radical intermediate to reduce Cu(II) to Cu(I) shown in Figure 2.14 and a triazole linked external ligand for photo click alkyne-azide cycloaddition process [59].

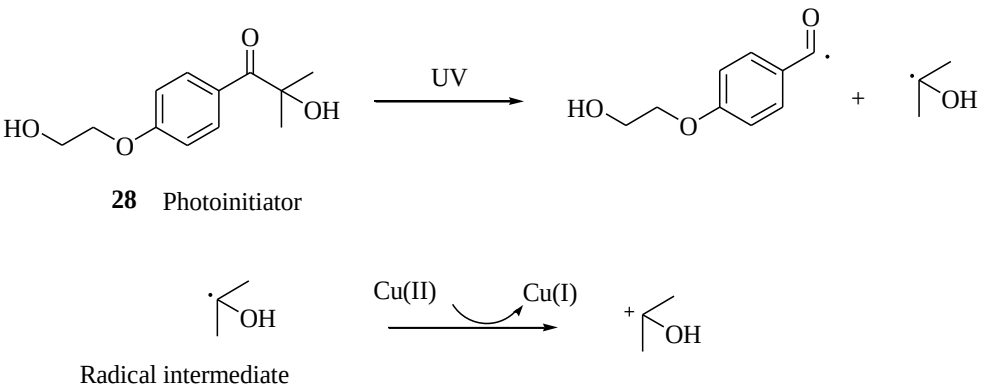

Figure 2.14: Conversion of Cu(II) to Cu(I) through electron transfer from radical intermediate

To enlarge the usefulness of photo-induced catalysis, B. Yin and co-workers, in 2019, performed a multicomponent one pot light induced CuAAC reaction followed by aza-michael addition using isopropylthioxanthone as photosensitizer and $CuCl_2$/Me_6TREN as catalyst. Very small amount of catalyst (1.7 mol%) generated 96% of product in just 20 min [60]. Moreover, the photoinduced CuAAC reactions are exceptionally controlled, where efficiency of reaction can be managed with the adjustment in intensity of light and exposure time [61]. Because of these characteristics, this plan of organic syntheses has amazing utility in material science and biochemistry involving the use of a variety of ligands along with photoinitiators [62-65].

2.2.3.3 One pot CuAAC using phase transfer catalyst along with Cu(I) source

The literature survey also claims multicomponent one pot synthesis of 1,2,3-triazole based molecules using terminal alkyne and alkyl halide or aryl halide in the presence of catalyst, $CuSO_4.5H_2O$ along with reducing agent (sodium ascorbate), KI and NaN_3 in aqueous medium at room temperature. The process did not involve

synthesis of organic azide separately but is carried out by the stirring of reaction mixture for about 1 h using phase transfer catalyst, followed by workup in cold water with good yield of isolated product. A study performed by Praveena *et al.* (2015) has reported reaction of 2-chloro-(3-chloromethyl) quinolone **29** with terminal alkyne **30** to yield a triazole derivative **31** used as cytotoxic agent under same reaction conditions along with tetrabutylammonium bromide salt as phase transfer catalyst as shown in Figure 2.15 [66].

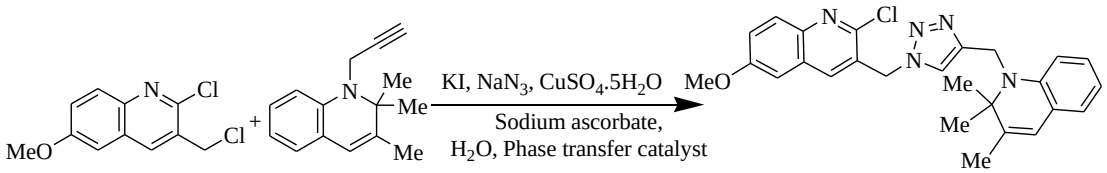

29 **30** **31**

Figure 2.15: Synthesis of 1,2,3-triazole derivative from quinoline derivatives using phase transfer catalyst

2.2.3.4 CuAAC using Cu(I) salts as catalyst

In addition to multicomponent catalytic systems, involving generation of Cu(I) from Cu(II) salts, the research contributions involving direct use of Cu(I) salts as catalyst have also been reported in literature. According to a research work by S. H. Kim and his coworkers in 2010, 1,8-dihydoxyanthraquinone based triazole derivative **34** with a yield of 35% was synthesized by cycloaddition reaction of 1,8-bis(prop-2-ynyloxy) anthraquinone **32** with 1,2-bis(2-azidoethoxy) ethane **33** catalyzed by CuI in DMF solvent as shown in Figure 2.16. The photophysical properties of probe **34** were investigated by UV-Visible as well as Fluorescence spectroscopy and results obtained showed sensitivity of synthesized molecule towards selective detection of Al(III) ions [67].

On the same note, Quinoline-functionalized homooxacalix [3] arene, a turn-On fluorescent chemosensor was synthesized by click reaction between alkyne of homooxacalix [3] arene and 8-azidomethyl quinoline using CuI as catalyst in THF/H_2O (v/v, 5:1). The reaction content was heated at 70 °C for 24 h to generate

fluorescent chemosensor with 65% yield. The probe exhibited a high deal of sensitivity and selectivity for Fe(III) ion [68].

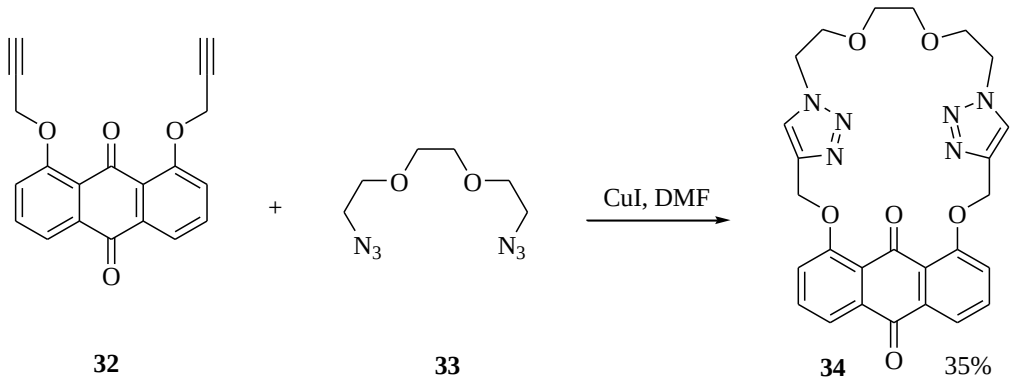

32 **33** **34**

Figure 2.16: CuAAC reaction of 1,8-bis(prop-2-ynyloxy) anthraquinone with 1,2-bis(2-azidoethoxy) ethane

2.2.3.5 CuAAC accelerated by external ligands

In order to decrease the usage of reducing agents, the direct utilization of Cu(I) salts have been preferred, but the stability/existence of Cu(I) in a particular solvent system is normally controversial [69]. It usually gets oxidized into Cu(II) form, a stable oxidation state of copper and as a result, low yield of product has been recorded as presented in section 2.2.3.4. In order to resolve this issue of conversion of oxidation state, the use of external ligand along with Cu(I) salt is found in various research contributions. Ligands with donor atoms such as N, O, S or P are most common that complexes with Cu(I) ion and inhibit its oxidation to Cu(II). In aqueous medium, these ligands also act as base that accelerates the formation of Cu-acetylide ion through the fast abstraction of terminal proton of alkyne substrate.

For CuAAC reactions, the external ligands having nitrogen atom as donor site has represented a major category and includes various molecules from monodentate to polydentate type as shown in Figure 2.17. Ligands having sp^3-hybridized nitrogen e.g., aliphatic amines are strongly basic and accelerates the mechanistic action of Cu(I) to large extent as compared to ligands having sp^2-hybridized nitrogen e.g., aromatic amines or pyridine-based ligands, whereas the protection from oxidation of

Cu(I) to Cu(II) is more with pyridine based polydentate ligands due to their strong chelation [70-73].

Aliphatic amines e.g., ethylenediamine, betaine, triethylamine (TEA), diisopropylethylamine (DIPEA) etc. that are basic in nature and found to increase the stability of Cu(I) by complexing with this ion, but at the same time promotes other side chain reactions such as homocoupling of triazole as well as alkyne and decreases the output of CuAAC [74-75]. TBTA, a ligand with tris (triazolylmethyl) amine backbone is a powerful stabilizer of Cu(I) in t-butanol:water (2:1) solvent system, however, it is partially soluble in water, whereas the ligands having hydrophilic substituents on tris(triazolylmethyl)amine skeleton such as THPTA and BTTAA have better stabilization of Cu(I) in aqueous medium due to their enhanced solubility in water [76-77].

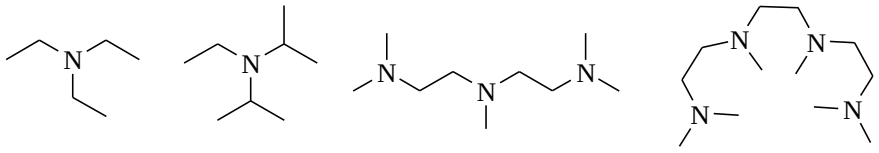

TEA DIPEA PMDETA HMTETA

A. Aliphatic amines as external ligands

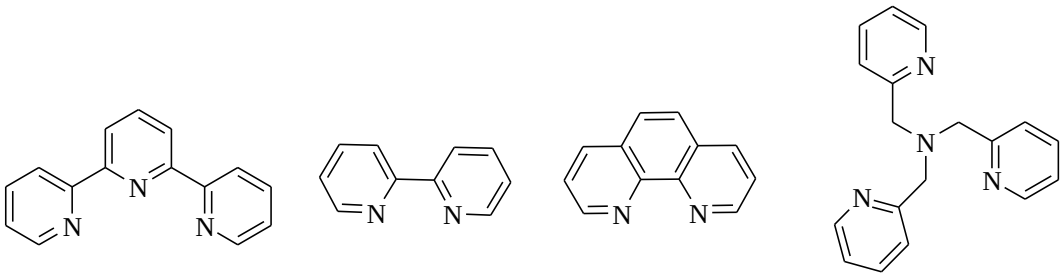

tpy bpy Phenanthroline TPMA

B. Pyridine based chelating ligands

Contd…

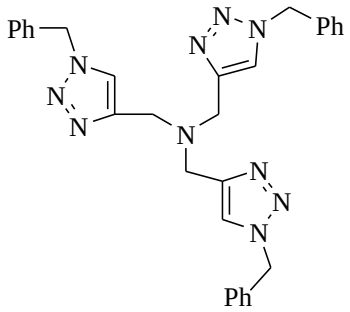

TBTA

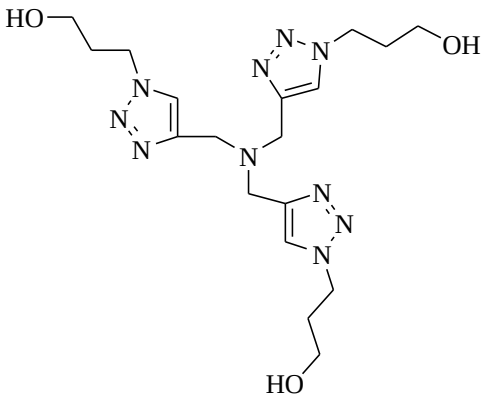

THPTA

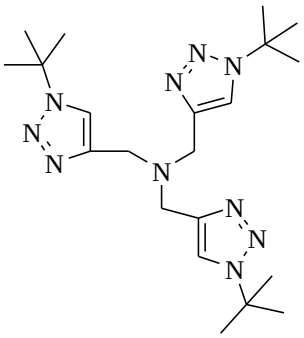

TTTA

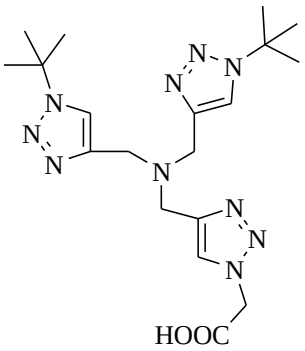

BTTAA

C. Tris(triazolylmethyl)amine based external ligands

Figure 2.17: Ligands with nitrogen atom as donor site used in CuAAC, **(A)** TEA; Triethylamine, DIPEA; Diisopropylethylamine, PMDETA; Pentamethyldiethyltriamine, HMTETA; Hexamethyltriethyltetraamine, **(B)** tpy; tripyridyl, dpy; dipyridyl, TPMA; Tris(pyridylmethyl)amine, **(C)** TBTA; Tris(benzyltriazolylmethyl)amine,THPTA; Tris(hydroxypropyltriazolylmethyl)amine, TTTA; Tris(t-butyltriazolylmethyl) amine, BTTAA; Bis(t-butyltriazolylmethyl) amino-methyltriazolylacetic acid.

2.2.3.6 CuAAC using Cu(I) coordination complexes as catalyst

The more advanced catalytic materials are the coordination complexes of Cu(I) having bulky organic species as ligands with enhanced stability of Cu(I). The coordination complexes, like $[CuI(P(OEt)_3)]$, $[CuBr(PPh_3)_3]$, $[Cu(MeCN)_4]PF_6$,

[$CuF(PPh_3)_3$], etc. are the most frequently employed Cu(I) sources with a great deal to act as catalysts for alkyne-azide cycloaddition reaction with minimum risk of oxidation of Cu(I) to Cu(II). Grooming research on CuAAC during the past few years, has witnessed the use of a variety of Cu(I) coordination complexes.

According to a research report, an ON-OFF and highly selective chemosensor **37** was prepared through CuAAC reaction between tripropargylamine **35** and pyrene based azide **36** as shown in Figure 2.18 in 82% yield. Fluorescence studies proved it as highly selective for Zn(II) ions among a set of different metal ions. The three triazole moieties have adopted a suitable geometry to bind with Zn(II) and modulate the fluorescence signal [78]

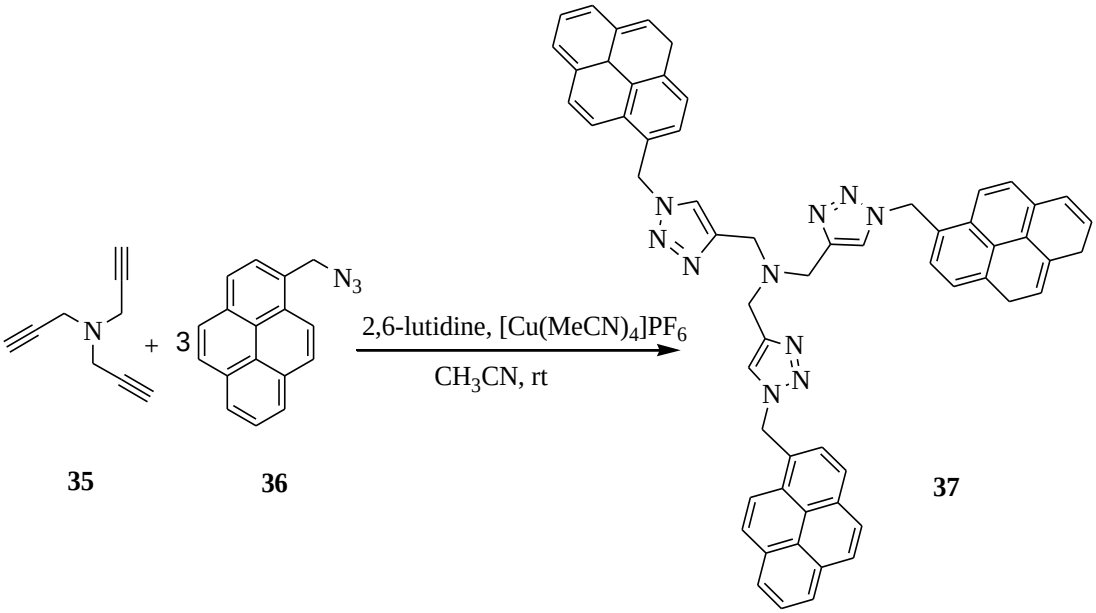

Figure 2.18: Synthesis of pyrene-based tris-triazole amine, a fluorescence ON-OFF sensor

A report by P. Kaur *et al.* presented an ON-OFF fluorescent system that has an excellent turn-on response with Co(II) and turn-OFF with Cd(II) metal ions. This 1,2,3-triazole linked fluorescent chemosensor **38** was synthesized from fluorescein **21** as starting material. In first step, fluorescein undergoes nucleophilic substitution with propargyl bromide **19** to get an alkyne **22**. Thereafter, this bimolecular alkyne was converted into 1,2,3-triazole linked fluorescein sensor **38** by 1,3-dipolar cycloaddition

reaction with benzyl azide **24** using catalytic amount of $[Cu(PPh_3)_3Br]$ in a good yield of 81%, as shown in Figure 2.19 [25].

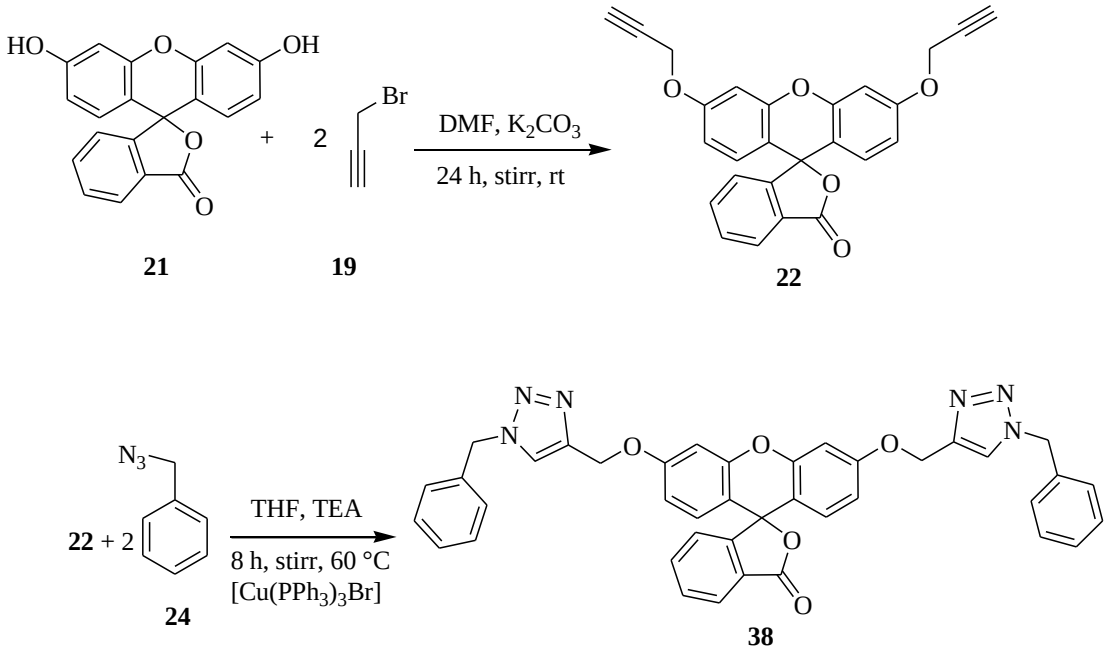

Figure 2.19: Synthesis of fluorescein based 1,2,3-triazole linked turn ON-OFF fluorescent chemosensor

2.3 Characterization techniques

The generation of any novel molecule requires its proper characterization for the authenticity of structure of designed molecule. The spectroscopic techniques like IR, NMR (^1H, ^{13}C), along with the mass spectroscopic analysis have been reported in literature that are generally used for the complete characterization of the molecules [79-80]. The synthesized molecules can also be analyzed for their UV-Visible active nature using UV-Visible and/or Fluorescence spectroscopic techniques.

For IR spectrum, molecules are irradiated with infra-red radiations within the frequency range 4000 to 500 cm^{-1}. The main contribution of this spectroscopy to structure elucidation is to find out the type of functional groups. IR waves cause vibrations of different bonds by absorbing radiations of different frequencies depending upon their bond strengths. For example, if IR spectrum indicates –**OH**

functional group, it should have broad band in IR range 3500-3350 cm^{-1} positively. Similarly, **C≡C** stretching in alkynes appear at frequency of vibration approximately equal to 2150 cm^{-1}, ≡**C–H** in the region of 3300 cm^{-1}, **C=O** stretch in range 1850-1680 cm^{-1} etc. 1,4-disubstituted 1,2,3- triazole derivatives, the ultimate products of the synthesis part of this research work can be confirmed by IR peak near 3100-3000 cm^{-1}, which corresponds to –C=**C-H** present in the aromatic triazole ring, at 1550-1200 cm^{-1} due to various modes of vibrations of –**C=C-** and **–N=N-** moieties in the heterocyclic triazole ring [81-83].

The NMR spectroscopy involves the use of radio waves of a particular frequency along with change in magnetic field. In ^{1}H NMR, magnetically non-equivalent protons show signal at different magnetic field values represented by chemical shifts (δ) that helps in identification of molecular structure, e.g., a singlet at δ = 8.4 ppm of proton at C_5 confirms the synthesis of 1,4-disubstituted 1,2,3-triazole ring [84]. Splitting of a particular signal indicates number of neighboring protons. The magnetic field of observed proton couples with field of neighboring protons to cause splitting of signal and extent of coupling expressed by coupling constant. Similarly, ^{13}C NMR spectrum shows signals corresponding to different types of carbons in a molecule e.g., according to one dimensional proton decoupled ^{13}C NMR spectra in $CDCl_3$, C_5 signal of 1,4-disustituted 1,2,3-triazole appears at approximately δ = 120 ppm, while in 1,5-disubstituted 1,2,3-triazole, the C_4 signal appears at δ = 133 ppm. It helps in distinguishing two isomeric triazoles. Research work shown in this thesis involved Cu(I)-catalyzed cycloaddition reaction of terminal alkyne with organic azide to produce 1,4-disustituted 1,2,3-triazole as the only product i.e., the reaction is highly stereospecific, so called as click reaction. Therefore, the ^{13}C NMR spectroscopy is very useful technique to prove the stereospecificity of this click alkyne-azide cycloaddition reaction. Thus, NMR proves to be a great technique in structure elucidation and estimation of purity of compound [85].

In addition to above, the mass spectroscopy is also used to determine the structure, chemical composition and more importantly, molecular mass of unknown molecules. In this technique, the molecules are firstly vaporized and converted into charged particles by electron ionization with further fragmentation or non-

fragmentation of molecular ions. The mass spectrometer measures the mass to charge ratio of ions and peaks appeared in mass spectrum against various mass to charge values vs. relative abundance of ions that helps in the characterization of molecules. Peak against highest mass to charge ratio corresponds to molecular mass. In this way, this technique is very useful in scientific research over the traditional methods of calculation of molecular masses and structure elucidation [86-87].

UV-Visible spectrum can be obtained by irradiating the molecules by radiations of wavelength range 200-800 nm. Irradiation by this wavelength range causes electronic transitions in the molecules from ground state to excited state and band appears in the spectrum corresponding to absorbed wavelength, from that the information can be drawn regarding functional groups. Generally conjugated molecules, aromatic molecules or molecules having non-bonded electrons on O, N or S atoms attached with double or triple bonds can be characterized by UV-Visible spectroscopy [88]. It becomes more meaningful in terms of structure elucidation when UV-Visible data is combined with IR and NMR results. In the absence of IR and NMR, information can be drawn as follows:

- A band in the wavelength range 250 to 360 nm with low intensity, indicates n→л* transition in N=N, C=O, –COOR, $–NO_2$, –COOH etc.
- Aromatic systems show two bands with medium intensity above 200 nm.
- Molecules (aldehydes, ketones, amides, esters etc.) having л-electrons with lone pair of electrons show two bands: one of high intensity at wavelength near 250 nm due to л→л* transition and other of low intensity at wavelength greater than 300 nm due to n→л* transition. Wavelength as well as intensity of absorption increases with conjugation.
- Bands of very high intensity above 210 nm indicate α, β-unsaturated aldehyde, ketone or a conjugated diene.
- Highly colored compounds show absorption in visible region.

Different molecules have different spectral data that helps in explaining their structural features. In this way, these spectral techniques proved very helpful and time saving for the characterization of newly synthesized molecules over the traditional

qualitative analysis of functional groups. Moreover, these techniques are great tools in the hands of researchers [89-90].

2.4 Applications of 1,2,3-triazole linkers in chemosensing

The sensing systems are in demand in many disciplines, including environmental sciences, chemistry, biology, etc. and depending upon the nature of analyte to be recognized, the designing and development of sensors are being practiced [91-98]. For the designing of fluorescent sensors, the material science, molecular recognition and device implementation are the main aspects that play vital role. An effective fluorescent chemosensor must convert the act of identification of target metal ion into highly sensitive and easily detectable fluorescent signal, as shown in Figure 1.6. Now a days, the designing and synthesis of chemosensors for the effective recognition of metal ions is an important task for clinical, biological and environmental applications [99-103]. Several examples and chemical methods of their synthesis are available in literature; few of them are as follows:

An ionophore (Z)-2-[(1H-1,2,4-triazole-3-ylimino) methyl] phenol **39**, as shown in Figure 2.20, that selectively detects Ce(III) ions, has been synthesized by reacting 3-amino-1H-1,2,4-triazole with salicylaldehyde in ethanol and modified into potentiometric electrode by mixing with graphite powder, silica nanoparticles and an ionic liquid to increase its stability in water. The synthesized Ce(III) selective carbon-based electrode and its junction with saturated calomel electrode were used for potentiometric measurements. The inductively coupled plasma-atomic emission spectrometer was used for the determination of Ce(III) [104].

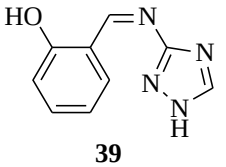

39

Figure 2.20: Phenol based ionophore for the detection of Ce(III) ions

An optical chemosensor named 2,6-bis (4-dimethylaminophenyl)-4-(dicyanomethylene)-cyclohexane-1,1-dicarbonitrile (BDC) **40** as shown in Figure

2.21 displayed high sensitivity and selectivity for Cu(II) ion in physiological pH range (pH=7.3) without the interference of other ions. Mechanism of chemosensing is attributed to the chelation of probe with metal ion that showed optical changes confirmed by UV-Visible and Fluorescence studies [105].

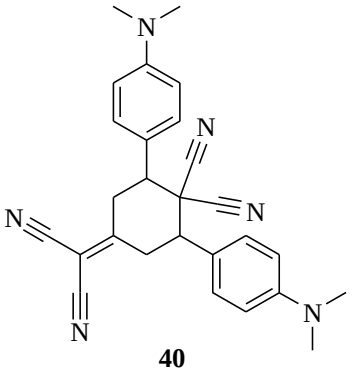

40

Figure 2.21: Optical chemosensor for sensing Cu(II) ion

The fluorescent sensor di-naphthoylatedoxacalix [4] arene **41** shown in Figure 2.22 was prepared by using naphthoyl chloride and tetranitrocalix [4] arene in acetone by stirring at room temperature for 24 h to detect Ce(III) ion, a rare earth metal. The naphthoyl moiety is observed as good fluorophore as it has absorption and emission in UV-Visible region. The decrease in emission intensity of sensor **41** was recorded with subsequent addition of Ce(III) ions without any interference of other metal ions.

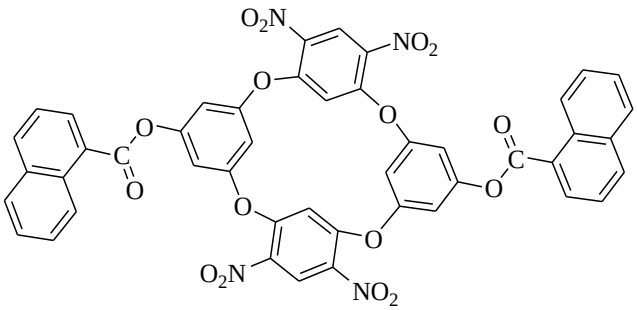

41

Figure 2.22: Di-naphthoylated oxacalix [4] arene fluorescent sensor for Ce(III) ion detection

The detection was obtained over a range of concentration between 18-20 µM. According to molecular geometry and based upon other studies, the nitro groups, bridged oxygens and naphthyl groups bent to bind with metal ion and a complex formation stabilizes the Ce(III) [106].

In a research paper, a series of macrocyclic ligands **42, 43** with ligating sites oxygen and nitrogen atoms having 8-hydroxyquinoline as fluorophoric unit were described as shown in Figure 2.23. The results indicated that the substitution of chloro group by nitro group on 8-hydroxyquinoline moiety increases the efficiency of probe towards the selective detection of mercury ions without interference of other metal ions. It may be due to participation of nitro group in complexation with metal ion that provided noticeable changes in fluorescence and absorption behavior of sensor [107].

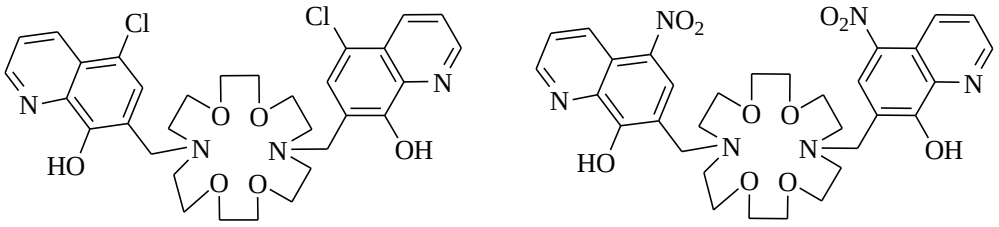

42 **43**

Figure 2.23: Macrocyclic ligands as fluorescent chemosensors for mercury ions

Y.B. Ruan *et al*. group has synthesized highly sensitive fluorescence turn-on sensor using Fenton reaction assisted amplification for the detection of Cu(II) ions. They have synthesized triazole linked fluorescein derivative and studied its sensing behaviour under different pH ranges [108]. A research work published by Jiang *et al*. has reported gold nanoparticles in conjugation with triazoles for the detection of Cu(II) ion [109]. M. Adlim *et al.* has published a review including sensors for the detection of mercury ions obtained by doing modifications in chitosan polymer, as chitosan has hydroxyl and amino groups that are good ligating sites for metal ions [110]. In another report, chitosan grafted with rhodamine derivative proved to have very high affinity for Hg (II) ions. The molecule proved to be good as colorimetric and fluorescent turn-ON senor for naked eye [111]. Another colorimetric sensor for

the detection of mercury ion is a composite of chitosan and silver nanoparticles with detection limit of 7.2 x 10^{-8} M [112].

The strategy of developing 1,2,3-triazole linked molecules as fluorescent chemosensors for selective detection of ions has emerged out as a promising approach in recent years. A study described the preparation of 1,2,3-triazole linked naphthyl fluorescent sensor **47** using materials and experimental steps shown in Figure 2.24. The terminal alkyne **20** prepared by nucleophilic substitution reaction between 2-hydroxy-1-naphthaldehyde **18** and propargyl bromide **19** reacted with 4-chloroaniline to get modified alkyne **44,** that was further treated with 3-azidopropyltriethoxysilane **45** through CuAAC reaction to get 1,4-disubstituted 1,2,3-triazole linked molecule **46**. To enhance the stability and applications of molecule **46** in aqueous medium, it was further treated with triethanolamine to get desired product **47**.

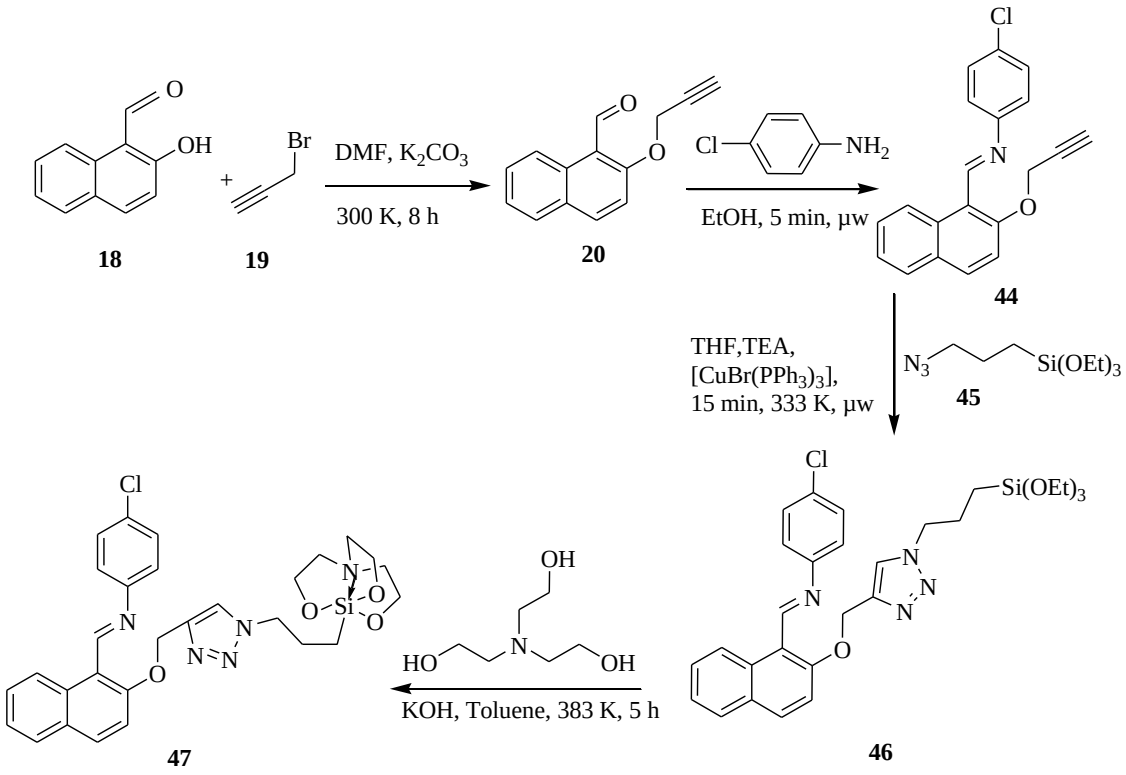

Figure 2.24: Synthesis of 1,2,3-triazole linked naphthyl fluorescent sensor **47** through CuAAC

Spectral behavior of fluorescent molecule **47** was analyzed for various metal ions using different solvent combinations through fluorescence spectroscopy and it was found best for sensing Ce(III), then **47**-Ce(III) conjugate was examined for various anions: NO_3^-, oxalate ion, CH_3COO^-, Cl^-, Br^-, I^- in DMSO:H_2O (v/v, 4:1) and was found sensitive for NO_3^- ion [24].

A research publication has reported the synthesis of ortho, meta and para isomers of chalcone linked 1,2,3-triazole silatranes and examined for their chemosensing behavior towards various metal ions. UV-visible spectral studies displayed more efficient sensing with ortho isomer **48** for the detection of two ions Cu(II) and Ni(II). Expected binding modes between sensor **48** and metal ions are shown in Figure 2.25 [113].

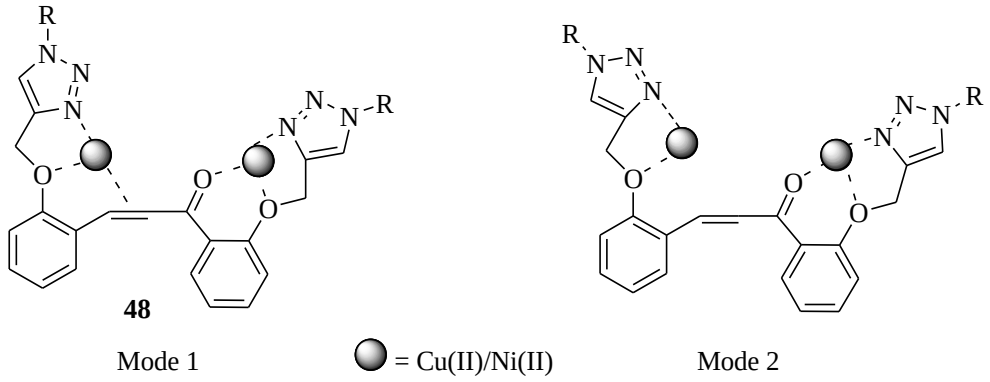

Figure 2.25: Expected binding modes between o-isomer **48** and metal ions

Sushil K. Dwivedi *et al.* research group has synthesized anthracene based triazole, a dual fluorophore. The complete process involved many steps including synthesis of anthracene-based azide **49** and terminal alkyne **50**. Thereafter, the azide **49** and alkyne **50** were reacted through CuAAC at 80 °C for 8 h in a round bottom flask containing DMSO-H_2O (v/v, 4:1) to get triazole based fluorescent sensor **51** as shown in Figure 2.26 with 62% yield. The probe was tested for chemosensing of various metal ions, anions and was found best for the detection of Cr(III) and PO_4^{3-} with the UV-Visible absorption and fluorescence studies. The probe is also used for fluorescent biological imaging of living cells [114].

8-Methylquinoline linked triazole **52**, a fluorescent chemosensor, was synthesized effectively by click reaction. Firstly, 2-Methyl-8-hydroxyquinoline undergoes nucleophilic substitution reaction with propargyl bromide to generate terminal alkyne that was further subjected to copper catalyzed alkyne-azide cycloaddition reaction with γ-azidopropyl-triethoxysilane at 55 °C for 20 h to generate 8-methyl-quinolinyl-1,2,3-triazolyl linked triethoxysilane **52**. This probe developed by click reaction was found effective for the sensing of Fe(II) and Fe(III) ions even in the presence of other ions in competition that was supported by UV-Visible and Fluorescence spectral studies. The expected binding for the developed probe and metal ion is shown in Figure 2.27 [115].

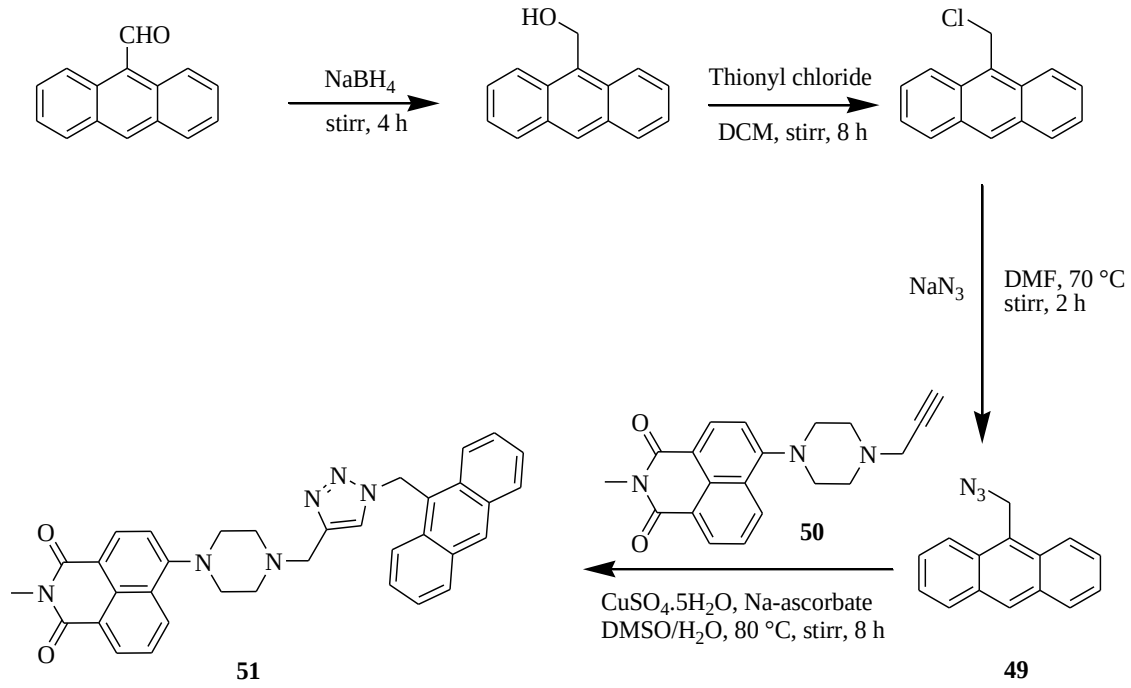

Figure 2.26: Synthetic route of anthracene based triazole, a dual fluorophore

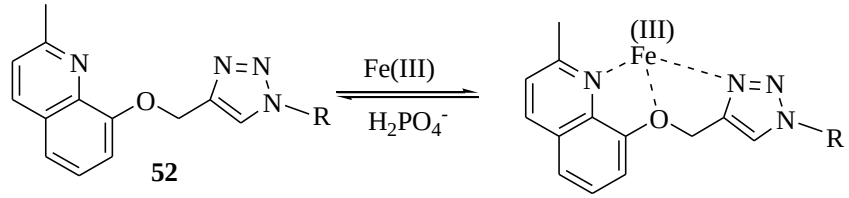

Figure 2.27: Expected binding mode for developed probe **52** and metal ion

In another report, the presented 1,2,3-triazole linked C-glycosyl pyrene based fluorescent chemosensors **53, 54** can selectively detect Au(III) in aqueous medium. 1,4-disubstituted triazole moiety not only act as linker between carbohydrate and pyrene (fluorophor), but acts as coordinating ligand to gold ion also that is proved with the results obtained from UV-Visible and Fluorescence measurements. 1,2,3-triazole linked C-glycosyl pyrene was prepared by Cu(I)-catalyzed cycloaddition reaction of azide of acetylated carbohydrate with terminal alkyne having pyrene group. With the deprotection of all acetate groups on the carbohydrate moiety under two different conditions, two different sensors were synthesized and are presented in Figure 2.28 were produced. The limit of detection of chemosensor with alcoholic group **54** (0.14 µM) for Au(III) was found to be more as compared to chemosensor with acyl group **53** (0.08 µM). Based upon the biological imaging studies, it was found that sensor **50** is permeable to cell membrane and is competent to detect gold ion in living cells [116].

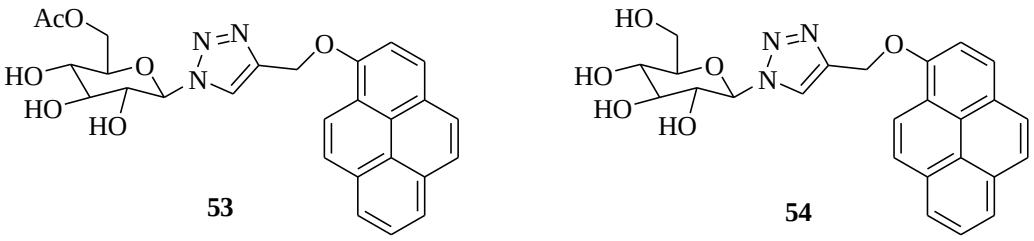

Figure 2.28: 1,2,3-triazole linked C-glycosyl pyrene based fluorescent chemosensors

Duxia Cao *et al*. group of researchers reported a number of coumarin based 1,2,3-triazole derivatives in a review article. Because of their biocompatibility and strong fluorescence emission, these molecules are found to have chemosensing applications and are used in various disciplines [117]. The study by A. J. Christensen and J. T. Fletcher has described the detection of Ni(II) ion by chemosensors having 2-(1,2,3-triazol-4-yl) pyridine as chelating moiety. The chemosensors containing two such chelating units displayed great changes in fluorescent signal when treated with different concentrations of Ni(II) ion without interference of other ions [118].

1,2,3-triazole-modified calix[4]crown **55** as a fluorescent ON-OFF chemosensor was prepared from bis-(O-propargyl)calix[4]arene that was treated with

tetraethyleneglycol-ditosylate in methyl cyanide using cesium carbonate and converted into bis-(O-propargyl)calix[4]crown which was further pass through click reaction with 9-(azidomethyl)anthracene and resulted into 1,2,3-triazole with 82% yield. The fluorescence of sensor **55** was strongly quenched by the addition of Pb(II) ions that was found to bind with two triazoles and enhanced with the addition of K(I) that fit into crown cavity, as shown in Figure 2.29 [119].

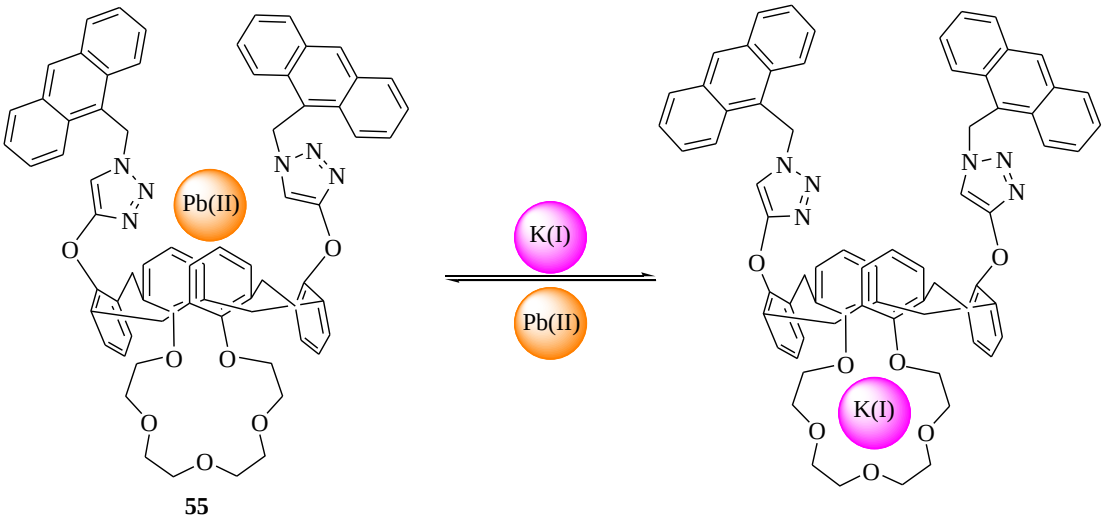

55

Figure 2.29: ON-OFF fluorescence behavior of 1,2,3-triazole-modified calix [4] crown sensor with the exchange of metal ion

A fluorescent chemosensor, with two anthracenetriazolymethyl groups linked to sugar-aza-crown ether exhibited high sensitivity and selectivity for Cu(II) and Hg(II) ions. The first step in the synthesis involved 'click' reaction of propargyl alcohol with 9-(azidomethyl) anthracene to yield triazole linked alcohol with 87% yield. After that, chloromethyl-1,2,3-triazole reacted with sugar aza crown ether using K_2CO_3, KI and n-Bu_4NI on refluxing in acetonitrile with 73% yield. Its fluoro-ionophoric properties were studied for various transition metal ions and found to have high selectivity and sensitivity for Cu(II) and Hg(II) ions [120].

Similarly, the triazole linked pyrano [2,3-c] pyrazolone, a colorimetric chemosensor, highly selective for Fe(III) and $H_2PO_4^-$ ions was synthesized by Cu(I)-catalyzed alkyne-azide cycloaddition [121]. The bis-glycoconjugated triazole, a

fluorescent chemosensor has been developed from D-glucose as starting material. Reaction mechanism involved series of steps and in final step, CuAAC reaction with 3-azidocoumarin in dichloromethane took place to generate bis-glycoconjugated triazole, found to be highly selective for detection of Cu(II) ions by means of fluorescence quenching [122]. The Table 2.1 summarizes the reaction conditions for the synthesis, yield and chemosensing behavior of few 1,2,3-triazole linked molecules.

Table 2.1: Summary of few 1,2,3-triazole linked chemosensors synthesized through CuAAC reaction

1,2,3-triazole linked molecules as chemosensors	**Reaction Conditions for synthesis**	**%Yield**	**Ions recognized**	**References**
2-hydroxy-1-naphthaldehyde based 1,2,3- triazole derivative	THF:TEA (v/v, 1:1), 15 min, 60 °C, µw, $[Cu(PPh_3)_3Br]$	87	Ce^{3+}, NO_3^-	[24]
Fluorescein based 1,2,3-triazole, an ON-OFF fluorescent sensor	THF:TEA (v/v, 1:1), 60 °C, 8 h, stirr, $[Cu(PPh_3)_3Br]$	81	Co^{2+}, Cd^{2+}	[25]
Quinoline-functionalized homooxacalix [3] arene	THF:H_2O (v/v, 4:1), 24 h, stirr, 70 °C, CuI	65	Fe^{3+}	[68]
Pyrene-linked tris-triazole amine fluorescent ON-OFF chemosensor	2,6-lutidine, $[Cu(MeCN)_4]PF_6$, CH_3CN, rt	82	Zn^{2+}	[78]
Anthracene based 1,2,3-triazole, a dual fluorophore	$CuSO_4.5H_2O$, Na-ascorbate, 80 °C, DMSO:H_2O (v/v, 4:1), 8 h, stirr	62	Cr^{3+}, PO_4^{3-}	[114]
8-methylquinoline based 1,2,3-triazole derivative	THF:TEA (v/v, 1:1), 55 °C, 20 h, stirr, $[Cu(PPh_3)_3Br]$	78	Fe^{2+}, Fe^{3+}	[115]

C-glycosyl pyrene based 1,2,3-triazole-I	$CuSO_4.5H_2O$, Na-ascorbate, 6 h, stirr, rt	53	Au^{3+}	[116]
C-glycosyl pyrene based 1,2,3-triazole-II	$CuSO_4.5H_2O$, Na-ascorbate, 8 h, stirr, rt	76	Au^{3+}	[116]
Pyridine based 1,2,3-triazole linked sensors I and II	$CuSO_4.5H_2O$, Na-ascorbate, 24 h, rt, t-BuOH:H_2O (v/v, 4:1)	93, 50	Ni^{2+}	[118]
1,2,3-triazole-modified calix [4] crown	24 h, stirr, 50 °C, CuI, THF:H_2O (v/v, 2:1)	82	Pb^{2+}, K^{+}	[119]
Sugar-aza-crown ether based 1,2,3-triazole linked fluorescent chemosensor	(i) $CuSO_4.5H_2O$, Cu, EtOH (ii) K_2CO_3, KI, n-Bu_4NI, CH_3CN	87 73	Cu^{2+}, Hg^{2+}	[120]
1,2,3-triazole-appended pyrano[2,3-c] pyrazolone	$CuSO_4.5H_2O$, Na-ascorbate, THF:H_2O (v/v, 2:1), overnight refluxing	82	Fe^{3+}, $H_2PO_4^-$	[121]
Coumarin based Bis-glycoconjugated 1,2,3-triazole derivative	CuI, DIPEA, DCM, 12 h, rt, stir	76	Cu^{2+}	[122]

From above data, it can be concluded that the synthesis by click reaction is high yielding, requires mild reaction conditions, wide in scope and results into formation of almost pure product or inoffensive by-products that can be removed by simple procedure under normal and environmentally amiable conditions. Synthesized molecules can be characterized easily by IR, NMR (^1H, ^{13}C) and mass spectroscopy. UV-Visible and Fluorescence studies help in explaining the chemosensing behavior of molecules.

2.5 Objectives and scope of thesis

A perusal of the literature survey shows a lot of scope for the synthesis of new molecules (terminal alkynes and organic azides) resulting into novel 1,2,3-triazole linkers. There is a lot of potential to explore the organic molecules with good chromo or fluorophoric units, whose functional groups can be modified to generate new terminal alkynes and organic azides that can further be subjected to CuAAC reaction to synthesize novel 1,2,3-triazole linked molecules. After characterization, the synthesized molecules can further be subjected to ion sensing. Based upon this observation, the objectives of this research work were coined as follows:

- To synthesize novel 1,2,3-triazole linked molecules using Cu(I)-catalyzed alkyne-azide cycloaddition (CuAAC) reaction.
- Characterization of newly synthesized compounds by spectroscopic tools like IR, NMR (^{1}H, ^{13}C), along with mass spectrometric studies.
- To study the chemosensing behavior of synthesized 1,2,3-triazole linkers for various ions using UV-Visible spectroscopy.

The goal of this thesis titled "**Synthesis and Characterization of 1,2,3-triazole linked chemo sensors using Cu(I) catalyzed alkyne-azide cycloaddition reaction"** was the development of new 1,2,3-triazole linked molecules and to explore their utility as optical sensors for the determination of various metal ions.

The transition or other metal ions can be toxic to humans or other living organisms when present in excess and their determination is therefore of tremendous interest. For example, as cobalt is a trace element, a key component of most common vitamin B12 that is responsible for smooth functioning of various biological activities, but the excess dietary intake of cobalt can lead to various diseases such as cardiac arrest, lung infection, asthma and/or dermatitis. In addition, hyperglycemia and polycythemia have been reported during cobalt administration, with a huge damage to alpha- cells in pancreas, whereas injection of cobalt in experimental animals has been known to induce cancer [123-124]. Therefore, continuous monitoring of cobalt concentration level in both biological as well as environmental specimens is of great concern for analytical scientists [125-126]. On the other hand, the heavy metal ions like Pb(II), Cd(II), Hg(II) etc. are very toxic to all kind of living organisms on earth.

These are very hazardous even at very low concentration level and cause serious health issues that are irreparable. For example, unnecessary exposure to lead metal can cause severe damage to central nervous system, increases blood pressure, causes anemia and severely affects the functioning of kidneys [127-128]. Similarly, other heavy metal ions are also very noxious to mankind and their qualitative as well as quantitative recognition is of utmost importance for their proper treatment. Various analytical techniques have been reported in literature, that is used to sense these metal ions, but most of those require high-cost analytical instruments and huge experimental setups. This thesis presents the synthesis of molecular sensors through CuAAC reaction, appended with organic moieties having excellent absorption in UV-Visible region, whose sensing potential can be explored by simple and highly reliable techniques, such as UV-Visible and Fluorescence spectroscopy. The titled molecules are having 1,2,3-triazole ring in their structure, that provides nitrogen atoms as binding sites to coordinate with metal ions and on ligand-metal complexation, the modulations in their absorption behavior can be studied by UV-Visible/Fluorescence spectroscopy. Therefore, these molecules and the techniques used for exploration of their sensing potential towards various metal ions are superior over conventional methods.

The synthetic approach leading to several chemosensors involves 'Click Chemistry' which follows the cyclization of organic azides with different terminal alkynes in the presence of Cu(I) as catalyst (CuAAC) and results into various 1,2,3-triazole linked molecules to be used as effective chemosensing materials. The simplicity and reliability of the CuAAC, has made this reaction an asset to have wide range of scientific applications. Now a day, the click reactions are being incorporated onto or into biomolecules, including introduction of synthetic amino acids with different reactive sites as well as modifications in DNA and nucleotides. Recently, in 2022, the Nobel Prize in chemistry was awarded to three scientists C. R. Bertozzi, M. P. Meldel and K. B. Sharpless for the 'Development of Click Chemistry and Bioorthogonal Chemistry' [129-130]. It would be impossible, in the context of this thesis, to give a complete overview of the numerous applications of the CuAAC in materials science, drug discovery, environmental chemistry, catalysis, chemosensing etc. [131-134]. With this perspective in mind, various 1,2,3-triazole linked derivatives

have been synthesized though Cu(I)-catalyzed alkyne-azide cycloaddition reaction and explored for their chemosensing behavior towards various metal ions.

References:

1. F. Tomas, J. L. M. Abboud, J. Laynez, R. Notario, L. Santos, S. O. Nilsson, J. Catalan, R. M. Claramunt, J. Elguero, *J. Am. Chem. Soc.* **1989**, 111, 7348.
2. A. Albert, P. J. Taylor, *J. Chem. Soc. Perkin Trans*. **1989**, 2, 1903.
3. J. A. Joule, K. Mills, Heterocyclic Chemistry, 5th Edition, J. Wiley & Sons, **2010**, ISBN 978-1-405-13300-5.
4. A. T. Balaban, D. C. Oniciu, A. R. Katritzky, *Chem. Rev.* **2004,** *104*, 2777.
5. A. Lauria, R. Delisi, F. Mingoia, A. Terenzi, A. Martorana, G. Barone, A. M. Almerico, *Eur. J. Org. Chem.* **2014**, 16, 3289.
6. G. Sandip, D. Agalave, R. Suleman, D. Maujan, S. Vandana, *Chem. Asian. J.* **2011**, 6, 2696.
7. S. M. Abdulghani, M. S. Al-Rawi, J. H. Tomma, *Chem. Method.* **2022**, 6, 59.
8. B. Aneja, M. Azam, S. Alam, A. Perwez, R. Maguire, U. Yadava, *ACS Omega*, **2018**, 3, 6912.
9. M. R. Aouad, D. J. O. Khan, M. A. Said, N. S. Al-Kaff, N. Rezki, A. A. Ali, *Chem. Select*, **2021**, 6, 3468.
10. S. K. Avula, M. Khan, S. A. Halim, A. Khan, S. A. Al-Riyami, R. Csuk, *Front. Chem.* **2021**, 9, 642614.
11. M. Bakherad, A. Keivanloo, A. H. Amin, A. Farkhondeh, *Heterocycl. Commun.* **2019**, 25, 122.
12. F. Celik, Y. Unver, B. Barut, A. Ozel, K. Sancak, *Mol. Chem.* **2018**, 14, 230.
13. R. Kharb, P. C. Sharma, M. Shahar Yar, *J. Enzy. Inhib. Med. Chem.* **2011**, 26, 3098.
14. B. S. Holla, M. Mahalinga, M. S. Karthikeyen, B. Poojary, P. M. Akberali, N. S. Kumari, *Eur. J. Med. Chem.* **2005**, 40, 1173.
15. M. D. Chen, S. J. Lu, G. P. Yuag. S. Y. Yang, X. L. Du, *Heterocycl. Commun.* **2000**, 6, 421.

16. E. A. Sherement, R. I. Tomanov, E. V. Trukhin, V. M. Berestovitskaya, *Russ. J. Org. Chem.* **2004**, 40, 594.
17. H. N. Hafez, H. A. Abbas, A. R. El-Gazzar, *Acta. Pharm*. **2008**, 58, 359.
18. S. Muller, B. Liepold, G. J. Roth, H. J. Bestmann, *Synlett.* **1996**, 6, 521.
19. E. Quesada, R. J. K. Taylor, *Tetrahed. Lett.* **2005**, 46, 6473.
20. C. Kuang, Q. Yang, H. Senboku, M. Tokuda, *Tetrahedron,* **2005**, 61, 4043.
21. A. K. Morri, Y. Thummala, V. R. Doddi, *Org. Lett.* **2015**, 17, 4640.
22. R. M. Singh, D. Nandini, K. C. Bharadwaj, T. Gupta, R. P. Singh, *Org. Biomol. Chem.* **2017**, 15, 9979.
23. G. F. Zha, W. Y. Fang, Y. G. Li, J. Leng, X. Chen, H. L. Qin, *J. Am.Chem. Soc.* **2018**, 140, 17666.
24. N. Kaur, G. Singh, J. Singh, A. Singh, P. Satija, G. Kaur, J. Singh, *RSC Adv.* **2018**, 8, 36445.
25. P. Kaur, B. Lal, N. Kaur, G. Singh, A. Singh, G. Kaur, J. Singh, *J. photochem. Photobio. A: Chem.* **2019**, 382, 111847.
26. R. Shaw, A. Elagamy, I. Althagafib, R. Pratapa, *Org. Biomol. Chem.* **2020**, 21, 5341.
27. A. Rani, G. Singh, A. Singh, U. Maqbool, G. Kaur, J. Singh, *RSC Adv.* **2020**, 10, 5610.
28. R. N. de-Oliveira, C. S. Santos, R. J. de-Oliveira, J. C. R. Freitas, *Arkivoc,* **2020**, 1, 219.
29. S. Neumann, M. Biewend, S. Rana, W. H. Binder, *Macromol. Rapid Commun.* **2020**, 41, 1900359.
30. M. Meldal, F. Diness, *Trends Chem.* **2020**, 2, 569.
31. A. N. Kursunlu, *RSC Adv.* **2015**, 5**,** 41025.
32. M. Sulak, A. N. Kursunlu, B. Girgin, O. O. Karakus, E. Guler, *J. Photochem. Photobiol. A: Chem.* **2017**, 349, 129.
33. P. Rani, K. Lal, V. D. Ghule, R. Shrivastava, *Curr. Analy. Chem.* **2020**, 16, 738.
34. W. He, R. Liu, Y. Liao, G. Ding, J. Li, W. Liu, L. Wu, H. Feng, *Anal. Biochem.* **2020**, 598, 113690.
35. G. Singh, G. Sharma, Sanchita, P. Kalra, P. Satija, Pawan, J. Singh, D. Aulakh, M. Wreidt, *Chem. Select.* **2020**, 5, 284.

36. G. Singh, A. Singh, Mohit, A. Saini, A. Devi, J. D. Kaur, P. Satija, Pawan, J. Singh, *J. Molecular Str.* **2021**, 1231, 129963.
37. S. Chakraborty, S. Rayalu, *Inorg. Chem. Commun.* **2019,** 112, 107963.
38. A.N. Kursunlu, M. Ozmen, E. Guler, *J. fluorescence*. **2019**, 29, 1321.
39. H. Tanimoto, K. Kakiuchi, *Nat. prod. Commun*. **2013**, 8, 1021.
40. S. Lang, J. A. Murphy, *Chem. Soc. Rev.* **2006**, 35, 146.
41. M. Kitamura, M. Yano, N. Tashiro, S. Miyagawa, M. Sando, T. Okauchi, *Eur. J. Org. Chem.* **2011**, 134, 458.
42. M. Kitamura, T. Koga, M. Yano, T. Okauchi, *Synlett.* **2012**, 23, 1335.
43. P. Molina, J. Alcántara, C. López-Leonardo, *Synlett.* **1995**, 36, 363.
44. Y. G. Gololobov, L. F. Kasukhin, *Tetrahedron*, **1992**, 48, 1353.
45. T. R. Chan, R. Hilgraf, K. B. Sharpless, V. V. Fokin, *Org. Lett.* **2004**, 6, 2853.
46. A. J. Link, D. A. Tirrell, *J. Am. Chem. Soc.* **2003**, 125, 11164.
47. A. E. Speers, G. C. Adam, B. F. Cravatt, *J. Am. Chem. Soc.* **2003**, 125, 4686.
48. S. Meunier, E. Strable, M. G. Finn, *Chem. Biol.* **2004**, 11, 319.
49. J. E. Hein, J. C. Tripp, L. B. Krasnova, K. B. Sharpless, V. V. Fokin, *Angew.Chem., Int. Ed.* **2009,** 48, 8018.
50. V. V. Rostovtsev, L. G. Green, V. V. Fokin, K. B. Sharpless, *Angew.Chem. Int. Ed.* **2002**, 41, 2596.
51. P. L. Rozas, M. Janeczko, K. Kubinaski, A. Amestey, M. Maslyk, A. E. Braun, *Molecules*, **2018**, 23, 199.
52. B. M. El-Zaatari, A. U. Shete, B. J. Adzima, C. J. Kloxin, *Phys. Chem. Chem. Phys.* **2016**, 18, 25504.
53. M. U. Kagveci, M. Ciftci, S. Evran, S. Timur, *Des. Mono. Polym.* **2015**, 18, 129.
54. M. Arslan, T. C. Bicak, B. A. Pulido, S. P. Nunes, Y. Yagci, *J. Eur. Polym.* **2018,** 100, 298.
55. M. A. Tasdelen, G. Yilmaz, B. Iskin, Y. Yagci, *Macromolecules*, **2012**, 45, 56.
56. M. A. Tasdelen and Y. Yagci, *Angew. Chem. Int. Ed*. **2013**, 52, 2.
57. M. A. Tasdelen, Y. Yagci, *Tetrahed. Lett.* **2010**, 51, 6945.
58. O. S. Taskin, G. Yilmaz, Y. Yagci, *ACS Macro. Lett.* **2016**, 5, 103.

59. R. T. Chen, S. Marchesan, R. A. Evans, K. E. Styan, G. K. Such, A. Postma, K. M. Mclean, B. W. Muir, F. Caruso, *Biomacromolecules,* **2012**, 13, 889.
60. B. Yin, C. C. Barghorn, C. Delaite, X. Allonas, *RSC Adv.* **2019**, 9, 4824.
61. B. S. Sumerlin, A. P. Vogt, *Macromolecules,* **2010**, 43, 1.
62. L. Harmand, S. Cadet, B. Kauffmann, L. Scarpantonio, P. Batat, G. Jonusauskas, N. D. M. Clenaghan, D. Lastecoueres, J. M. Vincent, *Angew. Chem. Int. Ed.* **2012**, 51, 7137.
63. T. Gong, B. J. Adzima, N. H. Baker, C.N. Bowman, *Adv. Mater.* **2013**, 25, 2024.
64. A. A. Alzahrani, A. H. Erbse, C. N. Bowman, *Polym. Chem.* **2014**, 5, 1874.
65. R. Beniazza, R. Lambert, L. Harmand, F. Molton, C. Duboc, S. Denisov, G. Jonusauskas, N. D. M. Clenaghan, D. Lastecoueres, J. M. Vincent, *Chem. Eur. J.* **2014**, 20, 13181.
66. K. S. S. Praveena, E. V. V. Shivaji, N. Y. S. Murthy, S. Akkenapally, C. G. Kumar, R. Kapavarapu, S. Pal, *Bioorg. Med. Chem. Lett.* **2015**, 13, 2012.
67. S. H. Kim, H. S. Choi, J. Kim, S. J. Lee, D. T. Quang, J. S. Kim, *Org. Lett*. **2010**, 12, 560.
68. C. Wu, C. Z. Wang, Q. Zhu, X. Zeng, C. Redshawd. T. Yamato, *Elsevier,* **2018**, 7, 15403.
69. S. I. Presolski, V. Hong, S. H. Cho, M. G. Finn, *J. Am. Chem. Soc.* **2010**, 132, 14570.
70. Y. L. Liu, L. Yang, L. Li, Y. Q. Guo, X. X. Pang, P. Li, F. Ye, Y. Fu, *Molecules*, **2019**, 24, 3093.
71. D. Soriano, W. Wang, H. Jiang, C. Besanceney, A. C. Yan, M. Levy, Y. Liu, F. L. Marlow, P. Wu, *J. Am. Chem. Soc.* **2010**, 132, 16893.
72. H. T. Le, J. G. Jang, J. Y. Park, C. W. Lim, T. W. Kim, *Anal. Biochem.* **2013,** 435, 68.
73. Y. Angell, K. Burgess, *Angew. Chem., Int. Ed.* **2007**, 46, 3649.
74. C. B. Webler, H. Jiang, T. Zheng, L. Feng, D. Soriano del Amo, W. Wang, L. M. Klivansky, F. L. Marlow, Y. Liu, P. Wu, *Angew.Chem.* **2011**, 123, 8201.
75. J. A. Shin, S. J. Oh, H. Y. Lee, Y. G. Lim, *Catal. Sci. Technol*. **2017**, 7, 2450.

76. Z. Zhu, H. Chen, S. Li, X. Yang, E. Bittner, C. Cai, *Catal. Sci. Technol.* **2017**, 7, 2474.
77. B. H. Lipshutz, Z. Boksovic, C. S. Crowe, V. K. Davis, H. C. Whittemore, D. A. Vosburg, A. G. Wenzel, *J. Chem. Educ.* **2013**, 90, 1514.
78. S. A. Ingale, F. Seela, *J. Org. Chem.* **2012**, 34, 5611.
79. R. Hiatt, *J. Chem. Educ.* **1989**, 66, 927.
80. L. A. Morrill, J. K. Kammeyer, N. K. Garg, *J. Chem. Educ.* **2017**, 94, 1584.
81. W. Edward, J. Castner, *J. Chem. Educ.* **2005**, 82, 43.
82. G. C. Pimentel, *J. Chem. Educ.* **1960**, 37, 651.
83. J. R. Ferraro, *J. Chem. Educ.* **1961**, 38, 201.
84. J. E. Pearson, *J. Chem. Educ.* **1967**, 50, 243**.**
85. M. Kandel, P. J. Tonge, *J. Chem. Educ.* **2001**, 78, 1208**.**
86. A. O. C. Nier, *J. Am. Chem. Soc.* **1958**, 80, 6696.
87. J. H. Bowie, D. H. Williams, S. O. Lawesson, G. Schroll, *J. Org. Chem.* **1966**, 31, 1792.
88. S. M. Barrett, P. S. Szalay, L. A. Zook-Gerdau, E. J. Schurter, *J. Chem. Educ.* **2020**, 97, 4097.
89. D. L. Pavia, G. M. Lampman, G. S. Kriz, J. R. Vyvyan, Spectroscopy, 6th Indian edition, **2011**, ISBN: 978–81–315–0576–2.
90. X. Creary, A. Anderson, C. Brophy, F. Crowell, Z. Funk, *J. Org. Chem.* **2012**, 77, 8756.
91. W. Xi, T. F. Scott, C. J. Kloxin, C. N. Bowman, *Adv. Funct. Mater.* **2014**, 24, 2572.
92. G. Singh, P. Satija, G. Sharma, Shilpy, J. Singh, *New J. Chem.* **2019**, 43, 5525.
93. G. Singh, S. S. Mangat, J. Singh, A. Arora, M. Garg, *J. Organomet. Chem.* **2014,** 769, 124.
94. M. Liu, Z. Xu, Y. Song, H. Li and C. Xian, *J. Lumin.* **2018**, 198, 337.
95. G. Singh, J. Singh, S. S. Mangat, A. Arora, *Tetrahedron,* **2014**, 55, 2551.
96. A. Rani, G. Singh, A. Singh, U. Maqbool, G. Kaur, G. Singh, *RSC Adv.* **2020**, 10, 5610.
97. V. S. Wills, J. I. Metzger, C. Allen, M. L. Varney, D. F. Wiemer, S. A. Holstein, *Bioorg. Med. Chem.* **2017**, 25, 2437.

98. R. K. Thatipamula, S. Narsimha, K. Battula, V. R. Chary, E. Mamidala, N. V. Reddy, J. Saudi, *Chem. Soc*. **2017**, 21, 795.
99. C. L. Su, C. L. Tseng, C. Ramesh, H. S. Liu, C. Y. F. Huang, C. F. Yao, *Eur. J. Med. Chem.* **2017**, 132, 90.
100. M. Allam, A. K. D. Bhavani, A. Mudiraj, N. Ranjan, M. Thippana, P. P. Babu, *Eur. J. Med. Chem.* **2018**,156, 43.
101. V. D. da Silva, B. M. de Faria, E. Colombo, L. Ascari, G. P. A. Freitas, L. S. Flores, Y. Cordeiro, L. Romao, C. D. Buarque, *Bioorg. Chem*. **2019**, 83, 87.
102. B. Mistry, R. V. Patel, Y. S. Keum, *Arabian J. Chem.* **2017**, 10, 157.
103. G. Wu, W. A. Zalloum, M. E. Meuser, L. Jing, D. Kang, C. H. Chen, Y. Tian, F. Zhang, S. Cocklin, K. H. Lee, X. Liu, P. Zhan, *Eur. J. Med. Chem*. **2018**, 158, 478.
104. A. Afkhami, T. Madrakian, A. Shirzadmehr, M. Tabatabaee, H. Bagheri, *Sens. Actuators: Chem.* **2012**, 174, 237.
105. S. M. Saleh, R. Ali, F. Alminderej, A. L. Ali, *Internat. J. of Anal. Chem.* **2019**, 6,1.
106. M. Panchal, A. Kongor, M. Athar, V. Mehta, P. C. Jha, V. K. Jain, *New. J. Chem.* **2017**, 12, 278.
107. L. Prodi, C. Bargossi, M. Montalti, N. Zaccheroni, N. Su, J. S. Bradshaw, R. M. Izatt, P. B. Savage, *J. Am. Chem. Soc.* **2000**, 122, 6769.
108. Y. B. Ruan, C. Li, J. Tang, J. Xie, *Chem. Commun.* **2010**, 46, 9220.
109. Y. Zhou, S. Wang, K. Zhang, X. Jiang, *Angew. Chem. Int. Ed.* **2008**, 47, 7454.
110. M. Adlim, F. Zarlaida, *AACL Bioflux.* **2015**, 8, 656.
111. D. Shi, F. Yan, M. Wang, Y. Zou, T. Zheng, X. Zhou, L. Chen, *Materials*, **2005**, 70, 958.
112. E. A. Nivethaa, V. Narayanan, A. Stephen, *Spectrochimica. Acta. Part A: Mole. Biomol. Spectro.* **2015**, 143, 242.
113. G. Singh, J. Singh, S. S. Mangat, J. Singh, S. Rani, *RSC Adv*. 2015, 5, 12644.
114. S. K. Dwivedi, R. C. Gupta, P. Srivastava, P. Singh, B. Koch, B. Maiti, A. Misra, *Anal. Chem.* **2018**, 90, 10974.
115. G. Singh, J. Singh, J. Singh, S. S. Mangat, *J. luminesc.* **2015**, 165, 123.

116. B. Dolai, S. K. Nayim, M. Hossain, P. Pahari, A. K. Atta, *Sens. Actuators B: Chem.* **2018**, 09, 105.
117. D. Cao, Z. Liu, P. Verwilst, S. Koo, P. Jangjili, J. S. Kim, W. Lin, *Am. Chem. Soc. Rev.* **2019**, 119, 10403.
118. A. J. Christensen, J. T. Fletcher, *Tetrahed. Lett.* **2014**, 55, 4612.
119. K. C. Chang, I. H. Su, A. Senthilvelan, W. S. Chung, *Org. Lett.* **2007**, 9, 3363.
120. Y. C. Hsieh, J. L. Chir, H. U. Wu, P. S. Chang, A. T. Wu, *Carbohyd. Res.* **2009**, 344, 2236.
121. H. Jain, N. Deswal, A. Joshi, C. N. Ramachandran, R. Kumar, *Anal. Methods*, **2019**, 11, 3230.
122. D. Kushwaha, R. S. Singh, V. K. Tiwari, *Tetrahed. Lett.* **2014**, 55, 4532.
123. Z. Liu, W. Wang, H. Xu, L. Sheng, S. Chen, D. Huang, F. Sun, *Inorg. Chem. Commun.* **2015,** 19, 62.
124. Y. L. Liu, L. Yang, L. Li, Y. Q. Guo, X. X. Pang, P. Li, F. Ye, Y. Fu, *Molecules*, **2019**, 24, 3093.
125. A. K. Jain, V. K. Gupta, L. P. Singh, U. Khurana, *Analyst*, **1997,** 122, 583.
126. Y. Jeong, Y. W. Choi, G. R. You, C. Kim, *Sens. Actuators B: Chem.* **2016**, 223, 234.
127. G. Flora, D. Gupta, A. Tiwari, *Interdiscip. Toxicol*. **2012**, 5, 47.
128. A. L. Wani, A. Ara, J. A. Usmani, *Interdiscip. Toxicol*. **2015**, 8, 55.
129. N. K. Devaraj, M. G. Finn, *Chem. Rev.* **2021**, 121, 6697.
130. "The Nobel Prize in Chemistry 2022", *Nobel Prize.org.* **2022**.
131. N. N. Reddy, S. J. Hung, M. K. Swamy, A. Sanjeev, V. S. Rao, R. Rohini, A. K. Raju, K. Bhaskar, A. Hu, P. M. Reddy, *Molecules*, **2021**, 26, 1952.
132. A. Pucci, G. Albano, M. Pollastrini, A. Lucci, M. Colalillo, F. Oliva, C. Evangelisti, M. Marelli, D. Santalucia, A. Mandoli, *Catalysts*, **2020**, 10, 434.
133. N. Touj, I. Ozdemir, S. Yasar, N. Hamdi, *Inorg. Chim. Acta.* **2017**, 467, 21.
134. M. A. Sierra, M. C. de la Torre, *ACS Omega*, **2019**, 4, 12983.

Chapter 3

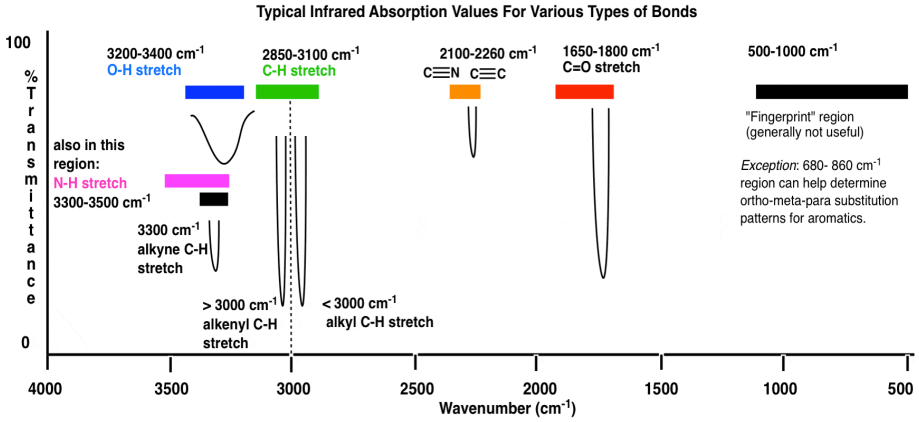

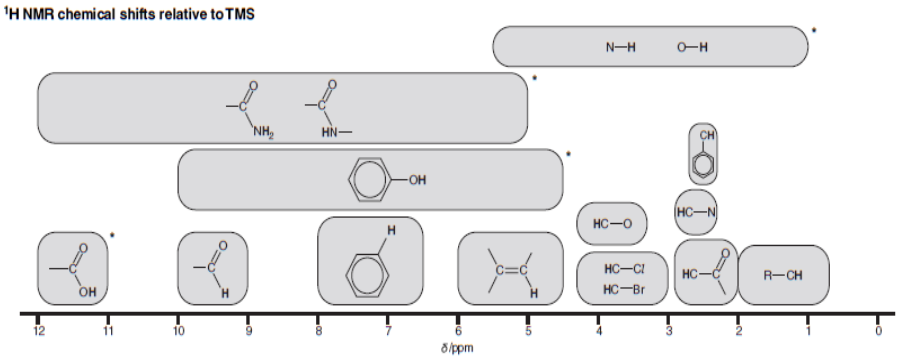

Experimental Data

This section includes detailed data regarding the experimental work done for the synthesis of various novel molecules along with their complete structural characterization that includes various studies like Color, yield, melting point, CHN analysis, IR, NMR, and HRMS.

3.1 General procedure for the synthesis of 1,2,3-triazole derivatives

General procedure adopted for the synthesis of 1,2,3-triazole linked molecules to pursue this research work includes following steps:

Step I: Synthesis of terminal alkyne

To the stirred solution of starting material (1.00 mol) in DMF, added dried potassium carbonate (5.00 mol) as base. Then propargyl bromide (1.30 mol) was added drop wise with stirring at room temperature. The growth of reaction was monitored by thin layer chromatography using various solvent combinations. At the end, the desired product was separated out using ice-cold water, for that whole of the reaction mixture was poured into ice-cold water and stirred well. The product was separated by filtration, washed with chilled water in order to remove solvent and dried in air till constant weight (if solid). For the liquid product, the solvent extraction process was followed.

Step II: Synthesis of organic azide

To proceed for the synthesis of an organic azide, first of all sodium azide was vacuum dried. Then dried sodium azide (5.00 mol) was added into the solution of organic halide (1.00 mol) in suitable amount of DMF used as solvent and set to stirring at 85-90 °C for 4-5 h. The product was isolated using ice cold water and ethylacetate through solvent extraction process.

Step III: Synthesis of 1,4-disubstituted 1,2,3-triazole derivatives

To the stirred solution of terminal alkyne (1.00 mol) in THF/TEA (v/v, 1:1), added accurately weighed (1.00 mol) amount of organic azide and dissolved into the same reaction mixture. After that catalytic amount of $[CuBr(PPh_3)_3]$ (0.001 mmol) complex was added and the reaction mixture was allowed to stir at 55-60 °C for 4-6 h. After the completion of reaction, the product was isolated from reaction mixture using ice-cold water and dried till constant weight. The general scheme involving all the steps is shown in Scheme 3.1.

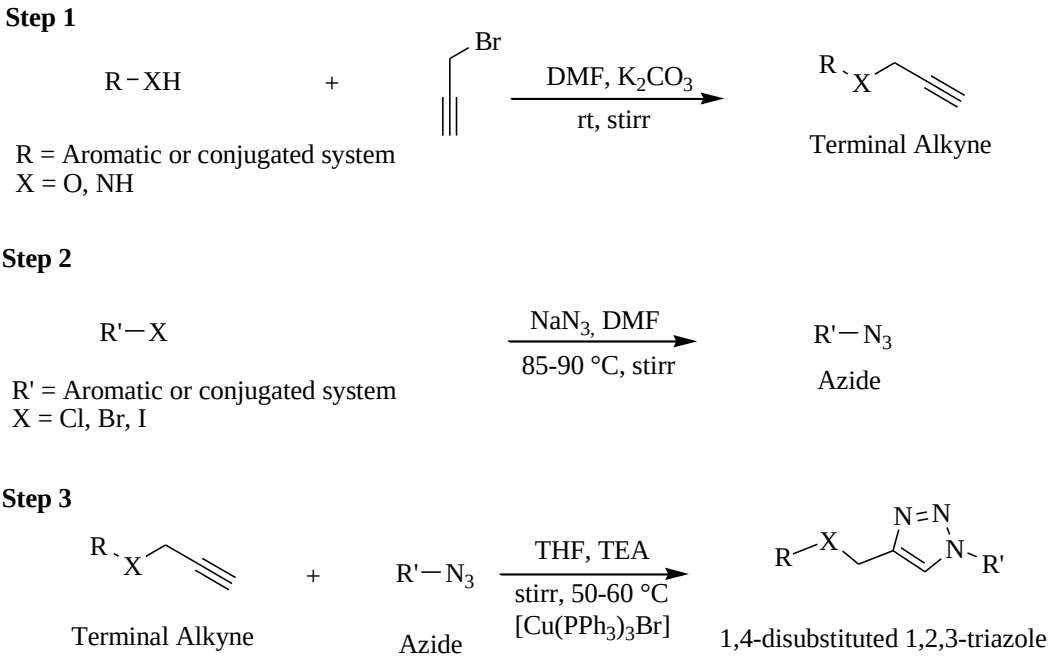

Scheme 3.1: General scheme for all the steps involved in the proposed research work, abbreviations used are DMF; N, N-dimethyl formamide, THF; Tetrahydrofuran, TEA; Triethylamine, stirr; stirring, rt; room temperature.

3.2 Synthesis of organic azides

3.2.1 Synthesis and characterization of benzyl azide

To the stirred solution of accurately weighed chloromethylbenzene **56** (5.00 g, 4.55 ml, 39.50 mmol) in DMF (50.00 ml), dried NaN_3 (12.87 g, 197.91 mmol) was added slowly and the reaction content was stirred for 5 h at 90 °C (Scheme 3.2), following the procedure in step-II of section 3.1.

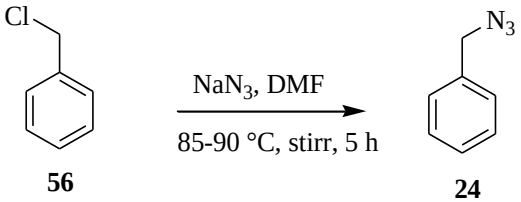

Scheme 3.2: Synthesis of benzyl azide

After 5 h, the product was isolated by solvent extraction method using ethyl acetate-water mixture. The organic layer collected from extraction process was dried over anhydrous sodium sulphate and vacuum evaporated to remove all the solvent to have pure azidomethylbenzene **24**.

Yield: 60%

Color/Texture: Light yellow oil

Molecular formula: $C_7H_7N_3$

IR (neat, cm^{-1}): 3051, 2930, 2091, 1675, 1345, 1250.

^{1}H NMR (500 MHz, $CDCl_3$): δ = 7.24-7.14 (m, 5H), 4.14 (s, 2H).

^{13}C NMR (126 MHz, $CDCl_3$): δ = 135.53, 128.91, 128.37, 128.31, 54.82.

3.2.2 Synthesis and characterization of azidomethylnaphthalene

To the solution of chloromethylnaphthalene **57** (5.00 g, 4.24 ml, 28.30 mmol) in DMF (50.00 ml), pure and dry sodium azide (9.20 g, 14.15 mmol) was added. The whole mixture was stirred for 6 h at 85-90 °C (Scheme 3.3). After the completion of reaction, the whole content was poured into ice-cold water and after that, the product was extracted by treating with ethyl acetate. The desired product azidomethylnaphthalene **58** was isolated from organic layer by vacuum evaporation of ethyl acetate.

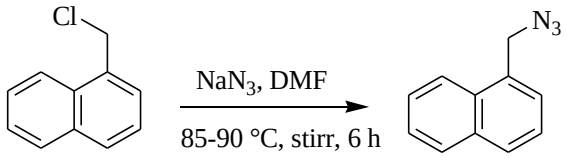

57 **58**

Scheme 3.3: Synthesis of azidomethylnaphthalene

Yield: 55%

Color/Texture: Light brown oil

Molecular Formula: $C_{11}H_9N_3$

IR (neat, cm^{-1}): 3049, 2930, 2090, 1460, 1345, 1253.

^{1}H NMR (500 MHz, $CDCl_3$): δ = 8.12 (d, 1H), 7.99 (d, 1H), 7.94 (dd, 1H), 7.65 (m, 2H), 7.53 (m, 2H), 4.78 (s, 2H).

^{13}C NMR (126 MHz, $CDCl_3$): δ = 134.05, 131.50, 131.15, 129.53, 128.07, 127.37, 126.86, 126.31, 125.37, 123.64, 53.02.

3.3 o-Cresolphthalein based alkyne 59a and 1,2,3-triazole derivatives 59b and 59c

3.3.1 Synthesis and characterization of alkyne 3,3-bis(3-methyl-4-(prop-2-ynyloxy) phenyl) isobenzofuran-1(3H)-one (59a)

The starting material **59** (o-cresolphthalein) was treated with propargyl bromide **19** to prepare terminal alkyne **59a** (Scheme 3.4) following the procedure mentioned in step-I of section 3.1. To do this, o-cresolphthalein (1.00 g, 2.87 mmol) was dissolved in DMF and then dried potassium carbonate (1.98 g, 14.40 mmol) was added into it, followed by slow and dropwise addition of propargyl bromide (0.89 ml, 7.50 mmol). The reaction content was set to stirring at room temperature and atmospheric pressure for 14 h. The growth of reaction was tracked with the thin layer chromatography in hexane:ethyl acetate (4:1) solvent system. Upon completion of reaction, the expected product **59a** was extracted using ethyl acetate-water as liquid mixture. In order to purify the extracted product, the impurities like base and DMF was removed by washing repeatedly with chilled water and dried for further use.

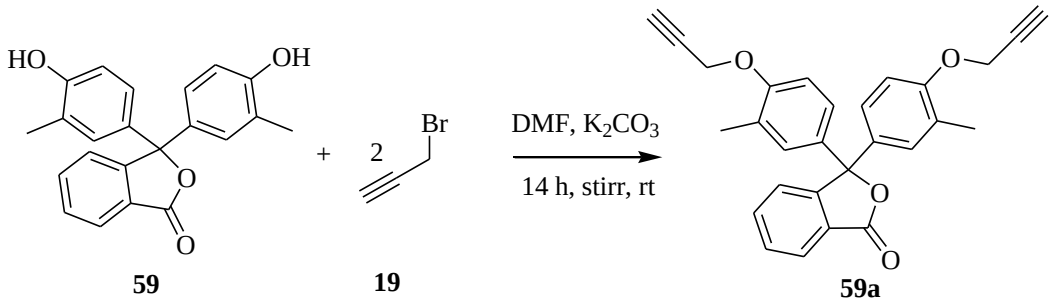

59 **19** **59a**

Scheme 3.4: Synthetic route of alkyne **59a**

Yield: 91%

Color/Texture: Highly viscous yellow oil

Molecular Formula: $C_{28}H_{22}O_4$

Elem. Anal. Calculated (%): C = 79.61, H = 5.24; **Found (%):** C = 79.58, H = 5.28

IR (neat, cm^{-1}): 3286, 2923, 2121, 1755, 1671, 1606, 1497, 1460, 1107, 750, 632.

^{1}H NMR (500 MHz, $CDCl_3$) δ = 7.81 (d, *J* = 7.6 Hz, 1H), 7.56 (s, 1H), 7.47-7.38 (m, 2H), 7.08-6.96 (m, 4H), 6.77 (d, *J* = 8.3 Hz, 2H), 4.57 (s, 4H), 2.41 (s, 2H), 2.06 (s, 6H).

^{13}C NMR (126 MHz, $CDCl_3$) δ = 169.98, 162.61, 155.88, 133.58, 129.83, 129.24, 127.40, 125.94, 125.70, 124.17, 111.02, 91.73, 78.70, 75.68, 55.94, 16.45.

3.3.2 Synthesis and characterization of 3,3-bis(4-((1-benzyl-1H-1,2,3-triazol-4-yl) methoxy)-3-methylphenyl) isobenzofuran-1(3H)-one (59b)

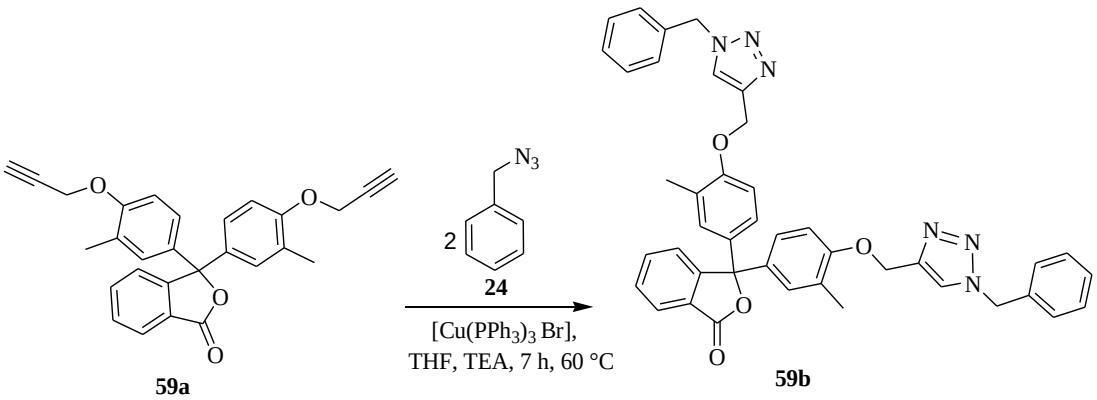

59a **59b**

Scheme 3.5: Schematic procedure of the synthesis of **59b**

The compound **59a** (1.00 g, 2.35 mmol) was dissolved in minimum amount of THF:TEA (v/v, 1:1) taken in 100.00 ml round bottom flask, to have a clear solution. It is then followed by addition of catalytic amount of [$CuBr(PPh_3)_3$] (0.001 mmol) and freshly prepared benzyl azide **24** (0.62 g, 0.59 ml, 4.74 mmol). The reaction was

allowed to refluxing for 7 h (Scheme 3.5). On pouring the reaction mixture into ice-cold water, a creamy white colored solid product **59b** was appeared, that was isolated by filtration. To purify the product, it was washed repeatedly with diethyl ether and finally, dried at room temperature to get constant yield.

Yield: 92%

Color/Texture: Creamy white powder

M. Pt. = 90-92 °C

Molecular Formula: $C_{42}H_{36}N_6O_4$

Elem. Anal. Calculated (%): C = 73.23, H = 5.26, N = 12.22; **Found (%):** C = 73.25, H = 5.24, N = 12.17

IR (neat, cm^{-1}): 3027, 2924, 1755, 1606, 1560, 1498, 1460, 1130, 1041, 941, 806, 750, 619.

^{1}H NMR (500 MHz, $CDCl_3$) δ = 7.91 (d, *J* = 7.6 Hz, 1H), 7.67 (s, 1H), 7.50 (d, *J* = 7.2 Hz, 4H), 7.47-7.30 (m, 6H), 7.26 (t, *J* = 3.6 Hz, 6H), 7.08 (d, *J* = 1.8 Hz, 3H), 6.85 (d, *J* = 8.5 Hz, 2H), 5.52 (s, 4H), 5.17 (s, 4H), 2.12 (s, 6H).

^{13}C NMR (126 MHz, $CDCl_3$) δ = 171.69, 170.19, 158.14, 152.69, 144.73, 134.43, 133.17, 129.91, 129.34, 129.01, 128.30, 128.29, 127.26, 126.10, 122.46, 110.90, 91.93, 66.06, 54.62, 16.64.

Molar Mass Calculated: 688.27; **Found (m/z)** = 689.28 $(M+1)^+$

3.3.3 Synthesis and characterization of 3,3-bis(4-((1-((naphthalen-1-yl)methyl)-1H-1,2,3-triazol-4-yl)methoxy)-3-methylphenyl)isobenzofuran-1(3H)-one (59c)

Alkyne **59a** (1.00 g, 2.36 mmol) was dissolved in THF:TEA (v/v, 1:1) to get a clear solution, added newly prepared azidomethylnaphthalene **58** (0.87 g, 4.74 mmol) along with $[CuBr(PPh_3)_3]$ (0.001 mmol) as catalyst and set to refluxing with constant stirring for 8 h (Scheme 3.6). A light brown solid **59c** was obtained with the addition of ice-cold water into the reaction mixture. The synthesized product was isolated by

filtration, washed thoroughly with chilled water and then stirred in diethyl ether for few minutes to remove any organic impurity, thereafter dried to get constant weight.

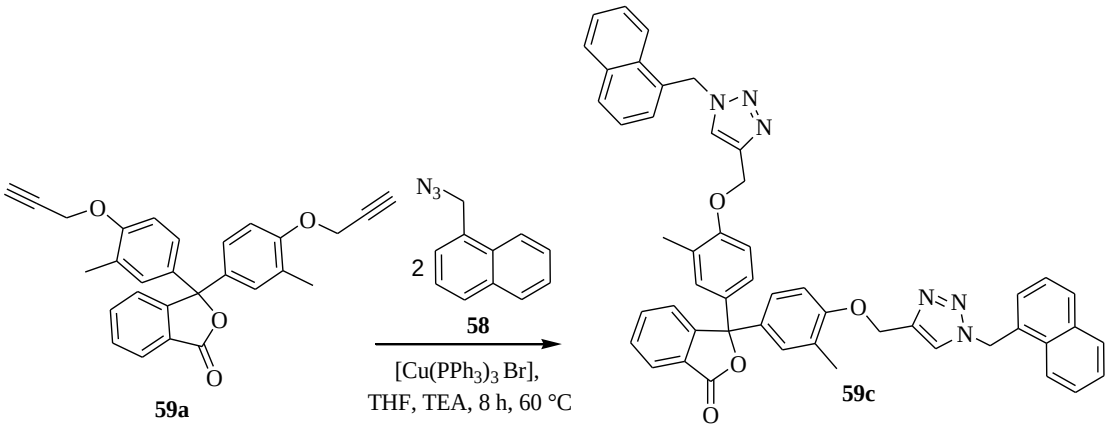

Scheme 3.6: Synthetic route of triazole **59c**

Yield: 95%

Color/Texture: light brown powder

M. Pt. = 130-132 °C

Molecular Formula: $C_{50}H_{40}N_6O_4$

Elem. Anal. Calculated (%): C = 76.12, H = 5.11, N = 10.65; **Found (%):** C = 76.09, H = 5.14, N = 10.57

IR (neat, cm^{-1}): 3025, 2964, 1753, 1499, 1464, 1252, 786.

^{1}H NMR (500 MHz, $CDCl_3$) δ = 7.92 (m, 4H), 7.69-7.46 (m, 8H), 7.43 (t, J = 11.1 Hz, 4H), 7.35 (s, 4H), 7.26 (s, 3H), 7.10-6.95 (m, 2H), 6.80 (d, J = 8.4 Hz, 2H), 5.98 (s, 4H), 5.10 (s, 4H), 2.05 (s, 6H).

^{13}C NMR (126 MHz, $CDCl_3$) δ = 169.89, 156.43, 152.63, 144.57, 133.94, 133.18, 130.13, 129.62, 128.98, 127.86, 127.32, 126.45, 125.74, 125.37, 122.84, 122.51, 110.95, 91.72, 62.31, 52.44, 16.39.

Molar Mass Calculated: 788.85; **Found m/z** = 789.32 $(M+1)^+$

3.4 1,4-Dihydroxyanthraquinone based terminal alkyne 60a and 1,2,3-triazole derivatives 60b and 60c

3.4.1 Synthesis and characterization of terminal alkyne 1,4-bis(prop-2-ynyloxy) anthracene-9,10-dione (60a)

1,4-dihydroxyanthraquinone **60** (1.00 g, 4.16 mmol) was dissolved in DMF (20.00 ml) taken in a round bottom flask, followed by addition of dry potassium carbonate (2.87 g, 20.76 mmol). Thereafter, the propargyl bromide **19** (1.24 ml, 8.34 mmol) was added dropwise into the flask and set to stirring at room temperature for 18 h (Scheme 3.7). Upon completion of the reaction that was regularly monitored by TLC, a mustard-colored solid product **60a** was obtained on pouring the reaction mixture into ice-cold water. The product was filtered, washed with chilled water to remove DMF and vacuum dried to get constant weight.

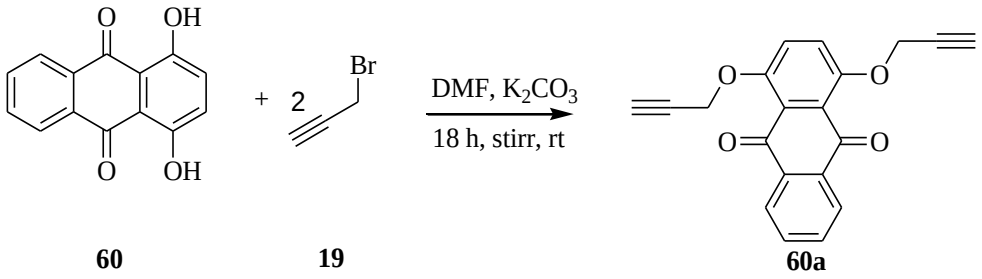

60 **19** **60a**

Scheme 3.7: Scheme for the synthesis of 1,4-dihydroxyanthraquinone based alkyne **60a**

Yield: 98%

Color/Texture: Mustard colored solid

M. Pt. = 160-162 °C

Molecular Formula: $C_{20}H_{12}O_4$

Elem. Anal. Calculated (%): C = 75.94, H = 3.82; Found **(%):** C = 75.90, H = 3.84

IR (neat, cm^{-1}): 3288, 3020, 2160, 2017, 1815, 1725, 1666, 1448, 1166, 642.

^{1}H NMR (500 MHz, $CDCl_3$) δ = 8.16 (dd, *J* = 5.7, 3.3 Hz, 2H), 7.72 (dd, *J* = 5.8, 3.3 Hz, 2H), 7.52 (s, 2H), 7.26 (s, 1H), 4.90 (s, 4H), 2.57 (s, 2H).

^{13}C NMR (126 MHz, $CDCl_3$) δ = 182.98, 152.86, 134.09, 133.52, 126.56, 124.74, 123.74, 78.19, 76.69, 58.28.

3.4.2 Synthesis and characterization of 1,4-bis((1-benzyl-1H-1,2,3-triazol-4-yl) methoxy) anthracene-9,10-dione (60b)

To the solution of alkyne **60a** (1.00 g, 3.16 mmol) and benzyl azide **24** (0.84 g, 0.78 ml, 6.31 mmol) in THF:TEA (v/v, 4:1) in a round bottom flask, added [$CuBr(PPh_3)_3$] (0.001 mmol) as catalyst (Scheme 3.8). The reaction was set to refluxing with stirring. In just 15 min, a yellow-colored solid appeared in the reaction mixture and within 30 minutes maximum amount of product was formed in the flask. The solid yellow colored product **60b** was obtained by filtration, washed thoroughly with water to remove solvents and dried.

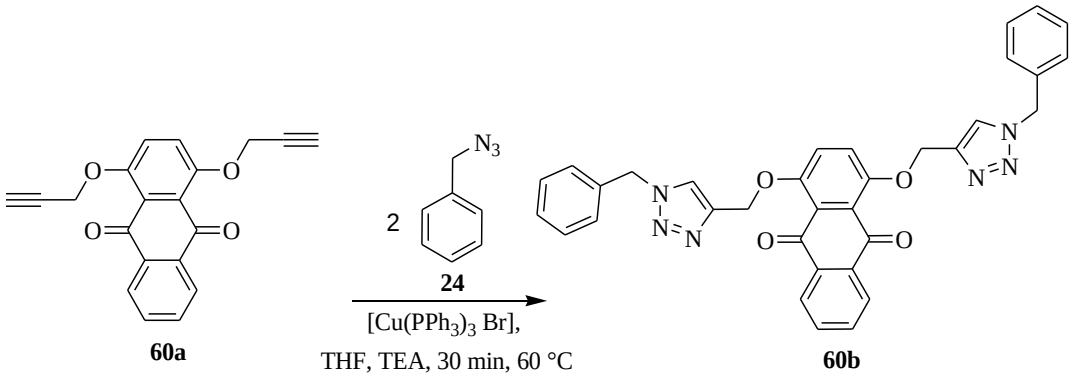

Scheme 3.8: Synthetic route of **60b**

Yield: 99%

Color/Texture: yellow powder

M. Pt. = 198-200 °C

Molecular Formula: $C_{34}H_{26}N_6O_4$

Elem. Anal. Calculated (%): C = 70.10, H = 4.47, N = 14.43; **Found (%):** C = 70.14, H = 4.43, N = 14.40

IR (neat, cm^{-1}): 3073, 1661, 1567, 1494, 1452, 1256, 1238, 1125, 1055, 989, 808, 717, 655.

^{1}H NMR (500 MHz, $CDCl_3$) δ = 8.12 (dd, *J* = 5.7, 3.3 Hz, 2H), 7.85-7.64 (m, 2H), 7.49 (s, 2H), 7.36-7.30 (m, 12H), 7.26 (s, 1H), 5.57 (s, 4H), 5.34 (s, 4H).

^{13}C NMR (126 MHz, $CDCl_3$) δ = 183.09, 153.32, 134.56, 134.12, 133.38, 129.12, 128.76, 128.06, 126.45, 123.39, 64.81, 54.29.

Calculated Molecular Mass: 582.21; **Observed m/z** = 583.21 $(M+1)^+$

3.4.3 Synthesis and characterization of 1,4-bis((1-methylnaphthyl-1H-1,2,3-triazol-4-yl) methoxy) anthracene-9,10-dione (60c)

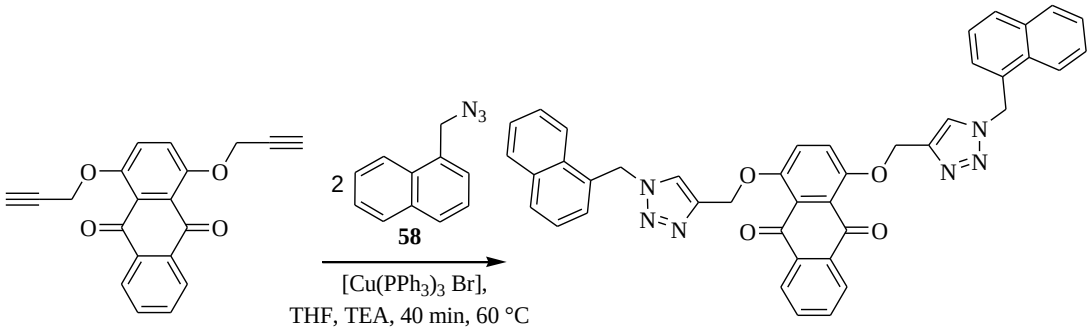

Scheme 3.9: Synthesis of **60c**

Following the procedure of step-III in section 3.1, the terminal alkyne **60a** (1.00 g, 3.15 mmol) was dissolved in THF:TEA (v/v, 4:1) in 100.00 ml round bottom flask, followed by the addition of azidomethylnaphthalene **58** (1.16 g, 6.33 mmol) and $[CuBr(PPh_3)_3]$ (0.001 mmol) as catalyst as shown in Scheme 3.9. The reaction mixture was set to stirring at 60 °C. In just 40 min, a maximum of yellow colored solid **60c** was collected in the reaction vessel. The solid product was separated by

filtration, washed thoroughly with water to remove solvents and dried to get constant weight.

Yield: 99%

Color/Texture: yellow powder

M. Pt. = 214-216 °C

Molecular Formula: $C_{42}H_{30}N_6O_4$

Elem. Anal. Calculated (%): C = 73.91, H = 4.39, N = 12.32; **Found (%):** C = 73.94, H = 4.36, N = 12.34

IR (neat, cm^{-1}): 3078, 1663, 1569, 1496, 1454, 1335, 1278, 1248, 1125, 1066, 997, 830, 798, 779, 721.

^{1}H NMR (500 MHz, DMSO) δ = 7.46-7.13 (m, 4H), 7.05 (dd, J = 13.0, 8.4 Hz, 6H), 6.90 (dd, J = 5.5, 3.5 Hz, 2H), 6.82-6.45 (m, 10H), 5.22 (s, 4H), 4.34 (s, 4H).

^{13}C NMR (126 MHz, DMSO) δ = 182.39, 153.01, 143.47, 134.12, 133.84, 131.96, 131.10, 129.56, 129.16, 127.71, 127.29, 126.68, 126.34, 126.04, 125.35, 123.97, 123.75, 123.24, 68.78, 57.40.

Calculated Molecular Mass: 682.21; **Observed m/z** = 683.35 $(M+1)^+$

3.4.4 Optimization of reaction conditions for the synthesis of 60b and 60c and product yield

A number of trials were taken out for this [3+2] cycloaddition process to get maximum yield of **60b** and **60c** with minimum time duration as presented in Table 3.1. The analysis of results shows no outcome of reaction at room temperature even on stirring the reaction mixture for 5-6 h, the conventional duration of cycloaddition reaction. On increasing the temperature up to 60 °C, an observable change in the yield has started appearing after 15 min. Within a time period of 15 min to 40 min, a maximum of yellow colored solid accumulated in the reaction vessel that was calculated as 99% for both **60b** and **60c**, the highest yield of product. At the

temperature above 60 °C, no further increase in yield was observed. From the whole practice, it was concluded that the cycloaddition reaction for the synthesis of these two 1,2,3-triazole linkers is very fast and get completed in just 30-40 min at 60 °C.

Table 3.1: Optimization of reaction conditions (temperature and time) for the generation of 1,2,3-triazole linkers **60b** and **60c**

S.No.	Temperature (°C)	Time (min)	% Yield	
			60b	**60c**
1	25	120	0	0
2	25	240	0	0
3	25	360	0	0
4	60	10	0	0
5	60	15	20	18
6	60	20	70	65
7	**60**	**30**	**99**	85
8	**60**	**40**	97	**99**
9	80	30	78	85
10	80	60	70	80

3.5 1-Naptholphthalein based terminal alkyne 61a and 1,2,3-triazole derivative 61b

3.5.1 Synthesis and characterization of terminal alkyne 3,3-bis(1-(prop-2-ynyloxy) naphthalen-4-yl) isobenzofuran-1(3H)-one (61a)

To the solution of starting material **61** (1-naptholphthalein, 1.00 g, 2.38 mmol) in DMF (10.00 ml) as solvent, potassium carbonate as base (1.65 g, 11.94 mmol) was added. Then propargyl bromide **19** (0.71 ml, 5.97 mmol) was added slowly into the reaction mixture and set to stirring for 28 h at room temperature and atmospheric conditions (Scheme 3.10). The growth of reaction was regularly watched with TLC and after 28 h, brown colored solid product **61a** was obtained on pouring the reaction

mixture into ice cold water. Solid product was filtered, washed thoroughly with chilled water to remove DMF and vacuum evaporated to get constant weight.

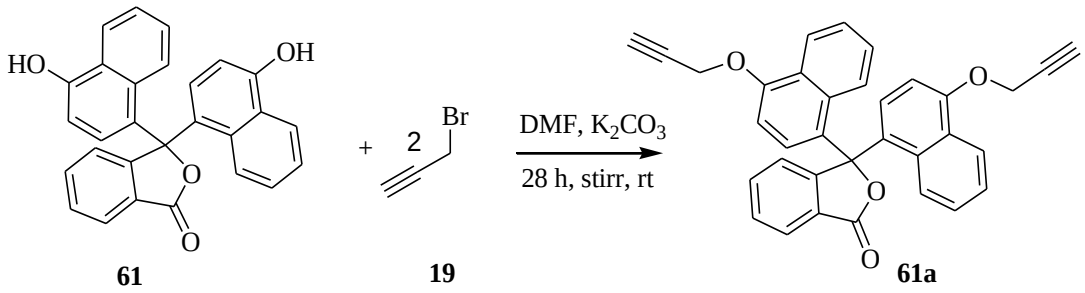

61 **19** **61a**

Scheme 3.10: Synthesis of alkyne **61a**

Yield: 90%

Color/Texture: brown colored solid

M. Pt. = 118-120 °C

Molecular Formula: $C_{34}H_{22}O_4$

Elem. Anal. Calculated (%): C = 82.58, H = 4.48; **Found (%):** C = 82.53, H = 4.50

IR (neat, cm^{-1}): 3287, 2034, 1758, 1627, 1587, 1459, 1157, 632.

^{1}H NMR (500 MHz, $CDCl_3$) δ = 8.27 (d, *J* = 8.4 Hz, 2H), 8.05-7.79 (m, 3H), 7.70-7.61 (m, 4H), 7.70-7.30 (m, 4H), 7.28-6.89 (m, 2H), 6.82 (d, *J* = 7.4 Hz, 2H), 4.87 (s, 4H), 2.54 (s, 2H).

^{13}C NMR (126 MHz, $CDCl_3$) δ = 170.12, 155.15, 153.38, 133.83, 131.95, 130.95, 130.30, 129.43, 126.83, 126.69, 126.47, 125.86, 125.33, 124.59, 122.50, 122.03, 103.95, 93.83, 78.25, 75.89, 56.12.

3.5.2 Synthesis and characterization of 3,3-bis(1-((1-((naphthalen-1-yl) methyl)-1H-1,2,3-triazol-4-yl) methoxy) naphthalen-4-yl) isobenzofuran-1(3H)-one (61b)

Synthesized alkyne **61a** (1.00 g, 2.02 mmol) was taken in 100.00 ml round bottom flask and the solvent mixture THF:TEA (v/v, 1:1) was added into it to get a clear solution. To the above solution, added freshly prepared azidomethylnaphthalene **58** (0.74 g, 4.04 mmol) along with catalytic amount of [$CuBr(PPh_3)_3$] (0.001 mmol) (Scheme 3.11). After stirring the reaction mixture at 60 ℃ for 8.5 h, a reddish brown colored solid **61b** was obtained on putting the ice-cold water into the reaction mixture. The reddish-brown solid was separated out from the reaction mixture by filtration, washed with ice-cold water to remove all the solvent and vacuum dried to get constant weight.

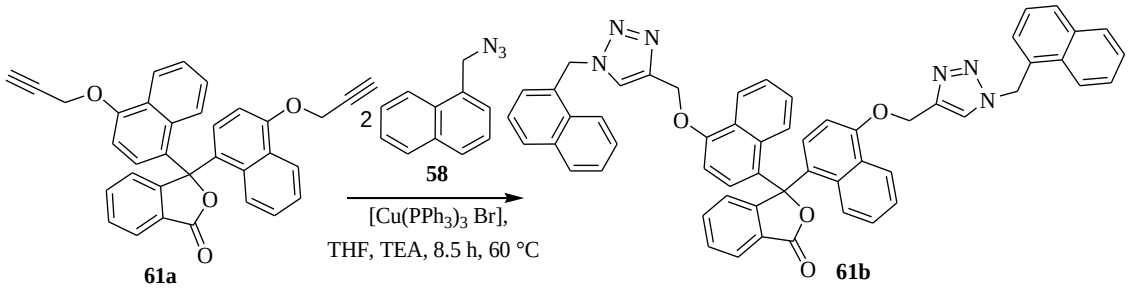

Scheme 3.11: Synthetic route of **61b**

Yield: 95%

Color/Texture: Reddish brown powder

M. Pt. = 220-222 °C

Molecular Formula: $C_{56}H_{40}N_6O_4$

Elem. Anal. Calculated (%): C = 78.12, H = 4.68, N = 9.76; **Found (%):** C = 78.09, H = 4.70, N = 9.79.

IR (neat, cm^{-1}): 3017, 2934, 1767, 1593, 1498, 1460, 1247, 1135, 1053, 941, 807, 761, 720, 619.

^{1}H NMR (500 MHz, $CDCl_3$) δ = 8.12 (d, J = 8.3 Hz, 2H), 8.08-7.82 (m, 4H), 7.54-7.48 (m, 18H), 7.45 (t, J = 7.5 Hz, 2H), 7.26 (s, 3H), 7.14 (s, 2H), 6.77 (s, 2H), 5.99 (s, 4H), 5.28 (s, 4H).

^{13}C NMR (126 MHz, $CDCl_3$) δ = 170.18, 154.80, 153.37, 144.17, 142.91, 141.87, 141.58, 133.96, 133.85, 131.16, 130.17, 129.96, 129.67, 129.43, 129.27, 129.00, 127,99, 127.95, 127.35, 126.46, 125.40, 125.11, 124.57, 123.97, 122.85, 122.76, 122.43, 122.33, 103.97, 93.88, 62.35, 52.49.

Molar Mass Calculated: 860.45; **Observed m/z** = 861.45 $(M+1)^+$

3.6 Sudan-IV dye based terminal alkyne 62a and 1,2,3-triazole derivatives 62b and 62c

3.6.1 Synthesis and characterization of 1-(3-methyl-4-(2-(prop-2-yn-1-yloxy) naphthalene-1-yl) diazenyl) phenyl)-2-(o-tolyl) diazene (62a)

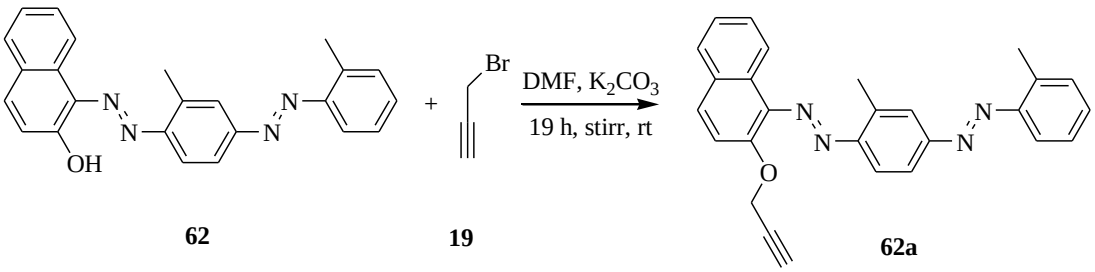

62 **19** **62a**

Scheme 3.12: Synthetic route of **62a**

For the synthesis of alkyne **62a**, the solution of organic dye **62** (Sudan IV, 1.00 g, 2.63 mmol) was prepared in DMF (20.00 ml) taken in a round bottom flask. Thereafter, potassium carbonate (1.82 g, 13.14 mmol) and propargyl bromide (0.31 g, 0.40 ml, 2.63 mmol) was added into the reaction vessel and set to stirring on a magnetic stirrer under normal temperature and pressure conditions (Scheme 3.12).

After 19 h, red colored solid product **62a** was obtained on pouring the reaction mixture into ice-cold water. The product was filtered, washed thoroughly with chilled water and vacuum dried to remove all the solvent to get constant weight.

Yield: 88%

Color/Texture: Red colored solid

M. Pt. = 130-132 °C

Molecular Formula: $C_{27}H_{22}N_4O$

Elem. Anal. Calculated (%): C = 77.49, H = 5.30, N = 13.39; **Found (%):** C = 77. 53, H = 5.28, N = 13.36.

IR (neat, cm^{-1}): 3280, 3050, 2985, 2100, 1550, 1504, 1456, 1274, 1219, 1146, 1057, 810, 679, 523, 556, 457.

^{1}H NMR (500 MHz, $CDCl_3$) δ = 7.98-7.81 (m, 5H), 7.68 (d, *J* = 8.0 Hz, 1H), 7.57 (s, 1H), 7.52 (m, 2H), 7.38 (d, *J* = 7.5 Hz, 2H), 7.27 (d, *J* = 18.0 Hz, 2H), 4.91 (s, 2H), 2.54 (s, 1H), 2.35 (s, 6H).

^{13}C NMR (126 MHz, $CDCl_3$) δ = 153.97, 153.02, 150.91, 147.58, 139.05, 138.54, 138.03, 131.40, 131.35, 131.24, 130.17, 128.51, 128.00, 127.95, 126.47, 125.98, 125.14, 123.79, 121.19, 117.71, 116.36, 115.43, 78.71, 76.08, 59.15, 18.13, 17.61.

3.6.2 Synthesis and characterization of 1-benzyl-4-(((1-((E)-(2-methyl-4-((E)-o-tolyldiazenyl) phenyl) diazenyl) naphthalene-2-yl) oxy) methyl)-1H-1,2,3-triazole (62b)

The synthesized terminal alkyne **62a** (1.00 g, 2.39 mmol) was put into the solvent system, THF:TEA (v/v, 4:1) to get a clear solution, followed by the addition of azidomethylbenzene **24** (0.32 g, 2.39 mmol) and catalytic amount of $[CuBr(PPh_3)_3]$ (0.001 mmol) (Scheme 3.13). The reaction content was refluxed with stirring for 5 h. Wine red colored solid **62b** was produced on treatment with ice-cold water. The solid

was separated out by filtration, washed thoroughly with water to remove solvents and dried to get constant weight.

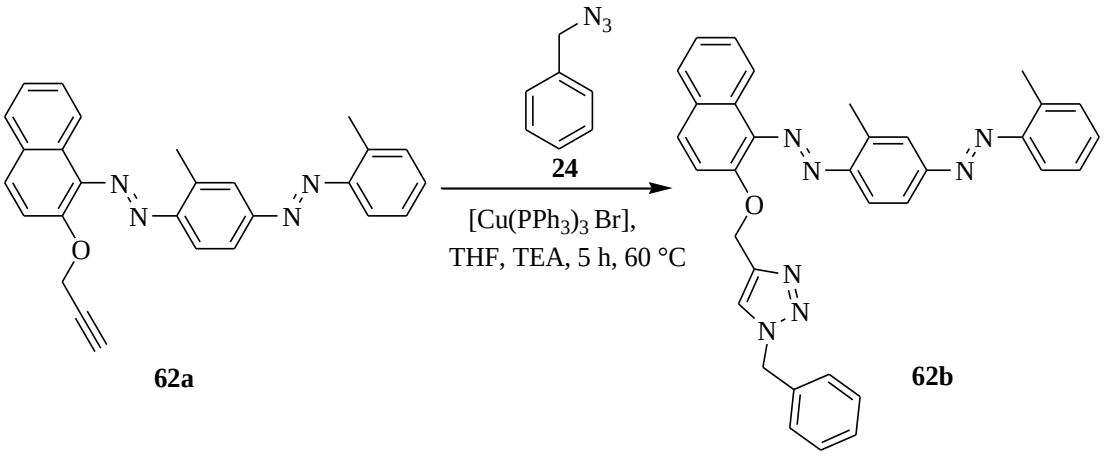

Scheme 3.13: Schematic procedure for the synthesis of **62b**

Yield: 92%

Color/Texture: Wine red solid

M. Pt. = 140-142 °C

Molecular Formula: $C_{34}H_{29}N_7O$

Elem. Anal. Calculated (%): C = 74.03, H = 5.30, N = 17.77; **Found (%):** C = 74.07, H = 5.27, N = 17.72.

IR (neat, cm^{-1}): 3051, 2921, 1561, 1590, 1510, 1455, 1422, 1269, 1250, 1212, 1150, 1044, 891, 828, 807, 763, 603, 493, 455.

^{1}H NMR (500 MHz, $CDCl_3$) δ = 7.98 -7.81 (m, 5H), 7.77 (d, *J* = 8.2 Hz, 1H), 7.73-7.45 (m, 2H), 7.49 (d, *J* = 9.3 Hz, 2H), 7.52-7.45 (m, 2H), 7.45 (s, 2H), 7.46-7.28 (m, 3H), 7.22 (d, *J* = 4.2 Hz, 2H), 7.11-7.02 (m, 1H), 5.45 (s, 2H), 5.43 (s, 2H), 2.79 (s, 3H), 2.65 (s, 3H).

^{13}C NMR (126 MHz, $CDCl_3$) δ = 153.92, 150.95, 147.71, 138.81, 138.52, 137.79, 134.38, 131.59, 131.40, 131.31, 129.84, 129.14, 129.04, 128.80, 128.68, 128.07,

127.98, 126.51, 126.04, 125.00, 123.59, 122.67, 121.14, 117.13, 116.26, 115.46, 65.33, 54.26, 17.82, 17.61.

Calculated Molecular Mass: 551.40; **Observed m/z** = 552.35 $(M+1)^+$

3.6.3 Synthesis and characterization of 4-(((1-((E)-(2-methyl-4-((E)-o-tolyldiazenyl) phenyl) diazenyl) naphthalene-2-yl) oxy) methyl)-1-(naphthalen-1-ylmethyl)-1H-1,2,3-triazole (62c)

To the solution of alkyne **62a** (1.00 g, 2.39 mmol) in THF:TEA (v/v, 4:1) taken in 100.00 ml round bottom flask, mixed newly prepared azidomethylnaphthalene **58** (0.44 g, 2.39 mmol) along with small amount of $[CuBr(PPh_3)_3]$ (0.001 mmol) (Scheme 3.14). The reaction content was allowed to stir at 60 °C for 5.5 h. Wine red colored product **62c** was produced upon addition of ice-cold water into the reaction mixture. The solid was separated by filtration, washed thoroughly with water to remove extra amount of solvent and dried to get constant weight.

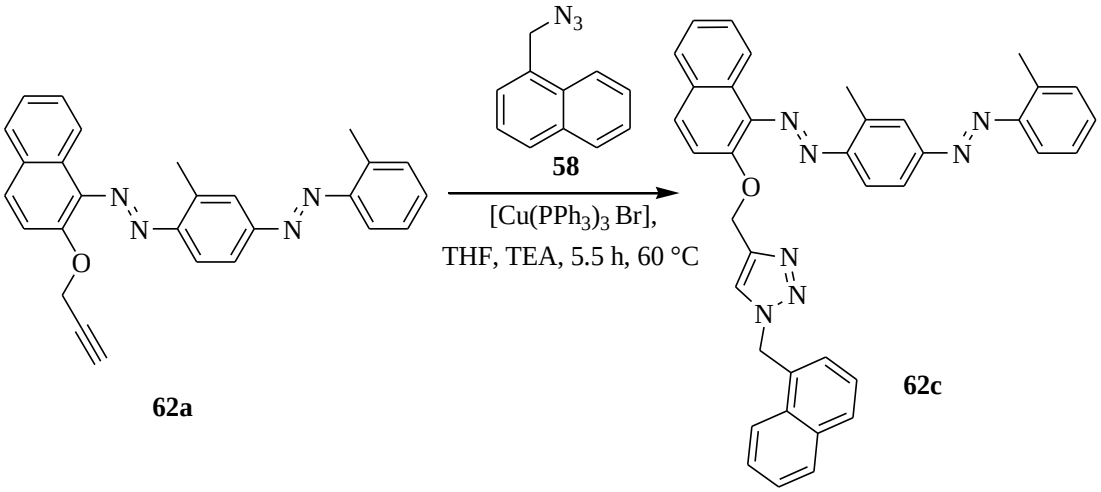

Scheme 3.14: Synthesis of **62c**

Yield: 91%

Color/Texture: Wine red colored solid

M. Pt. = 152-154 °C

Molecular Formula: $C_{38}H_{31}N_7O$

Elem. Anal. Calculated (%): C = 75.85, H = 5.19, N = 16.30; **Found (%):** C = 75.81, H = 5.21, N = 16.33.

IR (neat, cm^{-1}): 3090, 2919, 1592, 1510, 1457, 1270, 1250, 1215, 1151, 1094, 892, 799, 780, 746, 602, 493.

^{1}H NMR (500 MHz, $CDCl_3$) δ = 7.87 (ddd, *J* = 21.1, 18.6, 9.0 Hz, 6H), 7.74 (dd, *J* = 15.9, 8.2 Hz, 4H), 7.59-7.33 (m, 10H), 7.29 (s, 1H), 5.95 (s, 2H), 5.40 (s, 2H), 2.85 (s, 3H), 2.57 (s, 3H).

^{13}C NMR (126 MHz, $CDCl_3$) δ = 155.46, 152.49, 149.25, 140.34, 140.27, 140.06, 139.33, 135.92, 134.12, 133.13, 132.94, 132.84, 132.31, 131.37, 130.91, 130.67, 130.40, 130.34, 130.21, 129.61, 129.52, 128.05, 127.58, 126.54, 125.12, 124.21, 122.68, 118.67, 117.80, 117.00, 66.87, 55.80, 19.36, 19.14.

Calculated Molecular Mass: 601.4; **Observed m/z** = 602.43 $(M+1)^+$

3.7 1-Naphtholbenzein based terminal alkyne 63a and 1,2,3-triazole derivative 63b

3.7.1 Synthesis and characterization of 4-(phenyl (1-(prop-2-ynyloxy) naphthalen-4-yl) methylene) naphthalen-1(4H)-one (63a)

To the solution of compound **63** (1-naphtholbenzein, 1.00 g, 2.68 mmol) in DMF (15.00 ml), pure and dry potassium carbonate (1.84 g, 13.34 mmol) was added. To this solution, next was dropwise addition of accurately weighed propargyl bromide **19** (0.32 g, 0.40 ml, 2.67 mmol). After the addition of all the components of reaction, it was set to stirring at room temperature and observed for the progress of reaction through TLC (Scheme 3.15). After 22 h, rusty red colored solid product was obtained on pouring the reaction mixture into ice-cold water. The product was filtered, washed thoroughly with chilled water and vacuum dried to remove all the solvent to get constant weight. Dried sample was further subjected to its characterization through various spectroscopic techniques like IR and NMR, along with yield and melting point were also noticed.

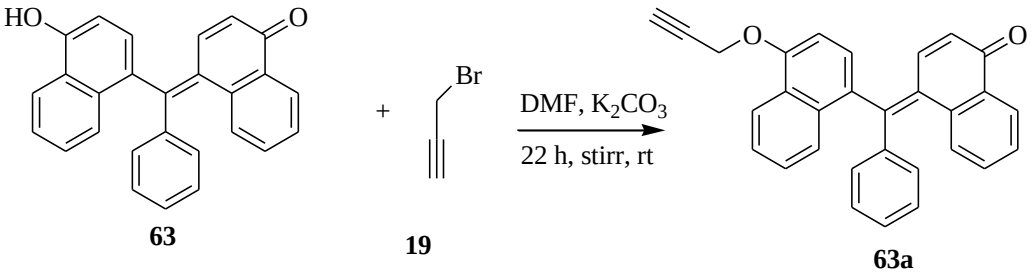

63 **19** **63a**

Scheme 3.15: Synthesis of terminal alkyne **63a**

Yield: 89%

Color/Texture: Rusty red solid

M. Pt. = 118-120 °C

Molecular Formula: $C_{30}H_{20}O_2$

Elem. Anal. Calculated (%): C = 87.36, H = 4.89; **Found (%):** C = 87.30, H = 4.91

IR (neat, cm^{-1}): 3288, 3057, 2982, 2104, 1736, 1561, 1508, 1456, 1234, 1219, 1157, 1078, 810, 679, 523, 556, 470.

^{1}H NMR (500 MHz, $CDCl_3$) δ = 8.13 (d, *J* = 7.9 Hz, 1H), 7.69 (d, *J* = 10.3 Hz, 1H), 7.53 (s, 2H), 7.22 (m, 12H), 6.94 (s, 1H), 6.47 (d, *J* = 10.3 Hz, 1H), 4.86 (s, 2H), 2.51 (s, 1H).

^{13}C NMR (126 MHz, $CDCl_3$) δ = 185.63, 155.53, 155.35, 155.17, 154.35, 144.92, 143.70, 131.50, 130.35, 130.21, 129.40, 129.07, 128.67, 128.56, 127.28, 127.21, 123.46, 106.2, 105.74, 79.02, 77.06, 57.23.

3.7.2 Synthesis and characterization of 1,2,3-triazole derivative 4-((1-((1-benzyl-1H-1,2,3-triazol-4-yl) methoxy) naphthalen-4-yl) (phenyl)methylene) naphthalen-1(4H)-one (63b)

The alkyne **63a** (1.00 g, 2.42 mmol) was dissolved in THF:TEA (v/v, 4:1) taken in 50.00 ml flask, followed by the addition azidomethylbenzene **24** (0.32 g, 2.42 mmol) along with [$CuBr(PPh_3)_3$] (0.001 mmol) (Scheme 3.16). After refluxing the

content of reaction for 4 h, an orange-colored product was separated out upon addition of ice-cold water into the reaction mixture. The solid product was obtained by filtration, washed thoroughly with water to remove solvents and dried well to get final weight of product **63b**.

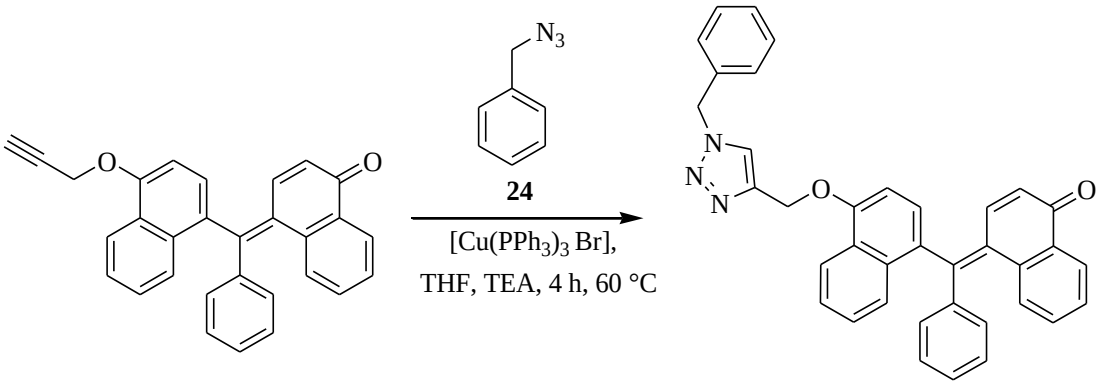

63a **63b**

Scheme 3.16: Schematic procedure for the synthesis of **63b**

Yield: 91%

Color/Texture: Orange colored solid

M. Pt. = 160-162 °C

Molecular Formula: $C_{37}H_{27}N_3O_2$

Elem. Anal. Calculated (%): C = 81.45, H = 4.99, N = 7.70; **Found (%):** C = 81.42, H = 5.01, N = 7.72.

IR (neat, cm^{-1}): 3010, 2964, 1761, 1591, 1440, 1357, 1327, 1246, 1210, 1159, 1051, 967, 812, 761, 721.

^{1}H NMR (500 MHz, $CDCl_3$) δ = 8.26 (s, 1H), 8.19 (m, 1H), 7.78 (d, *J* = 10.5 Hz 6H), 7.61 (m, 9H), 7.34 (s, 2H), 7.29 (s, 1H), 7.01 (dd, *J* = 14.9, 7.2 Hz, 2H), 6.92 (s, 1H), 6.57 (d, *J* = 8.2 Hz, 1H), 5.62 (s, 2H), 5.44 (s, 2H).

^{13}C NMR (126 MHz, $CDCl_3$) δ = 183.57, 154.41, 153.74, 153.46, 143.12, 143.02,

142.92, 139.36, 132.79, 131.12, 130.59, 130.18, 130.01, 129.53, 128.99, 128.59, 128.20, 127.89, 127.82, 127.41, 127.10, 126.52, 126.28, 125.30, 124.72, 122.90, 121.72, 121.59, 121.44, 110.12, 104.78, 61.43, 53.67.

Calculated Molecular Mass: 545.21; **Observed m/z** = 546.22 $(M+1)^+$

Chapter 4

Section I

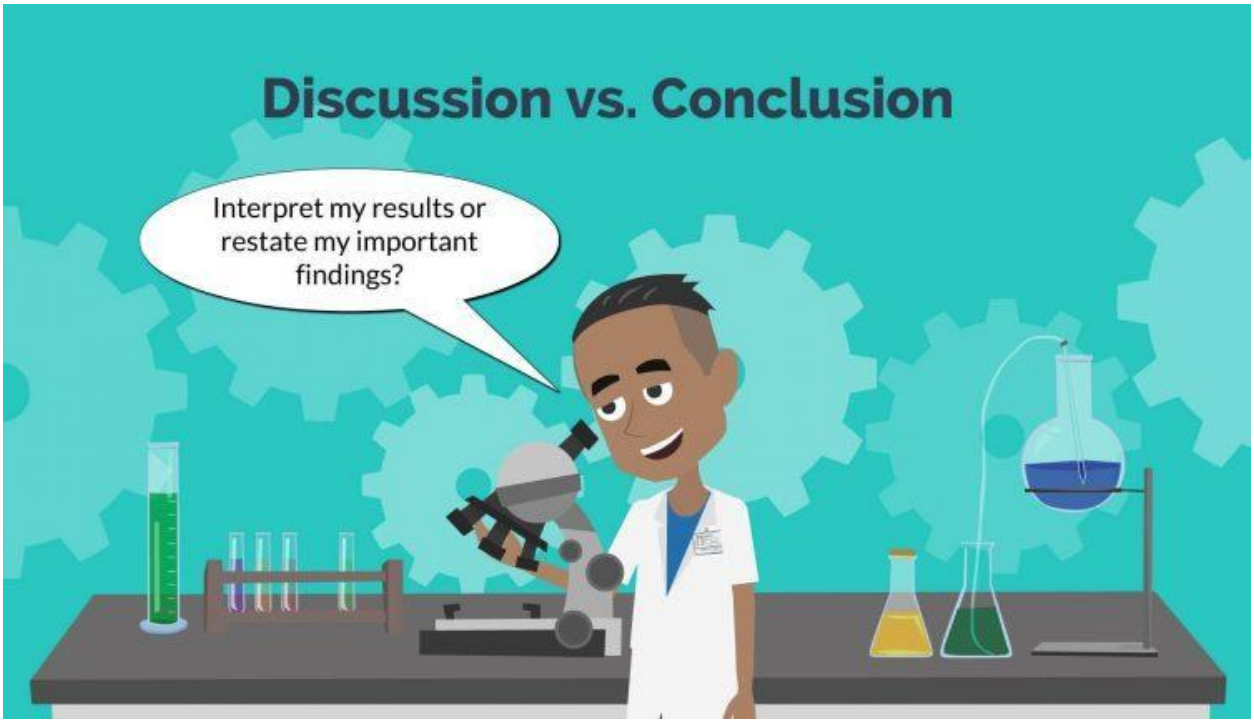

Results and Discussion of Spectroscopic Data

This chapter of thesis presents the findings and outcomes of present research contribution and reasons for those particular results in the form of text and figures.

4.1 Synthetic aspects

The 1,2,3-triazoles are the five membered heterocyclic compounds with three nitrogen atoms, that are aromatic, polar, thermally and chemically very stable and are inert to oxidation and reduction conditions, so considered as one of the most significant nitrogen containing compounds with a wide range of applications in a variety of organic syntheses, supramolecular chemistry, drug discovery, polymer chemistry, cell biology, chemosensing and material science [1-3]. Owing to their versatility in applications, the synthesis of 1,2,3-triazole linked molecules has been a concern of extensive scientific research.

Among the different approaches used to synthesize these magical molecules, the Cu(I)-catalyzed alkyne-azide cycloaddition (CuAAC) reaction has been identified as one of the most important contributions to synthetic organic chemistry [4-6]. The distinctive features of CuAAC reaction includes; high regioselectivity i.e generation of only 1,4-disubstituted 1,2,3-triazole molecule with less or innocuous by-products, excellent yield of product and scope under mild conditions [7-8]. This research work involves the synthesis of various 1,4-disubstituted 1,2,3-triazole derivatives through CuAAC reaction that includes following steps:

(i) Synthesis of terminal alkynes

The synthesis of terminal alkynes involved reaction of substrate having labile protons with propargyl bromide in the presence of suitable base. The labile protons of hydroxyl groups on starting materials get abstracted by base and substituted by propynyl group through nucleophilic substitution reaction on propargyl bromide, by stirring the reaction mixture at room temperature in DMF as solvent. The progress of reaction can be studied by TLC using various solvent combinations. The reaction time varies with change in substrate, as the tendency to lose a proton is different for different starting materials. The synthesized alkyne can be isolated from reaction mixture by filtration, if solid or extracted using suitable solvent, if liquid.

(ii) Synthesis of organic azides

The nucleophilic substitution reaction of aralkyl halide with dried sodium azide resulted into the generation of organic azides, preceded through the method reported by Lourdes et al. [9]. The reaction was carried out in suitable solvent on heating under precautionary measures in order to avoid explosion at higher temperature.

(iii) Cu(I)-Catalyzed alkyne-azide cycloaddition reaction

Terminal alkynes and organic azides undergo 1,3-dipolar cycloaddition reaction in the presence of a base and suitable solvent using a source of Cu(I) as catalyst. After stirring the reaction mixture at a particular temperature, 1,4-disubstituted 1,2,3-triazole linkers get formed as a result of click cycloaddition. Use of Cu(I) species as catalyst enhances the rate as well as stereo specificity of reaction.

4.2 Synthesis and spectral analysis of 1-(azidomethyl) benzene (24)

4.2.1 Synthesis

Benzyl azide **24** (Figure 4.1) was synthesized through the nucleophilic substitution reaction of chloromethylbenzene with dried NaN_3 in DMF as solvent on stirring for 5 h at 85-90 °C. As the azides are highly reactive and explosive at high temperature, the reaction conditions were properly controlled in order to avoid any accident. After extracting the benzyl azide by ethylacetate from reaction mixture, it was dried to remove all the solvents and then characterized by IR and NMR spectroscopy.

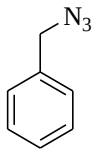

Figure 4.1: 1-(azidomethyl) benzene **24**

4.2.2 IR spectral analysis

The IR spectrum of freshly prepared benzyl azide was recorded as neat in the range 4000-500 cm^{-1} that displayed a strong peak at 2091 cm^{-1} characteristic to azide group indicating the substitution over benzyl chloride with azide group. Peak at 3050

cm^{-1} corresponds to vibration of aromatic **C-H** bond and at 2931 cm^{-1} is for symmetric stretch of **C-H** bond at benzylic carbon. Peaks in the fingerprint region are in line with the structure of synthesized azide molecule.

4.2.3 NMR spectral analysis

^{1}H NMR spectrum of benzyl azide obtained at 500 MHz in $CDCl_3$ with respect to tetramethylsilane as reference. It exhibited multiplet signal at δ = 7.24-7.14 ppm, which is due to five aromatic protons on benzene ring and a singlet at δ = 4.14 ppm, that corresponds to two protons on benzylic carbon.

^{13}C NMR spectrum of benzyl azide was also recorded in $CDCl_3$ and the data found was exactly in support of the structure of investigated azide. It has peaks at δ (ppm) = 135.53, 128.37, 128.91, 128.31 and 54.82. The signals in the range δ = 135.53-128.31 ppm belongs to carbons of benzene ring and at δ = 54.82 ppm corresponds to benzylic carbon.

4.3 Synthesis and spectral analysis of 1-(azidomethyl) naphthalene (58)

4.3.1 Synthesis

The nucleophilic substitution reaction of chloromethylnaphthalene with highly reactive sodium azide resulted into azidomethylnaphthalene **58** (Figure 4.2), an aromatic organic azide.

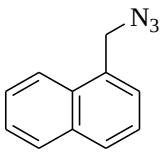

Figure 4.2: 1-(azidomethyl) naphthalene **58**

The reaction was conducted on stirring the components of reaction mixture at 85-90 °C in DMF that end up with brown oily product, extracted through ethylacetate. Extracted product was firstly dried over anhydrous sodium sulphate and then vaccum dried to found its exact yield. Thereafter, the pure product was characterized by IR and NMR spectroscopy to confirm its generation.

4.3.2 IR spectral analysis

The IR spectrum of azidomethylnaphthalene was recorded as neat in the range 4000-500 cm^{-1}. The high intensity peak at 2091 cm^{-1} confirms the presence of azide group and a signal at 3040 cm^{-1} corresponds to vibrational frequency of aromatic C-H bond. Rest of the peaks found in IR spectrum are due to different types of vibrational modes found in molecule **58** and are in well agreement with the structure of synthesized molecule.

4.3.3 NMR spectral analysis

^{1}H NMR spectrum of azidomethylnaphthalene was obtained at 500 MHz in $CDCl_3$, the peaks at δ (ppm) = 8.12, 7.99, 7.65, 7.53 corresponds to aromatic protons of naphthyl group and singlet obtained at δ = 4.78 ppm is for $–CH_2$ group attached to azide functionality. On the same note, the data obtained from ^{13}C NMR is in accordance with the expected results. The signals in the range δ = 134.05-123.64 ppm are due to carbon atoms of aromatic ring and at δ = 53.02 ppm corresponds to methylene carbon of synthesized molecule **58**.

4.4 Synthesis and spectral analysis of 3,3-bis(3-methyl-4-(prop-2-ynyloxy) phenyl) isobenzofuran-1(3H)-one (59a)

4.4.1 Synthesis

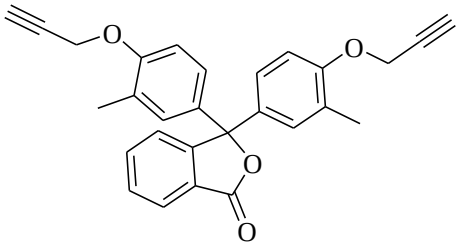

Figure 4.3: 3,3-bis(3-methyl-4-(prop-2-ynyloxy) phenyl) isobenzofuran-1(3H)-one **59a**

The terminal alkyne **59a** (Figure 4.3) was synthesized by nucleophilic substitution reaction of starting material (o-cresolphthalein) with 1.30 mol of 80%

propargyl bromide solution. With K_2CO_3 as base, labile proton of hydroxyl group on starting material was substituted by propynyl group by stirring at room temperature. Highly viscous and yellow colored oily product as terminal alkyne was extracted from reaction mixture for further use in cycloaddition reaction.

4.4.2 IR spectral analysis

The IR spectra of newly synthesized alkyne **59a** and starting material **59** were obtained in the range 4000-500 cm^{-1} as neat and compared, the data obtained was as per the expectation. The IR signal at 3287 cm^{-1} is for –C≡**C**−**H** group and at 2117 cm^{-1} is due to **−C≡C−** moiety in the newly prepared alkyne. Peak at 1759 cm^{-1} corresponds to carbonyl group in the molecule. No signal in region 3500-3350 cm^{-1} due to **−O−H** group confirms the moderation of –OH group on the starting molecule. Other peaks (fingerprint region) in the spectrum are due to a large number of vibrations of different types of bonds are in accordance with the molecular structure of **59a**.

4.4.3 NMR spectral analysis

In the ^{1}H NMR spectrum of compound **59a**, singlet at δ = 2.40 ppm is for proton of terminal alkyne group (≡C-**H**) and peak at δ = 4.57 ppm is for –C**H₂** of propynyl group indicates the formation of expected alkyne. No signal at δ = 5.38 ppm due to –O**H** group in the spectrum of compound **59a** confirms the modification of this group. Signals in the range δ = 7.82-6.76 ppm characterizes aromatic protons and singlet at δ = 2.06 ppm corresponds to protons of two methyl groups in the synthesized alkyne **59a**.

In the ^{13}C NMR spectrum of molecule **59a**, the peaks at δ (ppm) = 78.71, 75.69 corresponds to **−C≡C−** and singlet at δ = 55.94 ppm is for carbon of –**C**H_2−O− group ensures the generation of terminal alkyne **59a**. Signals in the range δ = 169.99-124.17 ppm corresponds to differently shielded aromatic carbons present in phthalein unit of molecule and at δ = 16.45 ppm represents the carbons of two methyl groups.

4.5 Synthesis and spectral analysis of 3,3-bis(4-((1-benzyl-1H-1,2,3-triazol-4-yl) methoxy)-3 methylphenyl) isobenzofuran-1(3H)-one (59b)

4.5.1 Synthesis

o-Cresolphthalein based 1,2,3-triazole derivative **59b** shown in Figure 4.4 was stereo selectively prepared by 1,3-dipolar cycloaddition reaction of alkyne **59a** with 1-(azidomethyl) benzene **24** using [$CuBr(PPh_3)_3$] (0.001 mmol) complex as catalyst in THF:TEA (v/v, 1:1) solvent mixture. Presence of Cu(I)-complex as catalyst defined the stereoselectivity of cycloaddition to get 1,4-disubstituted product only and triethyl amine base helped in easy abstraction of terminal proton on alkyne **59a** to facilitate 1,3-dipolar cycloaddition of azide **24.** The reaction completed in 5 h on stirring the components of reaction mixture at 60-65 °C. Solid product was obtained on treatment of reaction mixture with ice-cold water and was fully characterized by various spectroscopic techniques.

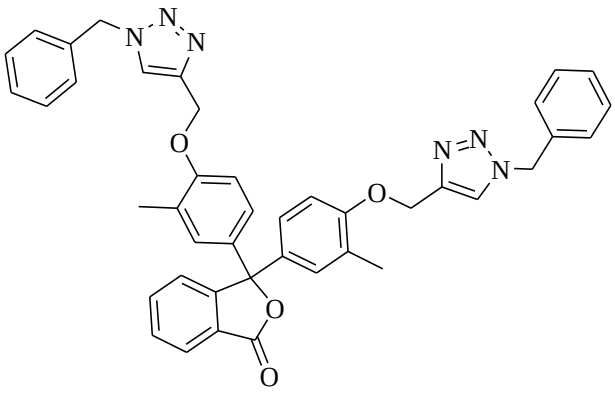

Figure 4.4: 3,3-bis(4-((1-benzyl-1H-1,2,3-triazol-4-yl) methoxy)-3 methylphenyl) isobenzofuran-1(3H)-one **59b**

4.5.2 IR spectral analysis

Vibrational spectrum of 1,2,3-triazole derivative **59b** was recorded as neat in the range 4000-500 cm^{-1}. It shows vibrational band at 3141 cm^{-1} that is due to –C=**C-H** group at C_5 carbon of 1,2,3-triazole ring. The absence of peaks at 3288 cm^{-1} for the vibration of –C≡**C**−**H** bond and at 2117 cm^{-1} corresponding to vibration of –**C**≡**C**−

moiety in the IR-spectrum of alkyne **59a** along with a signal at 2091 cm^{-1} for **$-N_3$** group in the spectrum of organic azide **24** proves the success of expected cycloaddition reaction between alkyne **59a** and azide **24** to generate heterocyclic molecule **59b** as shown in Figure 4.4. There are asymmetric stretching bands at 1606 cm^{-1} and 1498 cm^{-1}, that corresponds to –**C=C-** and –**N=N-** groups in the resulting molecule.

4.5.3 NMR spectral analysis

The ^{1}H NMR spectrum of compound **59b** strongly favors the cycloaddition of terminal alkyne **59a** with organic azide **24**. The peak at δ = 4.57 ppm is due to protons of –C**H_2** group linked to cresol oxygen, that gets downfield (δ = 5.52 ppm), because of desheilding caused by 1,2,3-triazole ring attached to this part of the molecule. The signal of proton of terminal alkyne group at δ = 2.40 ppm is absent, as it is now a part of aromatic triazole ring. The singlet at δ = 5.17 ppm belongs to benzylic –C**H_2** group of product **59b** as shown in Figure 4.5. Also, the ^{13}C NMR spectrum of heterocyclic compound **59b** verifies the successful outcome of cycloaddition reaction. The signal at δ = 55.94 ppm due to carbon atom of –**C**H_2−O− group in the spectrum of **59a** shifted downfield at δ = 66.06 ppm, as it is now directly linked to the triazole ring of molecule **59b**. A singlet at δ = 54.62 ppm observed in the spectrum of triazole linked molecule corresponds to –**C**H_2 of benzyl group. The signals at δ = 78.70 ppm and 76.58 ppm for **−C≡C−** present in the spectrum of alkyne gets down in aromatic region, as this moiety constituted triazole ring of molecule **59b**.

4.5.4 Mass spectral and elemental analysis

The molecular mass ‘M’ of newly synthesized triazole derivative **59b** is calculated as 688.28 and the mass spectrum obtained for this molecule shows a significant peak at m/z = 689.28 corresponding to $(M+1)^{+}$, confirms the successful generation of heterocyclic molecule **59b**, a product of Cu(I)-catalyzed cycloaddition reaction between o-cresolphthalein based terminal alkyne **59a** and benzyl azide **24**. As per the results of elemental analysis, the observed percentages of elements of molecule **59b** are in close agreement with the calculated percentages.

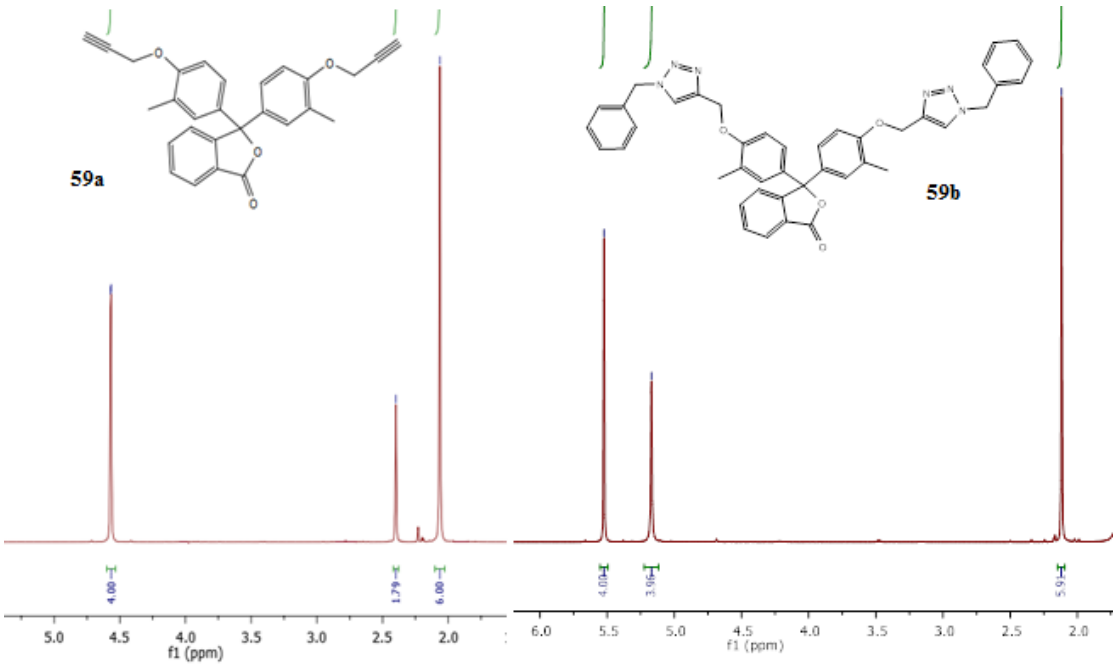

Figure 4.5: ^{1}H NMR spectra of compound **59a** and **59b** showing success of cycloaddition reaction

4.6 Synthesis and spectral analysis of 3,3-bis(4-((1-((naphthalen-1-yl) methyl)-1H-1,2,3-triazol-4-yl) methoxy)-3-methylphenyl) isobenzofuran-1(3H)-one (59c)

4.6.1 Synthesis

Using terminal alkyne **59a**, another triazole derivative **59c** was prepared through Cu(I)-catalyzed alkyne-azide cycloaddition reaction. The reaction involved use of azidomethylnaphthalene **58** as an organic azide that undergo cycloaddition with o-cresolphthalein based alkyne **59a** in the presence of [$CuBr(PPh_3)_3$] complex as Cu(I)-catalyst in THF:TEA (v/v, 1:1) as a solvent mixture upon stirring at 60-65 °C to give 1,2,3-triazole linker **59c** as a desired product shown in Figure 4.6.

4.6.2 IR spectral analysis

IR spectrum of heterocyclic compound **59c** was obtained as neat in the IR range 4000-500 cm^{-1}. No signal at 3287 cm^{-1} for –C≡**C**–**H** group and 2117 cm^{-1} due to –**C**≡**C**– part of alkyne in the IR spectrum of **59c** ensures the modification of

terminal alkyne**,** when treated with organic azide **58.** The signal at 3025 cm^{-1} is due to –C=**C-H** group at C_5 of 1,2,3-triazole ring and at 1499 cm^{-1} corresponds to –**N=N-** in the product of cycloaddition and at the same time, absence of peak at 2091 cm^{-1} for **–N_3** group ensures the favorable outcome of cycloaddition process as an expected product **59c** as depicted in Figure 4.6.

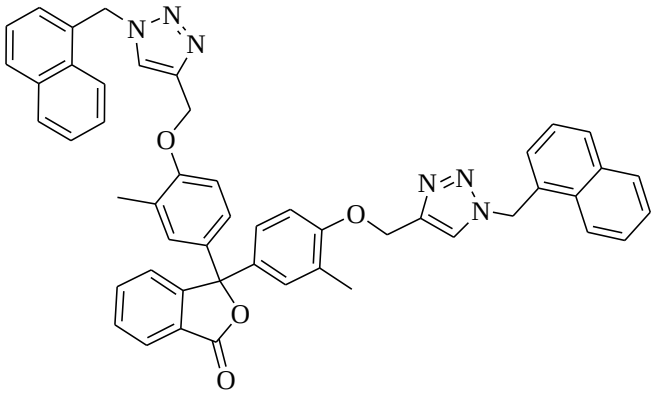

Figure 4.6: 3,3-bis(4-((1-((naphthalen-1-yl) methyl)-1H-1,2,3-triazol-4-yl) methoxy)-3-methylphenyl) isobenzofuran-1(3H)-one **59c**

4.6.3 NMR spectral analysis

The ^1H NMR spectrum of compound **59c** recorded at 500 MHz in $CDCl_3$ shows a number of signals in the range δ = 7.92-6.80 ppm that corresponds to aromatic protons in the heterocyclic product **59c.** Peak at δ = 4.56 ppm recorded in the spectrum of **59a** for –C**H_2** group with o-cresol oxygen has been shifted down at δ = 5.98 ppm in the spectrum of **59c** due to desheilding caused by triazole ring. The singlet due to terminal alkynyl proton at δ = 2.40 ppm has been lost, as it is then attached to C_5 of aromatic 1,2,3-triazole ring. The peak at δ = 5.10 ppm is due to –C**H_2** group bonded to naphthyl group of compound **59c**.

The data obtained from ^{13}C NMR spectrum of heterocyclic molecule **59c** also explains the success of cycloaddition reaction. The singlet at δ = 55.93 ppm due to the carbon of –**C**H_2–O– in the record of **59a** shifted downfield at δ = 62.31 ppm, as it is now linked to the 1,2,3-triazole unit in derivative **59c**. The signal at δ = 52.44 ppm

observed in the spectrum of triazole linked molecule corresponds to –**C**H_2 of naphthyl group.

4.6.4 Mass spectral and elemental analysis

HRMS obtained for molecule **59c** shows an observable peak at m/z = 789.32 that represents a peak at $(M+1)^+$ value, where 'M' is the molecular mass of newly synthesized triazole derivative **59c** which is calculated as 788.85. Parent ion peak and other signals due to fragment ions confirm the successful generation of heterocyclic compound **59c**, a product of Cu(I)-catalyzed cycloaddition reaction of o-cresolphthalein based terminal alkyne **5a** with azidomethylnaphthalene **58**. The calculated and observed percentage of component elements was also in favor of synthesized molecule.

4.7 Synthesis and spectral analysis of 1,4-bis(prop-2-ynyloxy) anthracene-9,10-dione (60a)

4.7.1 Synthesis

In the presence of potassium carbonate as base, the protons of hydroxyl functional groups on the substrate 1,4-dihydroxyanthraquinone were nuleophilicaly substituted by propargyl group to give terminal alkyne **60a**. The reaction took place by simple stirring at room temperature in DMF as solvent to produce a mustard-colored solid product shown in Figure 4.7 in good yield. The solid product was filtered, washed well to remove all the impurities and vacuum dried to find constant weight.

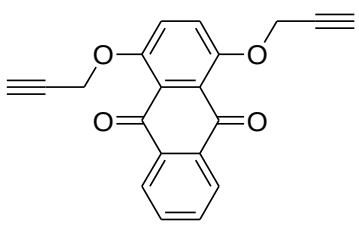

Figure 4.7: 1,4-bis(prop-2-ynyloxy) anthracene-9,10-dione **60a**

Melting point of product was recorded to check its purity. The exact structure of compound **60a** was elucidated by IR and NMR spectroscopy to confirm its successful generation for further use as one of the reactants of [3+2] cycloaddition reaction in order to generate 1,2,3-triazole derivatives.

4.7.2 IR spectral analysis

The synthesized alkyne molecule **60a** was characterized by IR spectroscopy in the range 4000-500 cm^{-1} and the data obtained was in line with anticipated values. IR peak found at 2160 cm^{-1} is the vibrational frequency of **−C≡C−** bond and at 3288 cm^{-1} corresponds to –C≡**C−H** stretching mode. Signal at 3020 cm^{-1} is due to aromatic **-C-H** stretch and for carbonyl group, IR peak is observed at frequency of vibration equal to 1725 cm^{-1}. Clear spectrum in the region 3500-3350 cm^{-1} due to vibration of –**O-H** bond confirms the substitution of protons on hydroxyl groups of starting material **60** with propynyl groups and confirms the formation of designed alkyne **60a**.

4.7.3 NMR spectral analysis

Interpretation of NMR spectrum of molecule **60a** strongly favors its generation. The singlet signal at δ = 2.57 ppm in the ^{1}H NMR of alkyne **60a** corresponds to alkynyl proton ≡C-**H** and peak at 4.90 ppm is due to protons of –C**H₂**–O– group attached to terminal alkyne. Signals from δ = 8.16 ppm to δ = 7.52 ppm are due to aromatic protons of anthraquinone moiety of compound **60a**. Data of ^{13}C NMR spectrum of this newly synthesized alkyne also favors its successful generation. The signals at δ = 78.19 ppm, 76.69 ppm are due to carbons of **−C≡C−** and at δ = 58.28 ppm is for carbon of –**C**H_2−O− ensures the synthesis of alkyne. Signals at higher δ values belong to carbons of aromatic part of this molecule.

4.8 Synthesis and spectral analysis of 1,4-bis((1-benzyl-1H-1,2,3-triazol-4-yl) methoxy) anthracene-9,10-dione (60b)

4.8.1 Synthesis

In order to prepare triazole linker 1,4-bis((1-benzyl-1H-1,2,3-triazol-4-yl) methoxy) anthracene-9,10-dione (**60b**) shown in Figure 4.8, the mustard yellow colored solid alkyne **60a** discussed in section 4.7 was treated with required amount of freshly prepared azidomethylbenzene **24** in THF:TEA (v/v, 4:1) as solvent system using catalytic amount of [$CuBr(PPh_3)_3$] (0.001 mmol) as a source of Cu(I). Use of [$CuBr(PPh_3)_3$] complex increases the rate as well as stereoselectivity of the reaction that yields 99% of heterocyclic compound **60b** as a result of [3+2] cycloaddition reaction between alkyne **60a** and organic azide **24**, completed in just 30 min on stirring the reaction components at 60 °C.

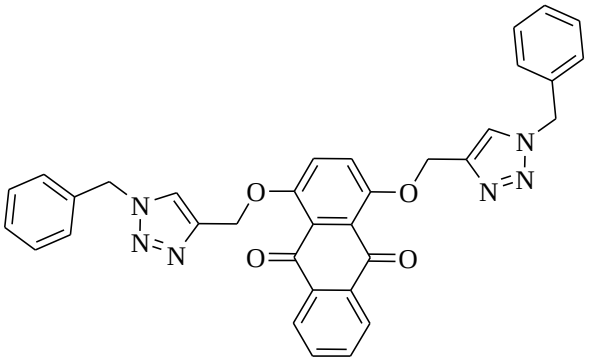

Figure 4.8: 1,4-bis((1-benzyl-1H-1,2,3-triazol-4-yl) methoxy) anthracene-9,10-dione **60b**

4.8.2 IR spectral analysis

In the IR spectrum of molecule **60b**, the signal at 3073 cm^{-1} is due to –C**=C-H** group of 1,2,3-triazole ring. The close comparison of IR spectra of starting materials related to CuAAC reaction, **60a** and **24** clearly signifies the formation of heterocyclic product **60b** as an outcome of the reaction. The fading of signals at 3288 cm^{-1} for the stretching vibration of –C≡**C**−**H** bond and at 2160 cm^{-1} due to –**C**≡**C**− accompanying a peak at 2091 cm^{-1} due to vibration of **–N_3** supports the success of [3+2] cycloaddition reaction to produce the designed triazole linker **60b**.

4.8.3 NMR spectral analysis

NMR spectral elucidation of molecules **60a** and **60b** shows the data as per the expected values. The peak at δ = 2.57 ppm for the alkynyl proton ≡C-**H** in ^{1}H NMR spectrum of alkyne **60a** is missing in the ^{1}H NMR spectrum of triazole derivative **60b**, indicates the moderation of alkyne molecule. The study of mechanism of reaction involving synthesis of product **60b** shows that this alkynyl carbon constitutes 1,2,3-triazole ring as a result of Cu(I)–catalyzed cycloaddition reaction among the terminal alkyne **60a** and azide **24**. The signal of this proton is now present in aromatic region. The peak at δ = 4.90 ppm in ^{1}H NMR spectrum of alkyne **60a** for the proton of –C**H$_2$**–O– get shifted downfield and appeared at δ = 5.57 ppm due to linking of this group with aromatic triazole moiety in the heterocyclic assembly **60b**. One more signal was recorded at δ = 5.34 ppm that was identified as a singlet due to four benzylic protons.

Peaks at δ = 78.19 ppm and 76.69 ppm due to **−C≡C−** (^{13}C NMR spectrum of alkyne **60a**) are extinct in the ^{13}C NMR spectra of 1,4-bis((1-benzyl-1H-1,2,3-triazol-4-yl) methoxy) anthracene-9,10-dione **60b** ensures merging of these alkynyl carbons into triazole ring during cycloaddition reaction and now appeared at higher δ values in the spectrum of **60b**.

4.8.4 Mass spectral and elemental analysis

Molar mass has been observed at m/z = 583.21 $(M+1)^{+}$ in the mass spectra (HRMS) of triazole derivative **60b** against the calculated molecular mass 'M' as 582.21 proved as strong evidence in favor of successful generation of this molecular framework. In elemental analysis the observed values of percentages of elements are in line with the calculated values.

4.9 Synthesis and spectral analysis of 1,4-bis((1-methylnaphthyl-1H-1,2,3-triazol-4-yl) methoxy) anthracene-9,10-dione (60c)

4.9.1 Synthesis

1,4-Dihydroxyanthraquinone linked triazole **60c** as shown in Figure 4.9 is prepared from alkyne **60a** on treatment with azidomethylnaphthalene **58** in the presence of catalytic amount of [$CuBr(PPh_3)_3$] complex through a Cu(I)-catalyzed alkyne-azide cycloaddition process, a worldwide popular form of 'Click Chemistry'**.** The reaction proceeded on stirring the component reactants at 60 °C in THF:TEA (v/v, 4:1) solvent system. The cycloaddition was so quick, that a maximum of yellow colored solid **60c** was collected in the reaction mixture in just 40 min as a pure component with an excellent yield of 99%. The purity and generation of designed triazole derivative was confirmed through various spectroscopic techniques.

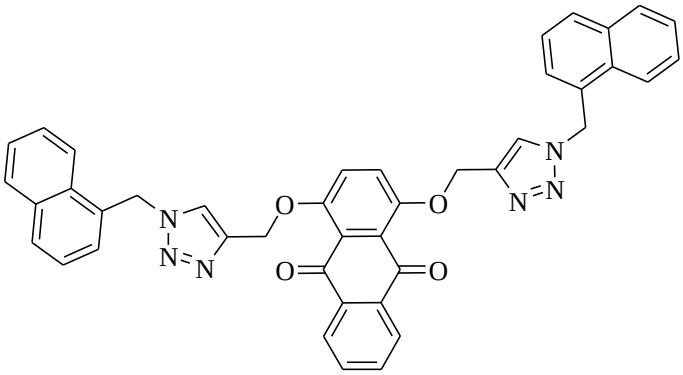

Figure 4.9: 1,4-bis((1-methylnaphthyl-1H-1,2,3-triazol-4-yl) methoxy) anthracene-9,10-dione **60c**

4.9.2 IR spectral analysis

IR spectrum of 1,4-dihydroxyanthraquinone based 1,2,3-triazole derivative **60c** was recorded as neat in range 4000-500 cm^{-1}. A signal at 3078 cm^{-1} found in the spectrum, corresponds to vibrational frequency of –C**=C-H** group of triazole ring. The signals at 3288 cm^{-1} for –C**≡C−H** stretching and at 2160 cm^{-1} for –**C≡C−** including a peak at 2091 cm^{-1} due to **$-N_3$** are absent in the spectrum of triazole linked molecule **60c** that ensures the success of reaction between alkyne **60a** and azide **58** to produce the expected compound. Other peaks are in accordance with the different functional groups and various types of bonds present in the newly generated molecule.

4.9.3 NMR spectral analysis

NMR spectrum of triazole derivative **60c** was recorded in DMSO as solvent using 500 MHz spectrometer. The aromatic protons of benzene rings as well as protons at C_5 of both the triazole rings, all shows NMR signals in range δ = 7.46-6.45 ppm. The protons which are more deshielded due to being attached with electron withdrawing groups appear more downfield i.e., at higher δ values as compared to others. The peak at δ = 2.57 ppm due to the proton ≡C-**H** group found in ^{1}H NMR spectrum of alkyne **60a** is lost in the ^{1}H NMR spectrum of triazole derivative **60c**, indicates modification of alkyne molecule during its reaction with azidomethylnaphthalene **58**. As the alkyne constitutes triazole ring during the cycloaddition process, the terminal proton changes to aromatic one (proton at C_5 of 1,2,3-triazole ring) and appeared very downfield. The peak at δ = 4.90 ppm in ^{1}H NMR of alkyne **60a** for the protons of –C**H$_2$**–O– group shifted downfield and appeared at δ = 5.22 ppm due to its bonding with aromatic triazole moiety in the heterocyclic compound **60c**. Signal at δ = 4.34 ppm was identified as a singlet due to four protons of methylene groups attached with naphthalene rings.

Peaks at δ = 78.19 ppm and 76.69 ppm for **−C≡C−** in the ^{13}C NMR of alkyne **60a** are missing in the ^{13}C NMR spectrum of **60c** proves the merging of these alkynyl carbons into triazole ring during cycloaddition reaction and appeared at higher δ values in the spectrum of **60c**. All other signals in the ^{13}C NMR of **60c** are in accordance with the expected data.

4.9.4 Mass spectral and elemental analysis

The peak at m/z = 683.35 $(M+1)^+$ for the ion of 1,2,3-triazole linker **60c** justifies the success of cycloaddition reaction for the generation of that particular compound. 'M' corresponds to molecular mass of parent ion which is calculated as 682.21. Other signals at lower m/z values explain fragmentation of parent ion. From the data obtained from elemental analysis, it is noticed that the observed percentages of constituent elements are quite similar to the calculated ones that supports the results obtained from other studies.

4.10 Synthesis and spectral analysis of 3,3-bis(1-(prop-2-ynyloxy) naphthalen-4-yl) isobenzofuran-1(3H)-one (61a)

4.10.1 Synthesis

The protons of two hydroxyl groups on starting material **61**(1-naphtholphthalein) undergoes nucleophilic substitution by propynyl groups to get a novel terminal alkyne **61a** (Figure 4.10) during the reaction of compound **61** with propargyl bromide **19** in the presence of potassium carbonate as base on stirring at room temperature. After a stirring of 28 h, the product **61a** was obtained as solid on treatment of reaction mixture with ice cold water. Solid was filtered and washed well with chilled water in order to remove extra solvent. The isolated solid was vacuum dried to get constant weight. Melting point was recorded to check the purity of alkyne **61a** and its generation was confirmed by IR and NMR spectroscopy for further use as starting material of CuAAC reaction to get chemosensing material.

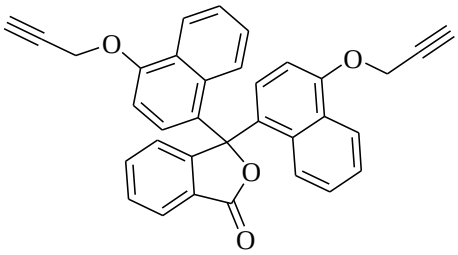

Figure 4.10: 3,3-bis(1-(prop-2-ynyloxy) naphthalen-4-yl) isobenzofuran-1(3H)-one **61a**

4.10.2 IR spectral analysis

IR spectra of both starting material **61** and **61a** were recorded as neat in the range 4000-500 cm^{-1} and compared for useful changes occurred during the reaction of compound **61** with propargyl bromide. There was no broad band near 3400 cm^{-1} due to hydroxyl group in the spectrum of product **61a** indicated modification over –OH functional group on starting molecule **61**. Peaks found at 3288 cm^{-1} corresponds to –C≡**C**−**H** and at 2034 cm^{-1} is due to −**C**≡**C**− group of terminal alkynes. Peaks in the range below 1500 cm^{-1} corresponds to various vibrational modes of bonds constituting unsaturated moiety in the synthesized alkyne.

4.10.3 NMR spectral analysis

^{1}H NMR spectrum of alkyne **61a** have a singlet at δ = 2.54 ppm that is due to protons of ≡C-**H** and at δ = 4.87 ppm represents –C**H₂** group attached with the oxygen of 1-naphthol unit of alkyne **61a** supported its successful generation from starting material **61**, whose NMR spectrum does not have these signals. Moreover, the signal at δ = 5.57 ppm corresponding to protons of –O**H** group present in the spectrum of compound **61** is absent in the spectrum of molecule **61a** that proves certain type of modification over -OH group.

Similarly, the data obtained from ^{13}C NMR supports the generation of expected product **61a.** The signals at δ = 78.25 ppm and 75.89 ppm corresponds to **−C≡C−** and at δ = 56.12 ppm notifies the carbon of –**C**H₂−O− group in the newly synthesized alkyne molecule **61a**. Peaks at higher chemical shift (δ values) represent aromatic carbons of 1-naphtholphthalein unit.

4.11 Synthesis and spectral analysis of 3,3-bis(1-((1-((naphthalen-1-yl) methyl)-1H-1,2,3-triazol-4-yl) methoxy) naphthalen-4-yl) isobenzofuran-1(3H)-one (61b)

4.11.1 Synthesis

Using catalytic amount of [CuBr(PPh₃)₃] complex, the highly acclaimed stereoselective click cycloaddition reaction of newly synthesized 1-naphtholphthalein based terminal alkyne **61a** and azidomethylnaphthalene **58** as an azide, the second reactant of Cu(I)-catalyzed cycloaddition reaction was conducted in a basic medium of THF:TEA (v/v, 1:1) to get 1-naphtholphthalein based 1,2,3-triazole derivative **61b** as the final product shown in Figure 4.11. The basic medium promotes easy abstraction of terminal alkynyl proton to form copper-acetylide intermediate that fuses with azide very stereoselectively to yield expected product. The triazole linker **61b** was characterized by various spectroscopic techniques like IR, NMR and mass discussed in next coming sections and was further investigated for its chemosensing applications through UV-Visible spectroscopy.

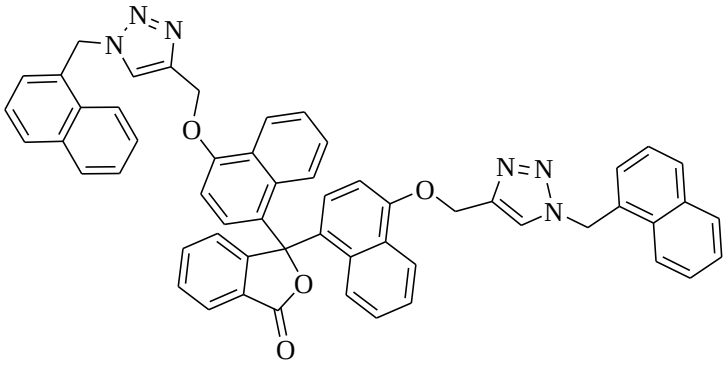

Figure 4.11: 3,3-bis(1-((1-((naphthalen-1-yl) methyl)-1H-1,2,3-triazol-4-yl) methoxy) naphthalen-4-yl) isobenzofuran-1(3H)-one **61b**

4.11.2 IR spectral analysis

IR spectra of all the newly synthesized compounds (terminal alkyne **61a**, azidomethylnaphthalene **58** and final product of cycloaddition **61b**) were obtained as neat in the range 4000-500 cm^{-1} and the results found were compared for the success of CuAAC reaction between terminal alkyne **61a** and azide **58**. IR peaks due to vibrational stretching of –C≡**C**−**H**, −**C**≡**C**− bonds of terminal alkyne found at 3287 cm^{-1} and 2034 cm^{-1} respectively were absent in the vibrational spectrum of click generated product **61b** confirms its generation. A signal at 2091 cm^{-1} in the IR spectra of azidomethylnaphthalene **58** due to **–N_3** group was also missing in the spectrum of cycloaddition product **61b** supports the expected outcome of CuAAC reaction. Signals at 3017 cm^{-1} in the spectrum of **61b** is due to –C=**C-H**, at 2934 cm^{-1} is for methylene –**C-H** stretching, at 1767 cm^{-1} signifies vibrations of carbonyl group and other peaks at 1498 cm^{-1} and 1247 cm^{-1} are due to vibrations of –**C=C-** and **–N=N-** moieties in the heterocyclic product **61b**.

4.11.3 NMR spectral analysis

^{1}H NMR spectrum of compound **61b** strongly authenticates the cycloaddition of alkyne **61a** with azidomethylnaphthalene **58**. The spectrum illustrates the downfield shifting of peak at δ = 4.87 ppm (spectrum of alkyne **61a**) due to –CH_2 linked with oxygen of 1-naphthol unit to δ = 5.99 ppm, as a result of its attachment with 1,2,3-triazole ring of molecule **61b** along with disappearance of the signal of

proton of terminal alkyne at δ = 2.54 ppm. During fusion of alkyne **61a** with azide **58**, the terminal alkynyl proton get converted into aromatic proton at C_5 of triazole ring and appeared in between δ = 7.20-7.00 ppm. A peak at δ = 5.28 ppm in the spectrum of heterocyclic product **61b** corresponds to $–CH_2$ of methylnaphthalene unit.

The ^{13}C NMR spectrum also favors the generation of molecule **61b**, depicting the signal at δ = 56.12 ppm for the carbon of $–CH_2–O–$ group in the spectrum of alkyne **61a** that has been shifted downfield at δ = 62.35 ppm, due to the formation of 1,2,3-triazole ring. The singlet at δ = 52.49 ppm is due to $–CH_2$ of methylnaphthalene unit. The peaks at δ = 78.71 ppm and 76.58 ppm corresponding to $–C≡C–$ in the spectrum of **61a** gets down in aromatic region, as these carbons account for 1,2,3-triazole ring in the desired product **61b**.

4.11.4 Mass spectrum and elemental analysis

In the high-resolution mass spectrum (HRMS) of triazole derivative **61b**, the molecular ion peak observed at m/z = 861.45 $(M+1)^+$ against the calculated molecular mass M = 860.45 confirms the generation of heterocyclic compound **61b**. The data obtained from elemental analysis proved the success of cycloaddition reaction of alkyne **61a** and azide **58**.

4.12 Synthesis and spectral analysis of 1-(3-methyl-4-(2-(prop-2-yn-1-yloxy) naphthalene-1-yl) diazenyl) phenyl)-2-(o-tolyl) diazene (62a)

4.12.1 Synthesis

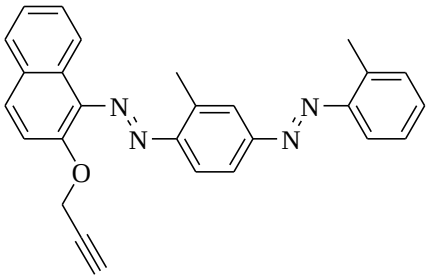

Figure 4.12: 1-(3-methyl-4-(2-(prop-2-yn-1-yloxy) naphthalene-1-yl) diazenyl) phenyl)-2-(o-tolyl) diazene **62a**

Azo-dye, Sudan IV was nucleophilicaly substituted at its hydroxyl group present on naphthyl ring with propargyl group on treatment with propargyl bromide involving abstraction of hydroxyl proton by potassium carbonate base on stirring at room temperature in DMF solvent. The reaction took 19 h to complete; the progress of reaction was monitored by TLC. Red colored solid **62a** shown in Figure 4.12 was obtained as a pure product on treatment of reaction mixture with ice cold water in a good yield of 88%.

4.12.2 IR spectral analysis

The IR spectrum obtained as neat in range 4000-500 cm^{-1} was viewed as in accordance with synthesized alkyne **62a**. Peaks found at 3280 cm^{-1} corresponds to stretching vibrations of –C≡**C-H** bond and at 2100 cm^{-1} is due to –**C≡C-** group of alkyne **62a** shown in Figure 4.12. Signal at 3050 cm^{-1} corresponds to asymmetric stretch of aromatic –**C-H** bond and at 2985 cm^{-1} illustrated stretching vibrations of aliphatic –**C-H** of methyl groups present in the molecule. Peaks in the range 1500-1200 cm^{-1} are due various types of vibrational modes of –**C=C-** and **–N=N-** bonds in newly synthesized alkyne **62a.** Signal at 1146 cm^{-1} explains vibration of etheral bond.

4.12.3 NMR spectral analysis

^{1}H NMR spectrum recorded for Sudan IV based alkyne **62a** in $CDCl_3$, using 500 MHz spectrometer with tetramethylsilane as internal standard. It shows a singlet at δ = 2.54 ppm that is for proton of ≡C-**H** and singlet at δ = 4.91 ppm represents –C**H₂** group attached to the oxygen of 1-naphthol unit in alkyne **62a.** Protons of two methyl groups have a singlet at δ = 2.35 ppm. Multiplets in range δ = 7.98-7.27 ppm represents all aromatic protons. No signal in the range δ = 5.00-3.00 ppm due to hydroxyl proton favors modification of this functional group on starting material **62** and confirms the generation of designed alkyne **62a** shown in Figure 4.12.

^{13}C NMR obtained for compound **62a** is also in accordance with the proposed structure. The signals at δ = 78.71 ppm and 76.08 ppm corresponds to **−C≡C−** and δ = 59.15 ppm notifies the carbon of –**C**H_2−O− group attached with propynyl unit in

the newly synthesized alkyne molecule **62a**. Singlets at δ = 18.13 ppm and 17.61 ppm represents carbons of two methyl groups. Peaks at higher δ values, from δ = 153.97-115.43 ppm corresponds to carbons of aromatic rings in the novel alkyne **62a**.

4.13 Synthesis and spectral analysis of 1-benzyl-4-(((1-((E)-(2-methyl-4-((E)-o-tolyldiazenyl) phenyl) diazenyl) naphthalene-2-yl) oxy) methyl)-1H-1,2,3-triazole (62b)

4.13.1 Synthesis

1,4-disubstituted 1,2,3-triazole derivative **62b** shown in Figure 4.13 was synthesized through CuAAC reaction between newly synthesized alkyne **62a** and freshly prepared azidomethylbenzene **24** in a basic medium of THF:TEA (v/v, 4:1) taken in 100.00 ml round bottom flask, followed by the addition of $[CuBr(PPh_3)_3]$ (0.001 mmol) as Cu(I) source.

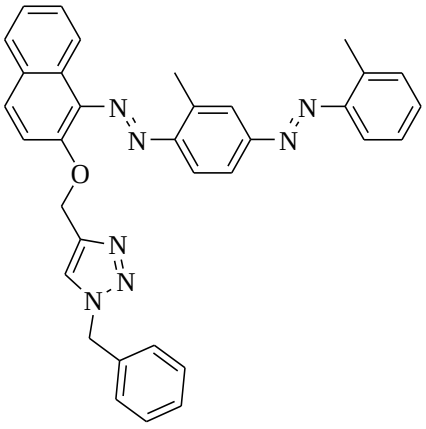

Figure 4.13: 1-benzyl-4-(((1-((E)-(2-methyl-4-((E)-o-tolyldiazenyl) phenyl) diazenyl) naphthalene-2-yl) oxy) methyl)-1H-1,2,3-triazole **62b**

The presence of Cu(I) restricts the stereospecificity of cycloaddition towards the synthesis of only 1,4-disubstituted product in pure form, whereas basic medium accelerates the abstraction of terminal proton of alkyne substrate. Wine red colored solid product **62b** was produced in a good yield of 92% by stirring the reaction mixture at 60 °C for 5 h. The generation of triazole linker **62b** was confirmed by IR,

NMR and Mass spectroscopic studies discussed in forthcoming sections and was further analyzed for its chemosensing applications through UV-Visible spectroscopy.

4.13.2 IR spectral analysis

IR spectral data obtained for heterocyclic compound **62b** was found in line with the expected values. Spectra of all the newly synthesized compounds (terminal alkyne **62a**, azidomethylbenzene **24** and final product of cycloaddition **62b** were compared for the favorable outcome of CuAAC reaction between terminal alkyne **62a** and azide molecule **24** and the search ended up with expected results. IR peaks due to vibrational stretching of –C≡**C**−**H**, −**C**≡**C**− bonds of terminal alkyne found at 3280 cm^{-1} and 2100 cm^{-1} respectively were missing in the vibrational spectrum of click generated product **62b** supports its generation. A signal at 2091 cm^{-1} in the IR spectrum of azidomethylbenzene **24** due to **–N_3** group was also absent in the spectrum of cycloaddition product **62b,** i.e., clear spectra around 2100 cm^{-1} indicates success of CuAAC reaction. Signals at 3051 cm^{-1} in the spectrum of **62b** corresponds to –C=**C-H** present in the aromatic rings, at 2921 cm^{-1} is for aliphatic –**C-H** stretching and at 1561-1212 cm^{-1} signifies various modes of vibrations of –**C=C-** and **–N=N-** moieties in the heterocyclic product **62b**.

4.13.3 NMR spectral analysis

^{1}H NMR spectral data of compound **62b** strongly favors the click cycloaddition of alkyne **62a** with azidomethylbenzene **24**. A singlet peak at δ = 2.54 ppm that was due to proton of terminal alkyne group ≡C-**H** in the spectrum of alkyne **62a** was missing in the spectrum of product **62b**. During cycloaddition, −**C**≡**C**− constituted 1,2,3-triazole ring and as a result terminal proton now behaved as aromatic proton and appeared downfield at around δ = 7.20 ppm. Singlet at δ = 4.91 ppm represents –C**H_2** group attached with the oxygen of 1-naphthol unit in alkyne **62a** went downfield at δ = 5.54 ppm due to its attachment with 1,2,3-triazole ring in molecule **62b**. A peak at δ = 5.28 ppm in the spectrum of heterocyclic compound **62b** corresponds to –C**H_2** of methylbenzene unit. Protons of two methyl groups appeared

as singlets at δ = 2.79 ppm and δ = 2.65 ppm. Multiplets in range δ = 7.99-7.02 ppm represents all aromatic protons.

The ^{13}C NMR spectrum also confirms the synthesis of 1,2,3-triazole derivative **62b,** showing a signal at δ = 65.33 ppm for carbon of –**C**H_2−O− group attached to 1,2,3-triazole ring. The singlet at δ = 54.26 ppm corresponds to −**C**H_2 of methylbenzene unit. The two signals at δ = 78.71 ppm and 76.08 ppm due to −**C**≡**C**− present in the spectrum of **62a** shifted downfield in the spectrum of molecule **62b**, as these carbons account for 1,2,3-triazole ring in the desired triazole derivative **62b** formed during cycloaddition reaction**.** Peaks at δ = 17.82 ppm and δ = 17.61 ppm corresponds to methyl carbons.

4.13.4 Mass spectral and elemental analysis

In the mass spectrum of triazole derivative **62b**, the molecular ion peak has been observed at m/z = 552.35 $(M+1)^+$ against the calculated molecular mass M = 551.40 confirms the formation of heterocyclic compound **62b**. The analysis of observed and calculated percentage of component elements of 1,2,3-triazole derivative **62b** for elemental analysis also supports the success of cycloaddition reaction of alkyne **62a** and organic azide **24**.

4.14 Synthesis and spectral analysis of 4-(((1-((E)-(2-methyl-4-((E)-o-tolyldiazenyl) phenyl) diazenyl) naphthalene-2-yl) oxy) methyl)-1-(naphthalen-1-ylmethyl)-1H-1,2,3-triazole (62c)

4.14.1 Synthesis

Sudan IV dye based 1,2,3-triazole linked molecule **62c** shown in Figure 4.14 was generated through Cu(I)-catalyzed alkyne-azide cycloaddition (CuAAC) reaction between newly synthesized terminal alkyne **62a** and freshly prepared azidomethylnaphthalene **58** as an organic azide in a solvent medium of THF:TEA (v/v, 4:1), followed by the addition of catalytic amount of $[CuBr(PPh_3)_3]$ (0.001 mmol). The presence of Cu(I) converts the reaction to a highly stereospecific one and directs the cycloaddition towards the synthesis of only 1,4-disubstituted product in pure form. Wine red colored solid **62c** was produced in a good yield of 91% by

stirring the reaction mixture at 60 ℃ for 5.5 h. The melting point of dried sample was recorded with electronic melting point apparatus and found as 152-154 ℃. The generation of 1,2,3-triazole linker **62c** was confirmed by IR, NMR and Mass spectroscopic studies discussed in next sections followed by investigation of its chemosensing behavior through UV-Visible spectroscopy.

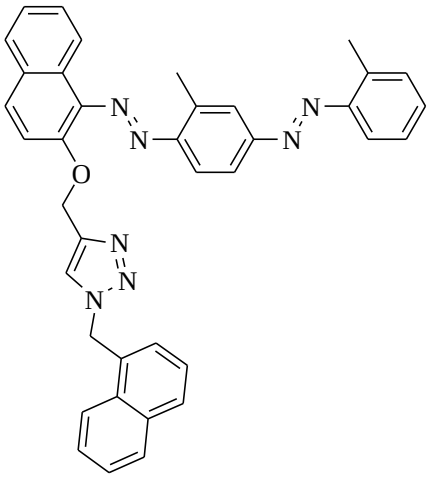

Figure 4.14: 4-(((1-((E)-(2-methyl-4-((E)-o-tolyldiazenyl) phenyl) diazenyl) naphthalene-2-yl) oxy) methyl)-1-(naphthalen-1-ylmethyl)-1H-1,2,3-triazole **62c**

4.14.2 IR spectral analysis

IR spectral data recorded for the molecule **62c** was found in accordance with the expected results. Spectra of starting material **62** and all the newly synthesized molecules (terminal alkyne **62a**, azidomethylnaphthalene **58** and resultant product of cycloaddition reaction **62c**) were viewed side by side for the evaluation of success of CuAAC reaction between terminal alkyne **62a** and organic azide **58** and the search ended up with awaited results. IR peaks due to vibrational stretching mode of –C≡**C**−**H**, −**C**≡**C**− bonds of terminal alkyne **62a**, found at 3280 cm^{-1} and 2100 cm^{-1} respectively were absent in the vibrational spectrum of click generated product **62c** that favors its generation. A signal at 2091 cm^{-1} in the IR spectra of azidomethylnaphthalene **58** due to **–N_3** group was also missing in the spectrum of cycloaddition product **62c,** i.e., clear spectra around 2100 cm^{-1} indicates modification of alkyne as well as azide groups during cycloaddition process. Signals at 3090 cm^{-1}

in the spectrum of **62c** corresponds to –C=**C-H** present in the aromatic rings, at 2919 cm^{-1} is for aliphatic –**C-H** stretching and at 1592-1215 cm^{-1} signifies various vibrational modes of –**C=C-** and **–N=N-** moieties in the novel heterocyclic compound **62c**.

4.14.3 NMR spectral analysis

^{1}H NMR spectral study of molecule **62c** and the recorded data strongly favors the successful conduct of click cycloaddition between alkyne **62a** and azidomethylnaphthalene **58**. In the spectrum of alkyne **62a**, a singlet peak at δ = 2.54 ppm that was for proton of terminal alkyne ≡C-**H** was found missing in the spectrum of product **62c** shown in Figure 4.14. In cycloaddition reaction, **−C≡C−** group involved in generation of 1,2,3-triazole ring and as a result terminal proton transformed into aromatic proton and has appeared downfield at around δ = 7.29 ppm. Signal at δ = 4.91 ppm represents –C**H₂** group linked with the oxygen of 1-naphthol unit in the alkyne **62a** moved downfield at δ = 5.95 ppm due to presence of 1,2,3-triazole ring in molecule **62c**. The peak at δ = 5.40 ppm in the NMR-spectrum of heterocyclic compound **62c** corresponds to –C**H₂** of methylnaphthalene unit. Protons due to two methyl groups appeared as singlets at δ = 2.85 ppm and δ = 2.57 ppm. Protons of shielded methyl protons generally appear at δ = 0.9 ppm and in this molecule **62c**, these are found downfield due to deshielding created by electron withdrawing azo-groups and aromatic rings. Multiplets in range δ = 7.87-7.33 ppm represents all the aromatic protons.

The ^{13}C NMR spectrum also substantiates the generation of cycloaddition product **62c,** has shown signal at δ = 66.87 ppm (s) due to carbon of –**C**H_2−O− group attached to 1,2,3-triazole ring that was earlier linked to terminal alkynyl moiety of molecule **62a.** In alkyne **62a**, the signal due to this carbon has appeared at δ = 59.13 ppm. The cause of this downfield shifting is strong deshielding effect of aromatic 1,2,3-triazole ring. The singlet at δ = 55.80 ppm has appeared due to **−C**H_2 of methylnaphthalene unit. The peaks at δ = 78.71 ppm and 76.08 ppm for the **−C≡C−** in the spectrum of **62a** gets down at higher δ values, as these carbons account for 1,2,3-triazole ring in the expected triazole derivative **62c** formed as a result of

cycloaddition reaction**.** Peaks at δ = 19.36 ppm and δ = 19.14 ppm corresponds to methyl carbons.

4.14.4 Mass spectral and elemental analysis

In the mass spectrum of 1,2,3-triazole derivative **62c**, the molecular ion peak was observed at m/z = 602.43 $(M+1)^+$, whereas the calculated molecular mass 'M' is equal to 601.40. Other peaks in the mass spectrum of **62c** correspond to various daughter ions formed through fragmentation of parent molecule. The data recorded from elemental analysis is in well agreement with the calculated values that is in favor of the generation of heterocyclic compound **62c** from the cycloaddition reaction of alkyne **62a** and organic azide **58.**

4.15 4-(phenyl (1-(prop-2-ynyloxy) naphthalen-4-yl) methylene) naphthalen-1(4H)-one (63a)

4.15.1 Synthesis

To get terminal alkyne 4-(phenyl(1-(prop-2-ynyloxy) naphthalen-4-yl) methylene) naphthalen-1(4H)-one **63a** shown in Figure 4.15, the labile proton of hydroxyl group on starting material **63** undergoes nucleophilic substitution by propynyl group on stirring with propargyl bromide **19** at room temperature. Reaction was conducted in the presence of potassium carbonate as base that facilitated the abstraction of proton from starting material, 1-naphtholbenzein **63**. After stirring the reaction mixture for 22 h, a rusty red colored solid **63a** with a yield of 89% was obtained on treating the content with ice cold water. Melting point of dried product **63a** was recorded that found as 118-120 °C. The generation of alkyne **63a** was confirmed by IR and NMR spectroscopy and further used as starting material for CuAAC reaction to get chemosensing material.

4.15.2 IR spectral analysis

IR spectra of both starting material **63** and terminal alkyne **63a** were recorded as neat in the range 4000-500 cm^{-1} and comparatively examined for the useful changes occurred during the reaction of compound **63** with propargyl bromide **19**. There was

no broad band near 3500-3350 cm^{-1} due to hydroxyl group in the spectrum of product **63a** claimed modification of –OH functional group during chemical reaction. Peaks found at 3280 cm^{-1} corresponds to –C≡**C**−**H** and at 2100 cm^{-1} is due to −**C**≡**C**− unit of molecule. IR signal at frequency 3050 cm^{-1} is for aromatic –**C**-**H** stretching vibrations occurring in the aromatic moiety of synthesized molecule **63a** and at 2985 cm^{-1} point to aliphatic –**C**-**H** stretching. Signal at 1146 cm^{-1} is for etheral –**C**-**O**– bond and other peaks in the spectrum signify various vibrational modes of –**C**=**C**- double bond.

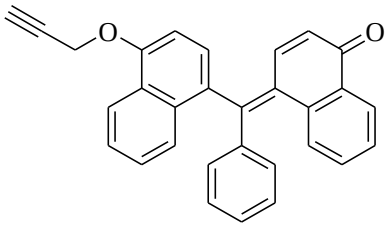

Figure 4.15: 4-(phenyl(1-(prop-2-ynyloxy) naphthalen-4-yl) methylene) naphthalen-1(4H)-one **63a**

4.15.3 NMR spectral analysis

^{1}H NMR spectrum of newly synthesized alkyne **63a** was recorded at 500 MHz that showed a singlet at δ = 2.51 ppm corresponding to one proton ≡C–**H** of terminal alkyne moiety and at δ = 4.86 ppm represents –C**H₂** group attached with the oxygen of 1-naphtholbenzein unit of alkyne **63a** supported its successful generation from starting material **63**, whose NMR spectrum did not have these signals. Moreover, the peak at δ = 5.57 ppm corresponding to proton of –O**H** functional group in the spectrum of compound **63** is absent in the spectrum of molecule **63a** that indicates certain type of reaction change on -OH functional group. Various signals in range δ = 8.13-6.46 ppm represent protons of large aromatic moiety of 1-naphtholbenzein unit.

Similarly, the data obtained from ^{13}C NMR supports the generation of desired product **63a.** The signals at δ = 79.02 ppm and 77.06 ppm represents carbons of −**C**≡**C**− group and at δ = 57.23 ppm notifies the carbon of –**C**H_2−O− group in the freshly synthesized alkyne molecule **63a**. A triplet at δ = 78.25-77.74 ppm is due to the carbon of deuterated chloroform used as solvent to conduct NMR spectrum.

Signals at higher δ values i.e., from δ = 155.53-105.74 ppm corresponds to carbons in aromatic part of molecule **63a**.

4.16 4-((1-((1-benzyl-1H-1,2,3-triazol-4-yl) methoxy) naphthalen-4-yl) (phenyl)methylene) naphthalen-1(4H)-one (63b)

4.16.1 Synthesis

Using catalytic amount of [$CuBr(PPh_3)_3$] (0.001 mmol) complex, a highly stereoselective click cycloaddition reaction of newly synthesized 1-naphtholbenzein **63** based terminal alkyne **63a** and azidomethylbenzene **24** as an azide, the second reactant of Cu(I)-catalyzed cycloaddition reaction was conducted in a basic solvent system of THF:TEA (v/v, 1:1) to get 1-naphtholbenzein linked 1,2,3-triazole molecule **63b** as a product shown in Figure 4.16. The basic medium promotes easy abstraction of terminal alkynyl proton to form copper-acetylide intermediate that further reacts with azide **24** very stereoselectively to yield expected product **63b** with a yield of 91% and melting point 160-162 °C. The triazole linker **63b** was characterized by various spectroscopic techniques like IR, NMR and mass discussed in next sections and was further analyzed for its chemosensing applications through UV-Visible spectroscopy.

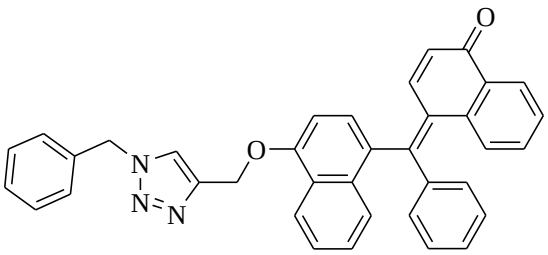

Figure 4.16: 4-((1-((1-benzyl-1H-1,2,3-triazol-4-yl) methoxy) naphthalen-4-yl) (phenyl)methylene) naphthalen-1(4H)-one **63b**

4.16.2 IR spectral analysis

IR spectra of all the synthesized molecules (terminal alkyne **63a**, azidomethylbenzene **24** and final outcome of click cycloaddition **63b**) were obtained as neat in the range 4000-500 cm^{-1} and the results were compared for the success of

CuAAC reaction between terminal alkyne **63a** and azide **24**. IR peaks due to vibrational stretching of –C≡**C**−**H**, −**C**≡**C**− bonds of terminal alkyne found at 3280 cm^{-1} and 2100 cm^{-1} respectively were absent in the vibrational spectrum of click generated product **63b** confirms its generation. A signal at 2091 cm^{-1} in the IR of azidomethylbenzene **24** due to **–N_3** group was also absent in the spectrum of cycloaddition product **63b** supports the expected result of CuAAC reaction. Signals at 3010 cm^{-1} in the spectrum of **62b** belongs to –C=**C–H**, at 2964 cm^{-1} is for methylene –**C–H** stretching vibrations and at 1761 cm^{-1} signifies vibrational frequency of carbonyl group. Peaks at 1591 cm^{-1} and 1246 cm^{-1} are for the vibrations of –**C=C**– and –**N=N**– moieties in the heterocyclic product **63b**.

4.16.3 NMR spectral analysis

^{1}H NMR spectrum of 1,2,3-triazole derivative **63b** strongly supports the click cycloaddition of terminal alkyne **63a** with benzylazide **24** in the presence of Cu(I) as catalyst. The spectrum illustrates the downfield shifting of signal at δ = 4.86 ppm observed in the spectrum of alkyne **63a** for the –C**H_2** protons linked with oxygen of 1-naphtholbenzein unit to δ = 5.62 ppm in the spectrum of molecule **63b**. This downfield shifting is due to the strong deshielding effect of 1,2,3-triazole ring in the molecule **63b.** The disappearance of the signal due to terminal alkynyl proton at δ = 2.51 ppm also favors success of cycloaddition reaction. During fusion of alkyne **63a** with azide **24**, the terminal alkynyl proton get converted into aromatic proton at C_5 of 1,2,3-triazole ring and appeared at δ = 7.29 ppm. A singlet at δ = 5.44 ppm in the spectrum of heterocyclic compound **63b** corresponds to –C**H_2** of methylbenzene unit. Signals in the range δ = 8.26-6.57 ppm belongs to the protons of aromatic system of molecule **63b**.

The ^{13}C NMR spectrum also confirms the generation of cycloaddition product **63b,** depicting the signal at δ = 57.23 ppm for the carbon of –**C**H_2−O− part in the spectrum of alkyne **63a** that has been shifted downfield at δ = 62.06 ppm in the spectrum of 1,2,3-triazole linker **63b** due to attachment of heterocyclic ring with this carbon. The singlet at δ = 53.96 ppm appeared due to carbon of −**C**H_2 of methylbenzene ring. This carbon was the part of benzyl azide **24**, a component of

cycloaddition reaction. The peaks at δ = 79.02 ppm and 77.06 ppm due to carbons of **−C≡C−** in the spectrum of **63a** shifted at higher δ values, as these carbons constituted 1,2,3-triazole ring in the expected product **63b.** Peaks in the range δ = 158.9-104.78 ppm corresponds to carbons of aromatic part of the synthesized heterocyclic compound **63b**.

4.16.4 Mass spectral and elemental analysis

In the high-resolution mass spectrum of 1,2,3-triazole derivative **63b**, the molecular ion peak observed at m/z = 546.22 $(M+1)^+$ against the calculated molecular mass M = 545.21 strongly proves the generation of heterocyclic molecule **63b**. The data obtained from elemental analysis was also in the line with the expected values and confirms the success of cycloaddition reaction of alkyne **63a** and azide **24**.

References:

1. K. M. Banu, A. Dinaker, C. Ananthnarayan, *Ind. J. Pharm. Sci*. **1999**, 61, 202.
2. L. P. Guan, Q. H. Jin, G. R. Tian, K. Y. Chai, Z. S. Quan, *J. Pharm. Sci.* **2007**, 10, 254.
3. S. Manfredini, C. B. Vicentini, M. Manfrini, N. Bianchi, C. Rustigliano, C. Mischiati, R. Gambari, *Bioorg. Med. Chem.* **2000**, 8, 2343.
4. L. Liang, D. Astruc, *Coordin. Chem. Rev.* **2011**, 255, 2933.
5. B. Schulze, U. S. Schubert, *Chem. Soc. Rev*. **2014**, 43, 2522.
6. J. T. Ngo, S. R. Adams, T. J. Deerinck, D. Boassa, F. Rodriguez-Rivera, S. F. Palida, *Nat. Chem. Bio.* **2016**, 12, 459.
7. X. Wang, B. Huang, X. Liu, P. Zhan, *Drug Discov. Today*. **2016**, 21, 118.
8. P. Wu, A. K. Feldman, A. K. Nugent, C. J. Hawker, A. Scheel, B. Voit, *Angew. Chem. Int. Edition.* **2004**, 43, 3928.
9. M. de Lourdes, G. Ferreira, L.C.S. Pinheiro, O.A. Santos-Filho, M.D.S. Pecanha, C.Q. Sacramento, V. Machado, V.F. Ferreira, T.M.L. Souza, N. Boechat, *Med. Chem. Res*. **2014**, 23, 1501.

Chapter 4

Section II

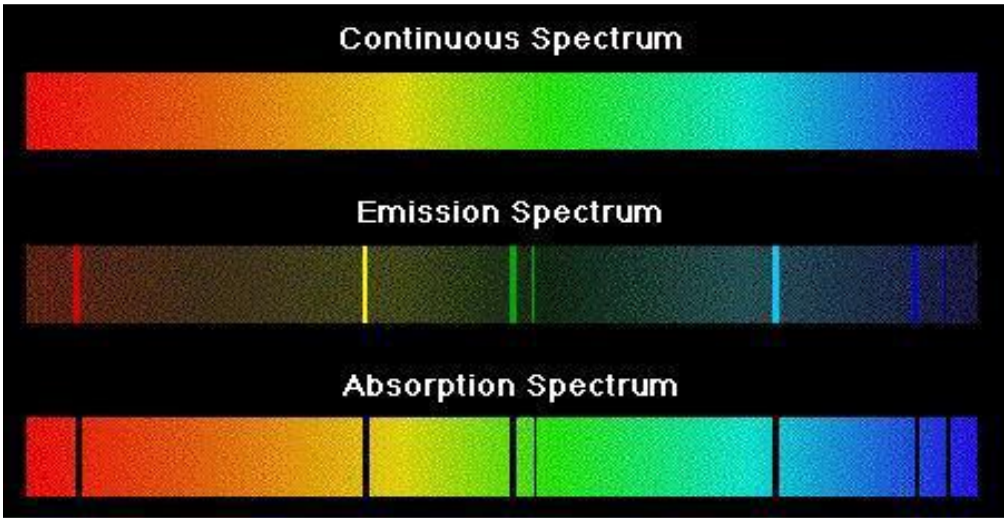

Analysis of photophysical properties

This section of chapter 4 presents detailed discussion of photophysical properties of newly synthesized 1,4-disubstituted 1,2,3-triazole derivatives studied by UV-Visible and Fluorescence spectroscopy. The molecules are analyzed for their chemosensing behavior to detect various metal ions.

4.17 Introduction to electronic spectroscopy

UV-Visible spectroscopy (electronic spectroscopy) is an analytical tool to determine the existence of various types of compounds, mainly aromatic compounds, organic molecules with extended conjugation, transition metal complexes and many more. With the absorption of UV-Visible light by a molecule, the electronic transitions take place from occupied molecular orbitals to empty molecular orbitals, where the most probable transition involves excitation of electron from highest occupied molecular orbital (HOMO) to lowest unoccupied molecular orbital (LUMO). A set of bonding (σ, π), antibonding (σ*, π*) and non-bonding (n) molecular orbitals are present in molecules, where the bonding orbitals are generally filled and antibonding are empty to receive electrons during excitation [1-3]. The energy level diagram and various types of excitations occurring in molecules are presented in Figure 4.17.

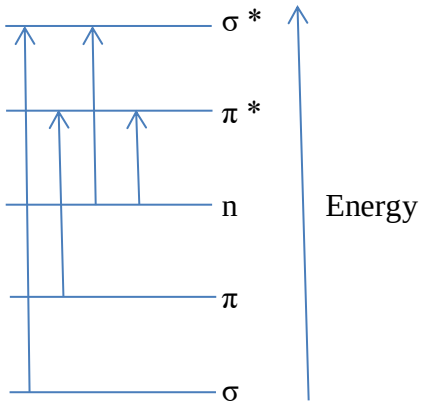

Figure 4.17: Molecular electronic energy levels and excitations

Based upon the nature of electrons present in a molecule, the different types of electronic transitions are σ-σ*, π-π*, n-σ* and n-π*. The transitions involving n and π-electrons happen by absorbing lesser amount of energy as compared to σ-electrons and show signals at higher wavelength of UV-Visible region (200-800 nm). Molecules having only σ-electrons generally absorb below 200 nm, which is not the feasible region for UV-Visible spectroscopy [4-5]. Hence, the electronic spectroscopy is more useful to study the molecules having n and/or π-electrons i.e., aromatic,

heterocyclic and unsaturated molecules. The objective of this research work was to synthesize novel molecules having chemosensing applications to be studied by UV-Visible spectroscopy. Therefore, the aromatic compounds have been selected as starting materials for the synthesis of chemosensors, whose sensing towards various metal ions has been analyzed by UV-Visible spectroscopy.

In addition to aromatic or unsaturated organic molecules, the transition metals or metal ions in their solutions also exhibit electronic transitions by absorbing UV-Visible light. Due to their low electronegativities, these metals generally exist as positively charged species or cations and don't move around one another, but attract species with high electron density and form coordination complexes [6]. The species with high electron density may be the solvent molecules or other foreign particles like the newly synthesized triazole derivatives, **59b-63b** and **59c-60c, 62c** discussed in this research work.

The transition metal complexes formed so far can interact with photons of variable energies when irradiated with the light of UV-Visible region. During this interaction, there is always a possibility of number of electronic transitions. These excitations might involve the metal ion itself or the binding ligands (ions or molecules that coordinate with metal ion). For transition metals, these electronic excitations are known as d-d transitions. During the complexation of metal ion with ligands, all the d-orbitals of metal ion are no longer degenerate i.e., undergoes splitting into different energy levels. When the light of particular frequency fall on these complexes, the electron from ground d-orbital gets excited into higher d-orbital by absorbing photons of suitable energy. The d-d transitions generally require less energy, but don't occur frequently, means very weak absorbance due to these excitations [7-9].

Another most common type of electronic transition is known as charge transfer transition that involves the excitation of most loosely held electrons from binding molecule (ligand) to the metal ion or vice versa and involves both the metal ion and ligand. Charge transfer transitions require much more energy, but occur frequently as allowed transitions and show stronger absorbances in the UV-Visible spectrum. The variations in the intensity of absorbance or wavelength of electronic

transitions on complexation of metal ions with different complexing agents form the basis of chemosensing of metal ions [10-11].

The chemosensing behavior of organic receptors can also be examined by fluorescence spectroscopy. Fluorescence is a kind of luminescence by electromagnetic radiations that causes excitation of a molecule, raising it to an excited electronic state, in other words, in fluorescence spectroscopy the molecules absorb a beam of light that excites its most loosely held electrons to higher energy states and then causes them to emit light of higher wavelength, means it is the wavelength of emitted light, which is being recorded in fluorescence spectroscopy. Wavelength of emitted light is always higher than the wavelength of light required for its excitation, because a molecule always needs higher energy for its electronic excitation than the emitted energy [12].

4.18 Chemosensing studies of 1,2,3-triazole derivatives 59b and 59c

4.18.1 UV-Visible spectroscopy for sensing studies of 59b

The newly synthesized compound **59b** has been investigated for its potential use in ion-sensing through UV-Visible spectroscopy, using a number of metal chlorides. o-cresolphthalein, the starting material used to synthesize the sensing probe **59b** has strong absorption in UV-Visible region, so considered as prime candidate to develop a chemosensor. On the other hand, the heterocyclic moiety incorporated as a result of CuAAC reaction creates a strong molecular framework with nitrogen donor atoms that can show complexation with various metal ions. In order to study the sensing behavior of heterocyclic molecule **59b**, the UV-Visible titrations of **59b** were performed with different metal ion solutions.

Solvents like methanol, methanol mixed with water and acetonitrile mixed with water were used in the UV-Visible experiments. Based upon the results, it was concluded that the acetonitrile-water (CH_3CN:H_2O::4:1) mixture is an optimal solvent system due to high solubility of the test sample and fine absorption bands. Using this solvent system, 0.20 mM solution of 1,2,3-triazole derivative **59b** and 0.50 mM solutions of metal salts such as Na(I), Cr(III), Mn(II), Fe(II), Co(II), Ni(II), Zn(II), Cd(II), Hg(II), Pb(II) and Ce(III) were prepared. To conduct ion analysis, 10 equiv. of

a 0.50 mM solution of each metal ion were added one by one into 0.20 mM solution of receptor **59b** in a series of UV-Visible titrations. Figure 4.18 displays the results seen in samples containing 10 equiv. of corresponding metal ions in the solution of compound **59b**. The sensitivity of manufactured probe for Pb(II) ions was declared by the maximum rise in absorbance value of ligand **59b** upon addition of Pb(II) ions in comparison to other metal ions.

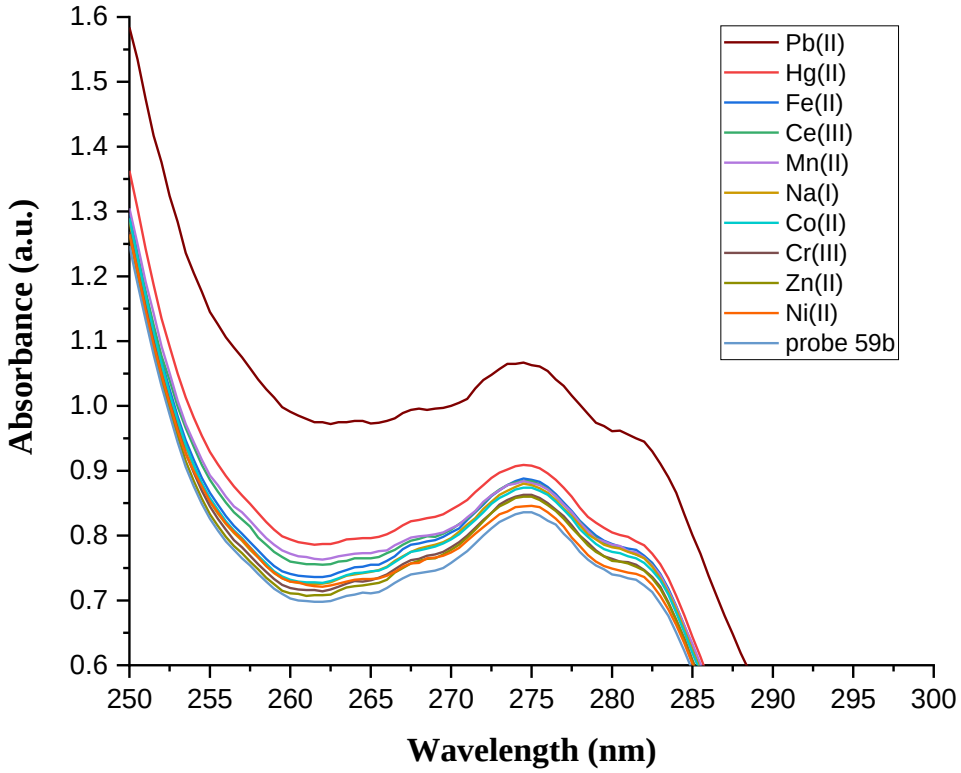

Figure 4.18: Absorption responses of molecule **59b** on adding 10 equiv. of each metal ion separately in 0.20 mM of probe **59b** in acetonitrile and water ($CH_3CN:H_2O$::4:1)

The changes in the electronic distribution between the metal ion and the ligand are responsible for the observable variation in absorbance. Figure 4.19 provides more illustrated information of probe **59b** towards different metal ions; here, a considerable

relative shift in the intensity of absorbance of UV-Visible spectrogram was seen for Pb(II) ions.

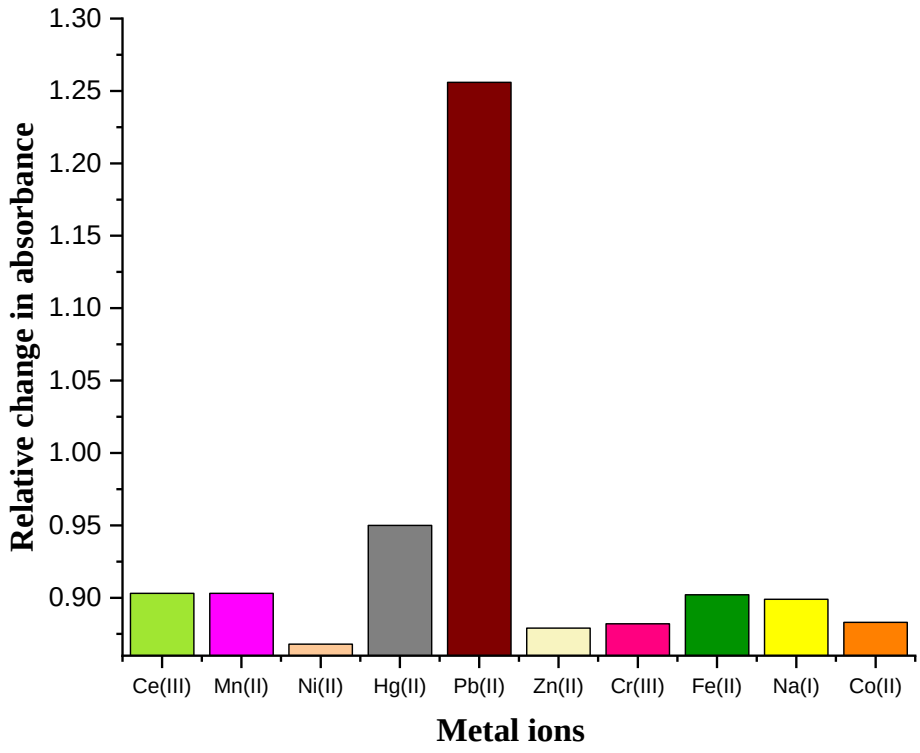

Figure 4.19: Relative change in absorbance of molecule **59b** with different metal ions, observed at λ_{max} = 275 nm

In order to investigate the complete sensing features of probe **59b**, the UV-Visible titrations were conducted by adding 20 equiv. of 0.50 mM Pb(II) ion solution successively into a 0.20 mM solution of testing probe **59b** and the results are depicted in Figure 4.20. In the beginning, the absorbance steadily increased with each new addition of metal ion solution, but after a specific concentration of Pb(II) ions, there was no longer any discernible rise in absorbance. In addition, there has been no observable shift in the wavelength, despite a very slight shortening (0.5-1.0 nm) in some additions. Figure 4.21(a) depicts the relative shift in absorbance maxima (An/Ao) with the subsequent addition of 20 equiv. of Pb(II) ions, where An = absorbance maxima with sequential addition of Pb(II) ions and Ao = Absorbance

maxima of ligand **59b** without metal ion. The binding ratio of probe **59b**:Pb(II) complex was calculated as 2:1 with binding constant of ligand-metal complexation as 2.8 x 10^4 M^{-1}, which shows strong chelation of receptor molecule with metal ions. From the correlation plot shown in Figure 4.21(b), the detection limit of Pb(II) ions was calculated as 13 µM.

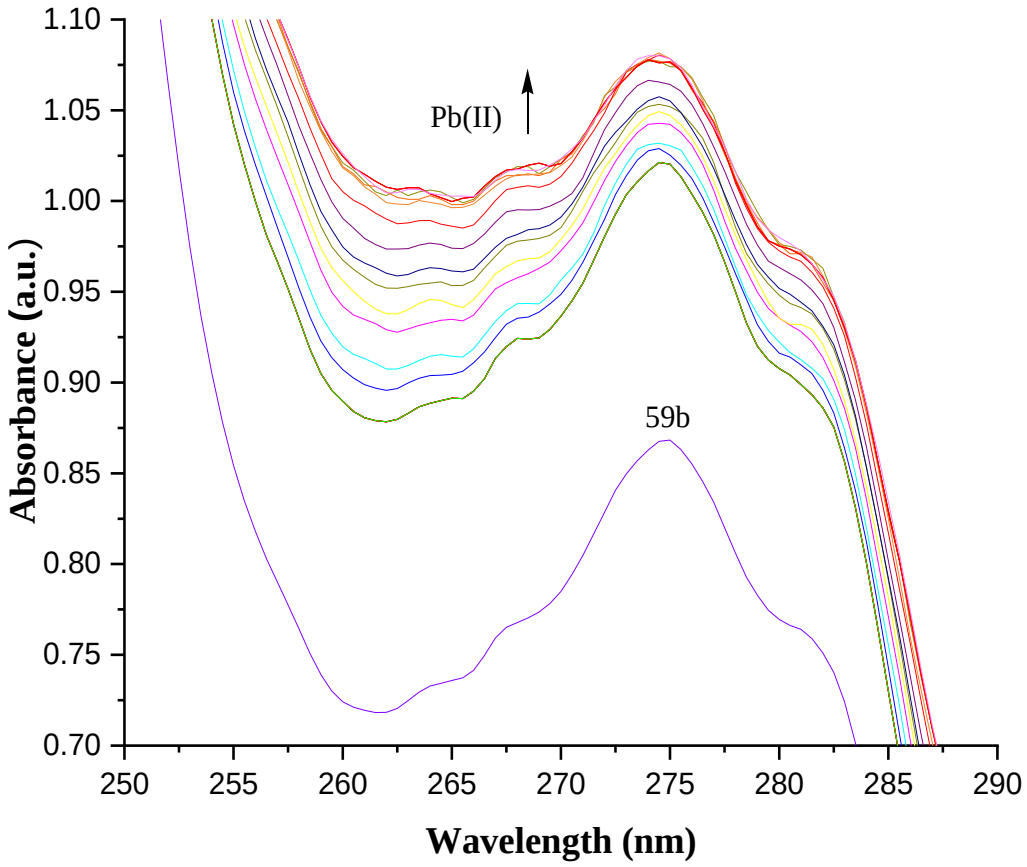

Figure 4.20: Absorbance responses of **59b** on adding 20 equiv. of 0.50 mM Pb(II) ion solution in 0.20 mM solution of chemosensor **59b** in acetonitrile and water ($CH_3CN:H_2O$::4:1

The synthesized probe **59b** was also analyzed for its ion sensing potential with a sample having a mixture of metal ions. No interference of other metal ions was detected, that declares high sensitivity of 1,2,3-triazole derivative **59b** towards Pb(II) ions.

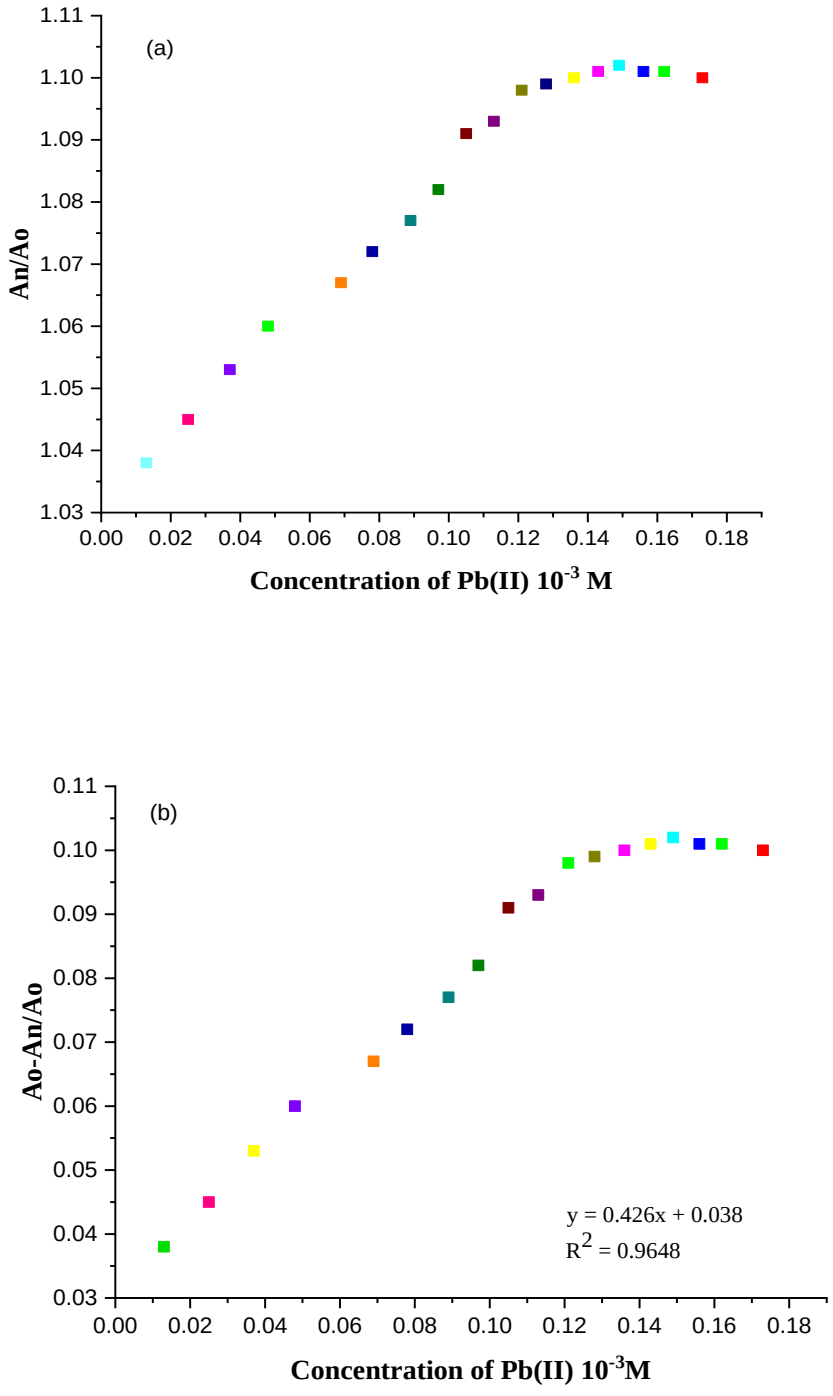

Figure 4.21: (a) Relative change in absorbance (An/Ao) of **59b** on adding 20 equiv. of 0.50 mM of Pb(II) ions. (b) Correlation plot [Ao-An/Ao vs. concentration of Pb(II) ions]

4.18.2 UV-Visible spectroscopy for sensing studies of 59c

On the same note, another o-cresolphthalein based probe **59c** has also been explored for its ion-sensing behavior by UV-Visible spectroscopy using various metal ion solutions. With a solvent system, acetonitrile-water ($CH_3CN:H_2O$::4:1), 0.20 mM solution of heterocyclic compound **59c** and 0.50 mM solutions of various metal ions such as as Na(I), Cr(III), Mn(II), Fe(II), Co(II), Ni(II), Zn(II), Cd(II), Hg(II), Pb(II) and Ce(III) were prepared. For ion detection, the UV-Visible studies were conducted for molecule **59c** on adding 10 equiv. of 0.50 mM solution of each metal ion in 0.20 mM of heterocyclic compound **59c**. The absorption responses recorded for each sample having 10 equiv. of respective metal ions in the sample of molecule **59c** were quite similar to the results recorded for the titrations with **59b** as shown in Figure 4.22. Here also, the maximum rise in absorbance (hyperchromic shift) of ligand **59c** was observed with Pb(II) ions as compared to other metals, indicating its selectivity towards Pb(II) ions.

In order to know the detailed sensing behavior of probe **59c** upon coordination with Pb(II) ion, the absorption titrations were conducted with only Pb(II) ions. Figure 4.22 shows the spectral responses recorded on adding 20 equiv. of metal ion in 0.20 mM solution of testing molecule **59c.** Initially, a noticeable rise in the intensity was found with each addition of Pb(II) ions, but after few additions, when whole ligand gets saturated with metal, no change in absorbance was recorded with further additions. Similar to the behavior of **59b**, no appreciable change in wavelength was recorded with the addition of Pb(II) ions.

Figure 4.23 (a) provides the relative shift in absorbance maxima (An/Ao) on adding 20 equiv. of Pb(II) ions in the sample of probe **59c**, where An = absorbance maxima with sequential addition of Pb(II) ions and Ao = Absorbance maxima of ligand **59c** without metal ion. The binding ratio of probe **59c**:Pb(II) complex was found as 2:1 with binding constant as 3.2×10^4 M^{-1}, from the correlation plot shown in Figure 4.23(b), the minimum limit of detection of Pb(II) ions was calculated as 11.2 µM.

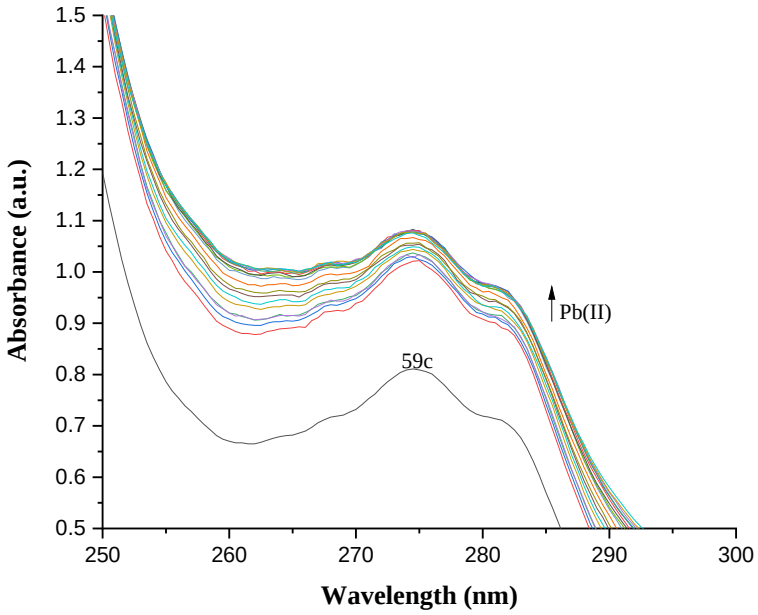

Figure 4.22: Absorbance responses observed during addition of 20 equiv. of 0.50 mM Pb(II) ion solution into 0.20 mM of probe **59c** in acetonitrile-water ($CH_3CN:H_2O$::4:1) mixture.

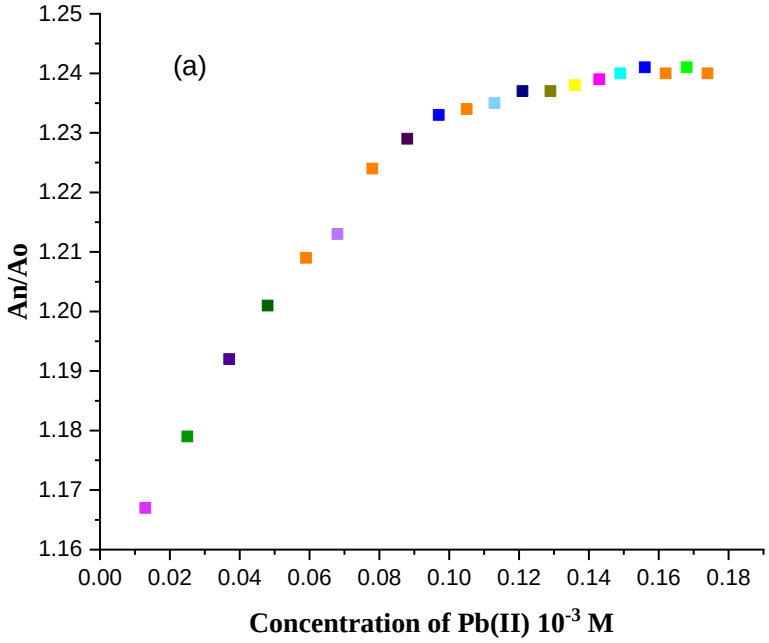

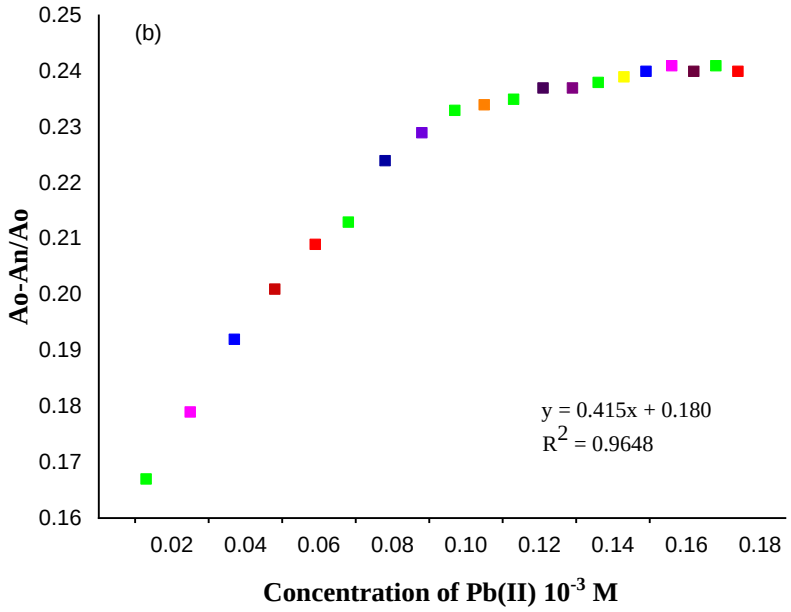

Figure 4.23: (a) Graph of relative shift in absorbance (An/Ao) vs. concentration of Pb(II) ions. (b) Plot of Ao-An/Ao vs. concentration of Pb(II)

These highly selective chemosensors **59b** and **59c** allow a direct quantitative assay of Pb(II) ions by UV-Visible spectroscopy with detection limited to 13 µM and 11.20 µM respectively.

4.18.3 Probable binding mode of 59b/59c with Pb(II)

According to the HSAB theory, Pb(II) is considered as borderline acid and can interact with a variety of ligands to exhibit a wide range of coordination modes. The synthesized 1,2,3-triazole derivatives **59b** and **59c** have more nitrogen and oxygen heteroatoms in their building blocks, making them capable to bind with Pb(II) ions. The computed 2:1 stoichiometry of the **59b/59c:**Pb(II) complex from the relative change in absorbance with the serial addition of Pb(II) ions implies the encapsulation of Pb(II) by two receptor units and the probable binding is as illustrated in Figure 4.24. Previous studies have shown that the Pb(II) ions, being bigger in size, are able to effectively combine with ligands that have cage-like structures and can stabilize a

high coordination number [13-14]. The two receptor units constitute a perfect cavity to retain the Pb(II) ion, which is in accordance with the reported stoichiometry.

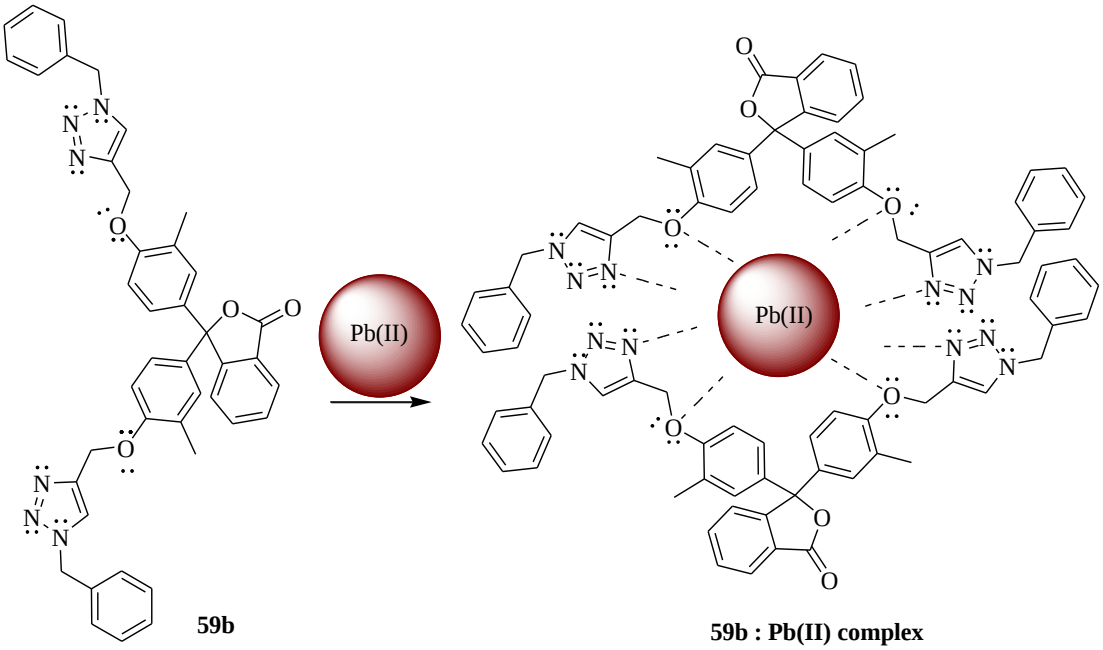

Figure 4.24: Possible complexation of probe **59b** with Pb(II) ions

4.19 Chemosensing studies of 1,2,3-triazole derivatives 60b and 60c

4.19.1 UV-Visible spectroscopy for sensing studies of 60b

The 1,2,3-triazole linker **60b** has been synthesized from 1,4-dihydroxyanthraquinone based alkyne, having strong absorption and emission in UV-Visible region i.e., 200-800 nm and on Cu(I)-catalyzed cycloaddition with azidomethylbenzene, the formation of 1,2,3-triazole ring with three nitrogen atoms creates a molecular system that can coordinate with a specific metal ion and the changes in spectral behavior of which on complexation with metal ion can be studied by UV-Visible spectroscopy. To study the sensing behavior of synthesized molecule **60b**, the UV-Visible analyses has been conducted in different solvent systems, like acetonitrile, methanol, acetonitrile-water and methanol-water combinations. Out of various solvent systems, the acetonitrile-water (CH_3CN:H_2O::4:1) mixture has been found as the best, because of the better solubility of testing 1,2,3-triazole molecule as

well as fineness of the absorption spectra at room temperature and natural pH conditions. With the optimization of concentration value, the 0.50 mM solution of testing probe **60b** and 0.50 mM solutions of various metal ions like, as Na(I), K(I), Ba(II), Cr(III), Mn(II), Fe(II), Fe(III), Co(II), Ni(II), Zn(II), Cd(II), Hg(II), Pb(II) and Ce(III) were prepared in selected solvent mixture. To examine the chemosensing nature of newly generated molecular assembly **60b**, the UV-Visible spectrophotometric titrations were done with the sequential addition of 10 equiv. of 0.50 mM solution of different metal ion separately into the solution of examining molecule. The analyte **60b** has shown significant change in the absorption peak on addition of Fe(II) ions as compared to other metal ions.

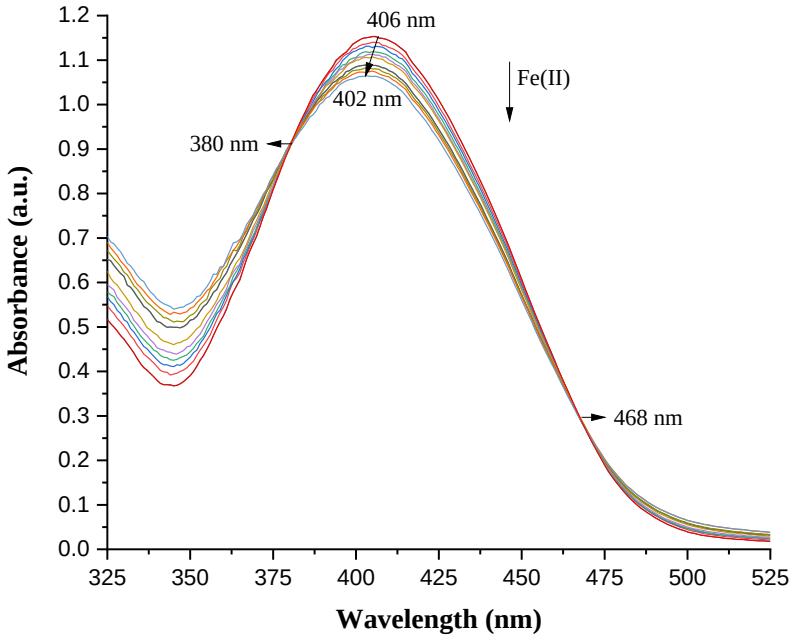

Figure 4.25: Absorption responses recorded with the subsequent addition of 15 equiv. of 0.50 mM of Fe(II) ions in 0.50 mM solution of receptor **60b** in acetonitrile-water ($CH_3CN:H_2O$::4:1) mixture as solvent system

Thereafter, the absorption titrations were performed for molecule **60b** with the subsequent addition of 15 equiv. of 0.50 mM of Fe(II) ions into 0.50 mM of triazole derivative **60b**, in order to study its complete chemosensing nature. An observable

decrease in absorption intensity has been recorded in between 380 nm and 468 nm along with hypochromic shifting in absorption maxima with each successive addition of Fe(II) ions into the solution of complexing agent **60b**, as presented in Figure 4.25, whereas a rise in absorption intensity was observed above 468 nm and below 380 nm, generating isosbestic points at these particular wavelengths. The absorption maximum at 406 nm shows a shift to lower wavelength of 402 nm with an increase in concentration of Fe(II) ions from 0.01 mM to 0.14 mM, causing hypsochromic shift of 4 nm.

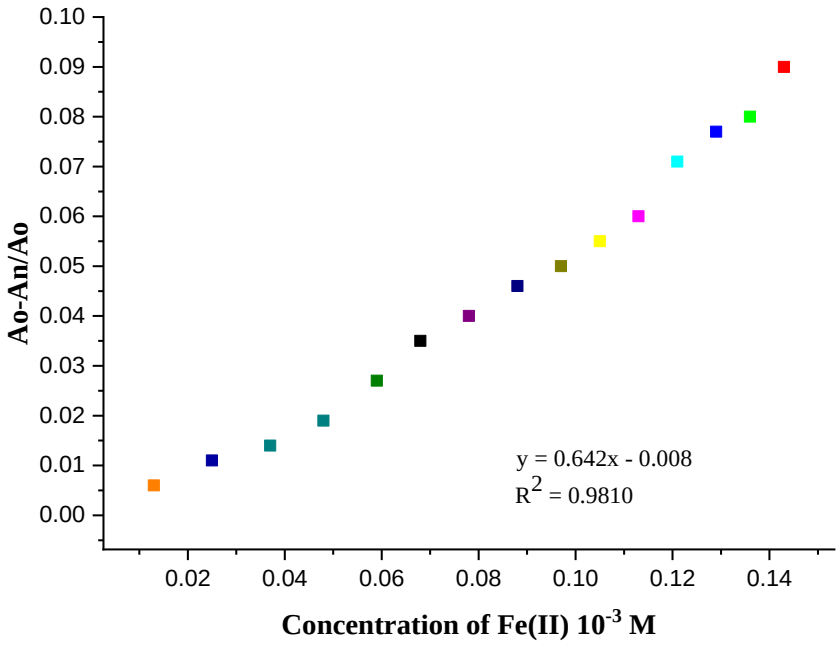

Figure 4.26: Relative shift in absorbance [Ao-An/Ao] vs. concentration of Fe(II) ions, An = Absorbance intensity with each addition of Fe(II) ions and Ao = Absorption maximum of 0.50 mM of triazole linker **60b**

The Figure 4.26 shows the relative shift in absorbance [Ao-An/Ao] of probe **60b** with the sequential addition of Fe(II) ions, where An = Absorbance maxima with each addition of Fe(II) ions and Ao = Absorption intensity of ligand **60b** without metal ion. From the correlation plot shown in Figure 4.26, the minimum detection

limit of Fe(II) ions by the receptor unit **60b** has been computed as 10 µM with 1:1 stoichiometry of **60b**: Fe(II) complexation.

4.19.2 UV-Visible spectroscopy for sensing studies of probe 60c

Following the same procedure, as practiced for the chemosensing analysis of probe **60b**, the 1,2,3-triazole derivative **60c** was also explored for its sensing quality. The sensing behavior of testing molecule **60c** (0.50 mM) was investigated with 0.50 mM solutions of various metal ions such as Na(I), K(I), Ba(II), Cr(III), Mn(II), Fe(II), Fe(III), Co(II), Ni(II), Zn(II), Cd(II), Hg(II), Pb(II) and Ce(III), each prepared in acetonitrile-water ($CH_3CN:H_2O$::4:1) solvent system through UV-Visible spectroscopy. The absorption titrations were conducted with the addition of 10 equiv. of 0.50 mM of different metal ion solutions separately into the solution of testing probe **60c**. The noticeable change in the absorption spectrum was observed with the addition of Fe(II) ions in the solution of **60c**.

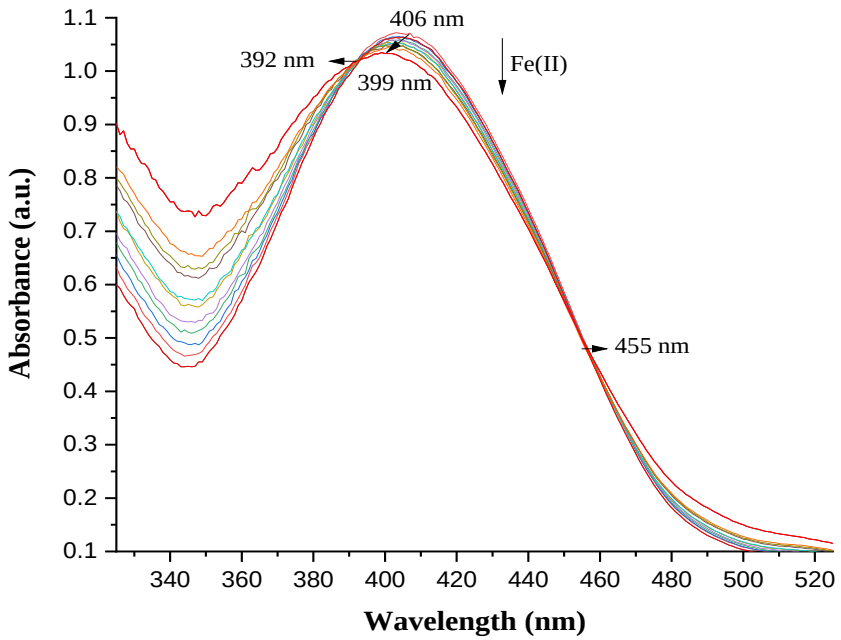

Figure 4.27: Absorbance responses recorded for probe **60c** (0.50 mM) with the addition of 15 equiv. of 0.50 mM Fe(II) ions in acetonitrile-water ($CH_3CN:H_2O$::4:1) solvent mixture

Thereafter, the UV-Visible spectrophotometric titrations were conducted with the successive addition of 15 equiv. of Fe(II) ions (0.50 mM) into the solution of molecule **60c** (0.50 mM) and the responses recorded are as presented in Figure 4.27. For 1,2,3-triazole derivative **60c**, the decrease in absorption intensity with each successive addition of Fe(II) ions and hypsochromic shift of 7 nm was recorded with an increase in concentration of Fe(II) ions from 0.01 mM to 0.14 mM along with the isosbestic points at 392 nm and 455 nm. In the region between isosbestic points, the decrease in absorption was recorded, whereas an increase in absorption was observed above 455 nm and below 392 nm with successive increase in concentration of Fe(II) ions. The lowest limit of detection for probe **60c** was calculated from corelation plot shown in Figure 4.28, which is found as 9.3 µM in acetonitrile-water ($CH_3CN:H_2O$::4:1) solvent mixture.

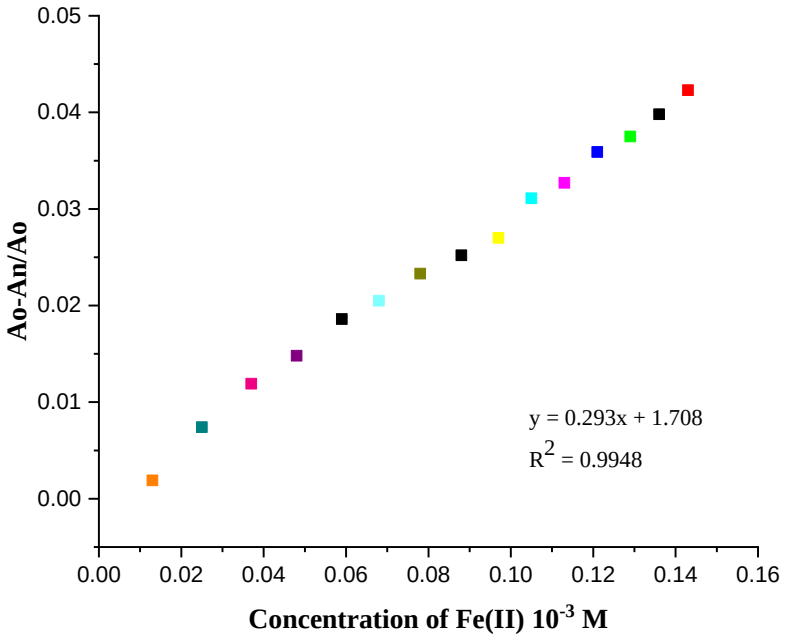

Figure 4.28: Graph presenting [Ao-An/Ao] vs. concentration of Fe(II) ions**,** An = Absorption intensity with each stepwise addition of Fe(II) ions and Ao = Absorption maximum of 0.50 mM of probe **60c** without metal ion

This exceptional behavior of complexing agents, **60b** and **60c** with Fe(II) ions with respect to other metals proves their sensitivity and selectivity towards the

detection of Fe(II) ions. The decrease in the absorption intensity along with the shifting of signal towards lower wavelength with every addition of Fe(II) ions for both **60b** and **60c** have shown that these changes are more significant for molecule **60c** indicating high sensitivity of probe **60c** towards the selective detection of these ions with a minimum limit of detection of Fe(II) ions with **60c** as 9.3 µM computed from the plot depicted in Figure 4.28.

4.19.3 Fluorescence spectroscopic studies with 60c

Similar to the UV-Visible titrations, the chemosensing nature of heterocyclic compound **60c** has also been explored through fluorescence spectroscopy. The fluorescence spectrometric titrations were conducted for **60c** with the subsequent addition of 12 equiv. of 0.10 mM solution of Fe(II) ions into 0.10 mM of testing molecule **60c** at λ_{ex} = 406 nm. With increase in concentration of Fe(II) ions from 0.003 mM to 0.025 mM, a noticeable decrease in emission intensity along with the shifting of emission bands from wavelength 563 nm to 551 nm was observed and shown in Figure 4.29.

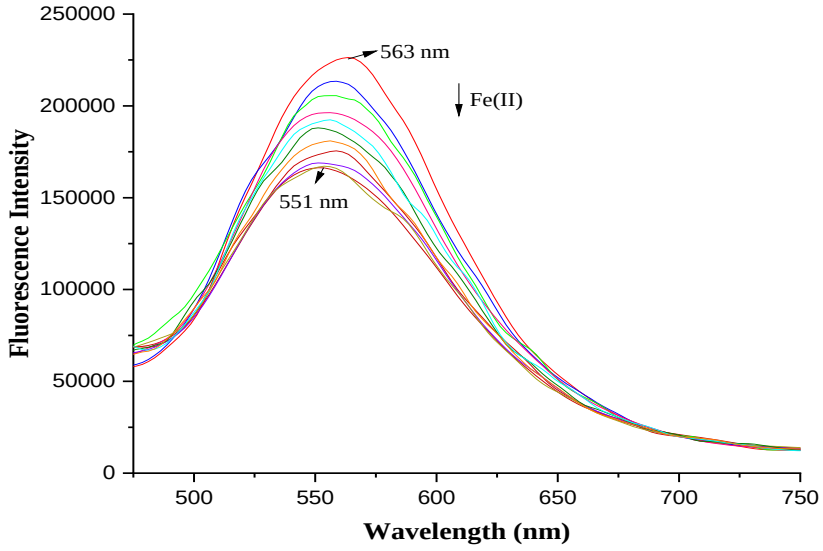

Figure 4.29: Emission responses of 1,2,3-triazole linker **60c** (0.10 mM) with the successive addition of 12 equiv. of 0.10 mM solution of Fe(II) ions in acetonitrile-water ($CH_3CN:H_2O$::4:1) solvent mixture at λ_{ex} = 406 nm

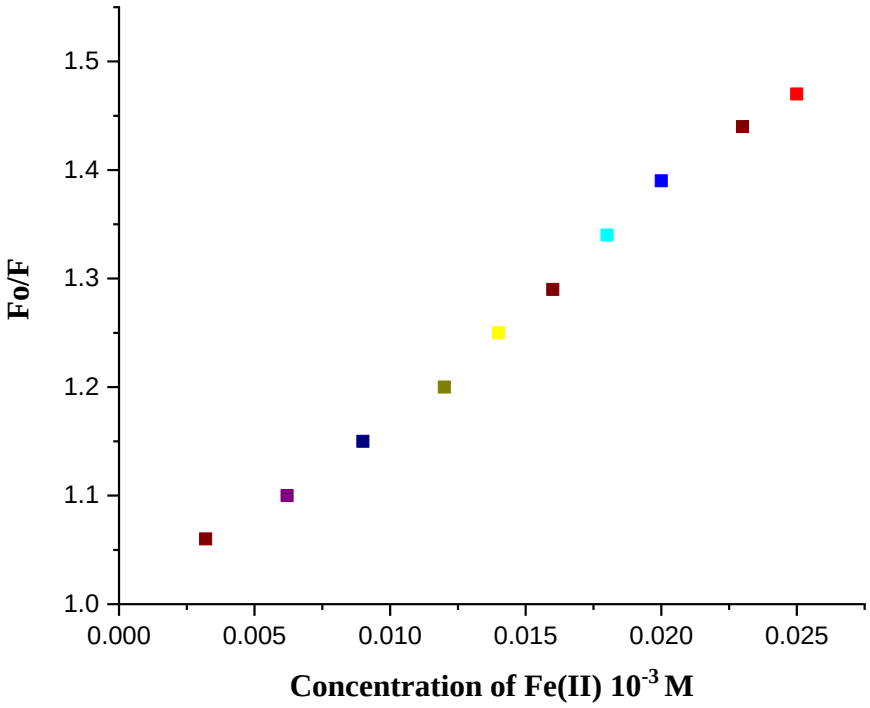

Figure 4.30: Emission intensity ratios (Fo/F) for **60c** in between 563 nm to 551 nm vs. concentration of Fe(II) ions varying from 0.003 mM to 0.025 mM at λ_{ex} = 406 nm

From the fluorescence data, a plot of fluorescence intensity ratio, Fo/F vs. concentration of Fe(II) ions was drawn, which shows a regular increase in fluorescence intensity ratio with an increase in concentration of Fe(II) ions as presented in Figure 4.30. Putting this data into Stern-Volmer equation, as given below, the binding coefficient for the ligand-metal interaction was calculated.

$Fo/F = 1 + Ksv\,[Q]$ (Stern-Volmer equation)

Fo in equation is the fluorescence intensity of molecule **60c** and F is the fluorescence intensity of molecule **60c** with the addition of Fe(II) ions at concentration Q. Ksv is the Stern-Volmer or binding coefficient of probe **60c** for the complexation with Fe(II) ions, which is calculated as $14.28 \times 10^4\ M^{-1}$.

4.19.4 Probable binding mode of 60b/60c with Fe(II)

As per the postulates of HSAB theory, the iron is identified as hard acid and has tendency to interact with hard bases i.e., ligands having oxygen and/or nitrogen atoms as donor sites. Literature survey on chemosensing of iron has revealed few reports, describing the synthesis of organic molecules having nitrogen and oxygen atoms and has been employed as chemosensor of Fe(II) ions. The data mentioned in those reports have witnessed the binding of Fe(II) ions with the organic complexing agents through nitrogen and oxygen atoms [15-17]. The organic molecules **60b** and **60c** synthesized in this research work are appended with 1,2,3-triazole rings having three nitrogen atoms and anthraquinone moiety with oxygen atoms can hold Fe(II) ions by coordinating through these atoms. The absorption responses recorded during the UV-Visible titrations of these linkers with the addition of Fe(II) ions declares the binding ratio of ligand:metal ion as 1:1.The possible binding mode of ligand **60b** with Fe(II) is presented in Figure 4.31. Fe(II) ions may bind with synthesized molecules through the acceptance of lone pair of electrons on binding atoms into their vacant orbitals.

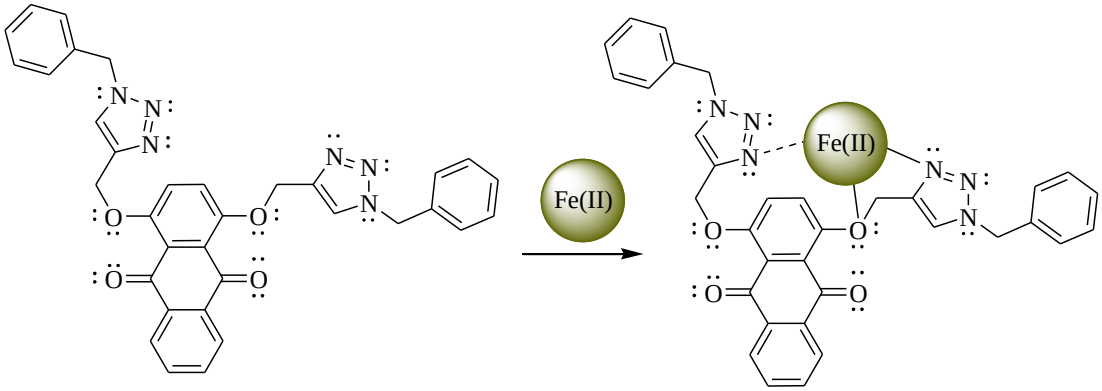

60b **60b: Fe(II)Complex**

Figure 4.31: Possible binding mode of synthesized 1,2,3-triazole derivative **60b** with Fe(II) ions.

4.20 Chemosensing studies of 1,2,3-triazole derivative 61b

4.20.1 UV-Visible spectroscopy for sensing studies of 61b

The probe **61b** has been analyzed for its ion-sensing behavior using solutions of a set of metal chlorides. The excellent absorption of 1-naphtholphthalein **61** in UV-Visible region make it a good choice to use as starting material for the synthesis of chemosensor and during the cycloaddition reaction, the generation of heterocyclic triazole ring with three snitrogen atoms provides a molecular moiety to coordinate with specific metal ion. The studies were performed using various solvents and among them, the combination of acetonitrile and water ($CH_3CN:H_2O$::4:1) was evaluated as the best solvent owing to the better solubility of testing analyte. Thereafter, the solutions of testing probe **61b** (0.50 mM) and metal salts of Na(I), K(I), Ba(II), Cr(III), Mn(II), Fe(II), Co(II), Ni(II), Zn(II), Cd(II), Hg(II), Pb(II) and Ce(III) each with concentration 1.00 mM were prepared using acetonitrile and water ($CH_3CN:H_2O$::4:1) mixture. To examine the ion-sensing potential, the absorption titrations were conducted for **61b** on adding 20 equiv. of 1.00 mM solution of each metal ion separately into 0.50 mM solution of receptor molecule at room temperature and the absorption responses recorded for different samples are as presented in Figure 4.32. The significant decrease in the absorbance of testing chemosensor **61b** at λ = 438 nm upon addition of Co(II) ions was noticed in contrast to rest of the metals that indicates the selectivity of newly prepared heterocyclic probe **61b** for Co(II). Figure 4.33 highlights the relative change in absorption of testing probe for various metal ions, where an abundant relative shift in the absorbance has been observed for Co(II) ions.

To examine the complete sensing characteristics of receptor **61b** with change in concentration of Co(II) ions, the absorption titrations were conducted with the serial addition of 15 equiv. of 1.00 mM Co(II) ions in 0.50 mM solution of the sample **61b** and the absorption results obtained were as depicted in Figure 4.34. A uniform dip in the absorption intensity was recorded with each addition of Co(II) ions without any significant change in λ_{max}. This decrease in absorption intensity of organic complexing moiety, on complexation with Co(II) ions has also been supported by various studies reported in literature [18-20].

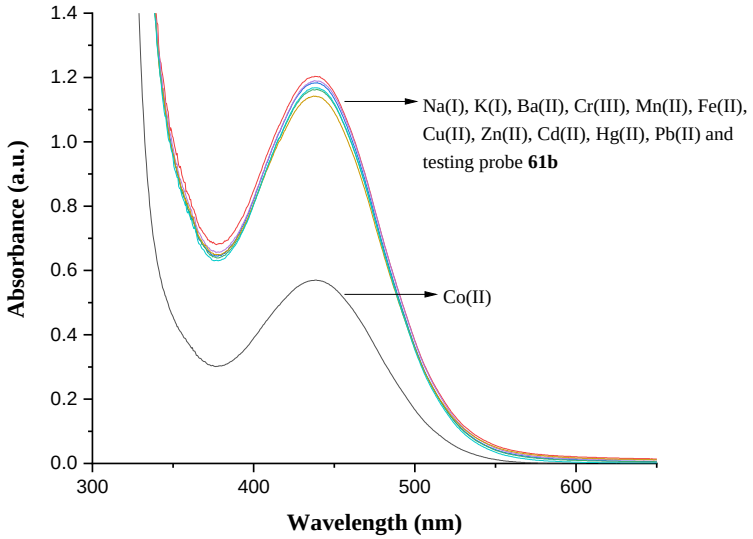

Figure 4.32: UV-Visible spectral responses recorded for testing probe **61b** on addition of 20 equiv. of different metal ions (1.00 mM) separately into 0.50 mM solution of **61b**

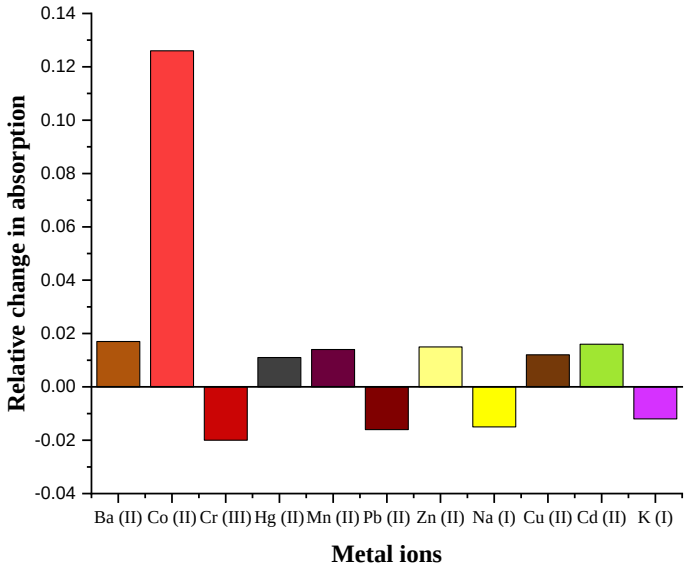

Figure 4.33: Relative change in absorption responses for probe **61b** with various metal ions in acetonitrile-water ($CH_3CN:H_2O$::4:1) as solvent system, observed at λ_{max} = 438 nm on adding 20 equiv. of each metal ion (1.00 mM) solution separately into 0.50 mM solution of chemosensor **61b**

The relative absorbance (An/Ao) with increase in concentration of Co(II) ions is presented in Figure 4.35(a), where An = Absorption intensity with each addition of Co(II) ions and Ao = Absorption intensity of probe **61b** without Co(II) metal ion. The minimum limit of detection of Co(II) with the synthesized probe has been calculated from plot shown in Figure 4.35(b) and was found as 1.87 µM with the stoichiometry of probe **61b**:Co(II) complex as 1:1. From absorption data, the binding constant for ligand-metal complexation was calculated as 5.7 x 10^4 M^{-1}.

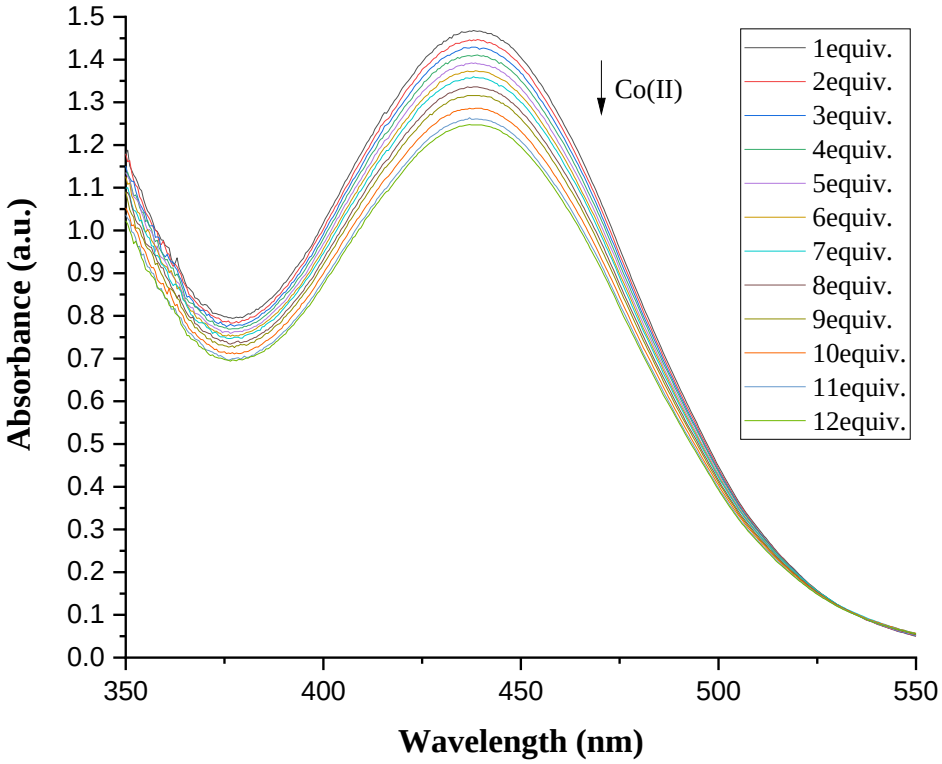

Figure 4.34: Absorbance responses recorded during each successive addition of 1.00 mM Co(II) ions in 0.50 mM of probe **61b** using acetonitrile-water (CH_3CN:H_2O::4:1) as solvent system.

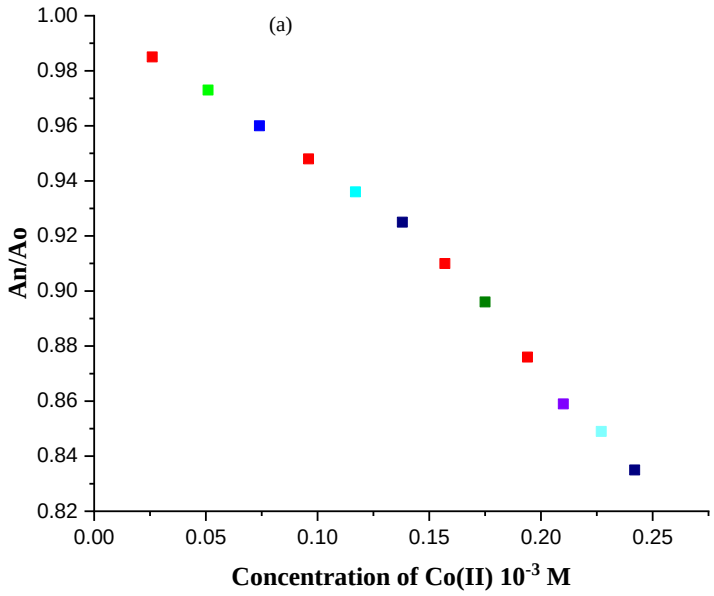

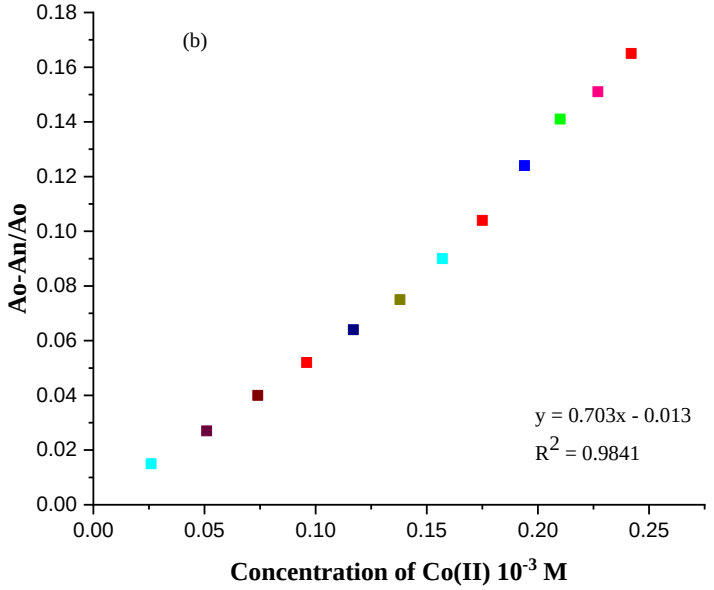

Figure 4.35: (a) Relative change in absorption intensity (An/Ao) of testing probe on adding 15 equiv. of 1.00 mM Co(II) ions. An = Intensity of absorption of **61b** for each addition of Co(II) ions and Ao = Intensity of absorption of chemosensor **61b** without Co(II) ions. (b) Plot of Ao-An/Ao vs. concentration of Co(II) ions.

4.20.2 Probable binding mode of 61b with Co(II)

According to HSAB theory, Co(II) is categorized as borderlines acid that has tendency to interact with receptors having both hard as well as soft basic moiety. Few searches related to Co(II) ion sensing have reported the coordination of this metal ion with nitrogen and oxygen donor atoms [21-22]. The newly synthesized compound **61b** has both these heteroatoms to coordinate with Co(II) ions through the transfer of lone pair of electrons present on these heteroatoms into vacant orbitals in the outermost shell of Co(II). The results of relative change in absorbance with change in concentration of metal ion shows 1:1 stoichiometry of **61b**:Co(II) complex. As per the observed stoichiometry, the two triazole rings of the synthesized heterocyclic probe constitute a perfect cavity to surround Co(II) and the possible binding mode for complexation is as shown in Figure 4.36.

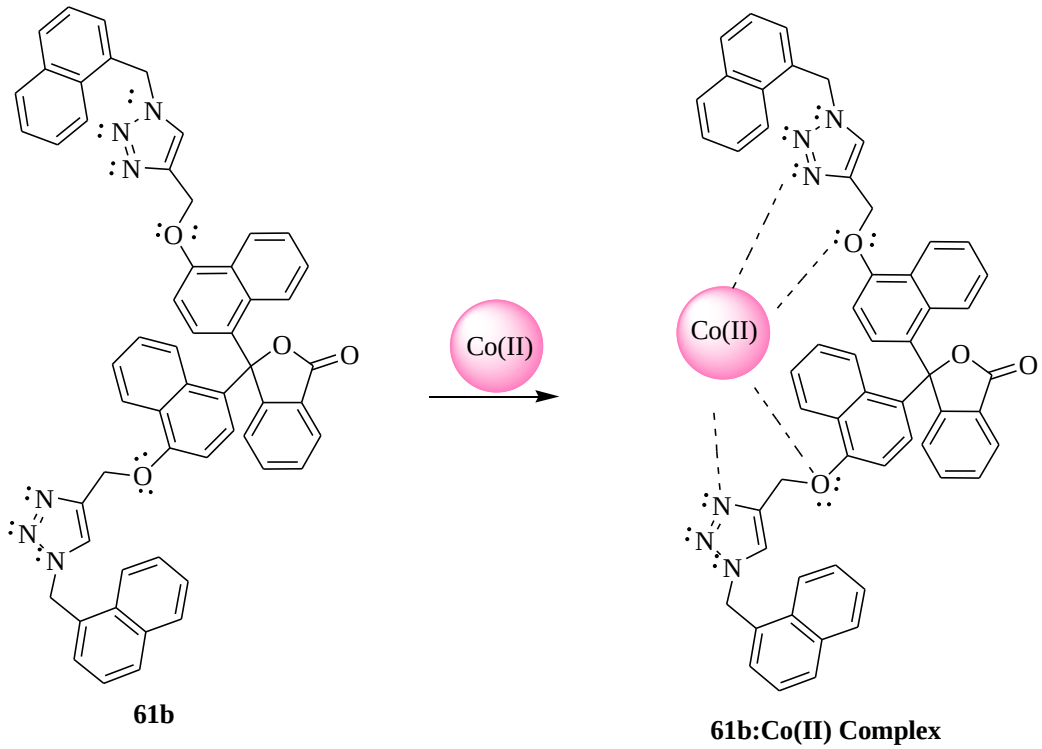

61b **61b:Co(II) Complex**

Figure 4.36: Plausible complexation of Co(II) ion with heterocyclic compound **61b.**

4.21 Chemosensing analysis of 1,2,3-triazole derivatives 62b and 62c

4.21.1 UV-Visible spectroscopy for sensing studies of 62b

Similar to the molecules **59b-61b** and **59c-60c**, the 1,2,3-triazole linked molecule **62b** has also been investigated for its chemosensing behavior by UV-Visible spectroscopy. In order to analyze its ion-sensing behavior, the absorption titrations were conducted with solutions of various metal ions. The significant absorption of sudan-IV dye **62** in UV-Visible region due to presence of azo-groups in its structure proves it a good choice to use as substrate for the synthesis of chemosensor **62b** and during the cycloaddition reaction between sudan-IV based terminal alkyne **62a** and benzylazide **24** in the presence of catalytic amount of $[CuBr(PPh_3)_3]$ complex, the generation of 1,4-disustituted 1,2,3-triazole ring with three nitrogen atoms produces an excellent system to coordinate with specific metal ions. The studies were performed using various solvents and out of those, the mixture of acetonitrile:water ($CH_3CN:H_2O$::4:1) was found as the suitable solvent system owing to the complete solubility of testing molecule **62b** along with clarity of absorption spectrum. Thereafter, the solutions of testing analyte **62b** (0.20 mM) and metal salts of Na(I), K(I), Ba(II), Cr(III), Mn(II), Fe(II), Fe(III), Co(II), Ni(II), Zn(II), Cd(II), Hg(II), Pb(II) and Ce(III) each of concentration 0.50 mM were made ready in the selected solvent system.

In order to analyze the sensing behavior of molecule **62b**, absorption titrations were conducted for sudan-IV appended 1,2,3-triazole derivative **62b** on adding 10 equiv. of 0.50 mM solution of each metal ion separately into 0.20 mM solution of receptor molecule at room temperature and the absorption spectra recorded for different samples are as depicted in Figure 4.37. The significant rise in absorbance of testing chemosensor **62b** at λ = 350 nm and λ = 422 nm with the addition of Fe(III) ions in contrast to other ions, describes the selectivity of newly prepared heterocyclic molecule **62b** for Fe(III) ions.

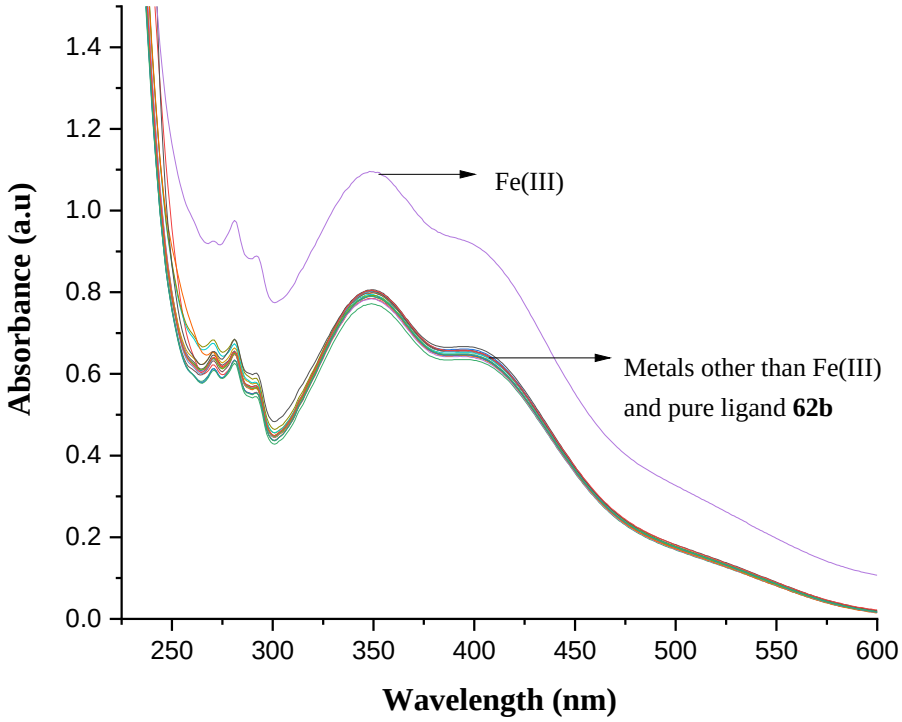

Figure 4.37: UV-Visible spectral responses for testing probe **62b** on addition of 10 equiv. of different metal ions (0.50 mM) separately into 0.20 mM solution of molecule **62b** in acetonitrile-water ($CH_3CN:H_2O$::4:1) mixture

In order to examine the sensing characteristics of receptor **62b** with the change in concentration of Fe(III) ions, the UV-Visible titrations were carried out with the addition of 20 equiv. of 0.50 mM Fe(III) ions in 0.20 mM of sample **62b** and the spectra recorded are as shown in Figure 4.38. Initially, a uniform rise in the absorption intensity was recorded with each addition of Fe(III) ions, whereas, after certain additions, no effect on absorption was recorded with increase in concentration of metal ion. The relative change in absorption intensity (An/Ao) with increase in concentration of Fe(III) ions is presented in Figure 4.39(a), where An = Absorbance with each stepwise addition of Fe(III) ions and Ao = Absorption intensity of probe **61b** without Co(II) metal ions. The minimum limit of detection of Fe(III) ions with the synthesized probe has been computed as 6.50 µM with the stoichiometry of complexation of probe **62b**: Fe(III) as 1:1 and binding constant as 1.8×10^4 M^{-1}, from graph presented in Figure 4.39 (b).

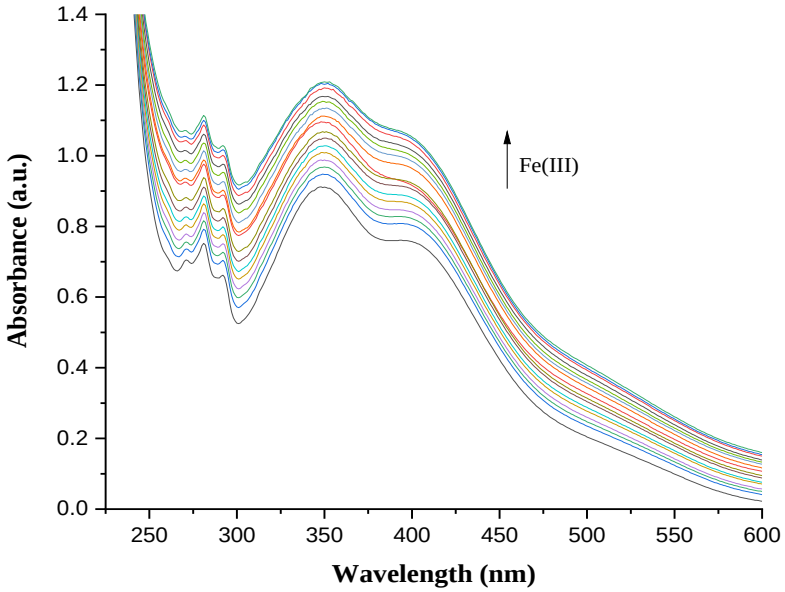

Figure 4.38: Absorbance responses of heterocyclic compound **62b** recorded with each addition of 20 equiv. of 0.50 mM of Fe(III) ions in 0.20 mM of **62b** in acetonitrile-water ($CH_3CN:H_2O$::4:1) mixture

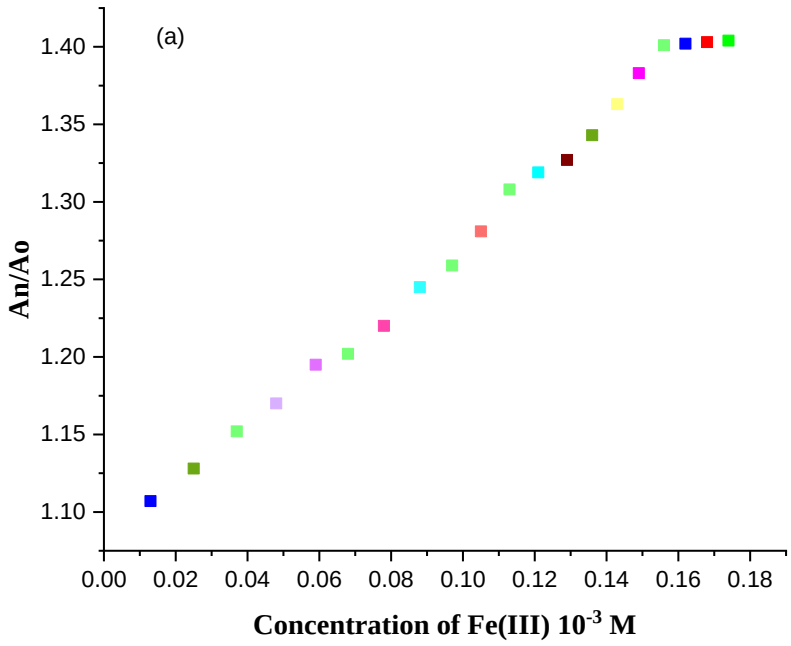

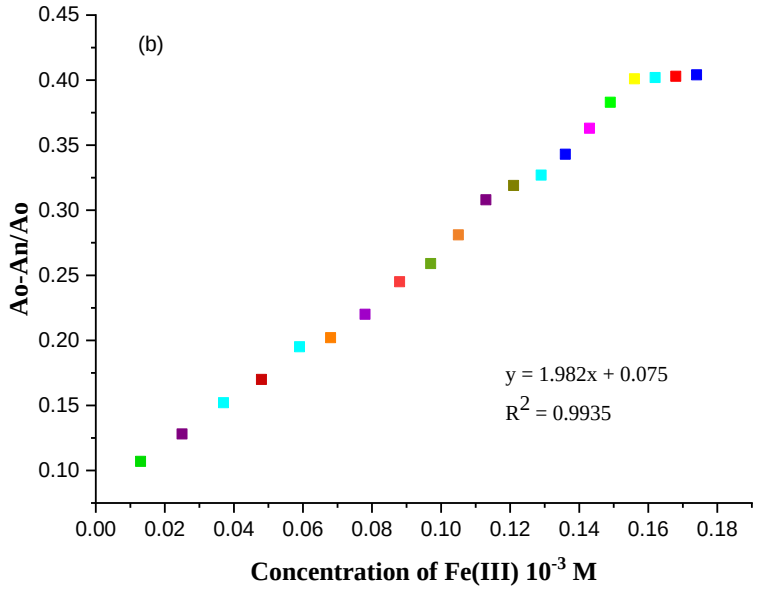

Figure 4.39: (a) Relative change in absorption intensity (An/Ao) of testing probe on addition of 20 equiv. of 0.50 mM Fe(III) ions into 0.20 mM of **62b**. An = Absorbance maxima for each addition of Fe(III) ions and Ao = Intensity of absorption of chemosensor **62b** without Fe(III) ions. (b) Plot of Ao-An/Ao vs. concentration of Fe(III) ions, where the limit of detection of Fe(III) ions was found as 6.5 µM

4.21.2 UV-Visible spectroscopy for sensing studies of molecule 62c

UV-Visible spectroscopic titrations were also performed to investigate the sensing behavior of another sudan-IV based 1,2,3-triazole derivative **62c**, that was prepared as a result of Cu(I)-catalyzed cycloaddition reaction of sudan-IV based alkyne **62a** with azidomethylnaphthalene **58**. Using acetonitrile-water ($CH_3CN:H_2O$::4:1) mixture as solvent system, 0.20 mM solution of heterocyclic compound **62c** and 0.50 mM solutions of various metal such as Na(I), K(I), Ba(II), Cr(III), Mn(II), Fe(II), Fe(III), Co(II), Ni(II), Zn(II), Cd(II), Hg(II), Pb(II) and Ce(III) were prepared. For ion detection, the absorption titrations were carried out for molecule **62c** with the addition of 10 equiv. of 0.50 mM solution of different metal ions separately in 0.20 mM of 1,2,3-triazole derivative **62c**. Similar to **62b**, a noticeable hyperchromic shifting of absorption was observed with the addition of Fe(III) ions in the 0.20 mM solution of receptor **62c**, indicating no change in sensing

behavior with the introduction of one more phenyl ring in the structure of organic azide.

The UV-Visible spectral results observed with the addition of 15 equiv. of 0.50 mM Fe(III) ion solution into 0.20 mM of molecule **62c** are presented in Figure 4.40. The noticeable increase in the absorption intensity was found with each addition of Fe(III) ions into the solution of ligand **62c** and after a stage, no change in absorbance was recorded with further additions. Figure 4.41 (a), presents the relative change in absorption (An/Ao) upon sequential addition of Fe(III) ions where An = Absorption intensity with each addition of Fe(III) ions and Ao = Absorption intensity of ligand **62c** without metal ion. The minimum detection limit of Fe(III) ions has been computed from the plot displayed in Figure 4.41(b) and was found as 6.38 µM with stoichiometry of complexation of **62c**: Fe(III) as 1:1 and and binding constant as 1.9 x 10^4 M^{-1}.

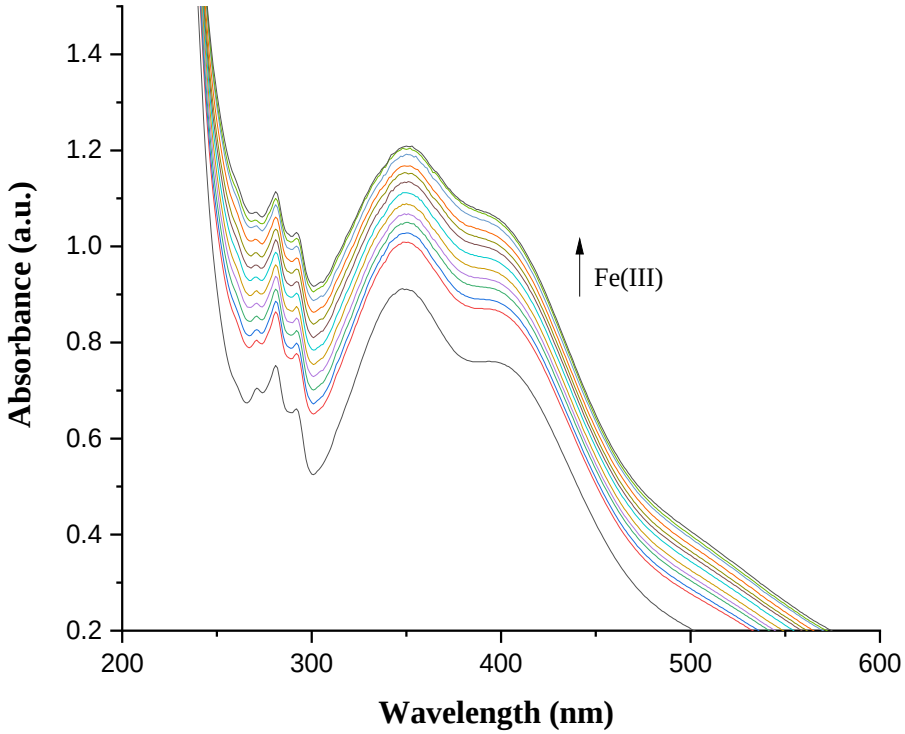

Figure 4.40: UV-Visible responses of 0.20 mM of ligand **62c** on addition of 15 equiv. of 0.50 mM of Fe(III) ions

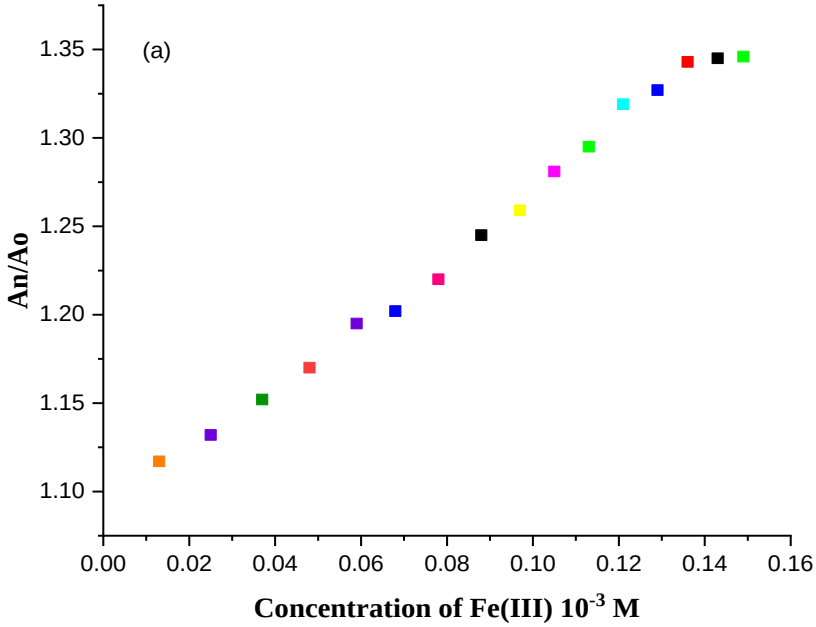

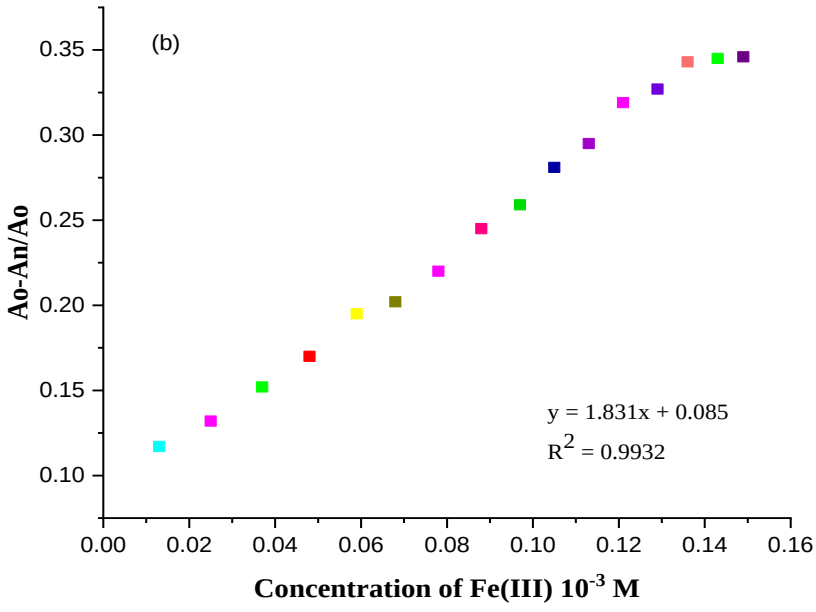

Figure 4.41: (a) Relative change in absorption intensity (An/Ao) of testing probe **62c** on addition of 15 equiv. of 0.50 mM Fe(III) ions into 0.20 mM of **62c**. (b) Plot of Ao-An/Ao vs. Concentration of Fe(III) ions, where the limit of detection of Fe(III) ions was found as 6.38 µM

4.21.3 Probable binding mode of 62b/62c with Fe(III)

According to HSAB theory, iron is classified as hard acid and likely to show binding with hard bases such as ligands having nitrogen and oxygen as binding sites. The literature studies regarding iron sensing have reported few organic receptor units equipped with oxygen and nitrogen atoms as coordinating sites to show complexation with Fe(III) ions [23-24]. The molecules **62b** and **62c** obtained as a result of CuAAC reaction contain heterocyclic 1,2,3-triazole moiety having three nitrogen atoms and sudan-IV linker with azo-groups to co-ordinate with Fe(III). From the plot of relative shift in absorption of molecules **62b** and **62c** with respect to change in concentration of Fe(III) ions, the binding ratio of ligand-metal complex was calculated as 1:1. In line with the observed stoichiometry, the possible binding of metal ion with 1,2,3-triazole derivative **62b** is given in Figure 4.42.

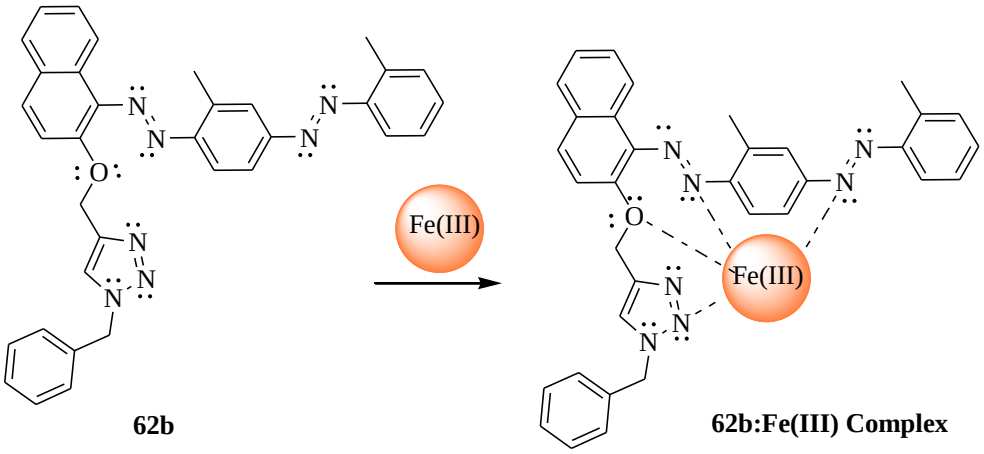

Figure 4.42: Possible binding mode of synthesized 1,2,3-triazole derivative **62b** with Fe(III) ions.

4.22 Chemosensing analysis of 1,2,3-triazole derivative 63b

4.22.1 UV-Visible spectroscopy for sensing studies of 1,2,3-triazole derivative 63b

1-naphtholbenzein based 1,2,3-triazole linker **63b**, synthesized through Cu(I)-catalyzed alkyne-azide cycloaddition of 1-naphtholbenzein based alkyne **63a** and azidomethylbenzene **24** has been investigated for its ion sensing behavior towards

several metal ions. The excellent absorption of 1-naphtholbenzein **63** and chloromethylbenzene **57** in UV-Visible region make them a better choice to use as starting materials for the synthesis of chemosensor **63b**. 1-naphtholbenzein was converted to terminal alkyne **63a**, the first reactant of CuAAC reaction that was generated by the substitution of proton of hydroxyl group on molecule **63** with propynyl group following a suitable procedure. Chloromethylbenzene was converted to azidomethylbenzene **24**, the second component of click cycloaddition, on treatment with sodium azide under suitable reaction conditions. During the cycloaddition reaction between 1-naphtholbenzein based terminal alkyne **63a** and azidomethylbenzene **24,** the generation of heterocyclic 1,2,3-triazole ring having three nitrogen atoms fabricates an excellent molecular setup for binding with metal ions. The molecular assembly **63b** has nitrogen as well as oxygen atoms to coordinate with a specific metal ion and make this molecule a chemosensor for the detection of that metal ion. Considering this specific feature of the molecule **63b,** the sensing studies were performed on UV-Visible spectrophotometer using various solvents and among them, the combination of acetonitrile and water ($CH_3CN:H_2O$::4:1) was analyzed as the best solvent in respect to solubility of testing analyte as well as fineness of absorption spectrum. Thereafter, the solutions of testing molecule **63b** (0.20 mM) and metal salts of Na(I), K(I), Ba(II), Cr(III), Mn(II), Fe(II), Fe(III), Co(II), Ni(II), Cu(I), Zn(II), Cd(II), Hg(II), Pb(II), Th(IV) and Ce(III) each of concentration 0.50 mM were made in acetonitrile-water ($CH_3CN:H_2O$::4:1) solvent mixture.

For ion detection, the absorption titrations were conducted for heterocyclic compound **63b** with the sequential addition of 10 equiv. of 0.50 mM of each metal separately in 0.20 mM of ligand molecule **63b** at room temperature. Ligand **63b** was showing two peaks with maximum intensity at λ = 426 nm and λ = 303 nm. No significant change in the absorption of ligand **63b** was observed with the addition of various metal ions except for Cu(II). Changes in the absorption responses recorded with an increase in concentration of Cu(II) ions from 0.013 mM to 0.174 mM are shown in Figure 4.43. The noticeable changes in the absorbance intensity of testing chemosensor **63b** was observed at λ = 426 nm and λ = 303 nm upon addition of Cu(II) ions into 0.20 mM solution of molecule **63b.**

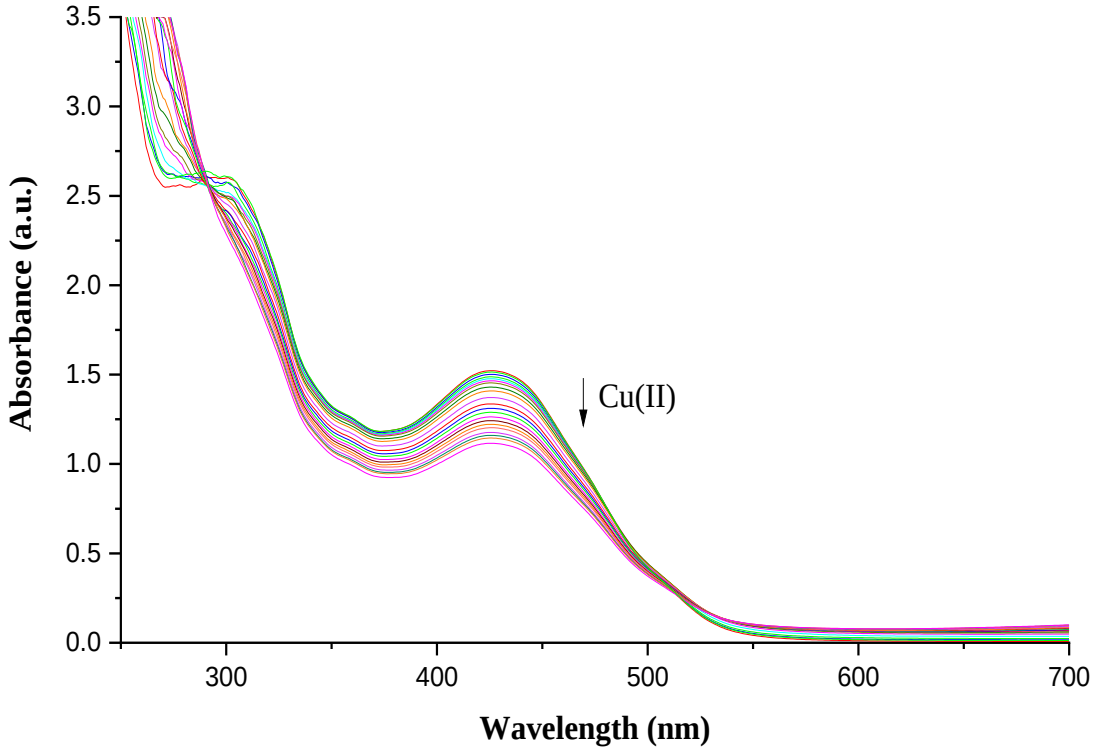

Figure 4.43: UV-Visible spectral responses of 1,2,3-triazole derivative **63b** with increase in concentration of Cu(II) ions from 0.013 mM to 0.174 mM in acetonitrile-water ($CH_3CN:H_2O$::4:1) mixture

With an increase in concentration of Cu(II) ions, hypochromic shifting in the intensity of absorbance was recorded at λ = 426 nm. In between λ = 500-520 nm, an isosbestic point was observed, above λ = 520 nm, an increase in intensity was noticed with increase in concentration of metal ion, whereas below λ = 500 nm, there is a regular decrease in intensity with each successive addition of Cu(II) ion. Highly significant change in the absorption pattern was recorded below and above λ = 290 nm, a visible isosbestic point, with rise in concentration of Cu(II) ions. The deep examination of results obtained from UV-Visible spectroscopy indicates the sensitivity of synthesized probe **63b** towards Cu(II) ions. In order to support the results obtained from UV-Visible titrations, the chemosensing studies has also been extended with Fluorescence spectroscopy.

4.22.2 Fluorescence spectroscopic studies of 63b

The fluorescence spectroscopic titrations were performed for heterocyclic molecule **63b** of concentration 0.10 mM with 0.01 mM of Cu(II) ions in acetonitrile-water ($CH_3CN:H_2O$::4:1) solvent system. Significant fluctuations in the emission spectra of testing probe were observed at wavelengths 372 nm, 579 nm and 730 nm at λ_{ex} = 290 nm as shown in Figure 4.44 (a). At wavelengths 372 nm and 730 nm, noticeable fall in emission intensity was recorded with increase in concentration of Cu(II) ions, whereas at wavelength 579 nm {Figure 4.44(b)}, the emission intensity goes on increasing with the successive addition of Cu(II) ions. This distinctive fluorescence response of **63b** towards Cu(II) ions makes this receptor selective for the recognition of these ions.

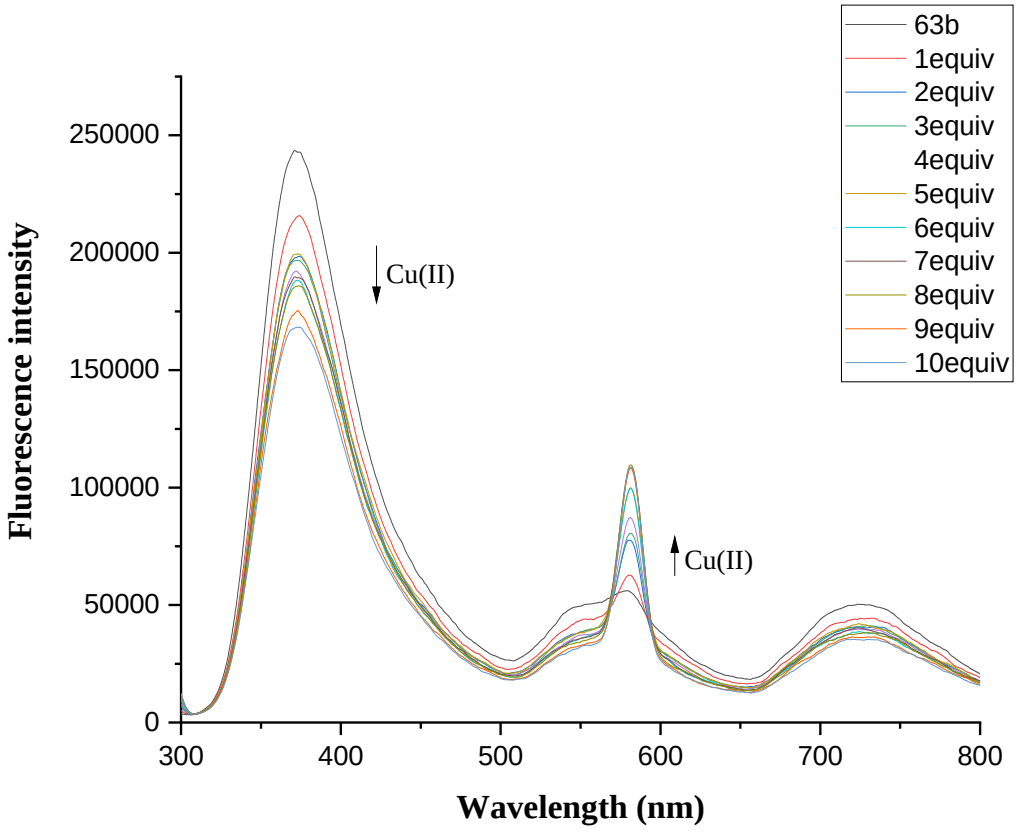

Figure 4.44(a): Emission spectra of testing analyte **63b** (0.10 mM) with the successive addition of 0.01 mM of Cu(II) ions in acetonitrile and water ($CH_3CN:H_2O$::4:1) mixture

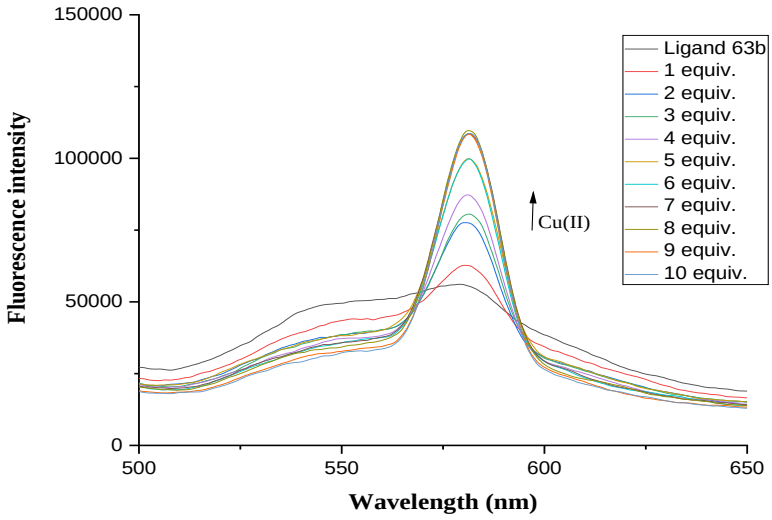

Figure 4.44(b): Fluorescence spectra for **63b** recorded at λ_{ex} = 290 nm showing increase in emission intensity at λ = 579 nm with increase in concentration of Cu(II) ions

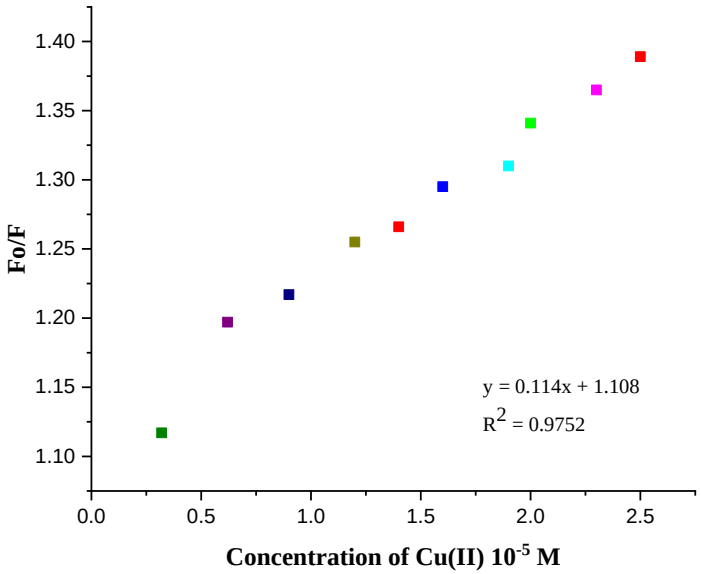

Figure 4.45: Relative change in emission intensity (Fo/F) with increase in concentration of Cu(II) ions from 0.32 x 10^{-5} M to 2.50 x 10^{-5} M at λ = 372 nm

The relative change in emission intensity (Fo/F) with increase in concentration of Cu(II) ions from 0.32 x 10^{-5} M to 2.50 x 10^{-5} M at wavelength λ = 372 nm is shown in Figure 4.45, where Fo is the fluorescence maximum of ligand **63b** without the addition of Cu(II) ions and F is the fluorescence intensity with each successive addition of Cu(II) ions in the solution of probe **63b**. From this graph, the minimum limit of detection of Cu(II) ions by heterocyclic molecule **63b** was calculated as 3.12 μM and on putting this fluorescence data into Stern-Volmer equation, the binding constant of this complexation was found as 0.15 x 10^{5} M^{-1}. Figure 4.46 shows the relative change in emission intensity (Fo/F) with change in concentration of Cu(II) ions at wavelength, λ = 579 nm, from where binding ratio of ligand-metal complexation has been calculated as 2:1.

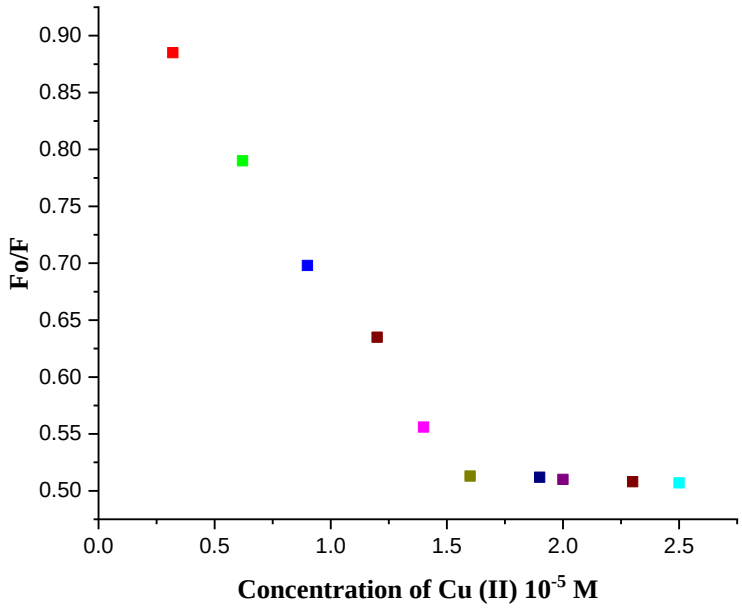

Figure 4.46: Relative change in emission intensity (Fo/F) with increase in concentration of Cu(II) ions from 0.32 x 10^{-5} M to 2.50 x 10^{-5} M at λ = 579 nm. The **63b**:Cu(II) complex ratio is found as 2:1

4.22.3 Probable binding mode of probe 63b with Cu(II)

Based upon the concept of HSAB theory, Cu(II) is classified as borderline acid and has potential to interact with receptor units having both hard as well as soft

basic sites. Literature survey has revealed various complexing units found to show interaction with Cu(II) ions through oxygen and nitrogen donor sites [25-27]. The newly synthesized complexing agent, 1,2,3-triazole derivative **63b** is enriched with oxygen and nitrogen atoms to coordinate with Cu(II) ions. The relative change in absorption intensity with change in concentration of metal ion shows binding ratio of **63b**:Cu(II) complexation as 2:1. As per the observed stoichiometry, the two 1,2,3-triazole linked molecules **63b** arrange themselves to create a cavity to encapsulate the Cu(II) ions and the possible binding mode for the complexation may be as per the interaction shown in Figure 4.47.

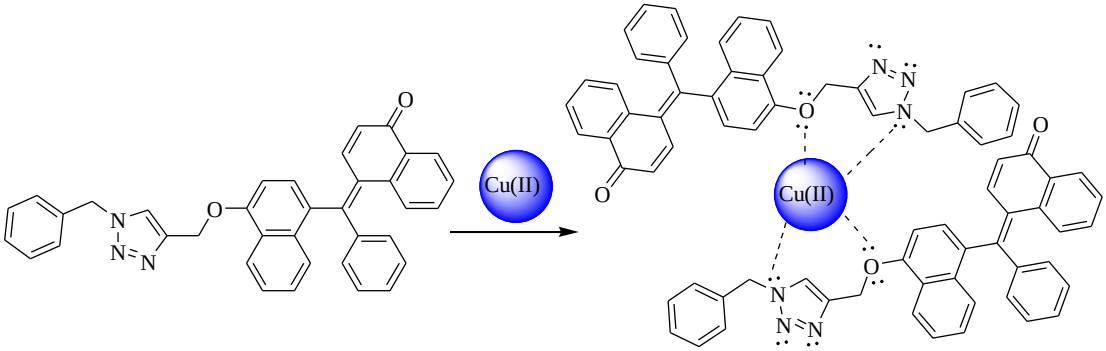

Figure 4.47: Possible binding of 1,2,3-triazole derivative **63b** with Cu(II) ions. From job's plot, the binding ratio of **63b**:Cu(II) has been found as 2:1

4.23 Conclusion

The 1,2,3-triazole linkers presented in this section are heterocyclic compounds having three nitrogen atoms in the triazole ring, that fabricate a perfect moiety to coordinate with metal ions. Each molecule is appended with good chromophoric unit in their structure, so have excellent absorption in UV-Visible region that helps in analyzing their sensing behavior through UV-Visible and Fluorescence spectroscopy. This section describes the chemosensing studies of various novel 1,2,3-triazole derivatives synthesized through CuAAC reaction of newly synthesized terminal alkynes with two different azides (azidomethylbenzene and azidomethylnaphthalene) and it was observed that 1,2,3-triazole derivatives prepared from cycloaddition of two different organic azides with same terminal alkyne do not differ much in their

chemosensing behavior. Both the molecules are showing their sensitivity towards same metal ion and almost to same extent. The observed spectral responses for different probes are shown in various figures, from where their specificity towards a particular metal ion is examined. The analytical calculations for the determination of limit of detection of metal ion, binding ratio of receptor:metal ion complex as well as binding constant for various newly synthesized 1,2,3-triazole linkers are done and reported in the text.

References:

1. X. Creary, A. Anderson, C. Brophy, F. Crowell, Z. Funk, *J. org. Chem.* **2012**, 77, 8756.
2. A. K. Brisdon, Inorganic Spectroscopic Methods, Oxford: Oxford UP, **1998**, ISBN: 978-01-985-5949-8.
3. D. L. Pavia, G. M. Lampman, G. S. Kriz, J. R. Vyvyan, Spectroscopy, 6th Indian edition, **2011**, ISBN: 978–81–315–0576–2.
4. N. S. Ginsberg, Y. C. Cheng, G. R. Fleming**,** *Acc. Chem. Res.* **2009**, 42, 1352.
5. F. Pointillart, T. Cauchy, Y. L. Gal, S. Golhen, O. Cador, L. Ouahab**,** *Inorg. Chem.* **2010**, 49, 1947.
6. M. Zhou, J. Dong, L. Miao, *J. Phy. Chem. A* **2004**, 108, 2431.
7. sL. M. A. Monzon**,** F. Burke, J. M. D. Coey, *J. Phy. Chem. C*, **2011**, 115, 9182.
8. N. Shao, Y. Zhang, S. Cheung, R. Yang, W. Chan, T. Mo, K. Li, F. Liu, *Analyt. Chem.* **2005**, 77, 7294.
9. J. E. Huheey, E. A. Keiter, L. K. Richard, Inorganic Chemistry: Principles of Structure and Reactivity, 4th edition, New York, NY: Harper Collins College, **1993**, ISBN: 978-00-604-2995-9.
10. Y. Yang, M. A. Ratner, G. C. Schatz**,** *J. Phy. Chem. C*, **2014**, 118, 29196.
11. R. S. Drago, Physical Methods for Chemists, 2nd edition, Ft. Worth: Saunders College Pub., **1992**, ISBN: 978-00-307-5176-9.
12. S. M. Barrett, P. S. Szalay, L. A. Zook-Gerdau, E. J. Schurter, *J. Chem. Educ.* **2020**, 97, 4097.
13. H. N. Kim, W. X. Ren, J. S. Kim, J. Yoon, *Chem. Soc. Rev.* **2012**, 41, 3210.

14. G. Singh, G. Sharma, Sanchita, P. Kalra, P. Satija, Pawan, B. Singh, D. Aulakh, M. Wreidt, *Chem. Select*, **2020**, 5, 284.
15. S. Sen, S. Sarkar, B. Chattopadhyay, A. Moirangthem, A. Basu, K. Dhara, P. Chattopadhyay, *Analyst*, **2012**, 137, 3335.
16. G. T. Selvan, C. Varadaraju, R. T. Selvan, I. V. M. V. Enoch, P. M. Selvakumar, *ACS Omega*, **2018**, 3, 7985.
17. S. Chakraborty, S. Rayalu, *Inorg. Chem. Comm.* **2019,** 112, 107963.
18. S. E. Enkuytu, E. T. Ecik, *Spectrochim. Acta. Mol. Biomol. Spectrosc.* **2018**, 198, 232.
19. S. E. Enkuytu, E. T. Ecik, *Spectrochim. Acta. Mol. Biomol. Spectrosc.* **2017**, 173, 863.
20. V. V. S. Mummidivarapu, V. K. Hinge, K. Tabbasum, R. G. Gonnade, C. P. Rao, *J. Org. Chem.* **2013**, 78, 3570.
21. Q. X. Liu, Z. L. Hu, Z. X. Zhao, *New j. Chem.* **2018,** 24, 20049.
22. D. Vashisht, K. Kaur, R. Jukaria, A. Vashisht, S. Sharma, S. K. Mehta, *Sens. Actuators: B. Chem.* **2018**, 10, 1016.
23. H. Jain, N. Deswal, A. Joshi, C. N. Ramachandran, R. Kumar, *Anal. Methods*, **2019**, 11, 3230.
24. M. Lievenbruck, B. Hartlaub, H. Ritter, *Poly. Internat.* **2016**, 65, 477.
25. N. Kursunlu, M. Ozmen, E. Guler, *J. fluorescence*, **2019**, 29, 1321.
26. G. Singh, J. Singh, S. S.Mangat, A. Arora, *Tetrahed. Lett.* **2014**, 55, 2551.
27. Y. C. Hsieh, J. L. Chir, H. H. Wu, P. S. Chang, *Carbohyd. Res.* **2009**, 344, 2236.

Summary

Thesis overview

This section packs down complete thesis into a compact form and briefly describes all the work done such as experimental data along with the results obtained.

The present research work involves the synthesis of 1,2,3-triazole linked molecules, their characterization by various spectroscopic techniques and chemosensing applications to detect various metal ions. Whole work is divided into four main parts: Introduction (Chapter 1), Review of literature (Chapter 2), Experimental details (Chapter 3) and Results and discussion (Chapter 4)

Chapter 1: Introduction

This chapter presents detailed discussion and outcomes of Cu(I)-catalyzed alkyne-azide cycloaddition reaction (CuAAC), an important class of 'Click Chemistry'. The chapter is divided into various sections and subsections describing several aspects of CuAAC reaction along with the importance of heterocyclic product obtained as a result of this cycloaddition reaction. First section introduces with the historical aspects of 'Click Chemistry' including contribution of Sir K. B. Sharpless, a noble laureate and founder of 'Click Chemistry' who introduced this term in 2001. 'Click Chemistry' is not a new set of synthetic chemistry, but an advanced form of previously discovered reactions to be conducted under simple and ambient reaction conditions to get pure product with high yield. Among the various types of click chemistry reactions, the main attraction of this chapter is the discussion of 1,3-dipolar cycloaddition reactions investigated in late 19th century to early 20th century with the invention of various types of 1,3-dipoles. Application part of this reaction was investigated with the research outcome of Rolf Huisgen 1,3-dipolar cycloaddition reaction shown in Figure S1, involving cycloaddition of organic azide as a dipole with an alkyne as a dipolarophile, but this reaction was suffering from the difficulty in separation of two isomers formed as a result of cycloaddition process.

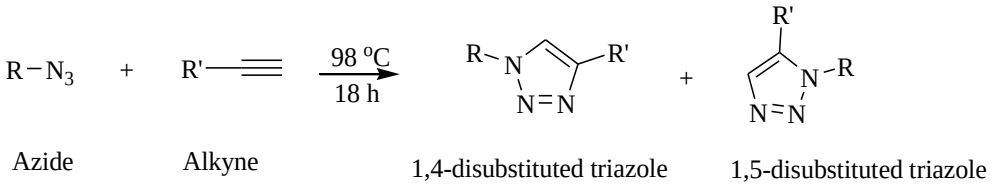

Figure S1: Rolf Huisgen 1,3-dipolar cycloaddition reaction to form two di-substituted 1,2,3-triazole products

The reaction gained extreme importance and worldwide popularity, when Dr. K. B. Sharpless, in 2001, performed the same reaction using Cu(I) as catalyst (Figure S2). Presence of catalytic amount of Cu(I) improved the rate as well as stereoselectivity of the reaction, i.e. generation of only 1,4-disubstituted 1,2,3-triazole as an exclusive product in high yield and purity under simple reaction conditions.

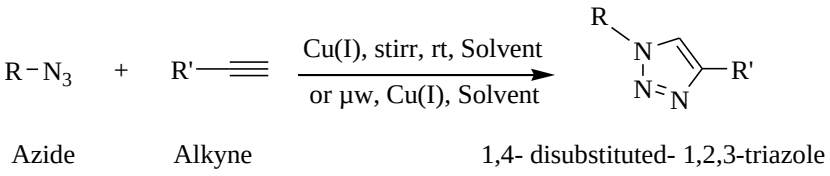

Figure S2: Scheme of Cu(I)-catalyzed alkyne–azide cycloaddition (CuAAC)

In order to support the stereoselectivity of alkyne-azide cycloaddition reaction in the presence of Cu(I), the catalytic action of Cu(I) was discussed in the mechanism of CuAAC reaction discovered by V. Fokin and K. B. Sharpless as shown in Figure 1.4a and 1.4b. In the next section, various catalytic systems as source of Cu(I) are described. A huge number of publications are found in literature using different types of catalytic systems.

Further sections familiarize with the importance as well as applications of 1,2,3-triazole linked molecules. As these molecules are aromatic with little basic character, highly stable to little thermal and chemical changes, therefore have great importance under physiological pH. The heterocyclic ring 1,2,3-triazole is found as core component of most of the drugs, so have wide pharmacological significance such as antiviral, anticancer, antimicrobial, anti-HIV etc. Due to the presence of nitrogen heteroatoms in ring, these molecules have great tendency to coordinate with various metal ions. This property leads to have their use as chemosensors to address certain environmental issues. The sensors constitute an effective analytical tool, when regular monitoring and real-time facts are required in the area of drug discovery, environmental study and process controlling. The chapter 1 involves detailed description of molecular sensors including their composition, features and mechanism of chemosensing. 1,2,3-triazole linkers appended with certain chromophoric or fluorophoric units have a great deal of sensing characteristics that can be examined through UV-Visible and Fluorescence spectroscopy. A brief description of

chemosensing analysis of molecules by UV-Visible and Fluorescence spectroscopy is presented in the last section of this chapter.

Chapter 2: Review of literature

This chapter has also been divided into various sections and subsections having the content of extensive literature survey related to the actual work done presented in this thesis. 1,2,3-triazole derivatives, the titled molecules of this research work are the heterocyclic compounds, so the first section shows general introduction of heterocyclic compounds along with a brief knowledge of isomeric forms of 1,2,3-triazole and their tautomerism. Next section focuses on the literature regarding methodologies used in the synthesis of expected heterocyclic compounds that are mentioned under following three headings:

- Synthesis of terminal alkynes
- Synthesis of organic azides
- Cu(I)-catalyzed cycloaddition of terminal alkynes and organic azides

Various types of chemical methods used for the synthesis of terminal alkynes are expressed, involving a variety of reactants and reaction conditions showing continuous growth and required modifications in terms of getting good yield of product, feasibility of reaction conditions and simplicity of experimental setup economically as well as experimentally. On the same note, next subsection describes the different methods of synthesis of aliphatic as well as aromatic organic azides under different azidation conditions.

Next to this, the literature review on [3+2] cycloaddition reaction organic azide with terminal alkyne has been elaborated showing a wide range of catalytic systems as Cu(I) sources. This section of thesis focuses on the evolutionary history of various Cu(I)-catalytic systems. Initially, the CuAAC reactions were being conducted using most common Cu(II) salts in combination with reducing agent e.g. $CuSO_4.5H_2O$ in combination with sodium ascorbate. Besides the use of reducing agent in combination with Cu(II) to convert it into Cu(I), a different technique has also been used for this reduction process, known as photo reduction, that involved reduction of Cu(II) to Cu(I) using UV-Visible light in the presence of a suitable photo-initiator in

spite of reducing agent. The literature survey also revealed one pot synthesis of 1,2,3-triazole based derivatives using terminal alkyne and alkyl halide or aryl halide in the presence of catalyst $CuSO_4.5H_2O$ along with sodium ascorbate, NaN_3 and KI in water at room temperature. The process did not involve synthesis of organic azide separately but is carried out by the stirring of reaction mixture for about 1h using phase transfer catalyst, followed by workup in cold water to isolate the product. In addition to multicomponent catalytic systems, involving generation of Cu(I) from Cu(II) salts, the research contributions involving direct use of Cu(I) salts as catalyst have also been reported in literature, but the stability/existence of Cu(I) in a particular solvent system is generally controversial. It usually gets oxidized into Cu(II) form, a stable oxidation state of copper and as a result, low yield of the product has been recorded. In order to resolve this issue of conversion of oxidation state, the use of external ligands along with Cu(I) salt is found in various research contributions. Ligands with donor atoms such as N, O, S or P are the most common that complexes with Cu(I) ion and inhibit its oxidation to Cu(II).

More advanced catalytic materials are the coordination complexes of Cu(I) having bulky organic species as ligands with enhanced stability of Cu(I). Coordination complexes, like $[CuI(P(OEt)_3)]$, $[CuBr(PPh_3)_3]$, $[Cu(MeCN)_4]PF_6$, $[CuF(PPh_3)_3]$, etc. are the most commonly employed Cu(I) sources with a great deal to act as catalysts for alkyne-azide cycloaddition reaction with minimum risk of oxidation of Cu(I) to Cu(II) and high yield of product. Various research reports have been discussed in this section of thesis as evidence in favor of regular advancements in catalytic material. Therefore, $[CuBr(PPh_3)_3]$ complex has been selected as Cu(I)-catalyst to generate novel 1,2,3-triazole derivatives reported in this research contribution.

Next section of this chapter briefly describes about various spectroscopic techniques like IR, NMR along with mass spectroscopy to be used, in order to characterize the synthesized molecules. In the last, applications of 1,2,3-triazole derivatives are discussed, among them more emphasis is laid on chemosensing. This section includes various examples of the molecular sensors and sensing techniques followed to analyze different analytes.

Chapter 3: Experimental details

This chapter provides detailed experimental work performed to achieve the proposed objectives. It contains complete description of all the experimental steps followed to synthesize novel 1,2,3-triazole linked molecules along with required analytical measurements in support of synthesis. The three step procedure was followed to prepare the designed molecules. First section of this chapter provides general course of action of all the three steps involved in the preparation of 1,2,3-triazole linkers. Next part describes the actual experimental work done to synthesize two different organic azides, azidomethylbenzene **24** and azidomethylnaphthalene **58,** including reaction conditions along with analytical data such as yield, color/texture, characterization data of IR and NMR (^{1}H, ^{13}C) of synthesized azides. Thereafter, the synthesis of novel terminal alkynes **59a-63a** presented in Figure S3 from starting materials **59-63** is described. The experimental conditions for each synthesis are expressed in detail separately in different sections. IR, NMR (^{1}H, ^{13}C) data of each alkyne is given in order to support their generation. Other features such as yield, color and melting points of each alkyne are also mentioned.

In the synthesis section, next is [3+2] cycloaddition reactions of synthesized alkynes with two different azides to get 1,2,3-triazole linked molecules **59b-63b** and **59c-60c, 62c** (Figure S4) has been elaborated in detail including all experimental conditions of each reaction properly. Product yield, melting point, color/texture, elemental analysis, IR, NMR (^{1}H, ^{13}C) and mass spectrum of each 1,2,3-triazole derivative were recorded on suitable instrument and the data is presented in this chapter, wherever required. Materials and methods including specification of instruments used during the research work are given in appendix A. IR spectra, NMR (^{1}H, ^{13}C) and mass spectra are provided in appendix B, C and D respectively.

Chapter 4: Results and discussion

This chapter gives detailed discussion of all the data expressed in experimental section. It is further divided into two sections based upon synthesis, spectral studies and application part of synthesized heterocyclic compounds.

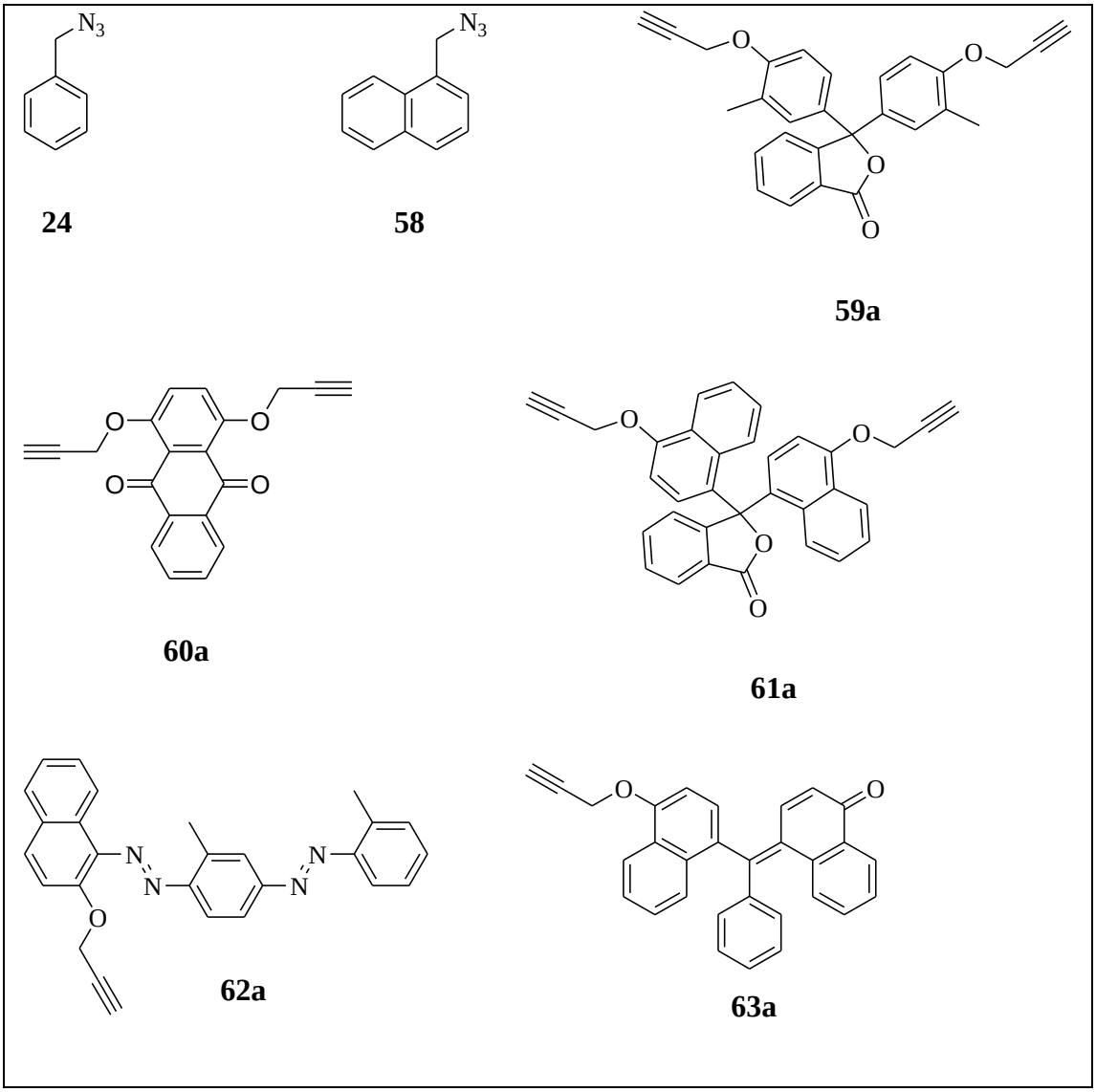

Figure S3: Organic azides **24** and **58** with terminal alkynes **59a-63a**

Section I: Results and discussion of spectroscopic data

Section II: Photophysical properties of 1,2,3-triazole linkers by UV-Visible/Fluorescence spectroscopy

Section I of this chapter displays synthetic aspects and discussion of spectroscopic data of all the synthesized molecules. For the generation of 1,2,3-triazole linkers, the three-step procedure was followed, where the different organic entities were reacted in suitable reaction conditions to result into expected molecules.

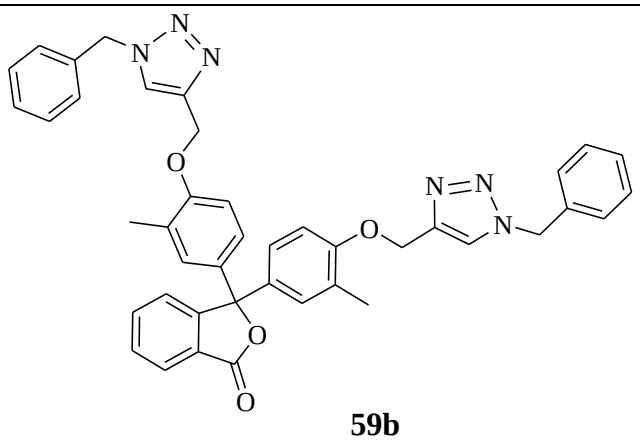

59b

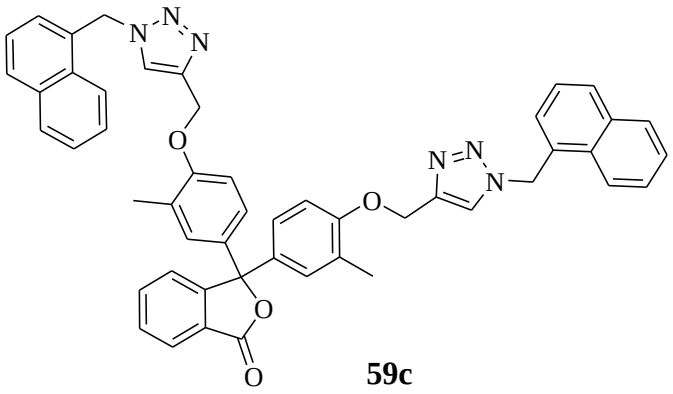

59c

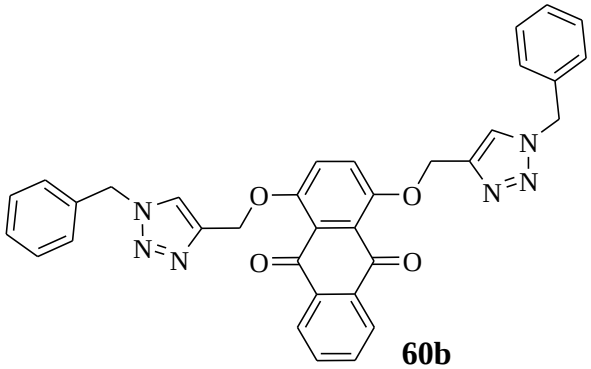

60b

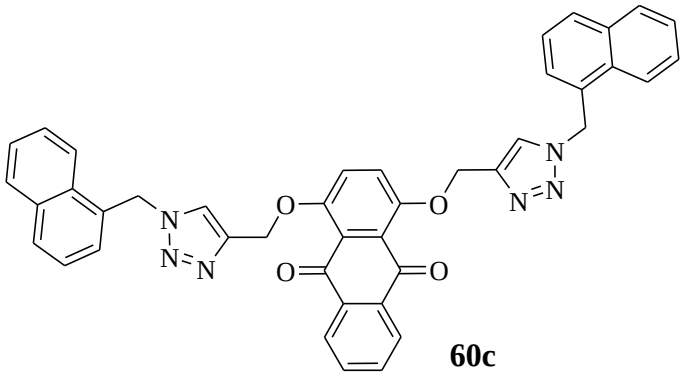

60c

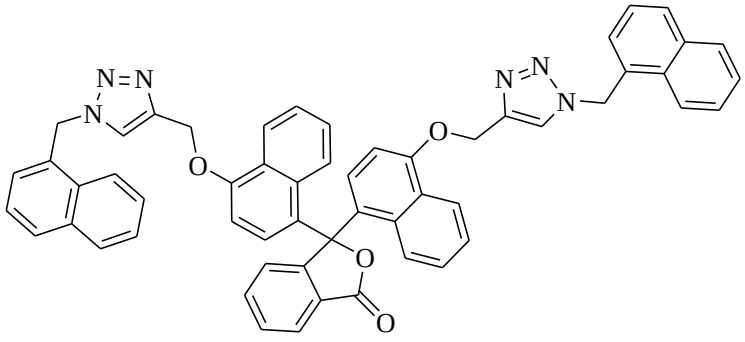

61b

Contd…

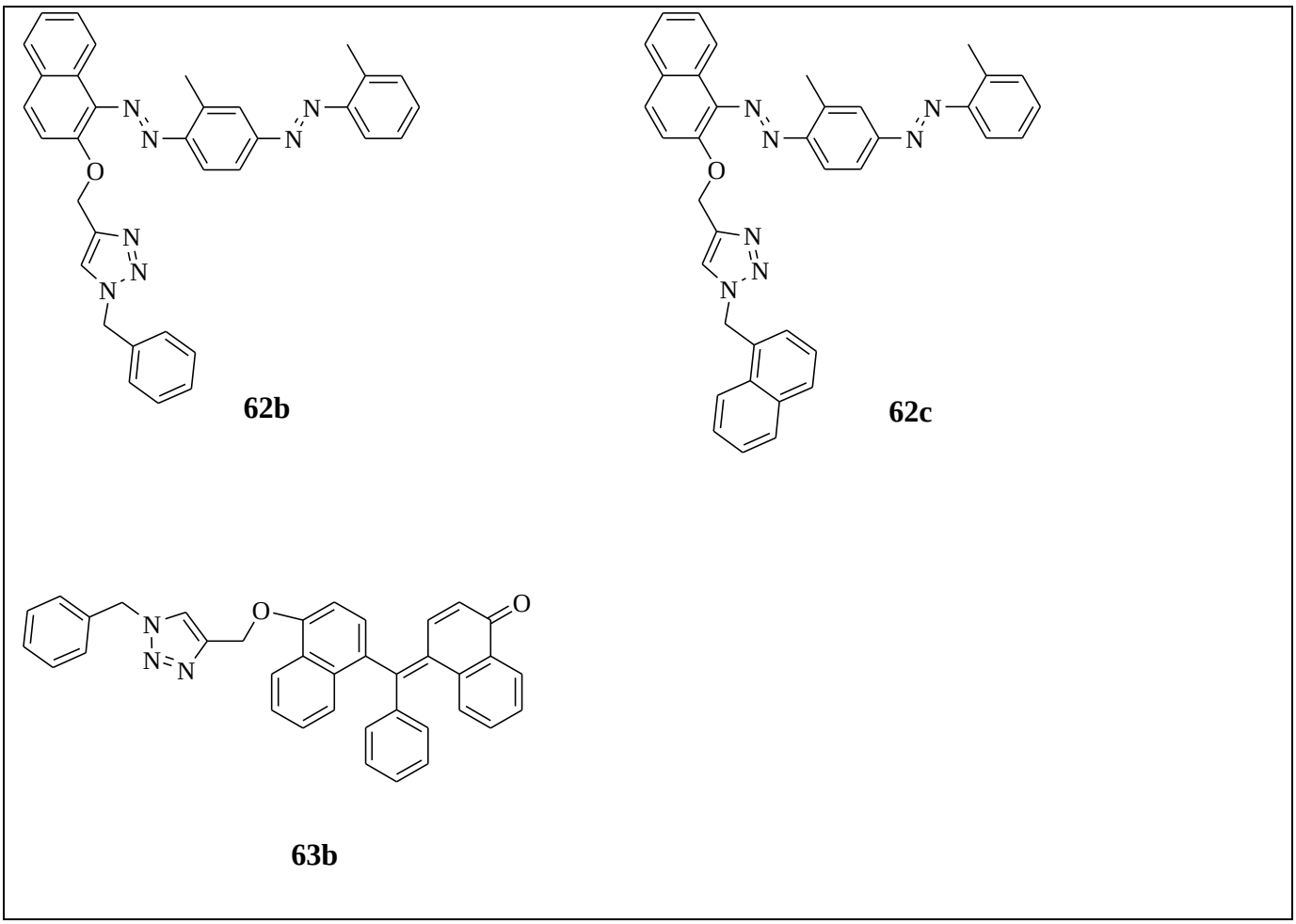

Figure S4: 1,2,3-triazole linked molecules **59b-63b** and **59c-60c, 62c**

Two different azides **24** & **58** were synthesized by the substitution reaction of benzyl chloride and chloromethylnaphthalene with sodium azide on stirring at 85-90 °C in DMF respectively. Both the azides are oily products at room temperature; whose generation was supported by IR and NMR spectroscopy. A strong peak at frequency of vibration 2091 cm^{-1} in the IR spectra of both the azides recorded as neat in range 4000-500 cm^{-1} characterizes $-\mathbf{N_3}$ group, whereas other peaks are in well agreement with the structures of synthesized azides. ^1H NMR spectra of both the azides were obtained at 500 MHz in $CDCl_3$, the peaks in range δ = 8.12-7.14 ppm corresponds to aromatic protons and singlet obtained at δ = 4.78-4.14 ppm is due to $-C\mathbf{H_2}$ group attached to azide functionality. The signal due to protons of $-C\mathbf{H_2}$ group is little bit more downfield in azidomethylnaphthalene as compared to benzylazide,

because of strong deshielding effect of naphthyl group than phenyl group. Similarly, the data obtained from ^{13}C NMR spectra is in accordance with the proposed structures. The signals in the range δ = 135.53-123.64 ppm are due to carbons of aromatic rings and at around δ = 54.82-53.02 ppm corresponds to methylene carbon in both the azides.

Same section describes the synthesis and characterization of all the alkynes, **59a-63a**. The generation of terminal alkynes involved the treatment of 1 mol of substrate, **59-63** having labile proton with 1.30 mol of 80% propargyl bromide solution in toluene in the presence of suitable base. Using K_2CO_3 as base, proton of hydroxyl group on each starting material get abstracted and substituted by propynyl group through nucleophilic substitution reaction on propargyl bromide, by stirring the reaction mixture at room temperature in DMF as solvent. Reaction time varies with change in substrate as the tendency to lose proton is different for different starting materials.

All the newly generated alkynes **59a-63a** were characterized and compared with their respective starting materials by IR spectroscopy in the range 4000-500 cm^{-1} as neat and the recorded data have fully supported the generation of expected product. IR peak observed at about 3287-3280 cm^{-1} in the spectra of different alkynes is for –C≡**C**−**H** group and at 2120-2100 cm^{-1} is due to −**C**≡**C**− moiety of alkyne. At the same time, no broad band in the range 3500-3350 cm^{-1} due to −**O**−**H** group indicates some changes over –OH group on the starting material of each alkyne. In ^{1}H NMR spectra of compounds **59a-63a**, a peak around δ = 2.47-2.40 ppm is for proton of alkyne, ≡C-**H** and at δ = 4.57-4.52 ppm corresponds to –C**H₂** of propynyl group in each newly synthesized alkyne molecule. No signal at around δ = 5.00-3.00 ppm for the proton of –O**H** group supports the substitution of this proton by propynyl group and confirms the formation of alkyne. Signals in the range δ = 8.20-6.87 ppm are characteristic of aromatic protons. In the ^{13}C NMR spectra of alkynes, the peaks at δ = 78.70-76.65 ppm are due to −**C**≡**C**− and at δ = 60.02-55.23 ppm corresponds to –**C**H_2−O− proves the synthesis of alkyne.

The alkynes **59a-63a** were converted into 1,2,3-triazole linked molecules **59b-63b** on cycloaddition reaction with benzyl azide **24** and **59c-60c, 62c** on treatment of alkynes with azidomethylnaphthalene **58** using small amount of [$CuBr(PPh_3)_3$] complex in THF:TEA (v/v, 1:1) as solvent system. All these heterocyclic compounds were characterized for IR, NMR and mass spectroscopic studies, which have clearly represented the success of cycloaddition reaction. The IR of azide molecules displayed a sharp signal at 2091 cm^{-1} and terminal alkynes in the region 2120-2100 cm^{-1}. After cycloaddition reaction, the IR spectra of products exhibited complete disappearance of these signals, indicating complete cyclization of respective alkyne and azide precursors. This behavior was also supported by NMR studies, where the disappearance of singlet at around δ = 2.47-2.40 ppm for the proton of alkyne group, ≡C-**H** indicated the success of cycloaddition reaction to produce 1,2,3-triazole linkers. The peak at around δ = 4.57-4.52 ppm due to –C**H₂** of propynyl group in each newly synthesized alkyne molecule has been shifted downfield due to formation of triazole ring, that has strong deshielding effect. In the ^{13}C NMR spectra of alkynes, the peaks at δ = 78.70-76.65 ppm, due to **−C≡C−** has been shifted downfield in the spectra of 1,2,3-triazole linkers, as these carbons have constituted triazole ring during cyclization. Other strong evidences in favor of the outcomes of CuAAC reactions in the form of heterocyclic compounds **59b-63b** and **59c-60c, 62c** are the mass spectra and elemental analysis data. Mass spectral and elemental analysis data of each 1,2,3-triazole linked molecule is in well agreement with their molecular structures.

Section II of chapter 4 illustrates the details of photophysical properties of all the novel 1,2,3-triazole derivatives by UV-Visible/Fluorescence spectroscopy to explore their ion sensing behavior. The selection of starting materials **59-63** to develop chemosensors **59b-63b** and **59c-60c, 62c** owes to their absorption in UV-Visible region and the incorporation of 1,2,3-triazole moiety during cycloaddition reaction provides nitrogen atoms as best coordinating sites for specific metal ions. The solutions of probes **59b-63b** and **59c-60c, 62c** and various metal ions were made in acetonitrile and water ($CH_3CN:H_2O$::4:1) as solvent system. In order to analyze the sensing behavior of synthesized heterocyclic compounds towards a particular metal ion, the UV-Visible/Fluorescence titrations were performed. The examination of

absorption responses recorded for receptors **59b** and **59c** with various metal ions explains their sensitivity for Pb(II) ions. Both the probes show significant hyperchromic shift with the increase in concentration of Pb(II) ions as shown in Figures S5 and S6. These highly selective chemosensors **59b** and **59c** allow a direct quantitative assay of Pb(II) ions by UV-Visible spectroscopy with the detection limited of 13 µM and 11.2 µM respectively. The limit of detection for each receptor unit has been calculated from job plots, discussed in detail in Section II of chapter 4.

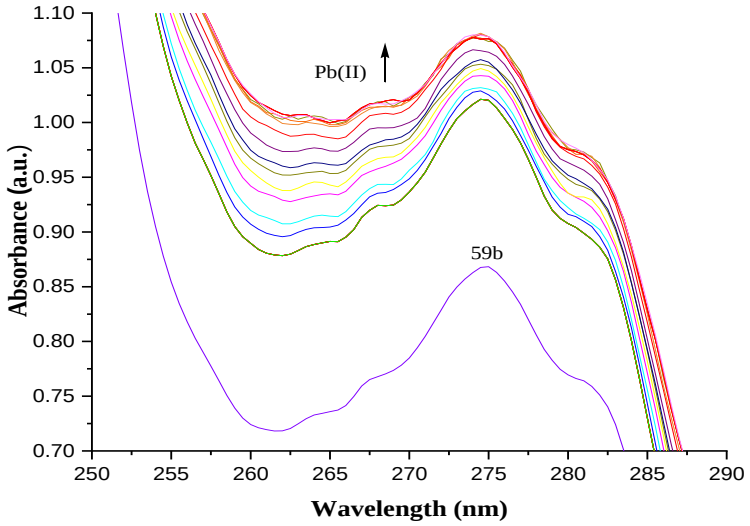

Figure S5: Absorption responses of **59b** with the addition of 20 equiv. of 0.50 mM Pb(II) ions into 0.20 mM solution of probe **59b** prepared in $CH_3CN:H_2O::4:1$

In the similar manner, the chemosensing activity of molecules **60b** and **60c** was explored by UV-Visible as well as Fluorescence spectroscopy. Both the probes have shown distinct results during the titration with Fe(II) ions. The absorption responses recorded with each sequential addition of 10 equiv. of 0.50 mM of Fe(II) ions into 0.50 mM solution of **60b** as well as **60c** in acetonitrile and water ($CH_3CN:H_2O::4:1$) mixture is presented in Figures S7 and S8. Absorption responses of **60b** with increase in concentration of Fe(II) ions illustrates an observable change in the absorbance intensity before and after isosbestic points at wavelengths 380 nm and 468 nm and hypsochromic shifting of absorption maxima recorded in between these wavelengths with significant decrease in intensity. Similarly, UV-Visible spectra of

60c shows same type of character on titration with Fe(II) ions with a hypochromic shifting of absorption maxima to an extent of 7 nm with increase in concentration of Fe(II) ions from 0.013 mM to 0.141 mM.

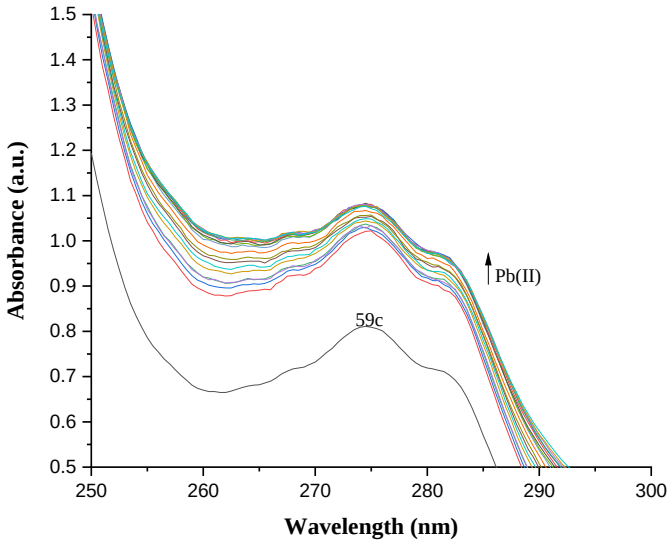

Figure S6: Absorbance responses observed during each addition of 20 equiv. of 0.50 mM Pb(II) ions in 0.20 mM solution of probe **59c**

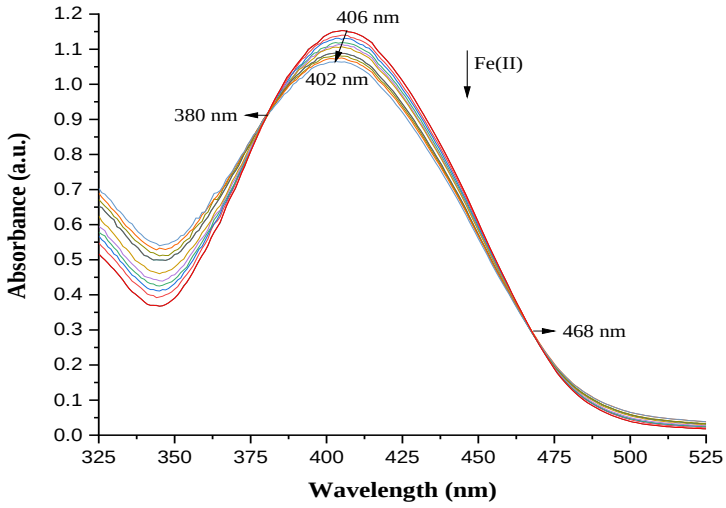

Figure S7: UV-Visible spectra of **60b** with the addition of 10 equiv. of 0.50 mM Fe(II) ion solution in 0.50 mM of its solution in acetonitrile and water ($CH_3CN:H_2O$::4:1) mixture

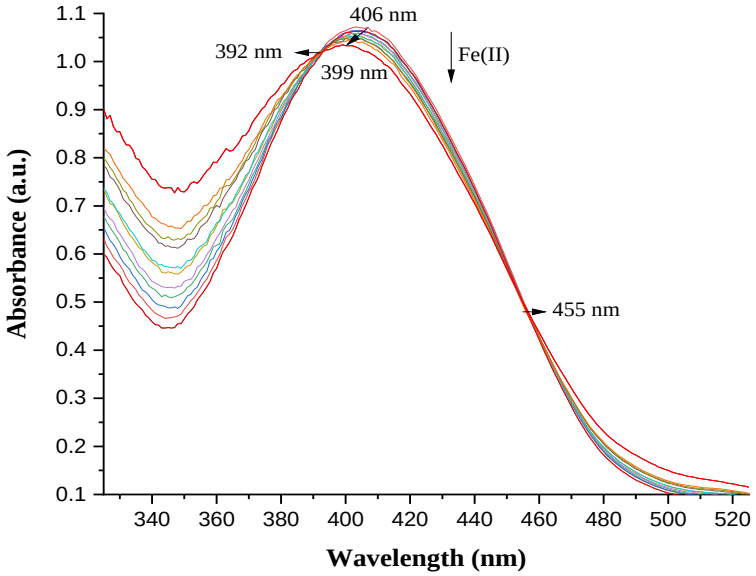

Figure S8: Absorption responses recorded for probe **60c** (0.50 mM) with the serial addition of 10 equiv. of 0.50 mM Fe(II) ions in acetonitrile and water ($CH_3CN:H_2O$::4:1) mixture

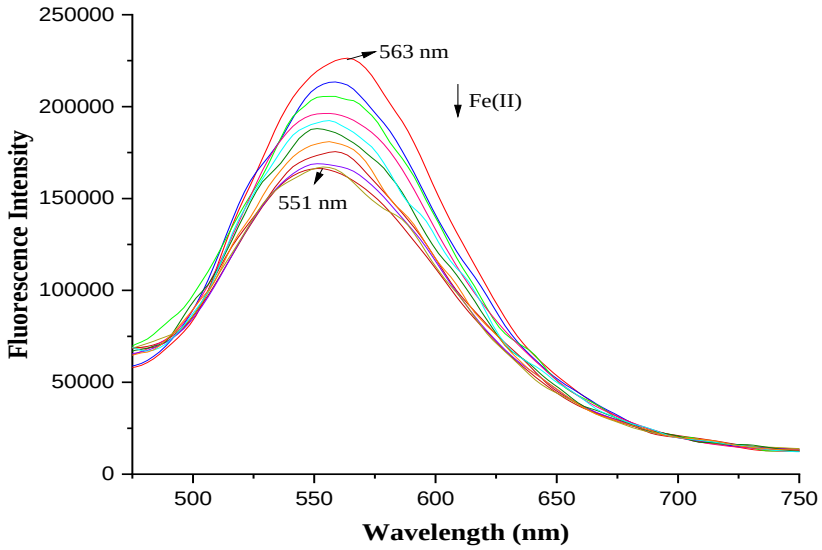

Figure S9: Emission responses of 1,2,3-triazole linker **60c** (0.10 mM) at λ_{ex} = 406 nm with the addition of 12 equiv. of 0.10 mM Fe(II) ions in acetonitrile and water ($CH_3CN:H_2O$::4:1) mixture

The chemosensing behavior of heterocyclic compound **60c** has also been studied through fluorescence spectroscopy. The fluorescence spectrometric titrations were conducted for **60c** with the subsequent addition of 12 equiv. of 0.10 mM solution of Fe(II) ions into 0.10 mM of testing molecule **60c** at λ_{ex} = 406 nm and the emission responses recorded are presented in Figure S9.

Similarly, the UV-Visible spectral studies of probe **61b** with various metal ions show its sensitivity with Co(II) ions. The absorption spectra recorded during the titration of 0.50 mM of receptor unit **61b** with 0.50 mM of Co(II) ions shows a regular decrease in absorption with an increase in concentration of metal ions from 0.026 mM to 0.242 mM as shown in Figure S10. The minimum limit of detection of Co(II) with the synthesized probe **61b** has been calculated as 1.9 µM with the complexing ratio of probe **61b**:Co(II) as 1:1.

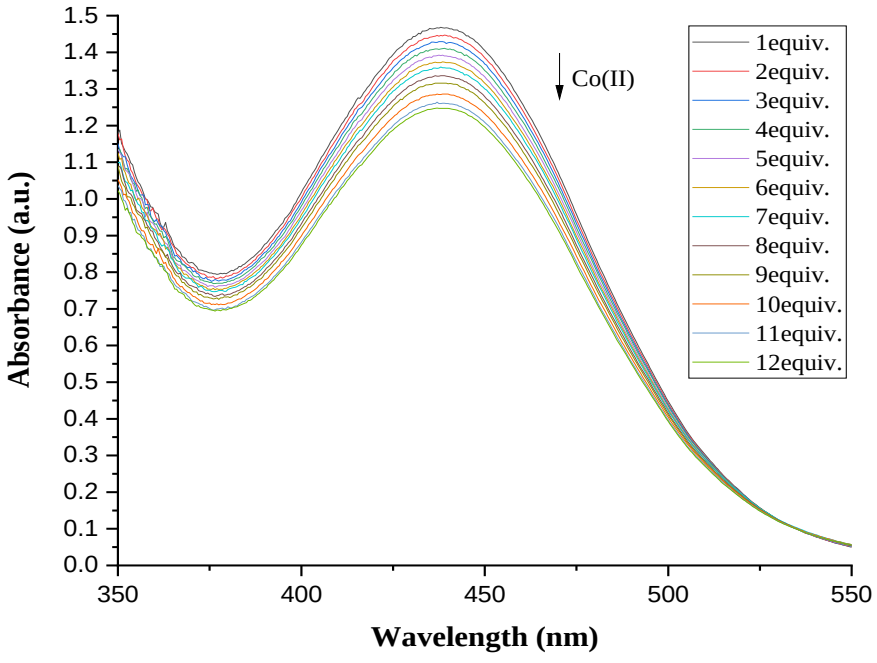

Figure S10: Absorbance responses recorded for each successive addition of 0.50 mM of Co(II) ions into 0.50 mM solution of 1,2,3-triazole linker **61b** in acetonitrile-water (CH_3CN:H_2O::4:1) mixture

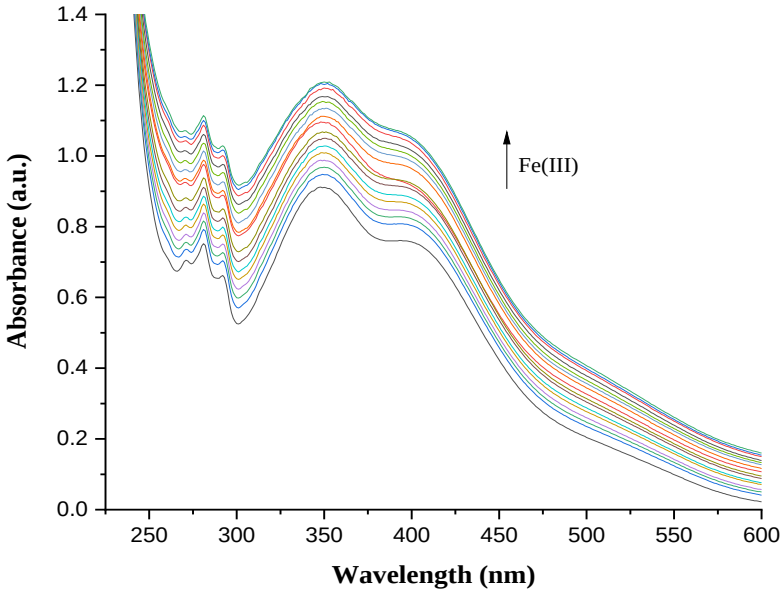

Figure S11: Absorption spectra of 0.20 mM of ligand **62b** with the addition of 20 equiv. of 0.50 mM of Fe(III) ions in acetonitrile-water ($CH_3CN:H_2O$::4:1) mixture

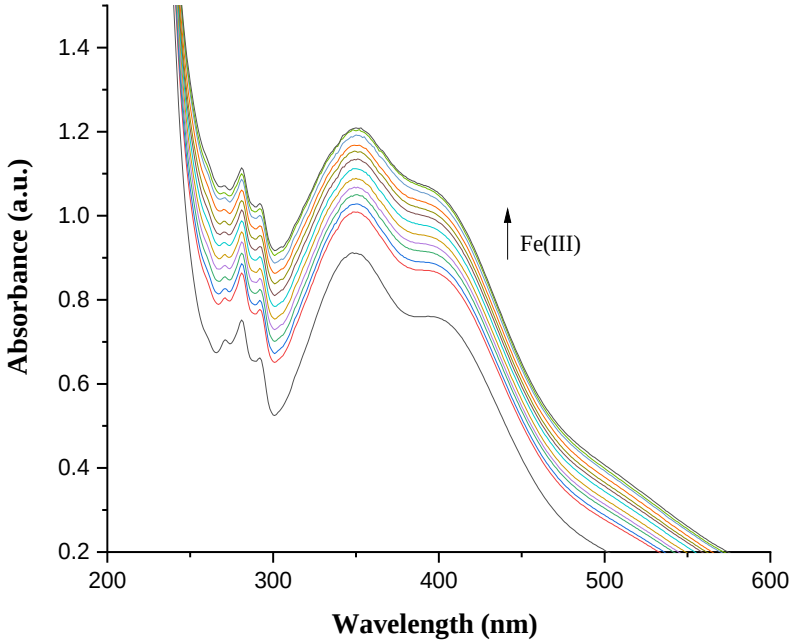

Figure S12: UV-Visible responses of 0.20 mM of ligand **62c** with the addition of 15 equiv. of 0.50 mM of Fe(III) ions in acetonitrile-water ($CH_3CN:H_2O$::4:1) mixture

Next part of this section presents chemosensing behavior of 1,2,3-triazole linkers **62b** and **62c** analyzed by UV-Visible spectroscopy. Studies were explored by performing absorption titrations of probes **62b** and **62c** (0.20 mM) with 0.50 mM of different metal chlorides in acetonitrile-water ($CH_3CN:H_2O$::4:1) mixture as solvent system. The results recorded have exhibited the selectivity of designed probes **62b** and **62c** for Fe(III) ions. The Figures S11 and S12 have shown the absorption responses of receptors **62b** and **62c** respectively with the successive addition of 0.50 mM of Fe(III) ions into the 0.20 mM solution of these receptors. The observable rise in absorption i.e., hyperchromic shifting was recorded with each successive addition of Fe(III) ions. The minimum limit of detection of Fe(III) ions with the synthesized probes **62b** and **62c** has been calculated from jobs plot as 6.50 µM and 6.38 µM respectively with the binding ratio of probe **62b/62c**:Fe(III) as 1:1.

One more 1,2,3-triazole linked molecule, **63b** was investigated for its chemosensing nature in the similar manner as for other molecules discussed earlier and the present molecule is responding to Cu(II) ions among a variety of metal ions. The results obtained from UV-Visible titrations of 0.20 mM solution of **63b** with each successive addition of 0.50 mM of Cu(II) ions prepared in acetonitrile-water ($CH_3CN:H_2O$::4:1) mixture are presented in Figure S13. The ligand **63b** was showing two peaks with maximum intensity at λ = 426 nm and λ = 303 nm. The noticeable change in the absorbance of testing chemosensor 63b was observed at these two wavelengths with successive increase in concentration of Cu(II) ions. Highly significant change in the absorption pattern was recorded below and above λ = 290 nm, a visible isosbestic point, with rise in concentration of Cu(II) ions.

The selectivity of ligand **63b** towards Cu(II) ions has also been supported by fluorescence spectroscopy. For the same, the fluorescence spectroscopic titrations were performed at λ_{ex} = 290 nm for heterocyclic molecule **63b** (0.10 mM) with Cu(II) ion (0.10 mM) solution and the results obtained are as shown in Figure S14. The 1,2,3-triazole derivative **63b** is showing significant changes in the emission spectra on interaction with Cu(II) ions. At wavelengths 372 nm and 730 nm, noticeable fall in emission intensity was recorded with increase in concentration of Cu(II) ions, whereas

at wavelength 579 nm, the emission intensity goes on increasing with each addition of Cu(II) ions.

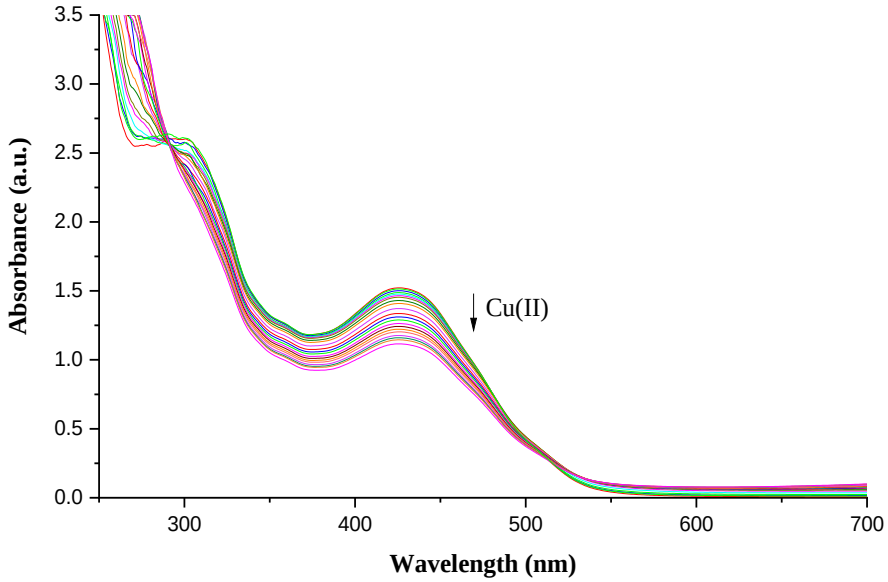

Figure S13: UV-Visible responses for probe **63b** (0.20 mM) with the sequential addition of 20 equiv. of 0.50 mM of Cu(II) ions in acetonitrile-water ($CH_3CN:H_2O$::4:1) mixture

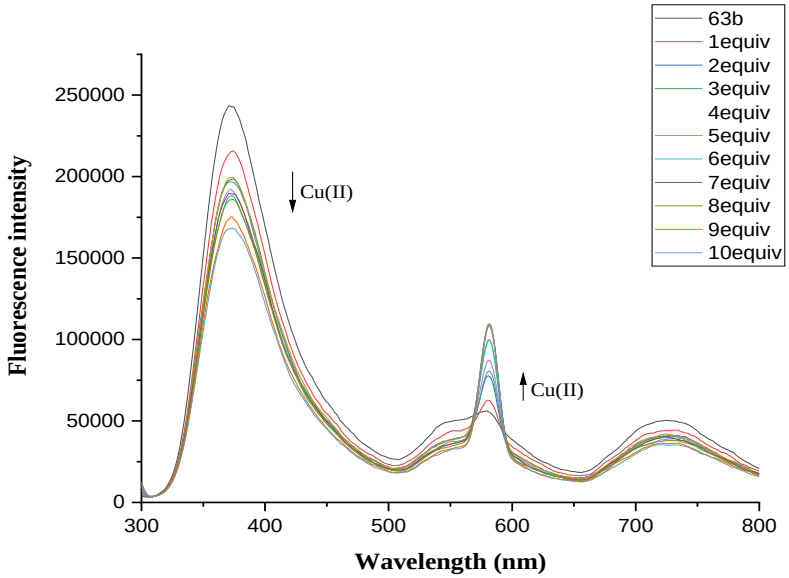

Figure S14: Emission responses of probe **63b** (0.10 mM) with the addition of 10 equiv. of 0.10 mM of Cu(II) ions in acetonitrile-water ($CH_3CN:H_2O$::4:1) mixture

Appendix A

Chemicals and Instruments

Appendix A illustrates all the chemicals, reagents, catalysts and solvents involved in chemical syntheses and analytical study of synthesized molecules. This section also mentions instruments used for various studies.

Experimental techniques:

1. Infrared spectra

Infrared spectra were recorded on SHIMADZU FTIR-8400S Spectrometer in the range 4000-500 cm^{-1} at CIF department, LPU Phagwara.

2. NMR spectra

^{1}H and ^{13}C NMR spectra were recorded with respect to TMS as standard reference. ^{1}H NMR spectra of the samples were recorded in $CDCl_3$ and DMSO-d6 on BRUKER-ADVANCE HD III 500MHz spectrometer and ^{13}C NMR in $CDCl_3$ and DMSO-d6 on BRUKER-ADVANCE HD III 126 MHz spectrometer at Emerging Life Sciences Department (Central Instrumentation Facility), GNDU Amritsar.

3. Mass spectra

Mass spectral measurements (HRMS) were carried out on Waters Q-TOF Micro mass spectrometer at SAIF, Panjab University, Chandigarh.

4. Fluorescence spectra

Fluorescence spectral study was performed on Perkin Elmer LS6500 Fluorescence Spectrophotometer at CIF, LPU Phagwara.

5. UV-Visible spectra

UV-Visible spectra were recorded on SHIMADZU UV-1800 Spectrometer using quartz cuvettes and standard solutions at Department of Chemistry, LPU, Phagwara.

6. CHNS Analysis

CHNS analyses were obtained on a Perkin Elmer Model 2400 CHNS elemental analyzer at Department of Chemistry, Panjab University, Chandigarh.

7. Melting Point

Melting points were measured in a Mel Temp II device using sealed capillaries at Department of Chemistry, LPU, phagwara.

8. General materials

Bromotris(triphenylphosphine)copper(I) [$CuBr(PPh_3)_3$] (Aldrich), propargyl bromide solution (80% by weight in toluene) (CDH), N,N-dimethylformamide (DMF) (CDH), benzyl chloride (Loba chemie), tetrahydrofuran (THF) (CDH), triethylamine (CDH), diethylether (Qualigens), potassium carbonate (Nice), sodium azide (Nice), diethyl ether (CDH), hexane (Nice), ethylacetate (Nice), chloromethylnaphthalene (Loba chemie), o-cresolphthalein (Sigma aldrich), 1,4-dihydroxyanthraquinone (Loba chemie), 1-naphtholphthalein (CDH), 1-naphtholbenzein (Loba chemie), sudan-IV (Nice).

Appendix B

IR of azidomethylbenzene 24

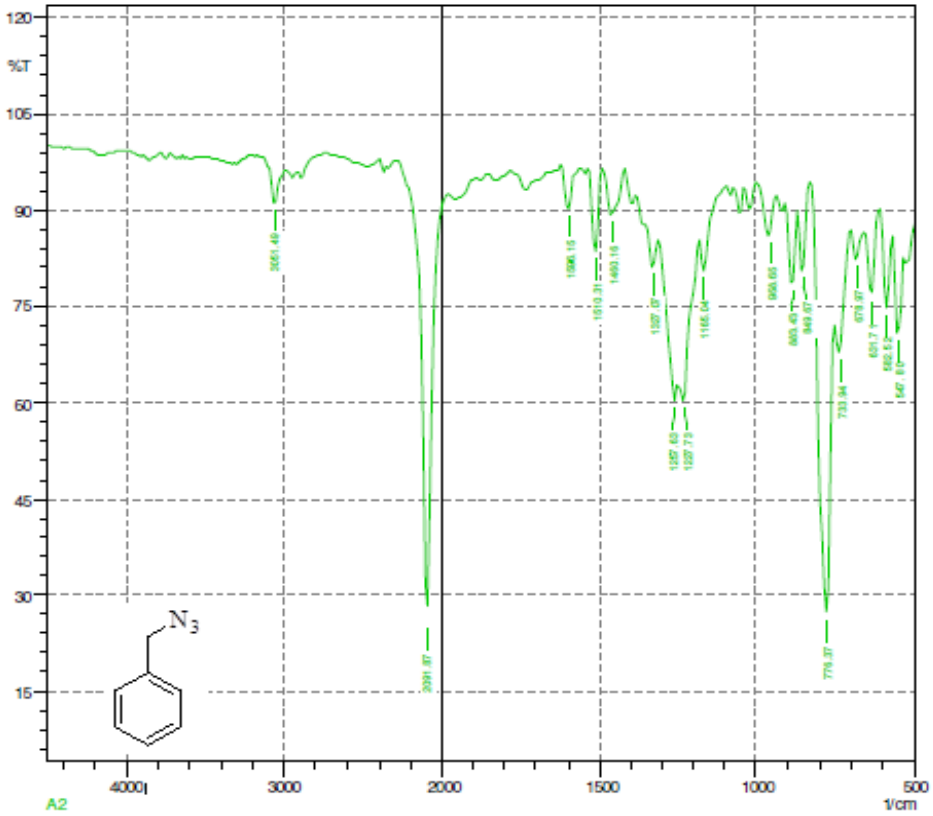

SHIMADZU

No.	Peak	Intensity	Corr. Inte	Base (H)	Base (L)	Area	Corr. Area
1	547.8	70.898	13.701	564.2	525.62	4.48	1.626
2	582.52	74.85	13.077	603.74	564.2	3.524	1.34
3	631.71	76.785	11.517	652.93	610.49	3.564	1.268
4	678.97	82.358	4.64	698.25	652.93	3.233	0.48
5	733.94	26.999	9.344	750.33	698.25	6.531	1.354
6	776.37	26.999	53.404	820.74	750.33	21.439	15.555
7	849.67	80.646	11.53	866.07	830.38	2.327	1.093
8	883.43	78.669	11.788	904.64	866.07	2.873	1.205
9	958.65	85.868	7.378	1001.09	933.58	2.952	0.982
10	1165.04	80.466	6.501	1179.51	1093.67	4.6	0.532
11	1227.73	60.284	9.003	1247.02	1179.51	10.356	1.244
12	1257.63	60.205	6.517	1307.78	1247.02	9.115	0.884
13	1327.07	81.023	5.403	1352.14	1307.78	3.297	0.52
14	1460.16	89.286	7.279	1490.06	1416.76	2.465	1.351
15	1510.31	83.424	13.111	1529.6	1490.06	1.907	1.302
16	1596.15	90.106	6.31	1616.4	1576.86	1.242	0.618
17	2091.87	25.811	68.746	2273.19	1976.14	38.319	31.816
18	3051.49	91.196	0.22	3053.42	3018.7	1.072	-0.001

IR of azidomethylnaphthalene 58

SHIMADZU

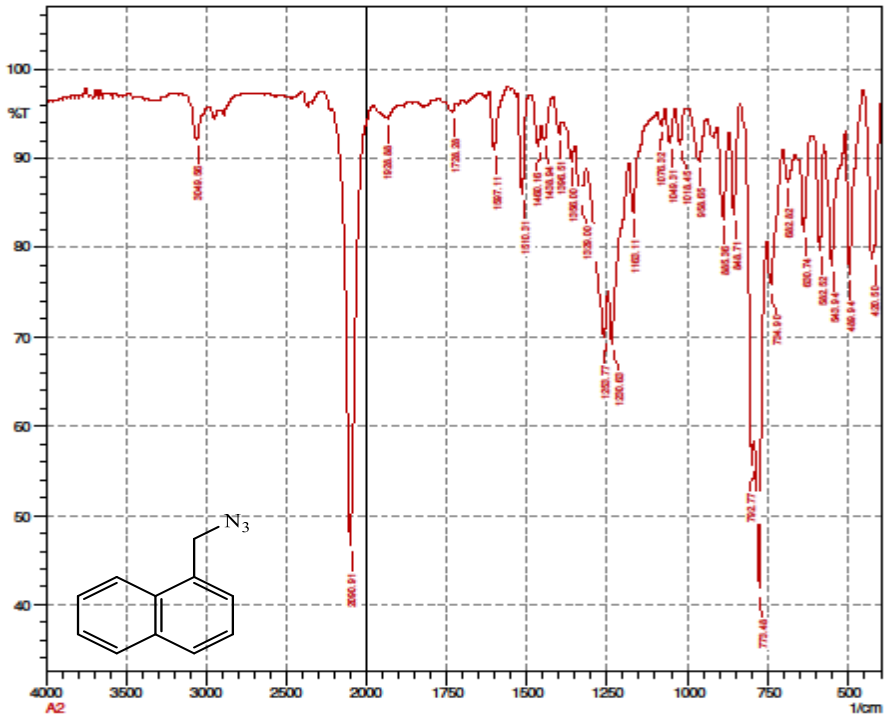

No.	Peak	Intensity	Corr. Inte	Base (H)	Base (L)	Area	Corr. Area
1	420.5	78.784	18.305	445.57	399.28	2.465	1.879
2	489.94	77.088	17.038	503.44	445.57	3.04	1.831
3	543.94	78.033	11.131	567.09	530.44	2.76	1.019
4	582.52	79.662	12.34	599.88	567.09	2.068	0.886
5	630.74	81.718	9.852	659.68	607.6	2.844	0.822
6	682.82	87.405	3.363	698.25	659.68	1.959	0.324
7	734.9	75.52	7.891	748.41	698.25	4.302	0.93
8	773.48	41.572	24.581	786.98	748.41	8.919	2.603
9	792.77	55.638	7.662	831.35	786.98	4.646	-0.916
10	848.71	83.716	10.757	864.14	831.35	1.554	0.756
11	885.36	83.189	10.064	902.72	864.14	2.026	0.85
12	958.65	89.687	5.244	995.3	935.51	1.986	0.67
13	1018.45	91.551	3.998	1031.95	995.3	0.986	0.264
14	1049.31	91.814	3.796	1064.74	1031.95	0.92	0.28
15	1076.32	93.618	1.857	1089.82	1064.74	0.621	0.116
16	1163.11	83.928	6.329	1178.55	1147.68	1.82	0.446
17	1230.63	69.145	8.702	1242.2	1178.55	6.578	1.136
18	1253.77	69.883	7.685	1309.71	1242.2	7.158	1.263
19	1329	85.368	4.891	1346.36	1309.71	2.094	0.449
20	1356	89.676	2.432	1384.94	1346.36	1.406	0.145
21	1396.51	92.713	2.464	1413.87	1384.94	0.728	0.142
22	1438.94	92.153	2.561	1450.52	1413.87	0.904	0.133
23	1460.16	91.431	3.119	1489.1	1450.52	0.958	0.161
24	1510.31	86.007	11.277	1525.74	1489.1	1.237	0.793
25	1597.11	90.922	6.677	1612.54	1556.61	1.179	0.618
26	1728.28	95.095	1.082	1753.35	1712.85	0.767	0.088
27	1928.88	94.481	0.347	1936.6	1892.23	0.935	0.006
28	2090.91	45.648	49.096	2204.71	1973.24	23.051	18.683
29	3049.56	92.18	3.294	3140.22	3022.55	2.625	0.573

Comment;
A2

Date/Time; 6/24/2021 3:19:34 PM
No. of Scans;
Resolution;
Apodization;

IR of alkyne 59a

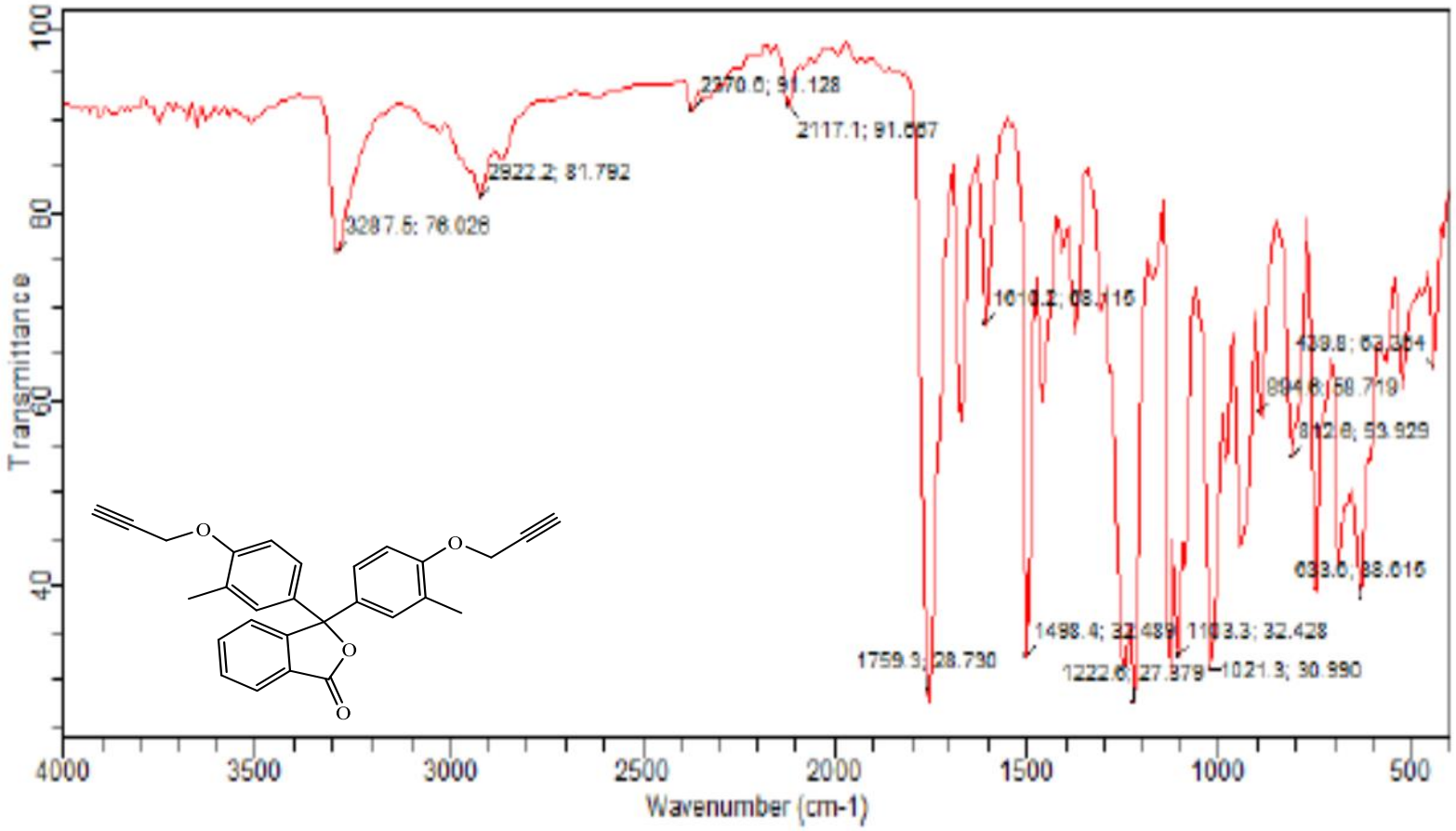

IR of triazole 59b

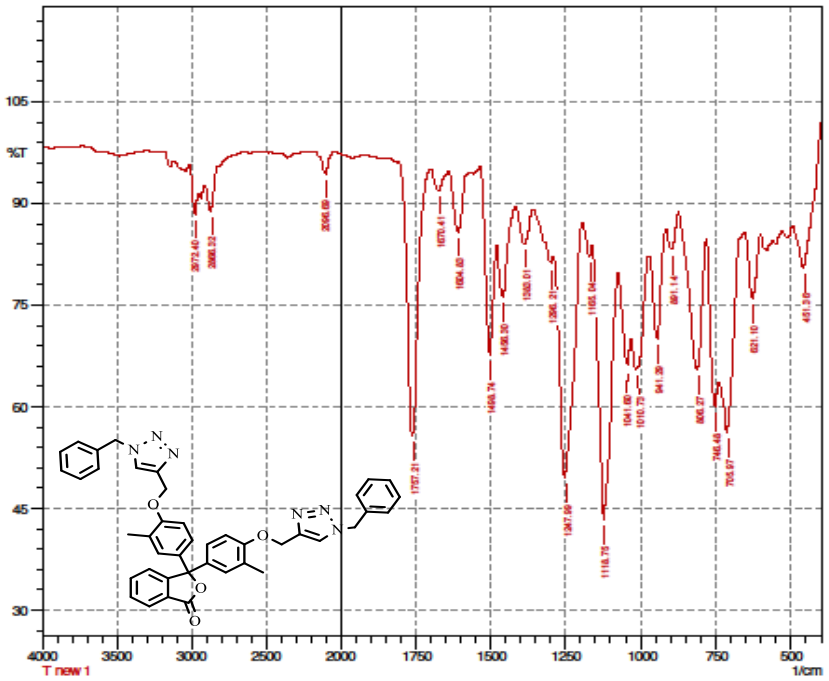

SHIMADZU

No.	Peak	Intensity	Corr. Inte	Base (H)	Base (L)	Area	Corr. Area
1	451.36	80.597	12.236	486.08	399.28	5.346	3.032
2	621.1	76.002	9.666	645.17	594.1	4.902	1.403
3	705.97	56.243	15.465	731.05	665.46	12.094	3.305
4	746.48	59.997	10.953	775.41	731.05	7.577	1.624
5	806.27	65.406	20.766	868	775.41	10.941	5.258
6	891.14	83.185	4.388	910.43	868	2.935	0.511
7	941.29	70.026	14.088	966.37	910.43	6.234	2.088
8	1010.73	65.421	7.754	1026.16	966.37	8.869	1.697
9	1041.6	65.774	7.834	1068.6	1026.16	6.35	0.995
10	1118.75	43.313	38.734	1157.33	1068.6	18.541	10.785
11	1165.04	82.215	2.343	1190.12	1157.33	2.437	0.199
12	1247.99	49.473	34.691	1284.63	1190.12	17.344	10.521
13	1296.21	81.037	2.342	1354.07	1284.63	4.97	0.279
14	1383.01	84.035	5.226	1411.94	1354.07	3.661	0.805
15	1456.3	76.143	9.573	1477.52	1411.94	5.417	1.333
16	1498.74	67.638	20.999	1529.6	1477.52	5.464	2.96
17	1604.83	86.67	9.012	1635.69	1564.32	3.012	1.312
18	1670.41	91.805	3.092	1699.34	1635.69	1.882	0.431
19	1757.21	55.633	40.09	1803.5	1699.34	10.644	8.631
20	2096.69	94.25	3.431	2169.99	2040.76	2.063	0.748
21	2866.32	88.843	5.107	2904.89	2820.02	3.227	0.975
22	2972.4	88.285	4.852	3009.05	2949.26	2.378	0.661

Comment;
T new 1

Date/Time; 1/9/2021 3:33:56 PM
No. of Scans;
Resolution;
Apodization;

IR of triazole 59c

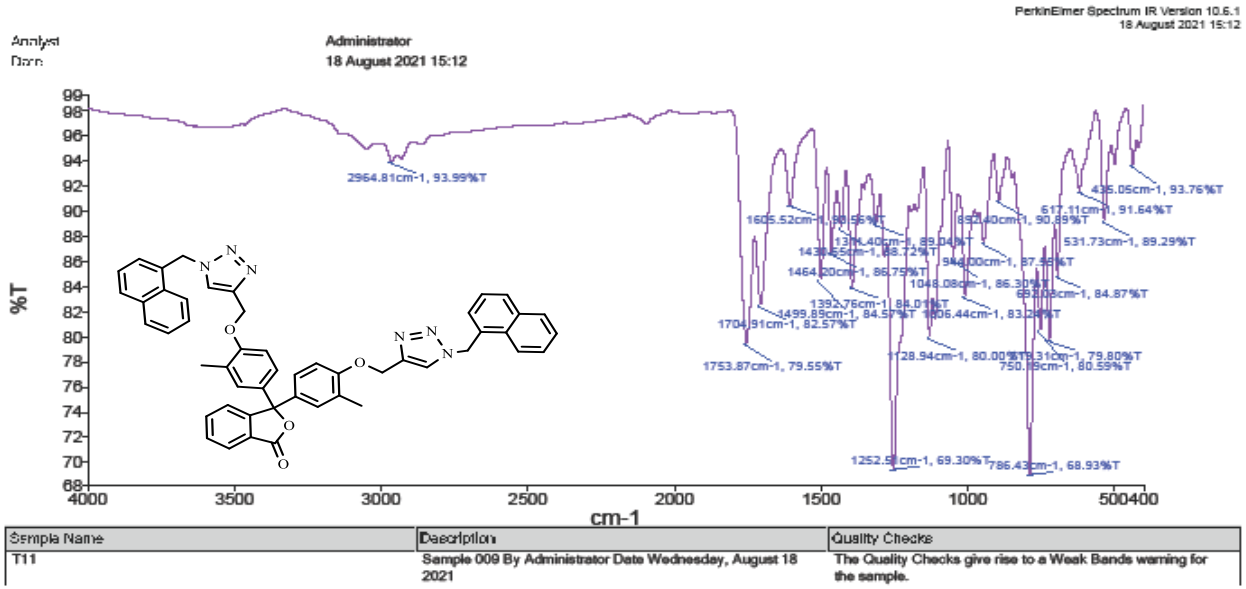

Page 1

IR of alkyne 60a

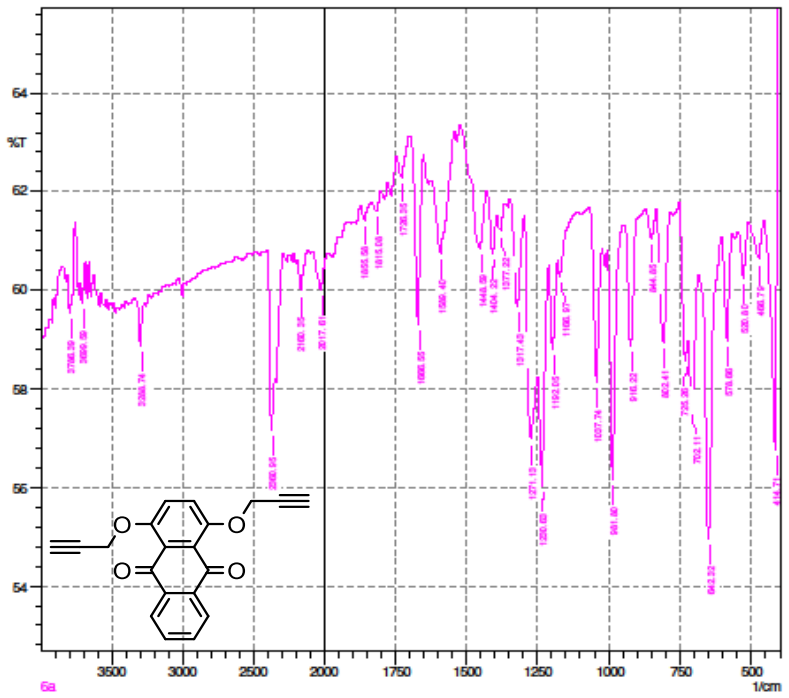

SHIMADZU

No.	Peak	Intensity	Corr. Inte	Base (H)	Base (L)	Area	Corr. Area
1	414.71	56.75	16.795	449.43	399.28	10.602	2.718
2	466.79	60.62	0.789	501.51	449.43	11.174	0.143
3	520.8	60.233	1.036	538.16	501.51	7.92	0.124
4	578.66	58.982	2.154	597.95	559.38	8.514	0.27
5	642.32	54.967	5.711	678.97	597.95	18.627	1.07
6	702.11	57.589	1.885	715.61	678.97	8.468	0.243
7	725.26	58.554	1.301	746.48	715.61	6.897	0.131
8	802.41	58.949	2.666	827.49	779.27	10.593	0.452
9	844.85	61.037	0.616	866.07	827.49	8.188	0.085
10	916.22	58.863	2.56	939.36	866.07	15.849	0.365
11	981.8	56.157	4.8	999.16	939.36	13.47	0.661
12	1037.74	58.137	3.085	1060.88	1018.45	9.452	0.421
13	1166.97	60.28	0.438	1174.69	1109.11	14.036	-0.003
14	1192.05	58.795	1.754	1207.48	1174.69	7.332	0.19
15	1230.63	56.021	3.162	1246.06	1207.48	9.154	0.426
16	1271.13	56.96	3.013	1294.28	1246.06	11.258	0.521
17	1317.43	59.682	1.999	1340.57	1294.28	10.045	0.33
18	1377.22	61.166	0.469	1388.79	1359.86	6.121	0.044
19	1404.22	60.744	1.023	1421.58	1388.79	6.969	0.11
20	1448.59	60.851	1.531	1518.03	1421.58	20.039	0.469
21	1589.4	60.746	1.874	1622.19	1539.25	17.375	0.574
22	1666.55	59.306	3.57	1697.41	1647.26	10.562	0.47
23	1726.35	62.257	0.58	1741.78	1697.41	9.018	0.088
24	1815.08	61.599	0.291	1830.51	1795.79	7.268	0.035
25	1855.58	61.406	0.345	1869.08	1830.51	8.115	0.041
26	2017.61	59.996	0.766	2075.47	1984.82	19.854	0.241
27	2160.35	59.958	0.688	2179.63	2102.48	16.874	0.144
28	2360.95	57.175	1.944	2393.74	2343.59	11.608	0.302
29	3288.74	58.866	0.901	3308.03	3257.88	11.334	0.121
30	3699.59	59.729	0.562	3713.09	3674.52	8.541	0.082
31	3786.39	59.539	1.083	3801.82	3747.81	11.947	0.295

Comment;
6a

Date/Time; 6/24/2021 3:29:42 PM
No. of Scans;
Resolution;
Apodization;

IR of triazole 60b

SHIMADZU

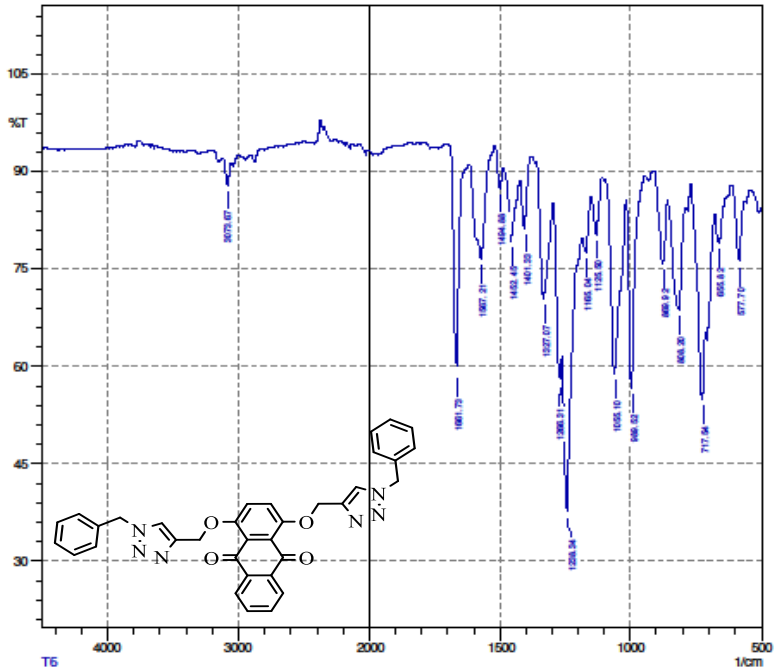

No.	Peak	Intensity	Corr. Inte	Base (H)	Base (L)	Area	Corr. Area
1	577.7	76.046	10.44	606.63	558.41	4.117	1.132
2	655.82	79.027	5.48	670.29	623.03	3.955	0.613
3	717.54	55.05	14.933	761.91	705.97	9.053	2.355
4	808.2	68.629	3.111	813.02	783.13	3.632	0.183
5	869.92	75.746	11.646	902.72	849.67	4.55	1.58
6	989.52	56.682	29.991	1008.8	939.36	7.993	3.952
7	1055.1	58.932	19.316	1091.75	1032.92	8.299	2.566
8	1125.5	80.305	7.332	1145.75	1103.32	3.215	0.794
9	1165.04	77.496	5.391	1180.47	1145.75	3.278	0.5
10	1238.34	37.457	28.562	1256.67	1199.76	14.892	5.418
11	1256.31	57.574	10.905	1289.46	1256.67	5.667	1.068
12	1327.07	70.506	18.477	1354.07	1289.46	6.66	3.198
13	1401.33	81.299	8.973	1418.69	1373.36	2.793	0.856
14	1452.45	79.295	10.664	1481.38	1418.69	4.395	1.494
15	1494.88	87.332	4.895	1511.28	1481.38	1.434	0.404
16	1567.21	76.549	6.192	1580.72	1524.78	4.165	0.477
17	1661.73	59.133	32.638	1683.91	1639.55	5.268	3.609
18	3073.67	87.979	3.636	3106.46	3044.74	2.865	0.524

Comment;
T6

Date/Time; 7/28/2021 5:00:56 PM
No. of Scans;
Resolution;
Apodization;

IR of triazole 60c

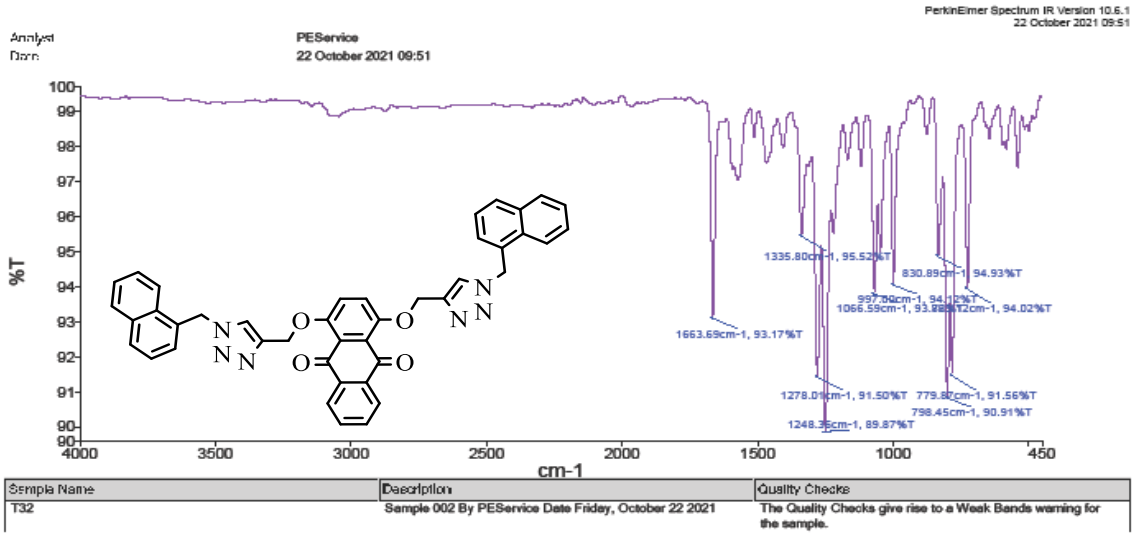

Page 1

IR of alkyne 61a

SHIMADZU

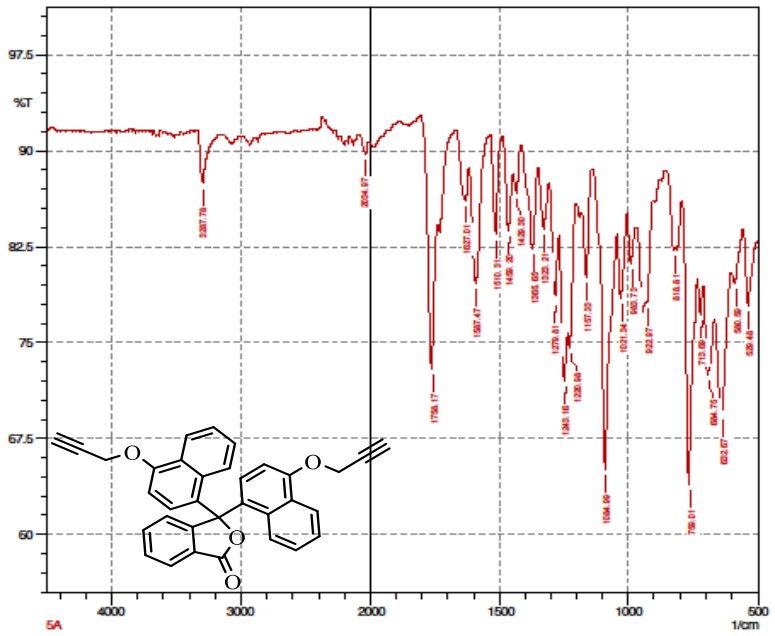

No.	Peak	Intensity	Corr. Inte	Base (H)	Base (L)	Area	Corr. Area
1	529.48	77.875	5.609	548.77	499.58	4.488	0.608
2	580.59	79.615	1.952	596.02	548.77	4.257	0.227
3	632.67	69.372	8.993	659.68	596.02	8.29	1.641
4	684.75	72.415	5.946	704.04	659.68	5.556	0.811
5	713.69	77.177	2.592	725.26	704.04	2.238	0.158
6	759.01	63.89	19.524	786.02	725.26	7.676	2.766
7	816.81	82.251	0.935	850.64	813.99	2.451	-0.064
8	922.97	78.088	1.369	927.79	896.93	2.726	0.077
9	983.73	81.131	3.551	999.16	960.58	3.126	0.318
10	1021.34	78.469	5.774	1039.67	999.16	3.622	0.621
11	1084.99	65.051	20.81	1136.11	1039.67	10.153	3.823
12	1157.33	80.062	6.556	1173.72	1136.11	2.868	0.558
13	1220.98	74.6	3.831	1229.66	1196.87	3.32	0.254
14	1243.16	71.941	6.795	1254.38	1229.66	4.096	0.635
15	1279.81	78.291	6.86	1300.07	1254.38	3.048	0.602
16	1323.21	83.91	4.27	1344.43	1300.07	2.914	0.484
17	1365.65	82.321	7.035	1410.98	1344.43	4.201	1.045
18	1429.3	86.656	2.46	1440.87	1410.98	1.645	0.185
19	1459.2	83.707	5.881	1480.42	1440.87	2.426	0.556
20	1510.31	83.431	7.787	1528.64	1480.42	2.647	0.719
21	1587.47	79.619	9.801	1610.61	1537.32	4.978	1.576
22	1627.01	86.111	3.454	1663.66	1610.61	2.904	0.508
23	1758.17	72.91	14.332	1800.61	1735.99	5.257	1.817
24	2034.97	89.725	0.088	2084.15	2033.04	2.174	-0.036
25	3287.78	87.318	4.052	3326.35	3191.33	6.396	1.031

Comment;
5A

Date/Time; 7/28/2021 4:58:07 PM
No. of Scans;
Resolution;
Apodization;

IR of triazole 61b

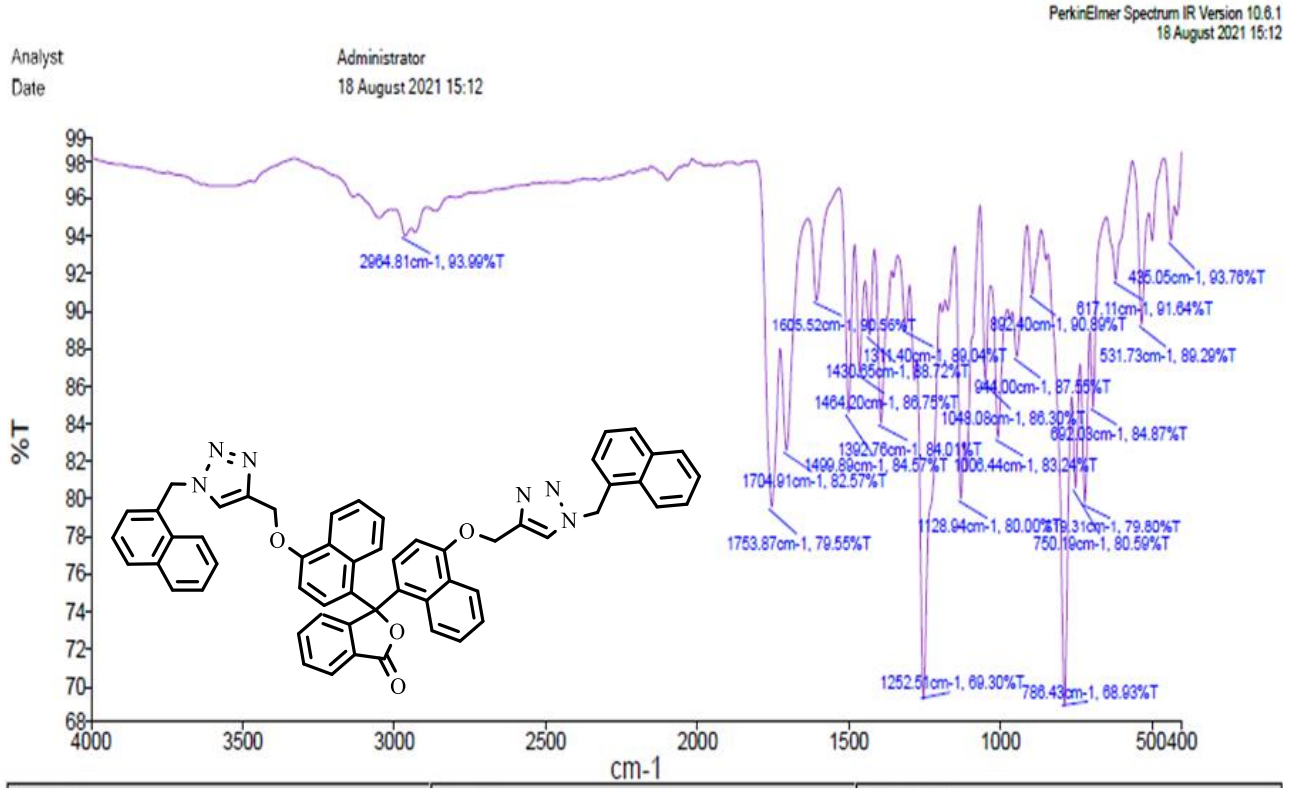

IR of alkyne 62a

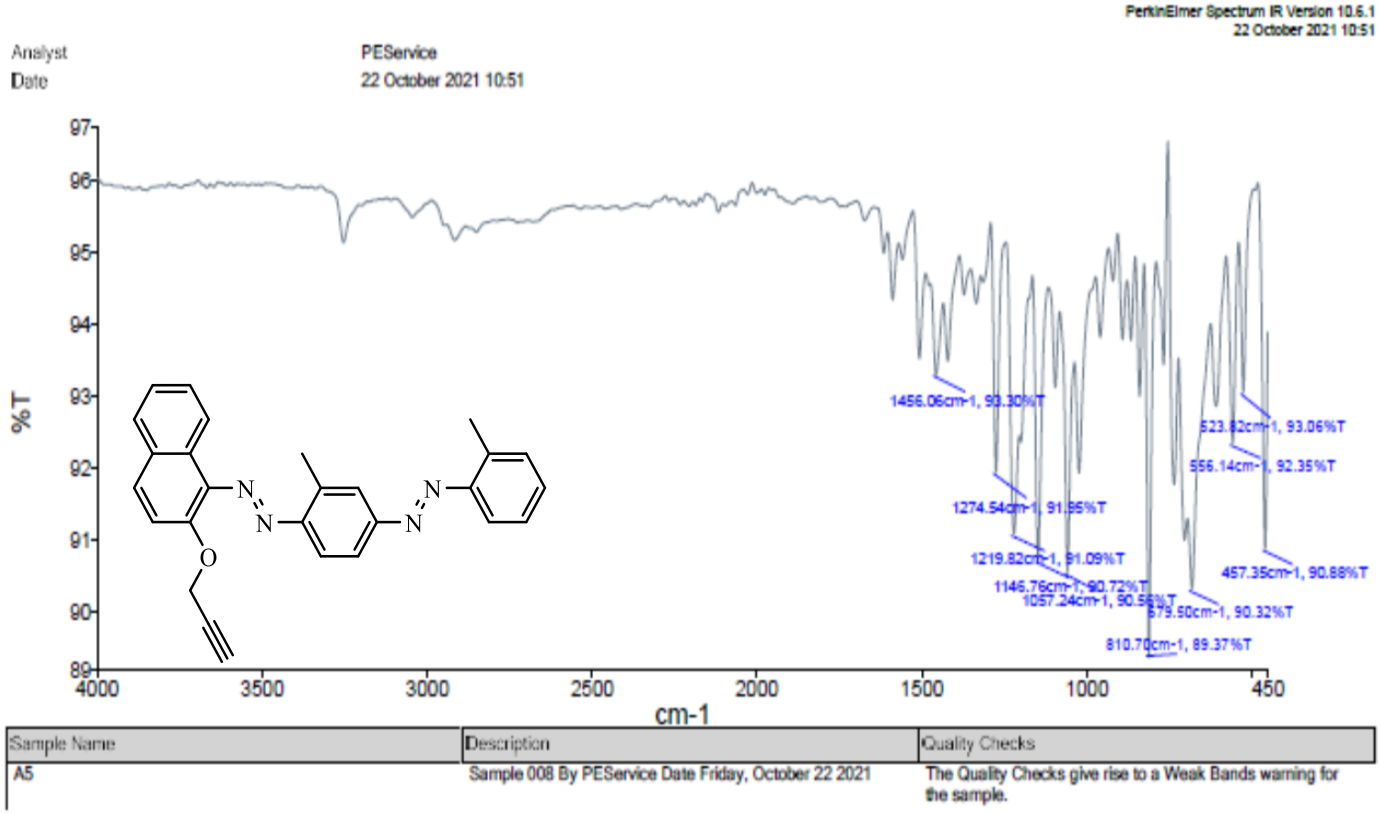

IR of triazole derivative 62b

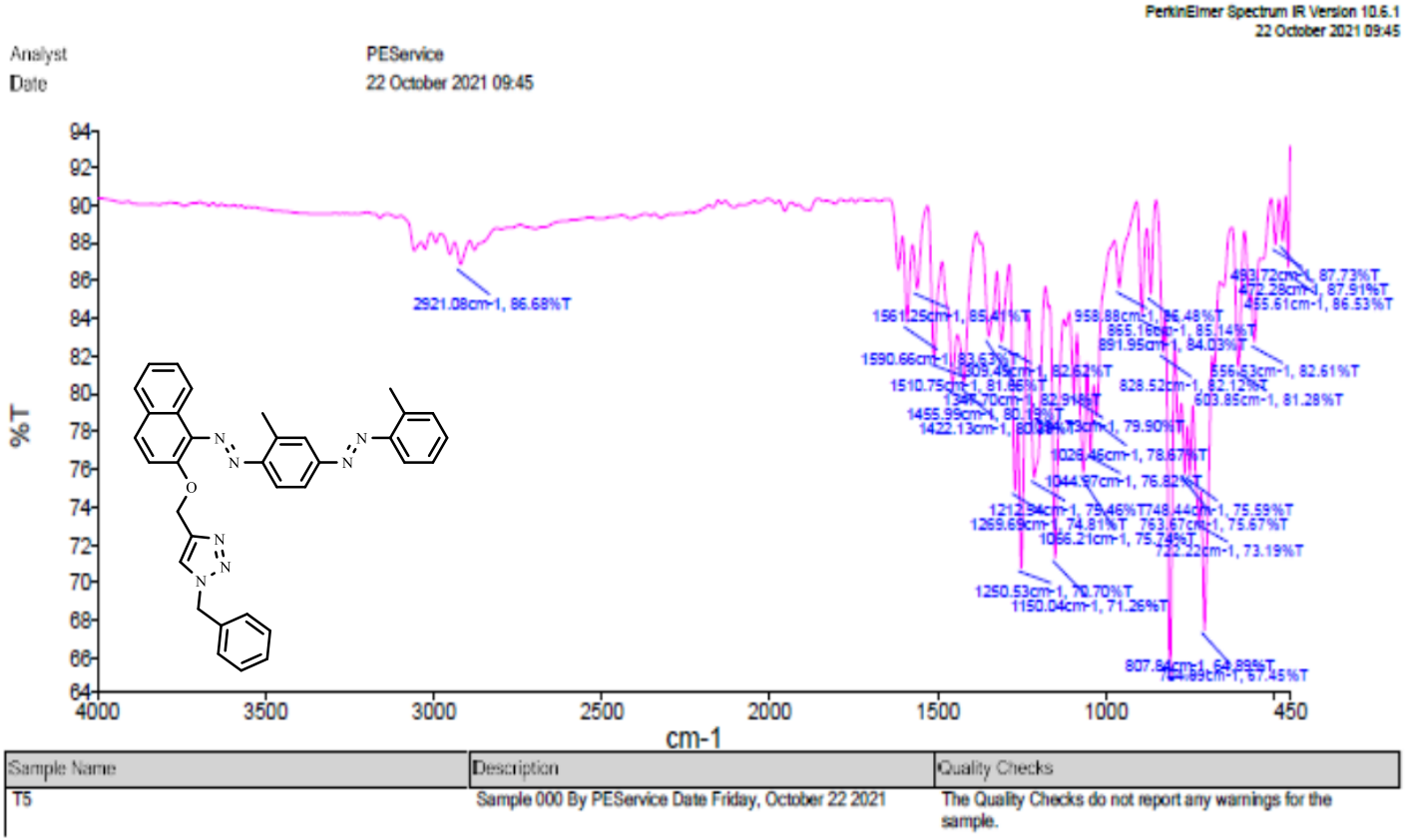

IR of triazole derivative 62c

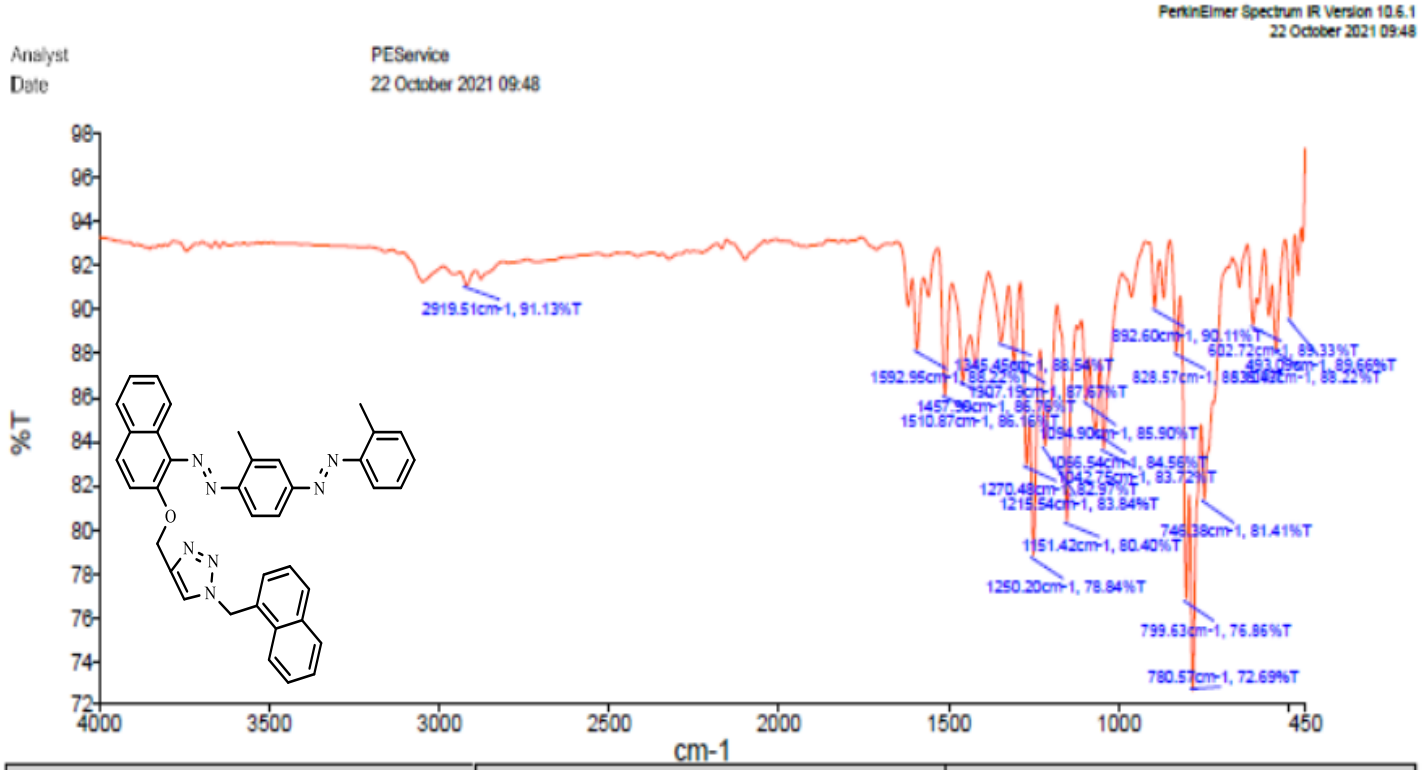

IR of alkyne 63a

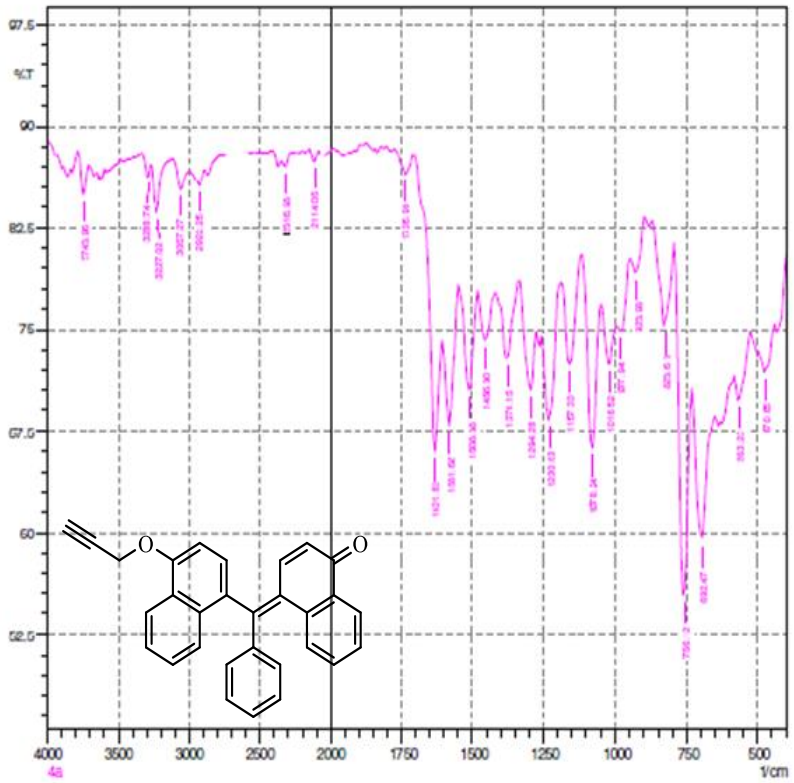

SHIMADZU

No.	Peak	Intensity	Corr. Inte	Base (H)	Base (L)	Area	Corr. Area
1	470.63	71.069	2.224	489.94	434	7.619	0.439
2	563.28	69.837	2.519	576.74	520.8	8.08	0.509
3	692.47	59.537	10.242	727.19	646.17	15.378	2.643
4	756.12	55.382	20.324	788.91	727.19	11.578	4.169
5	823.63	75.311	6.859	864.14	788.91	7.894	1.5
6	923.93	79.196	2.248	945.15	893.07	4.936	0.37
7	977.94	74.805	2.049	993.37	945.15	5.61	0.324
8	1016.52	72.445	3.598	1045.45	993.37	6.799	0.557
9	1078.24	66.226	12.486	1114.89	1045.45	9.607	2.42
10	1157.33	72.363	6.998	1186.26	1114.89	8.514	1.428
11	1250.63	66.336	7.566	1295.7	1186.26	9.636	1.532
12	1294.20	70.010	5.099	1332.06	1274.99	7.700	1.109
13	1379.15	72.834	5.309	1415.8	1332.86	9.981	1.129
14	1456.3	74.198	3.458	1481.38	1427.37	6.554	0.618
15	1508.38	70.515	7.493	1546.96	1481.38	8.475	1.413
16	1581.68	67.904	7.964	1606.76	1546.96	8.462	1.392
17	1631.53	66.961	11.717	1706.13	1606.76	10.841	1.719
18	1736.00	86.468	0.806	1746.64	1706.13	2.449	0.106
19	2114.05	87.376	0.893	2142.99	2085.12	3.278	0.142
20	2316.58	87.032	0.613	2341.66	2278.01	3.721	0.097
21	2922.25	85.617	0.855	2955.04	2889.46	4.284	0.144
22	3057.27	85.309	1.829	3109.35	2995.55	7.276	0.452
23	3227.02	00.000	3.079	3301.74	3124.79	0.000	0.790
24	3288.74	86.319	1.152	3331.18	3261.74	4.196	0.193
25	3743.96	84.936	2.764	3778.68	3705.38	4.709	0.521

IR of triazole derivative 63b

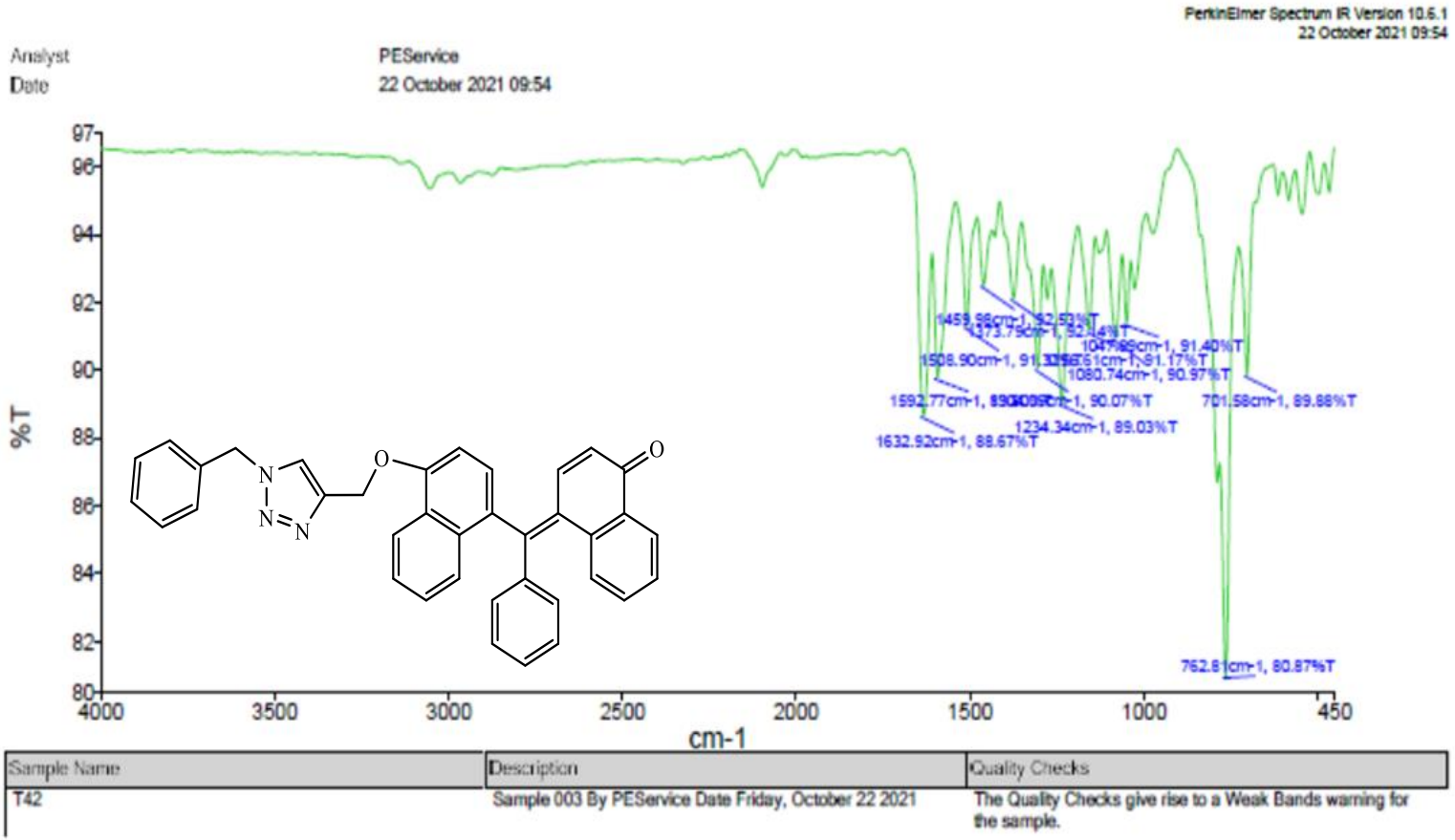

Appendix C

NMR Spectra ^{1}H, ^{13}C

^{1}H NMR of azidomethylbenzene 24

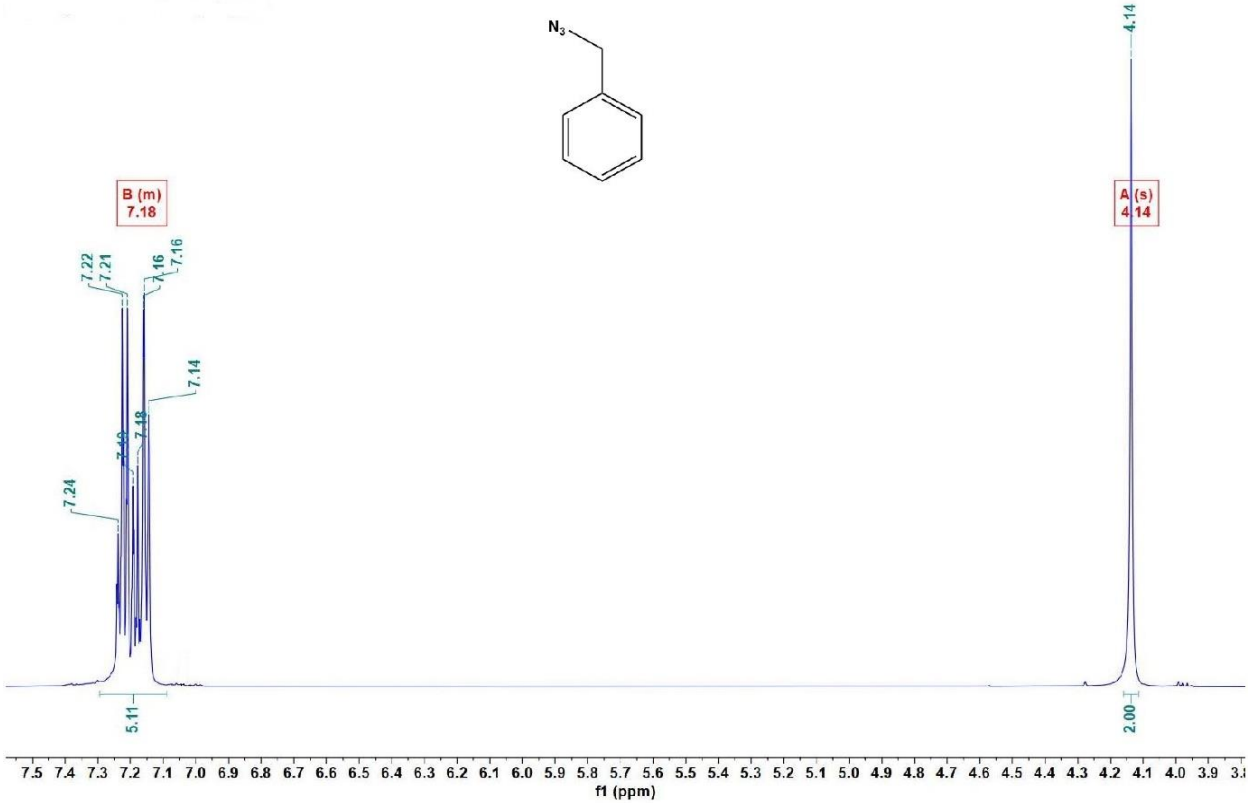

^{13}C NMR of azidomethylbenzene 24

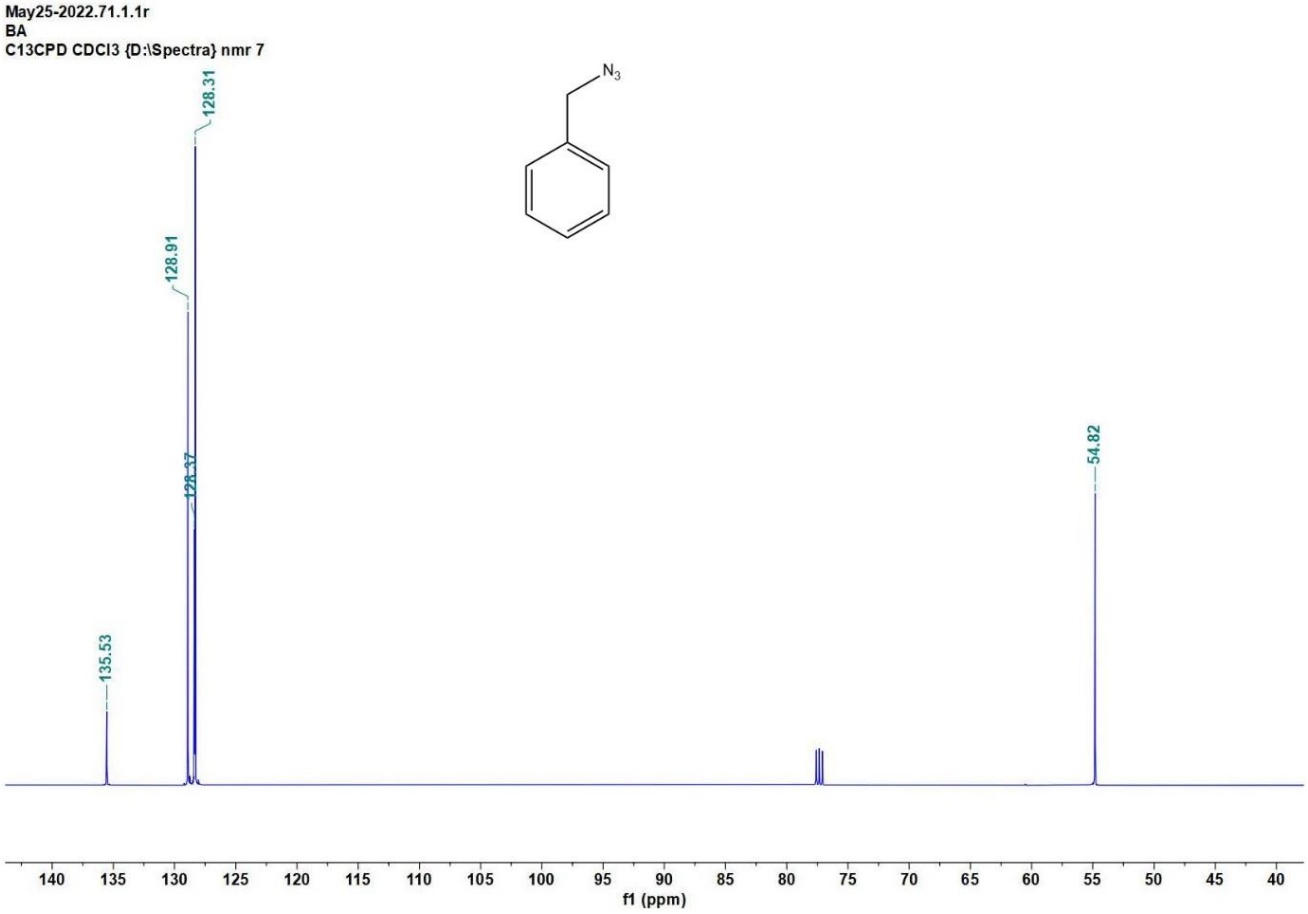

^{1}H NMR of azidomethylnaphthalene 58

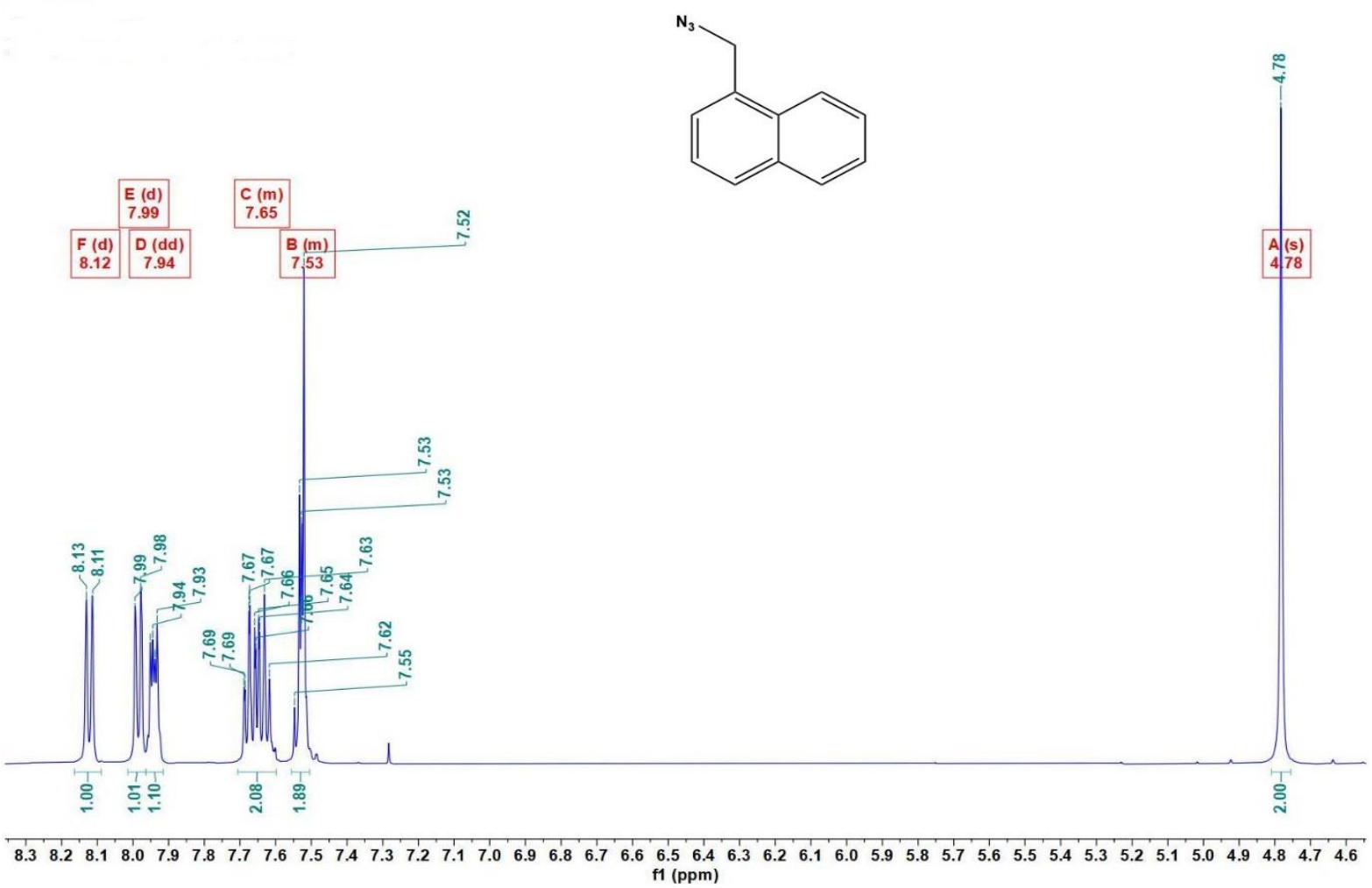

^{13}C NMR of azidomethylnaphthalene 58

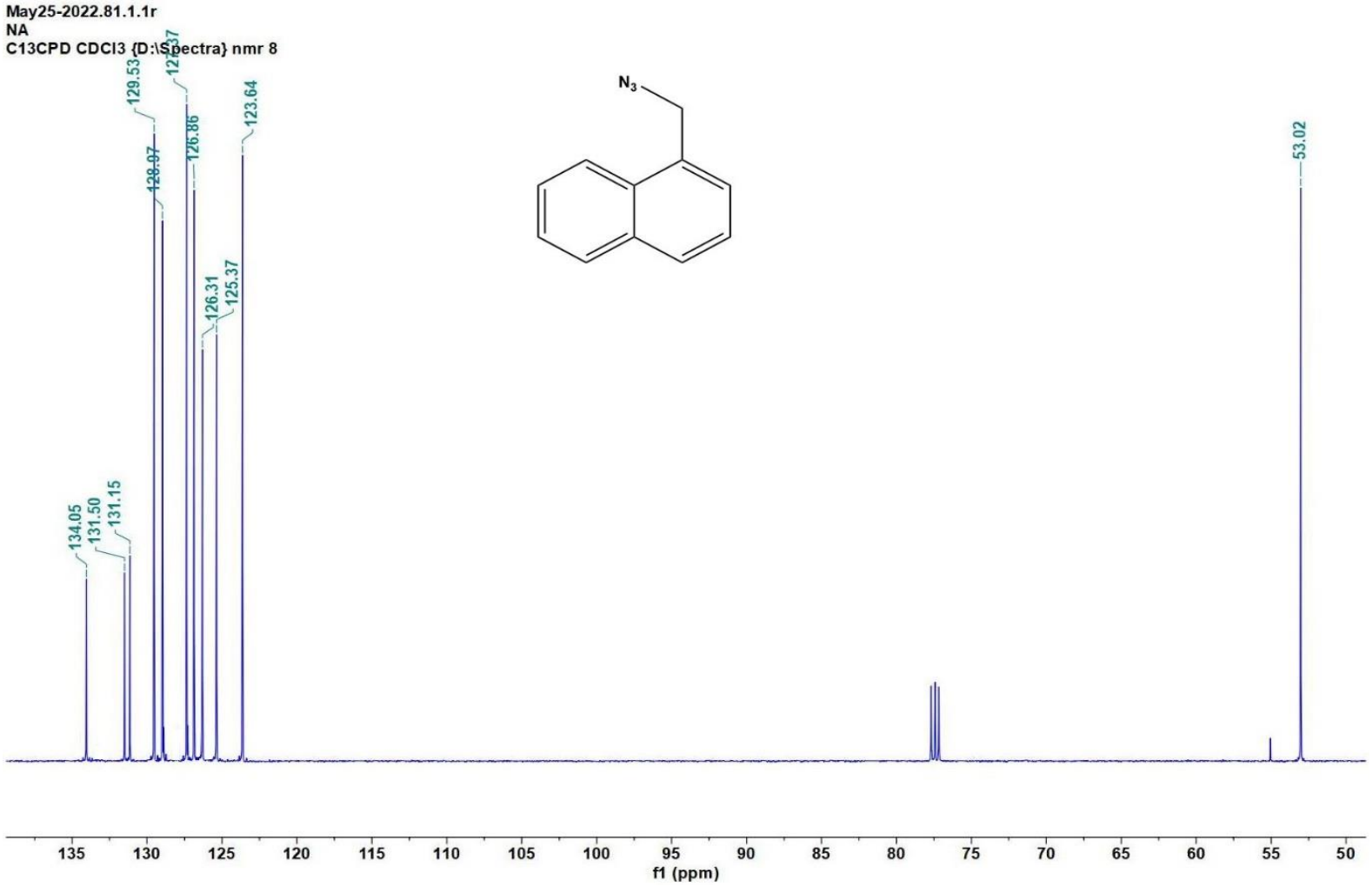

^{1}H NMR of alkyne 59a

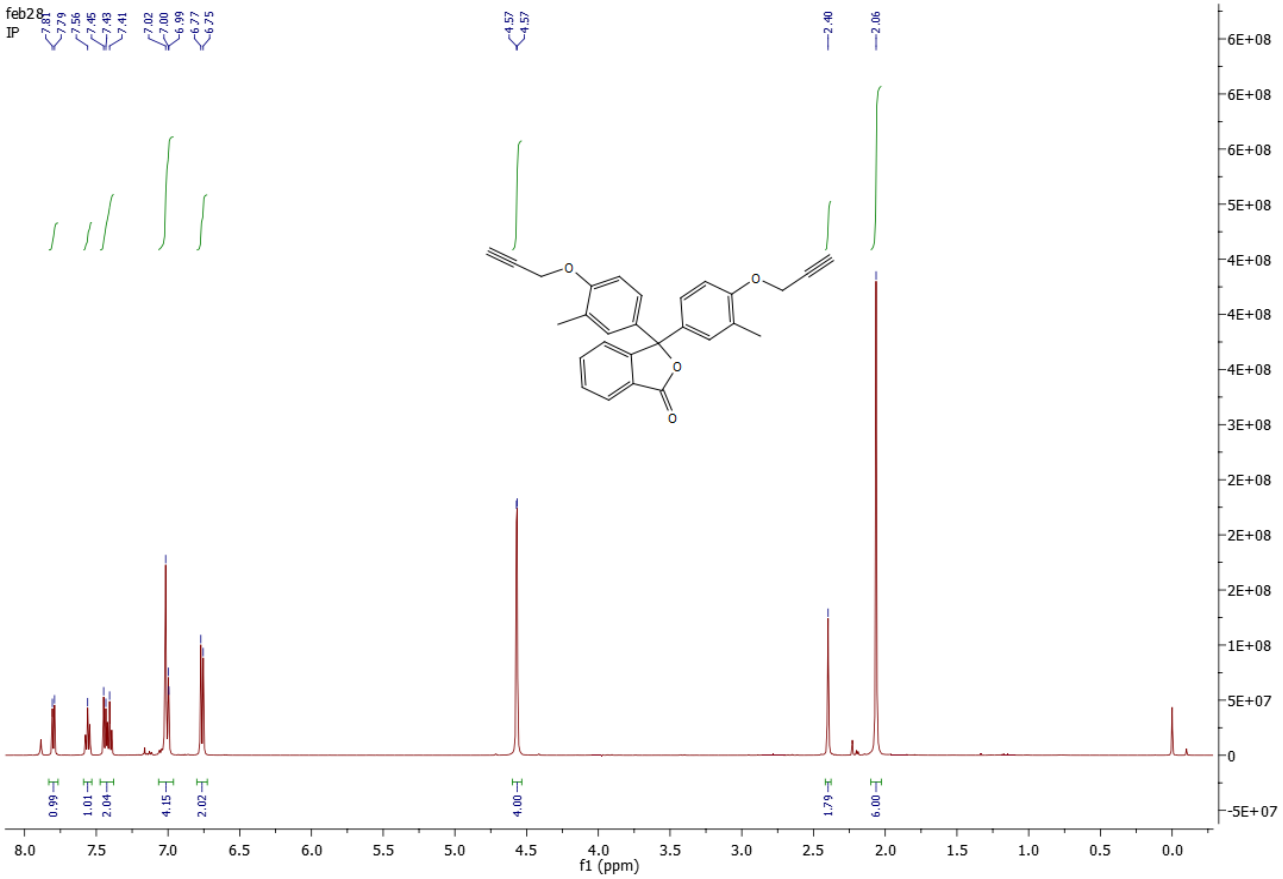

^{13}C NMR of alkyne 59a

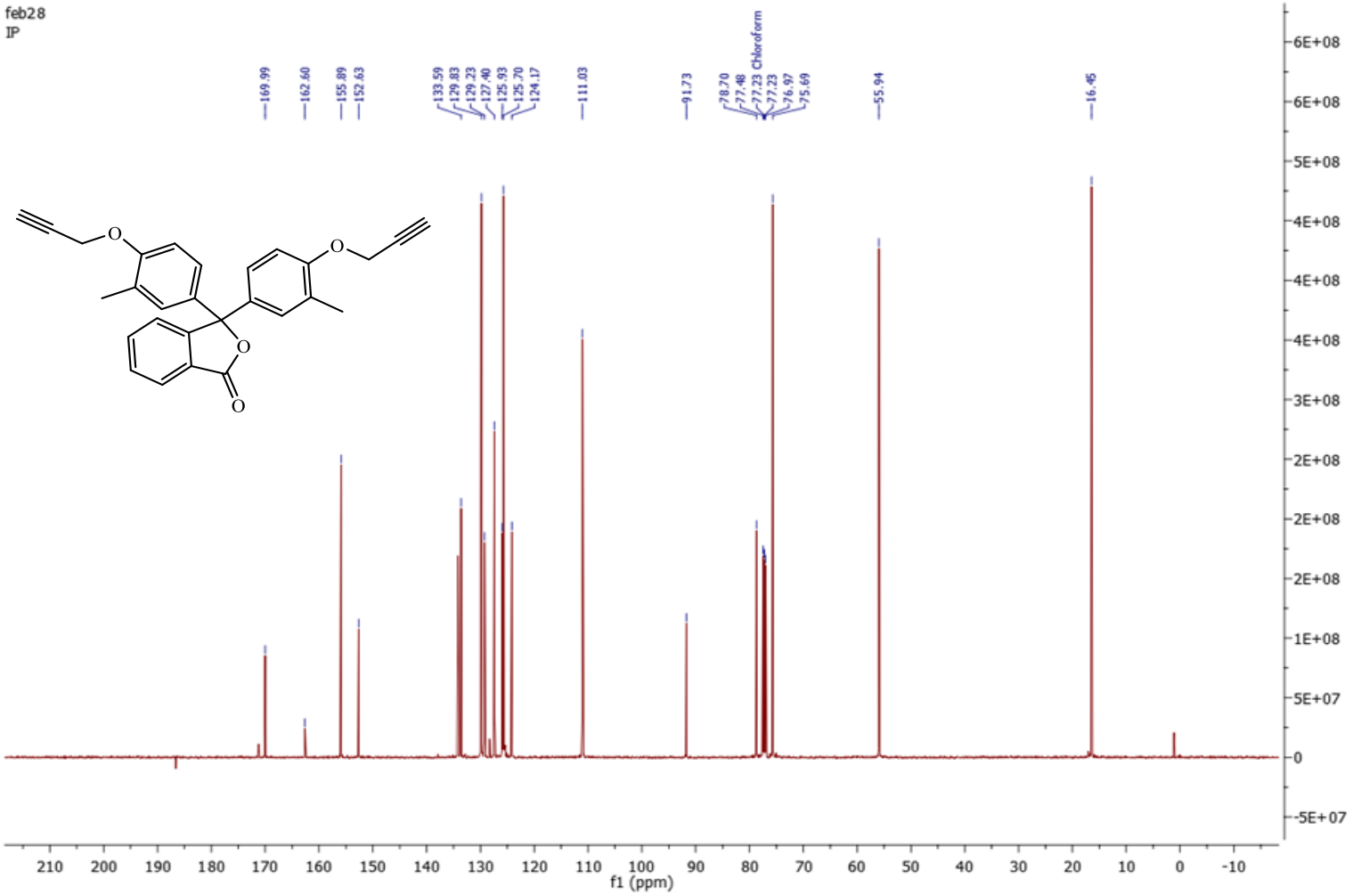

^{1}H NMR of 1,2,3- triazole derivative 59b

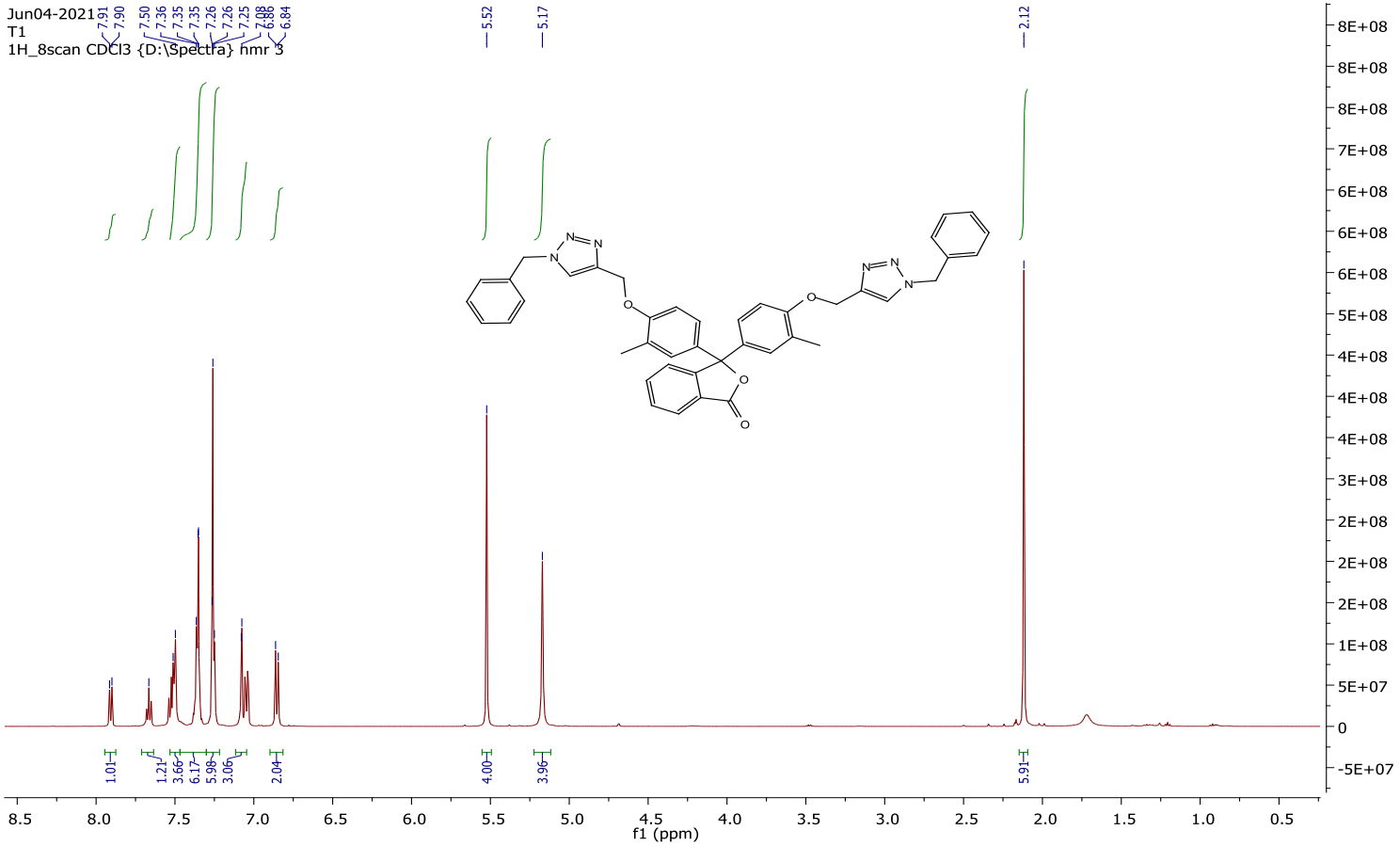

^{13}C NMR of 1,2,3- triazole derivative 59b

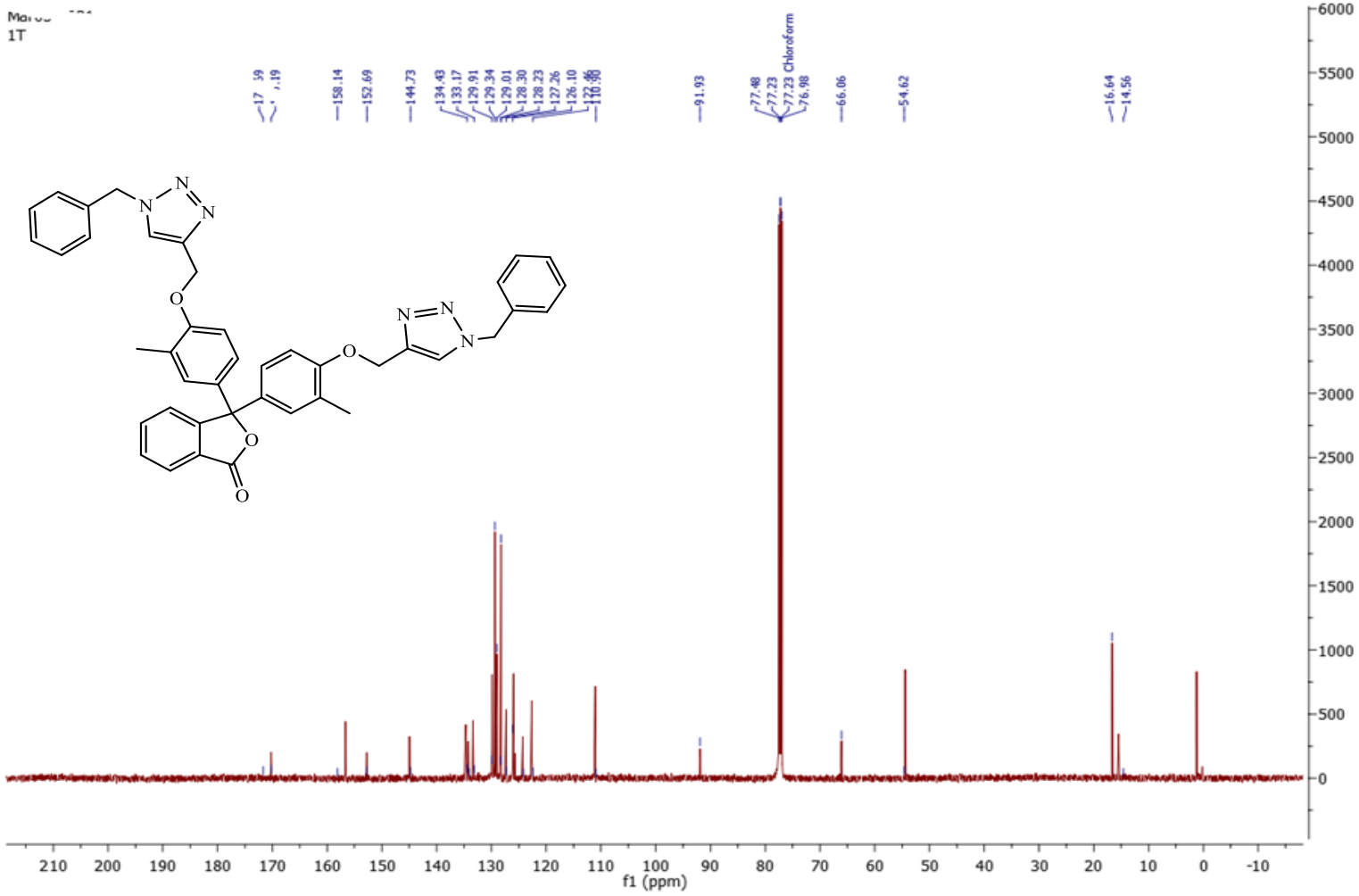

^{1}H NMR of 1,2,3-triazole derivative 59c

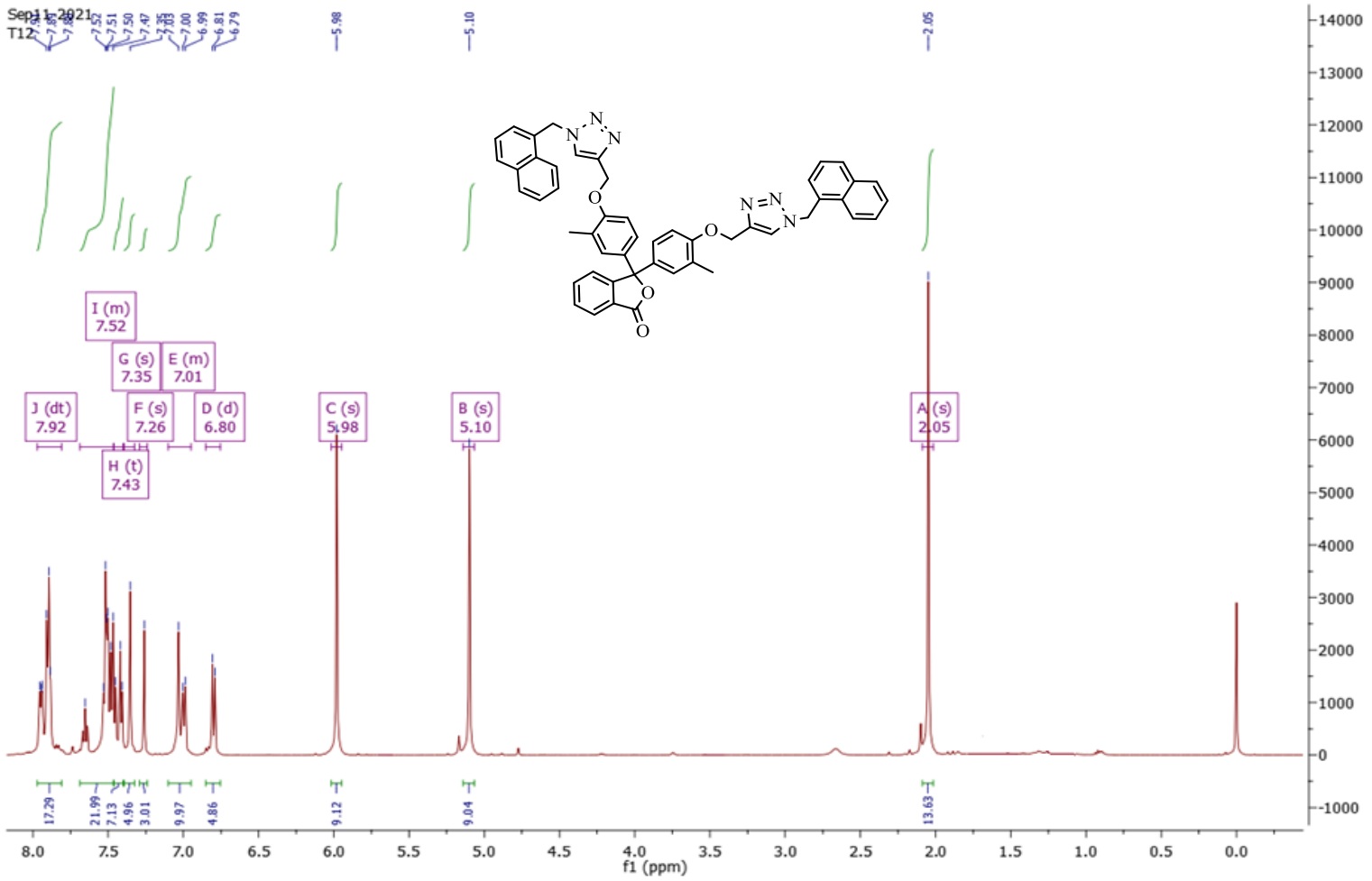

^{13}C NMR of 1,2,3-triazole derivative 59c

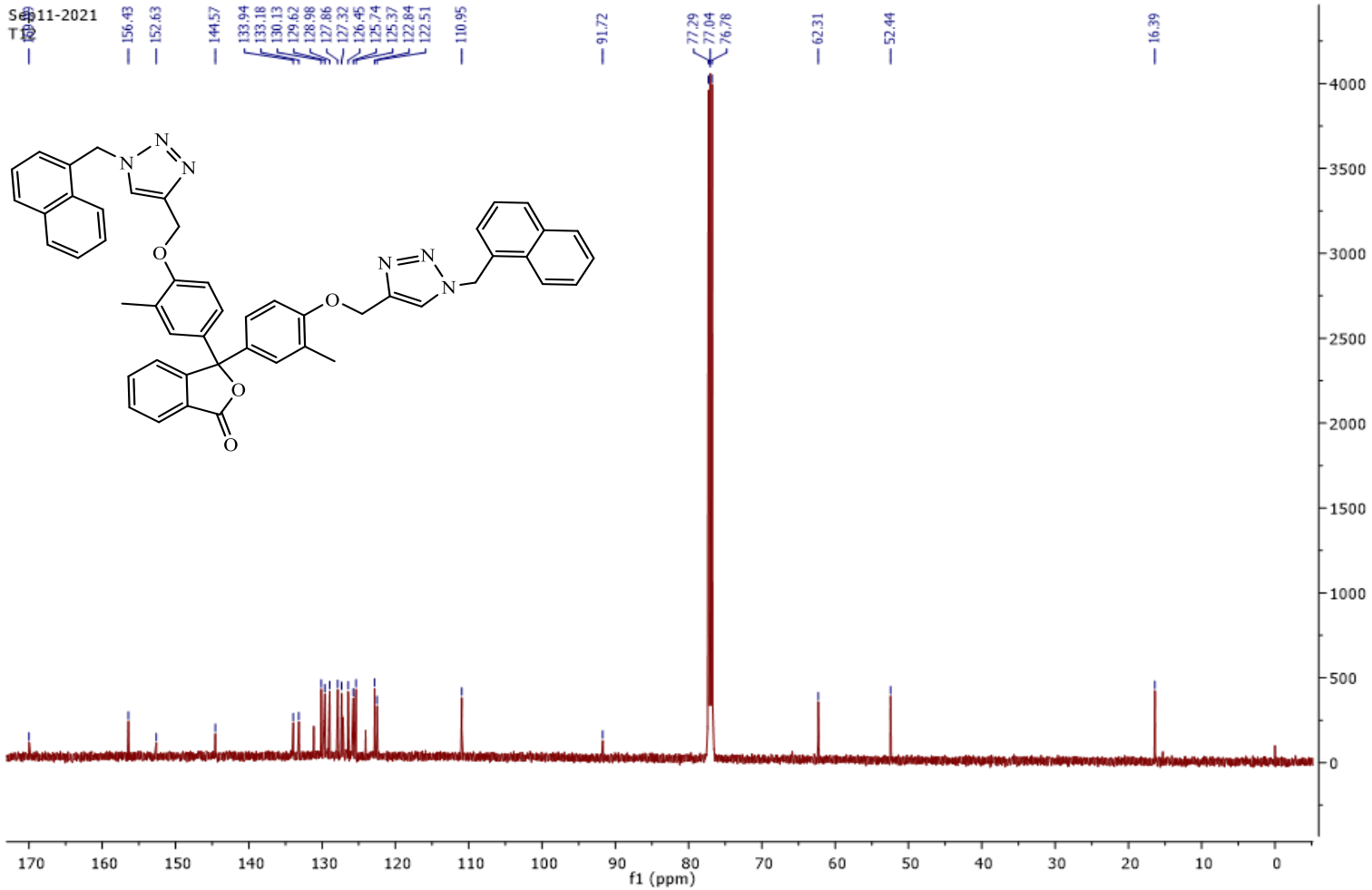

^{1}H NMR of alkyne 60a

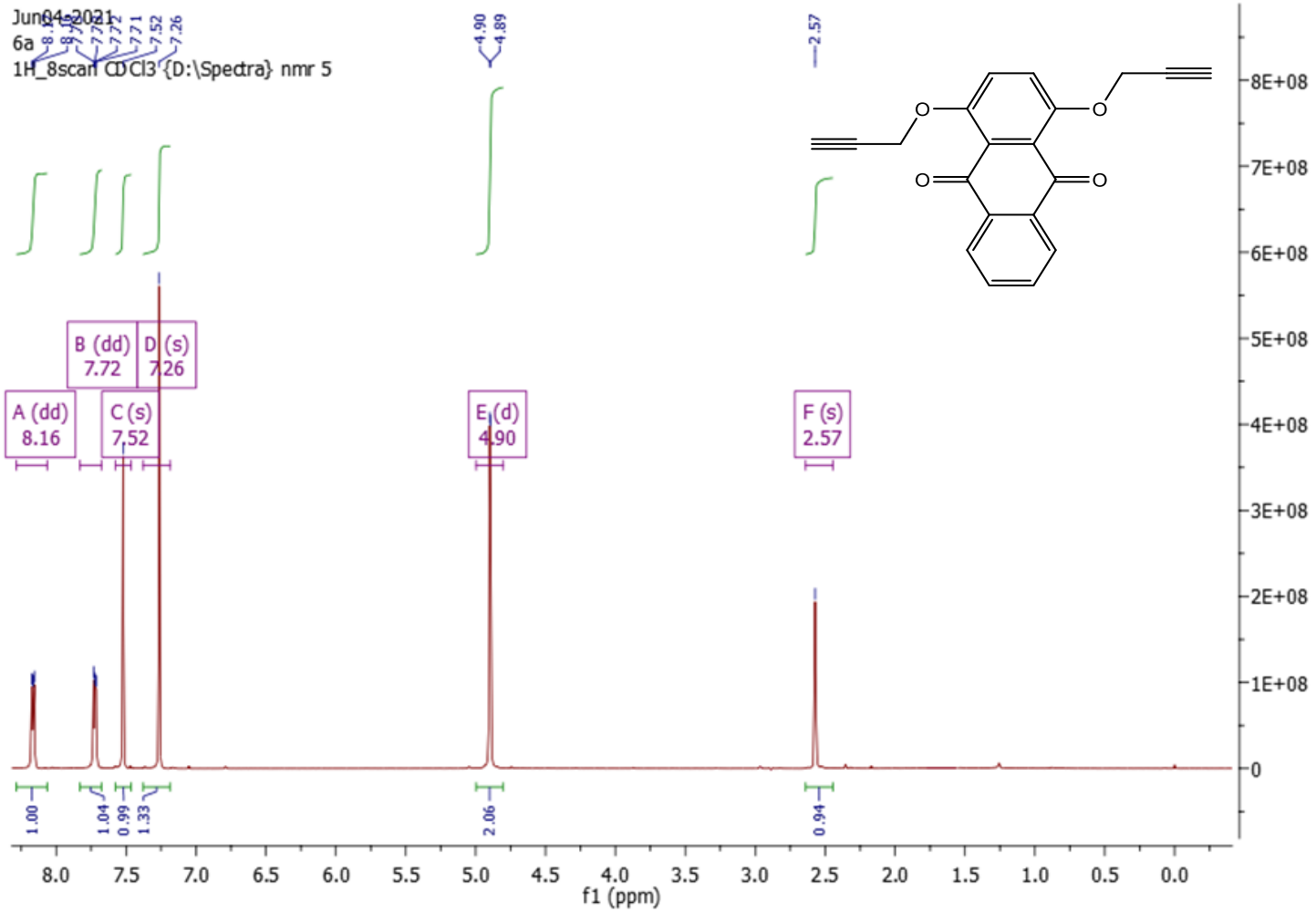

^{13}C NMR of alkyne 60a

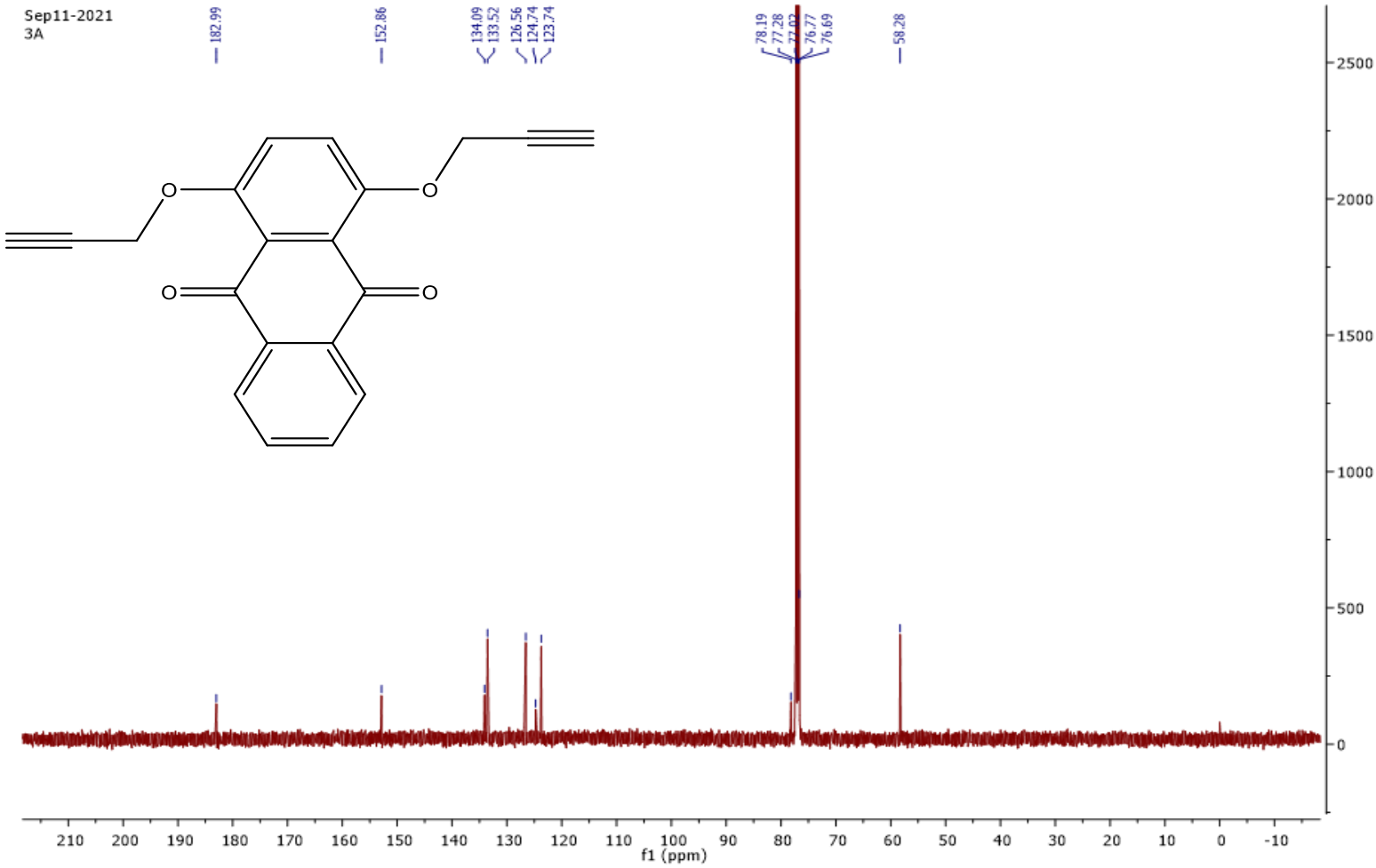

^{1}H NMR of 1,2,3-triazole derivative 60b

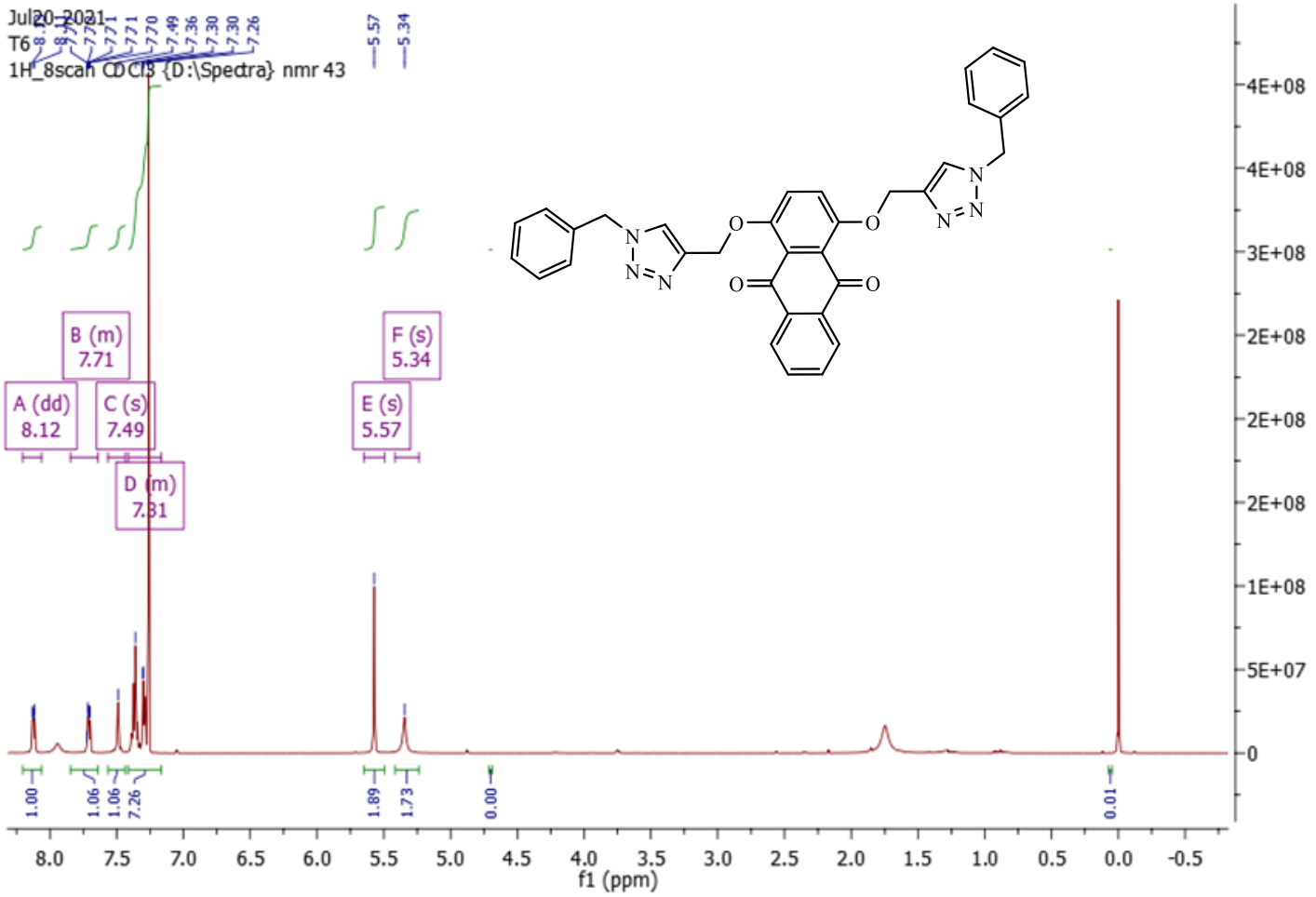

^{13}C NMR of 1,2,3-triazole derivative 60b

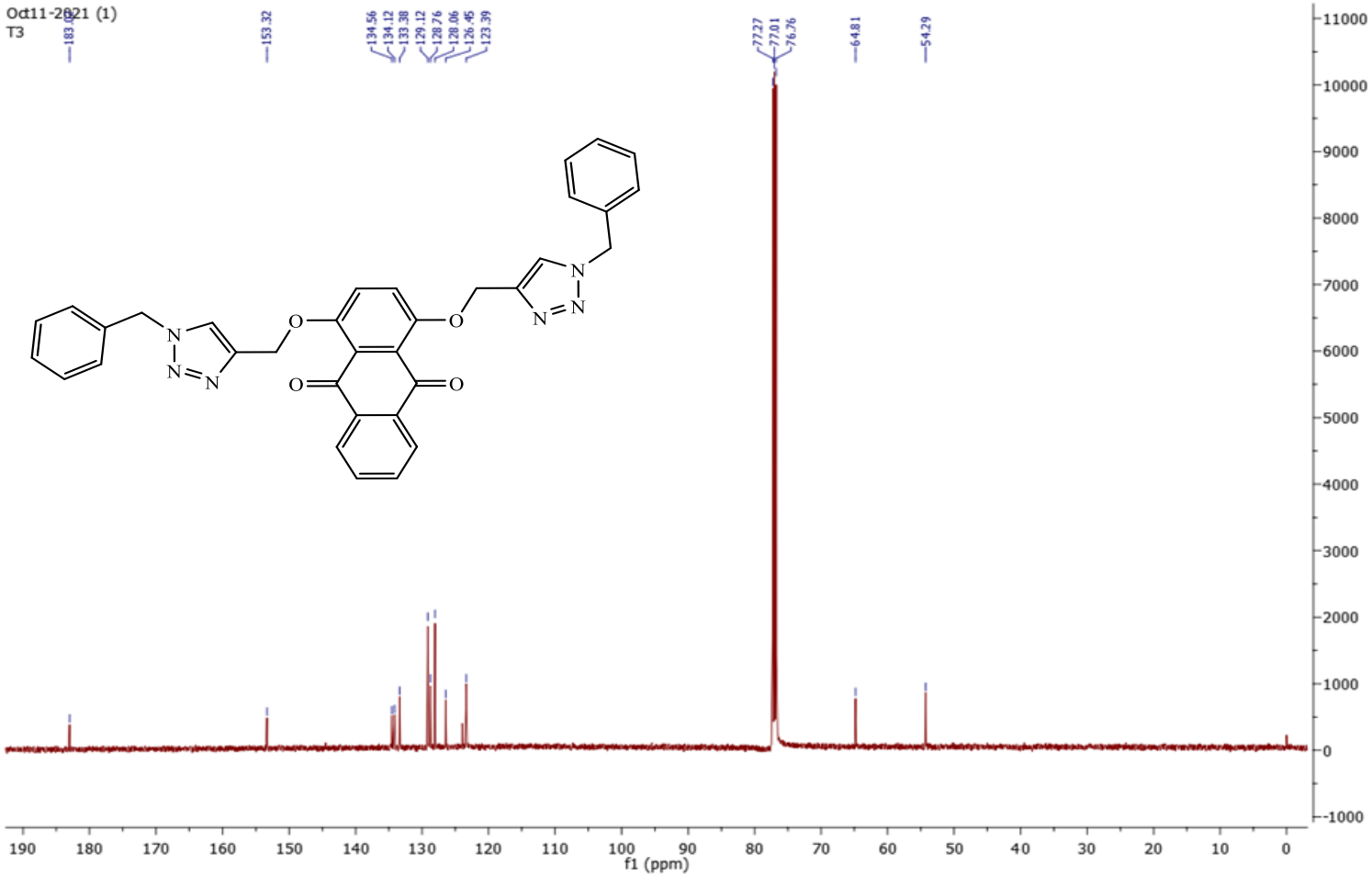

^{1}H NMR of 1,2,3-triazole derivative 60c

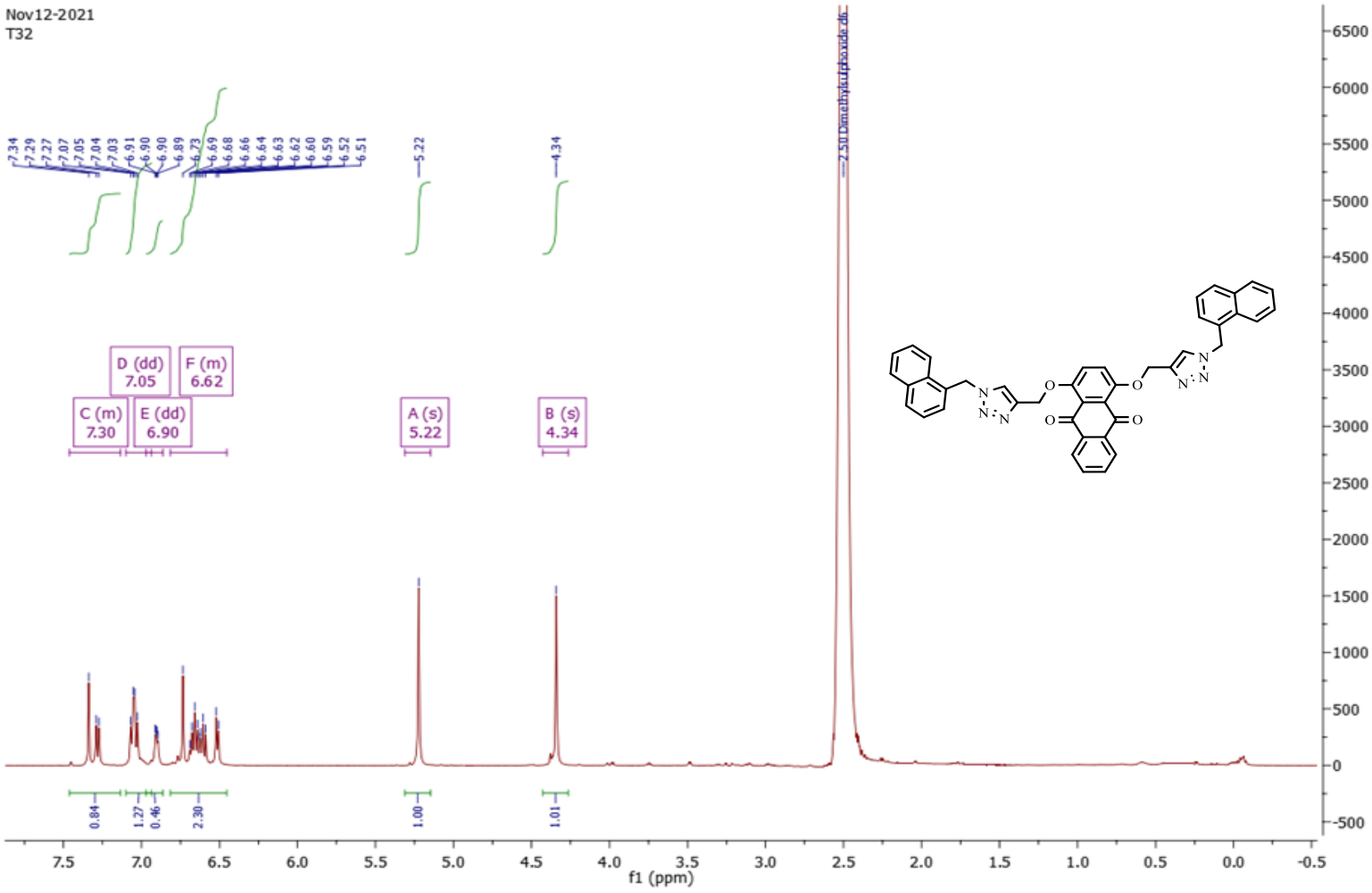

^{13}C NMR of 1,2,3-triazole derivative 60c

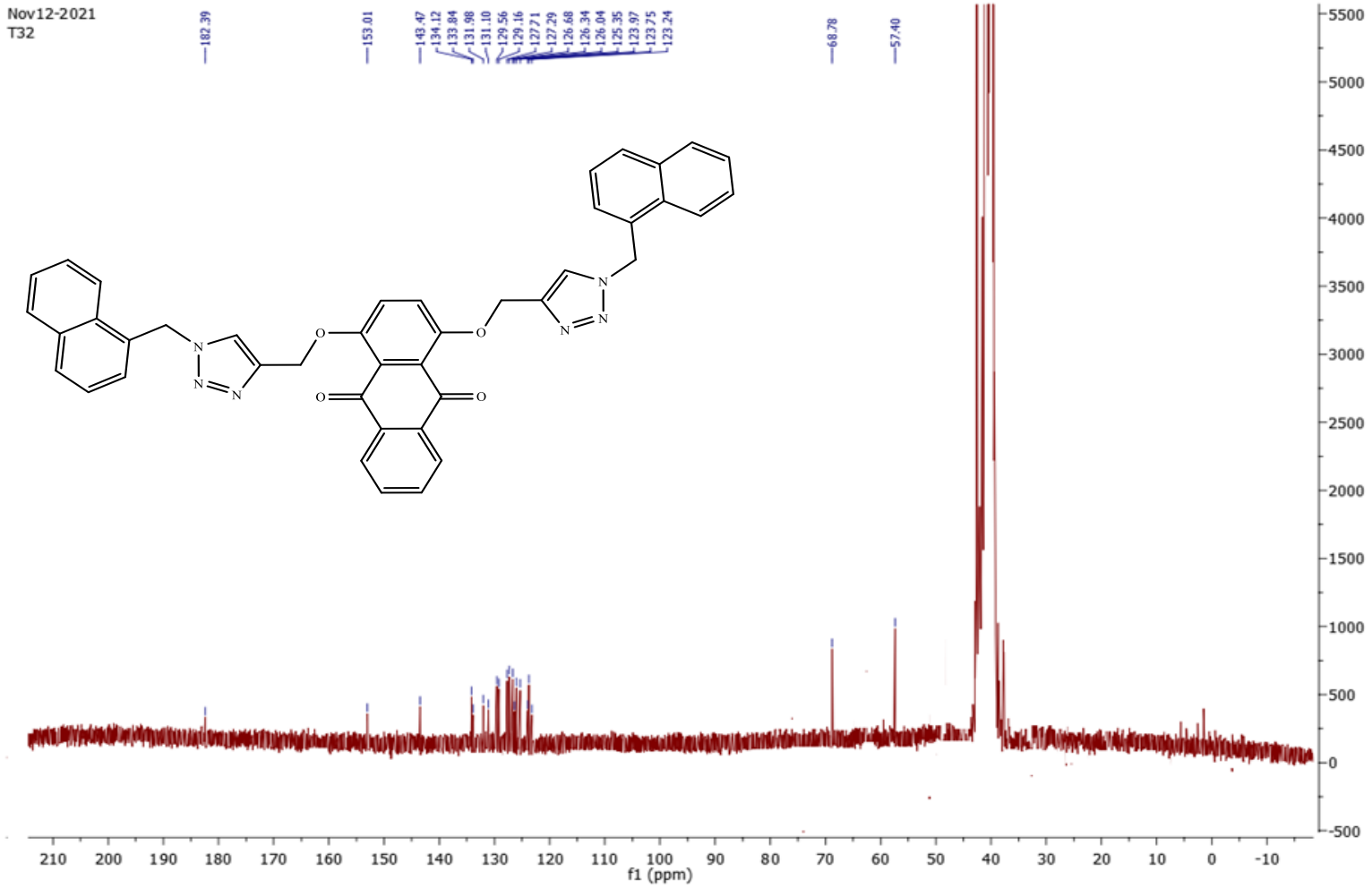

^{1}H NMR of alkyne 61a

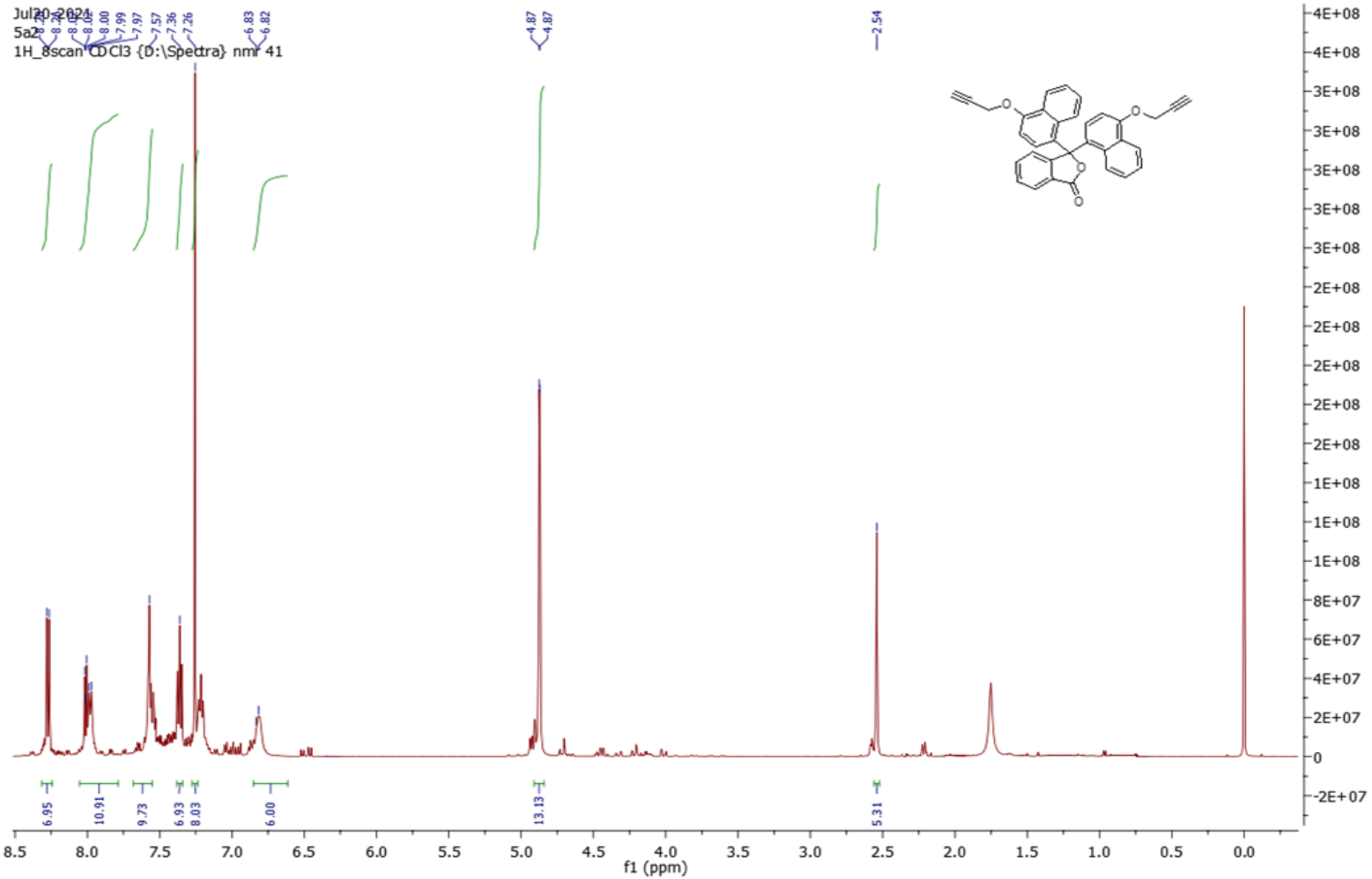

^{13}C NMR of alkyne 61a

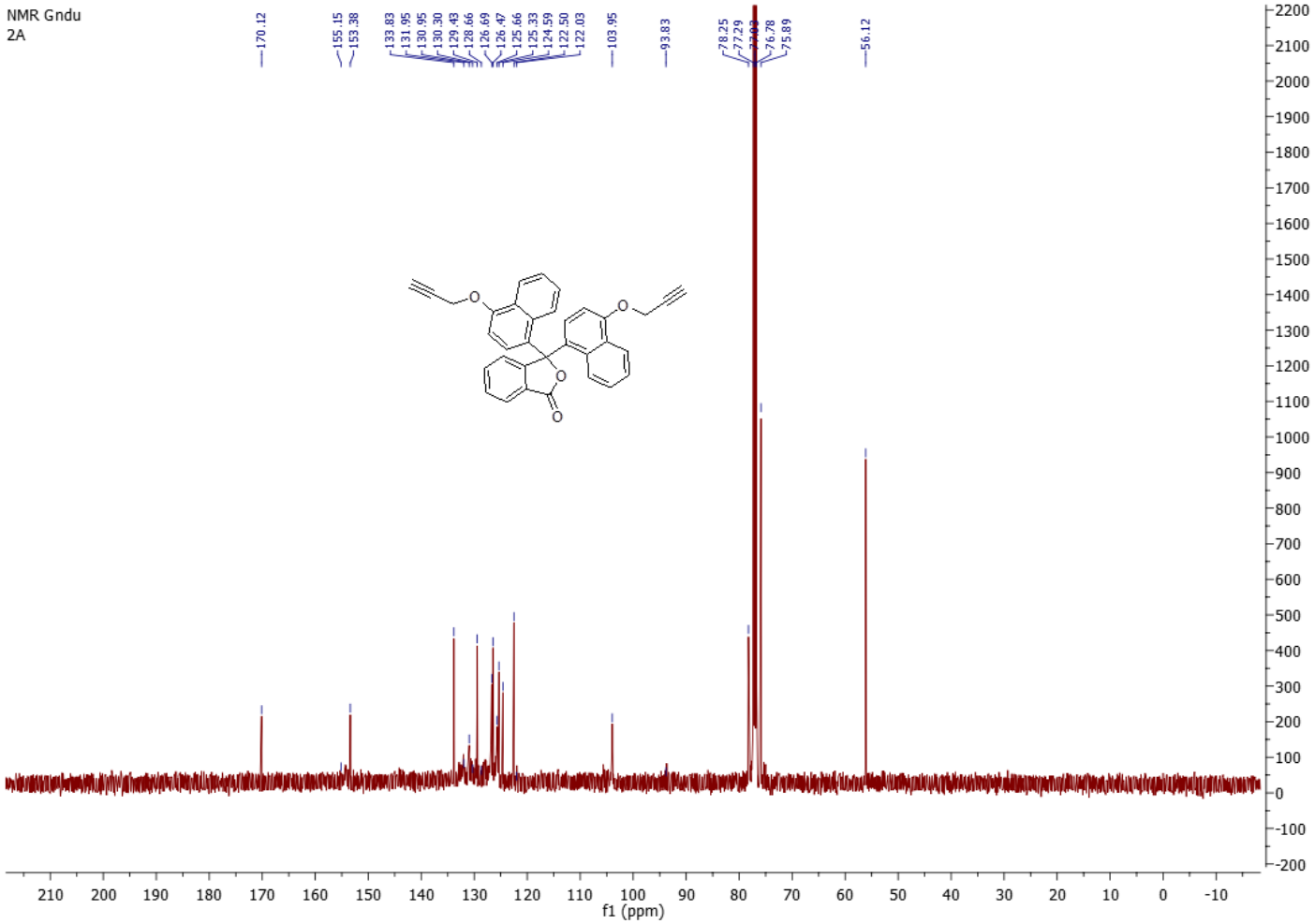

^{1}H NMR of 1,2,3-triazole derivative 61b

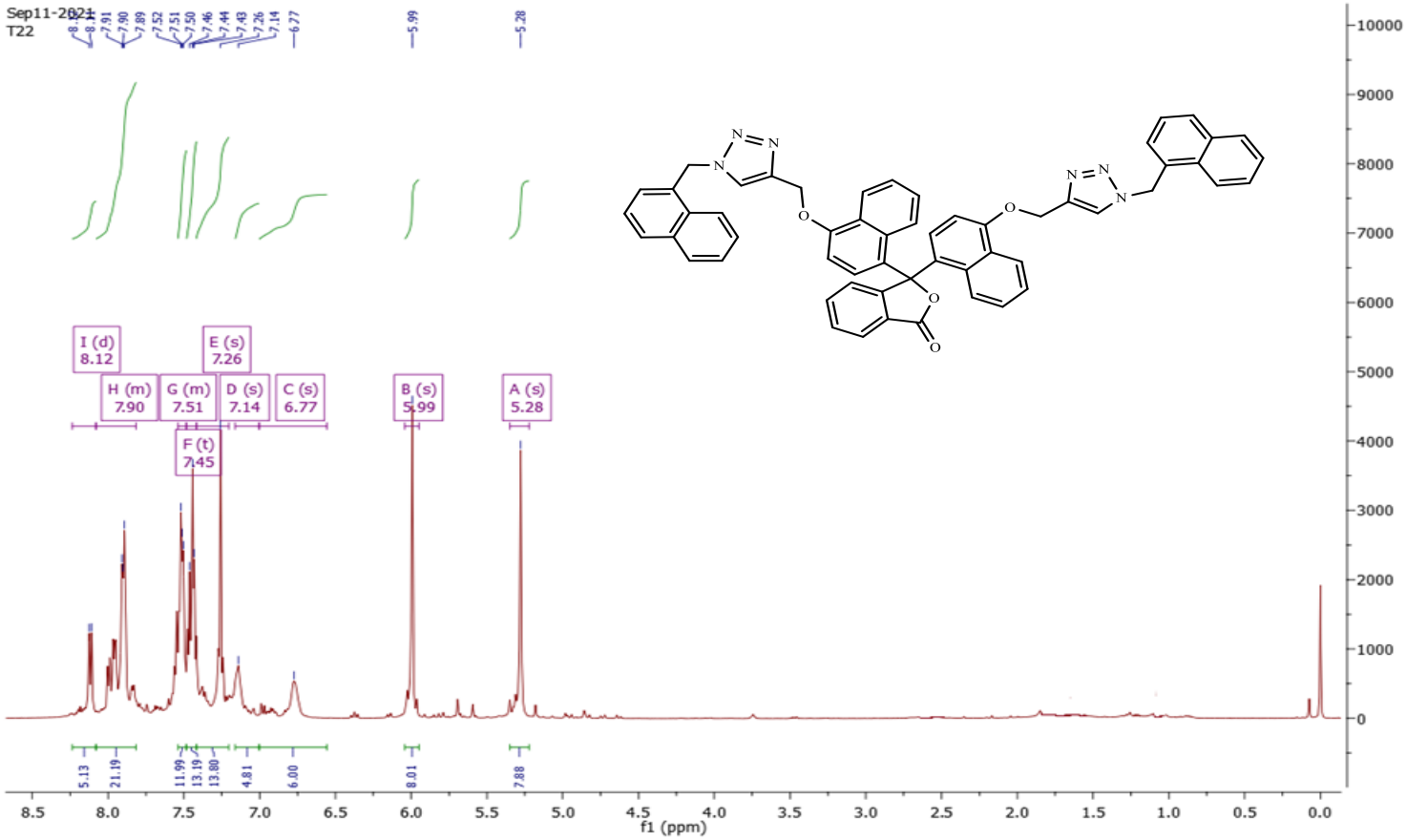

^{13}C NMR of 1,2,3-triazole derivative 61b

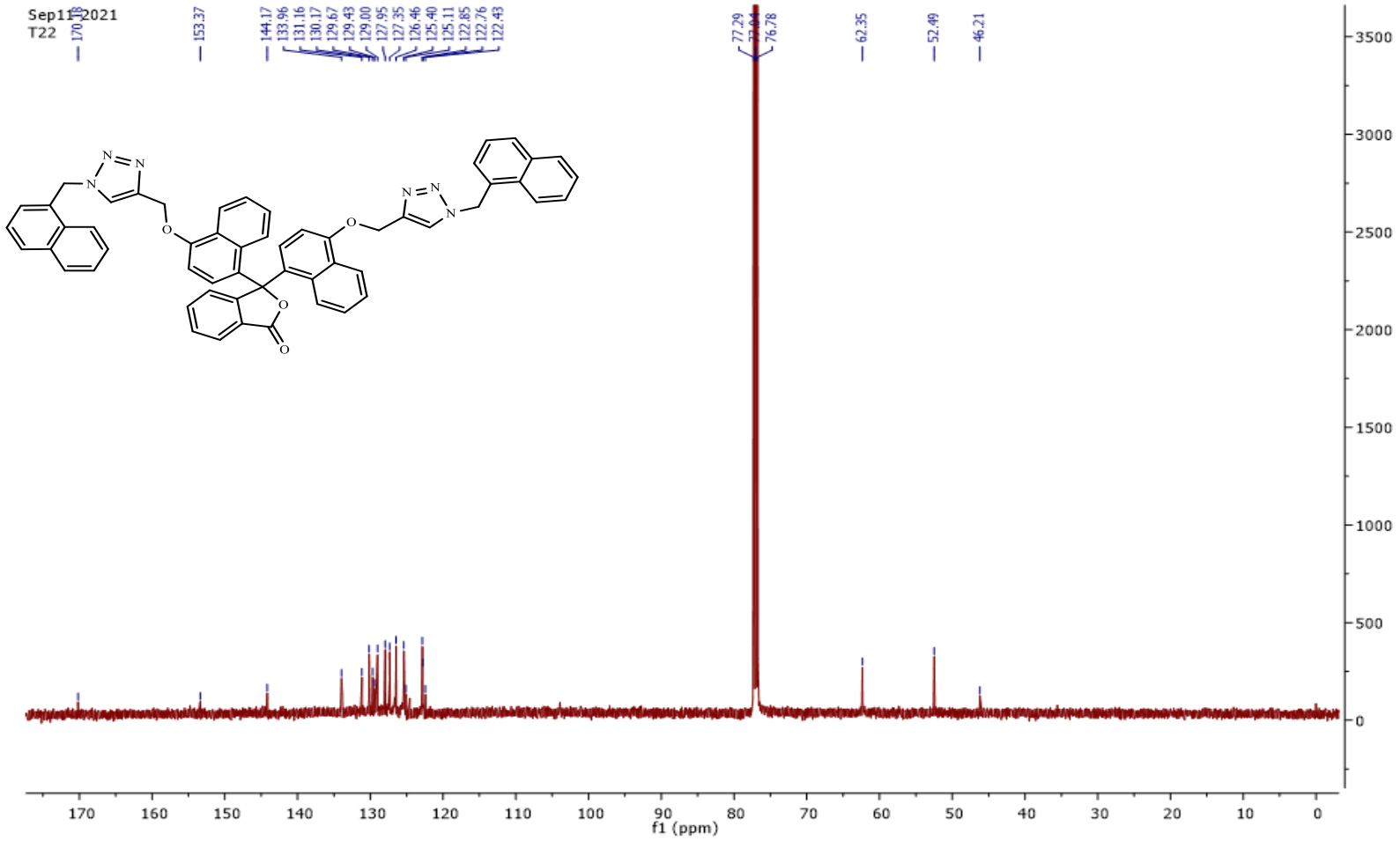

^{1}H NMR of alkyne 62a

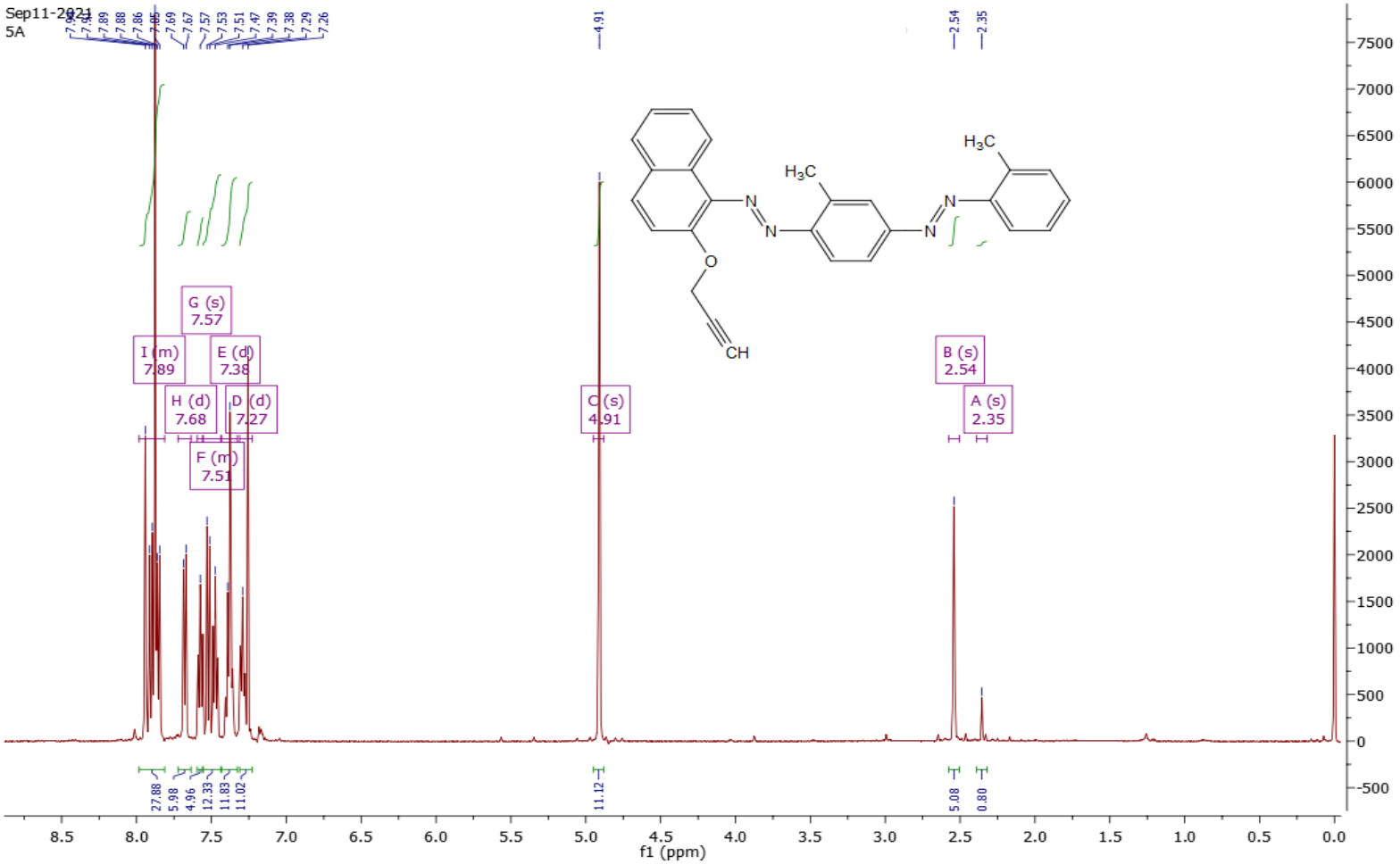

^{13}C NMR of alkyne 62a

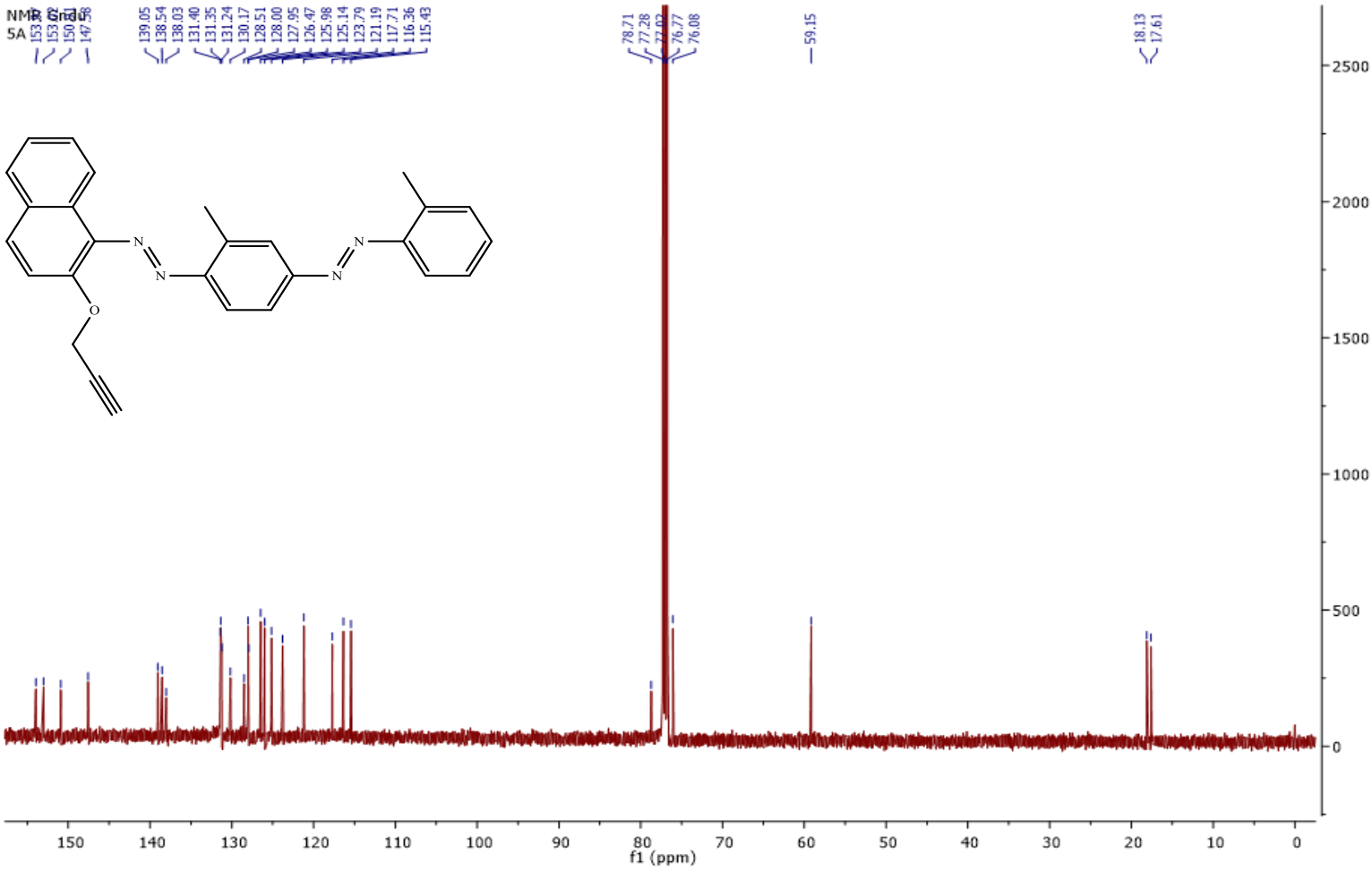

^{1}H NMR of 1,2,3-triazole derivative 62b

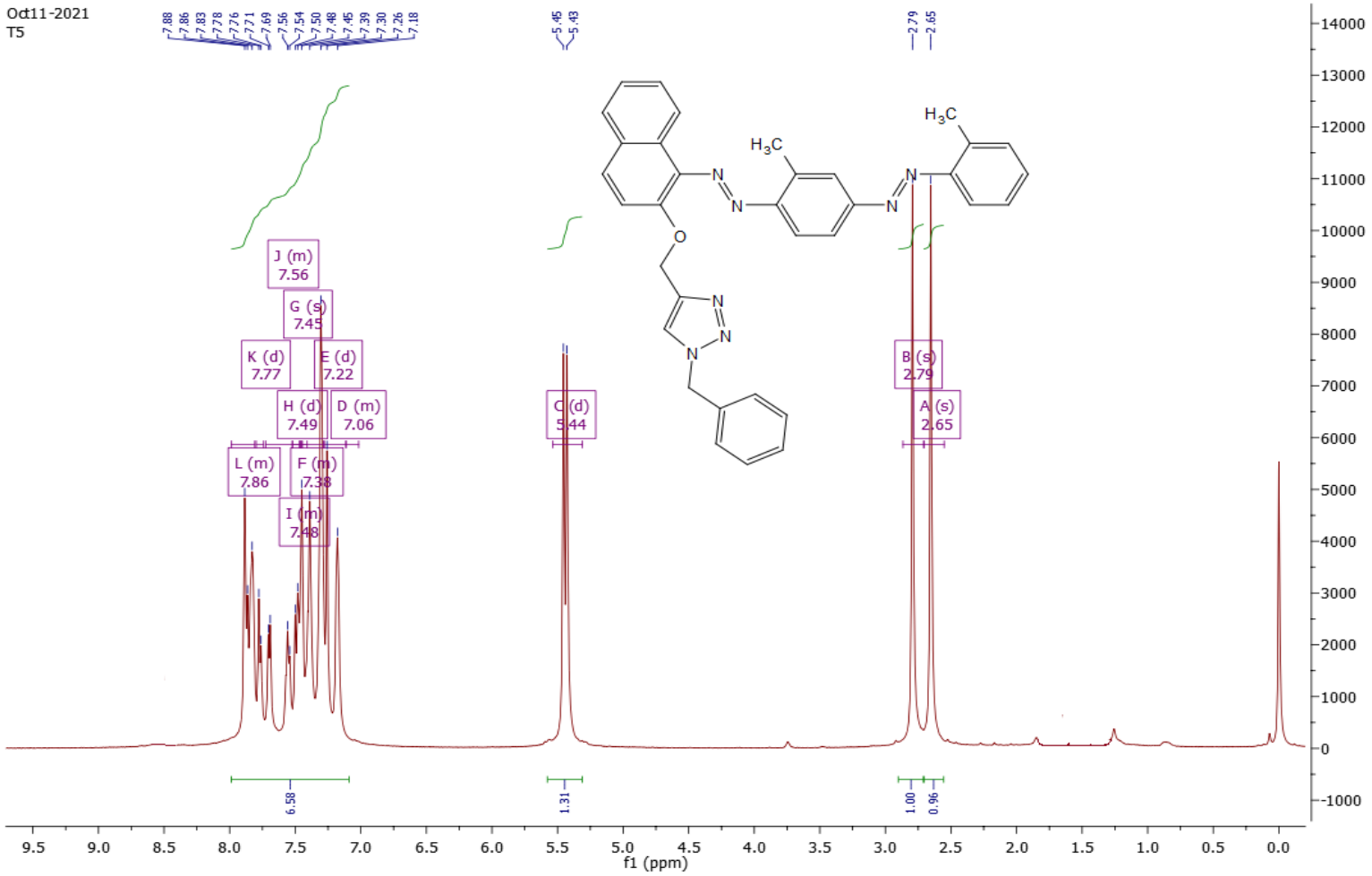

^{13}C NMR of 1,2,3-triazole derivative 62b

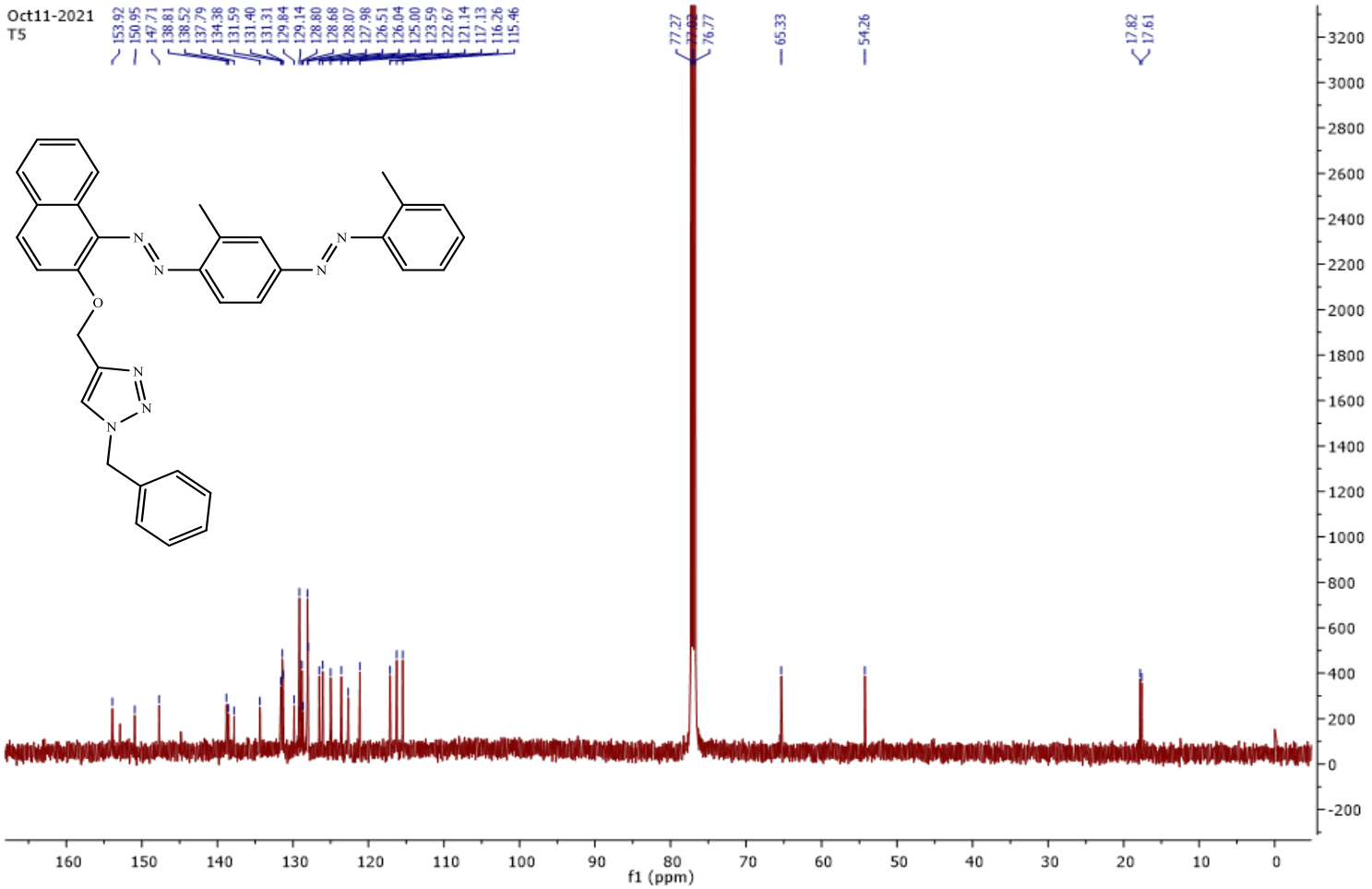

^{1}H NMR of 1,2,3-triazole derivative 62c

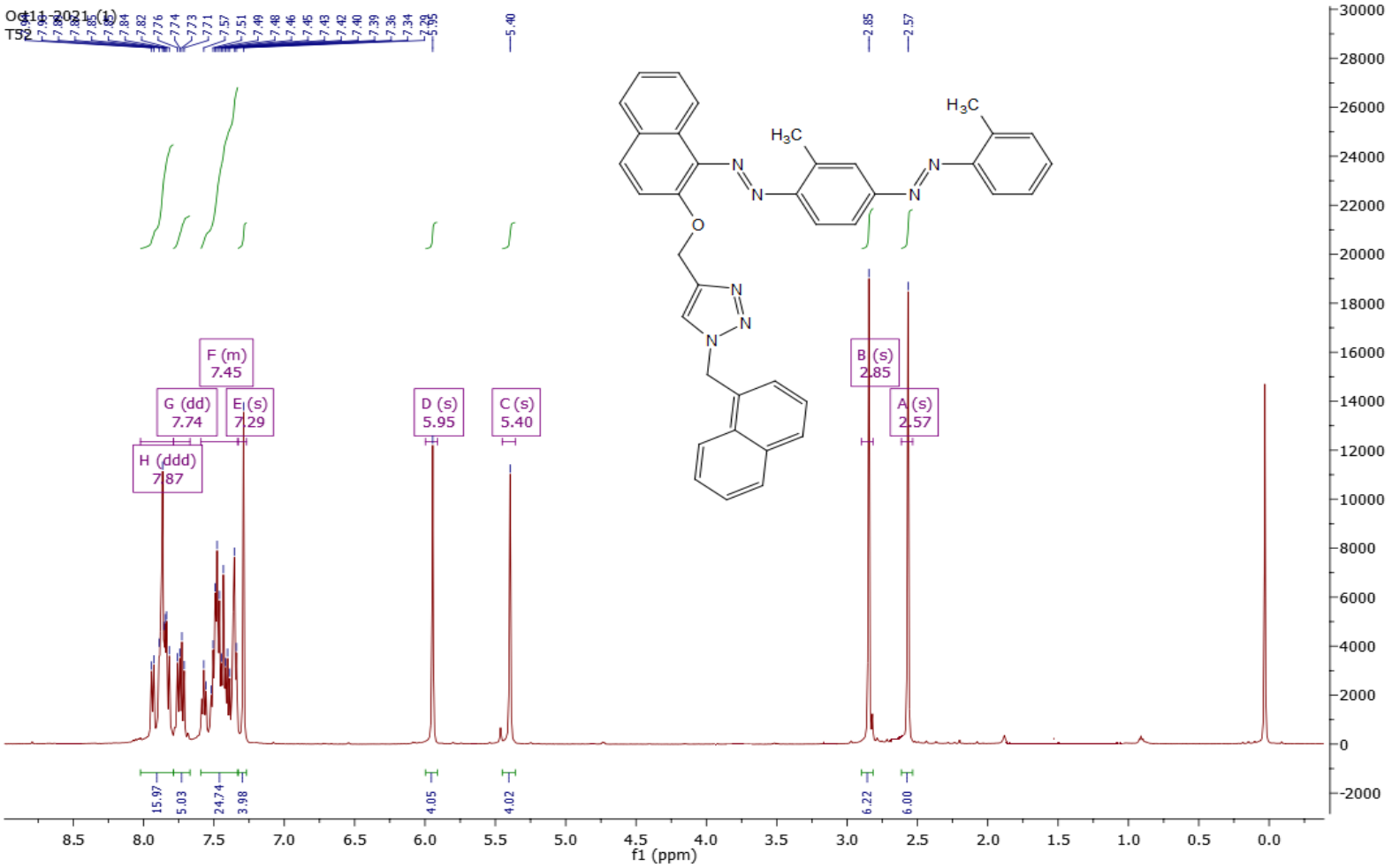

^{13}C NMR of 1,2,3-triazole derivative 62c

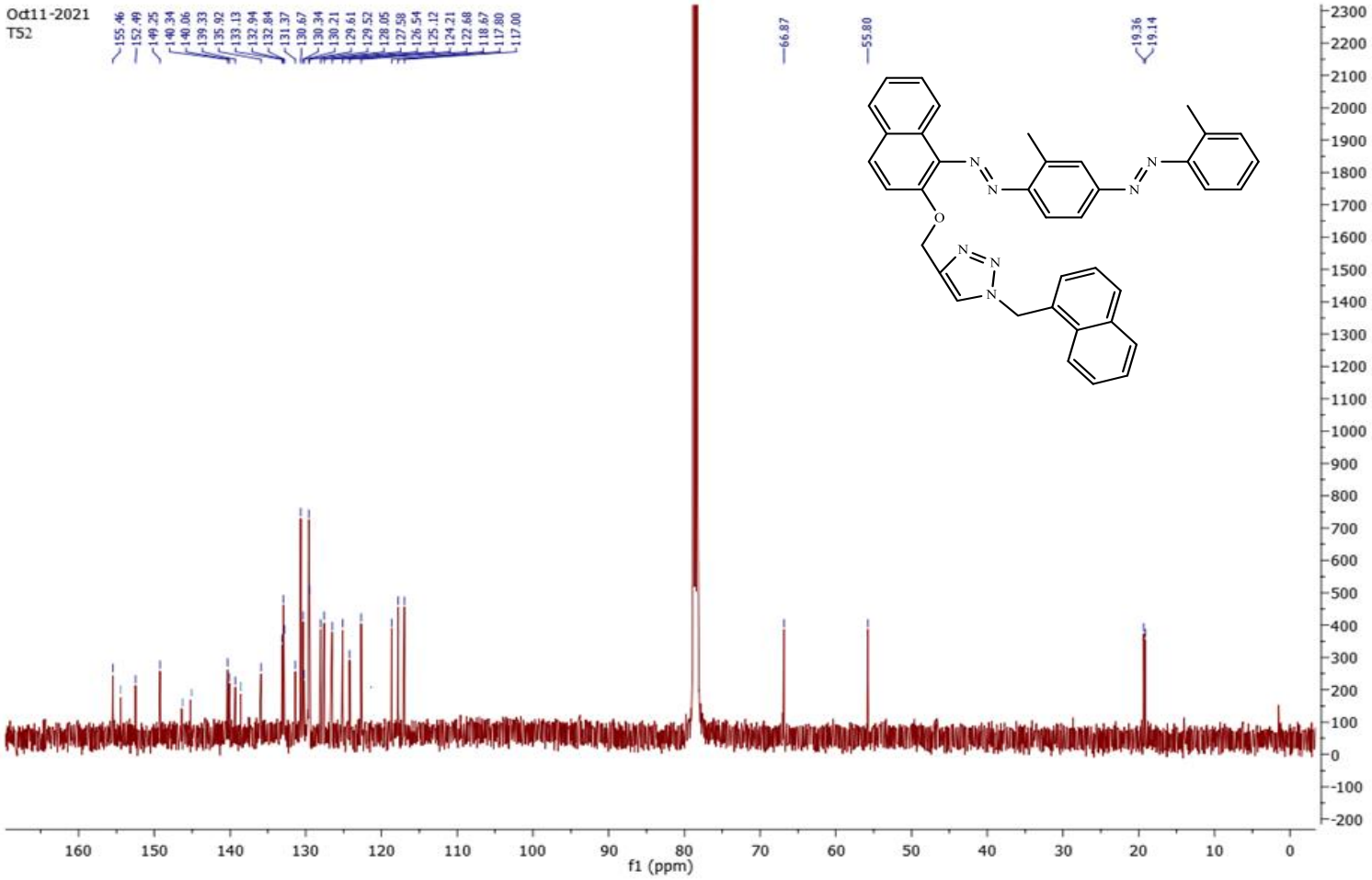

^{1}H NMR of alkyne 63a

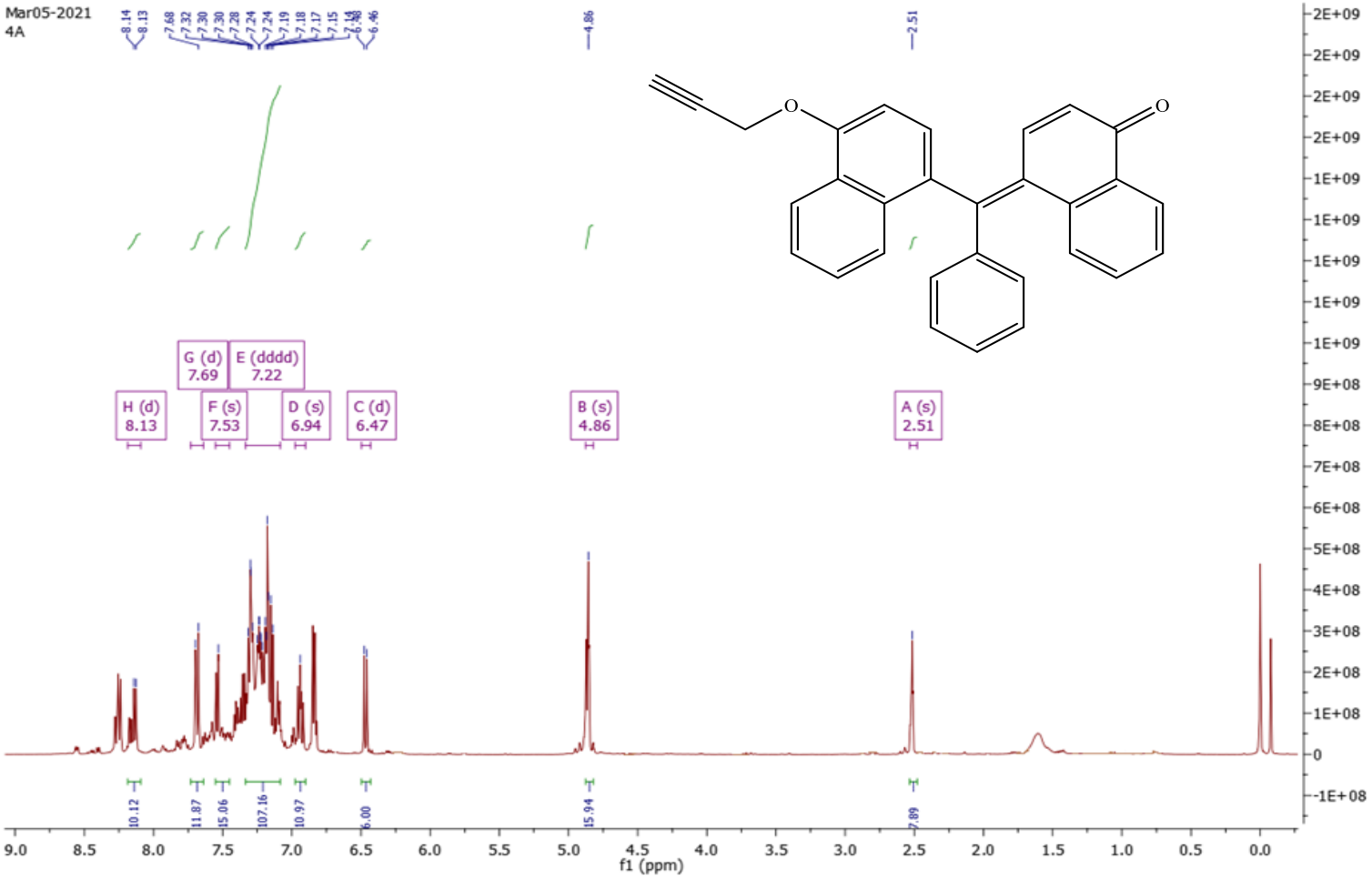

^{13}C NMR of alkyne 63a

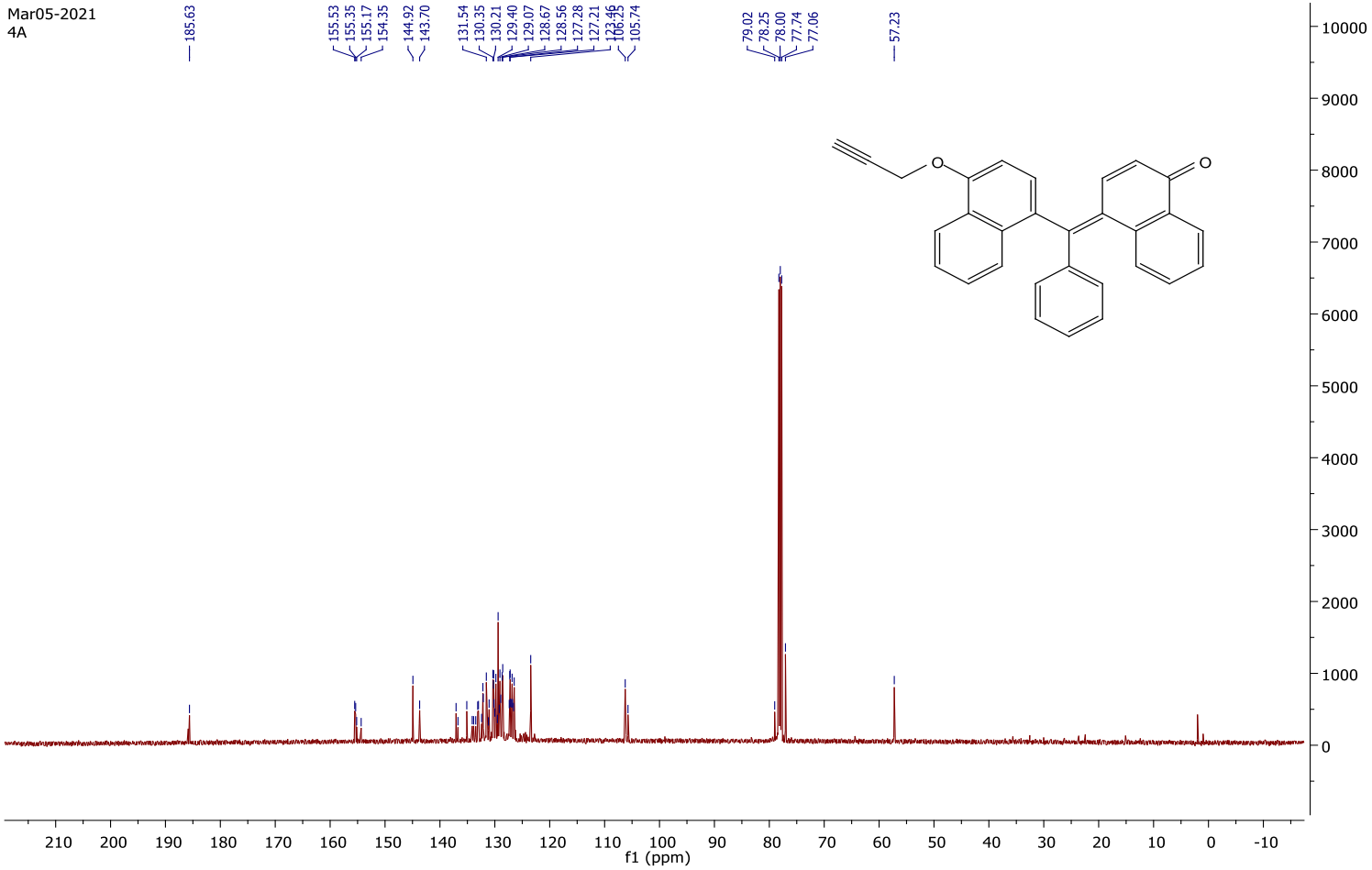

^{1}H NMR of 1,2,3-triazole derivative 63b

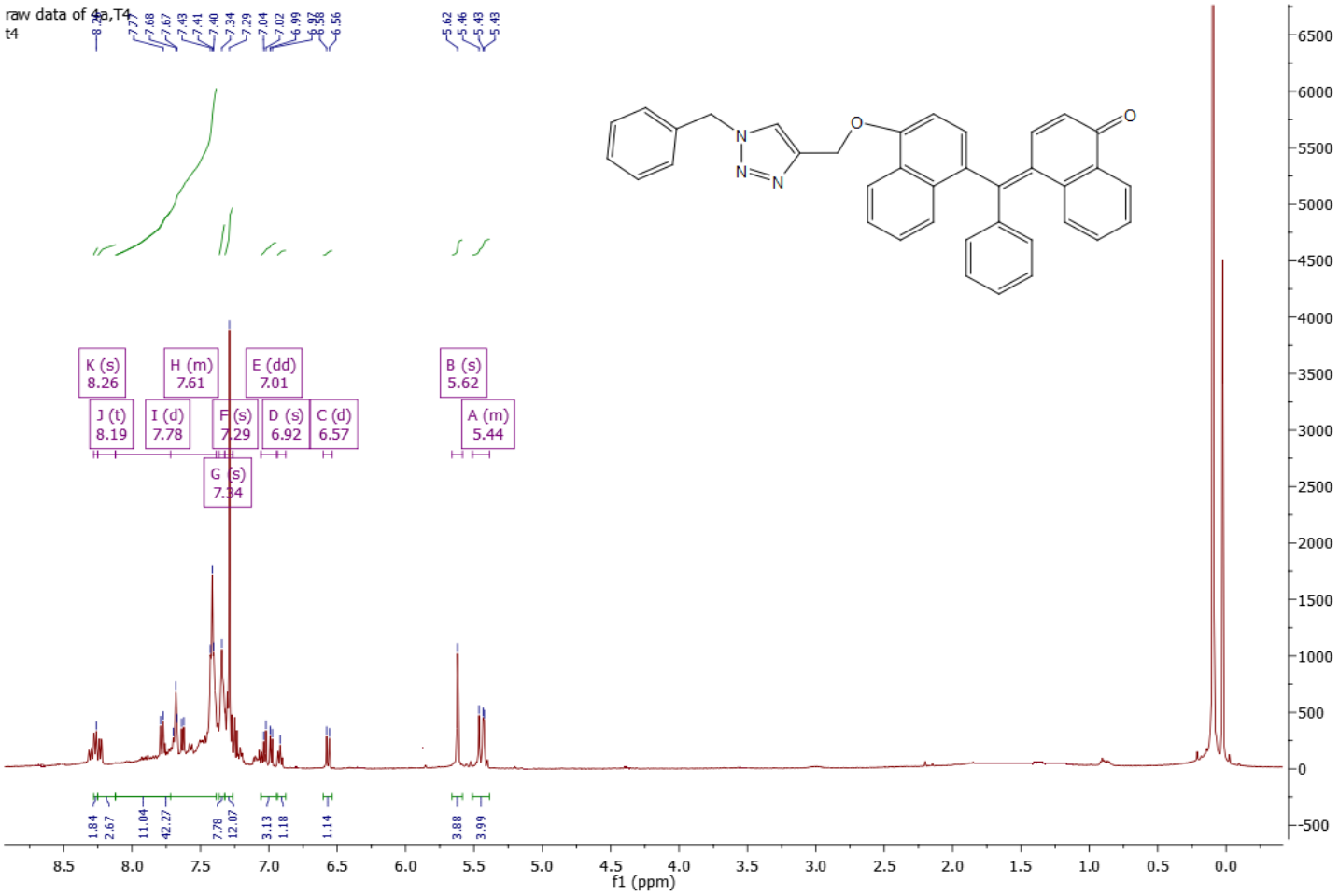

^{13}C NMR of 1,2,3-triazole derivative 63b

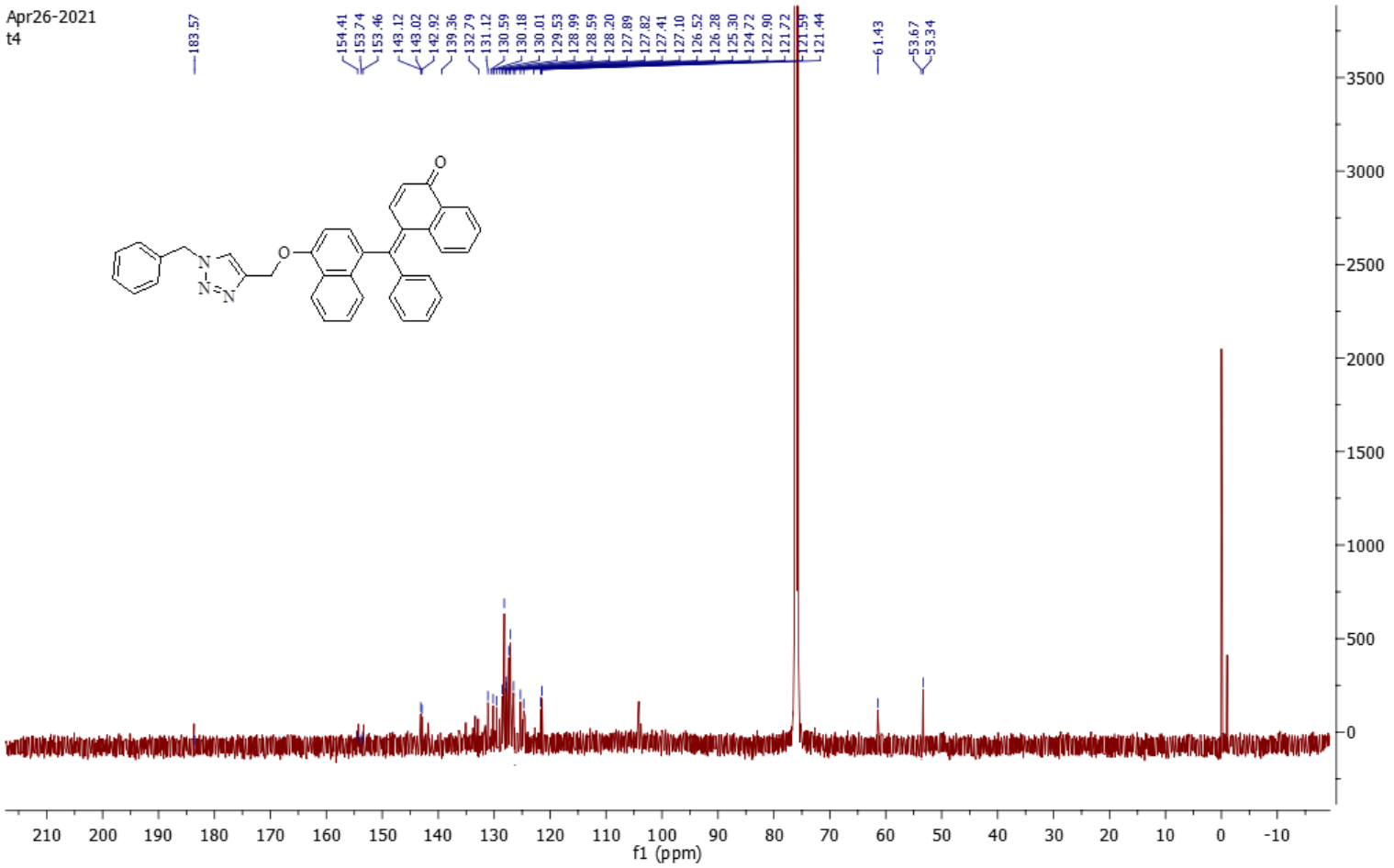

Mass spectrum of 59b

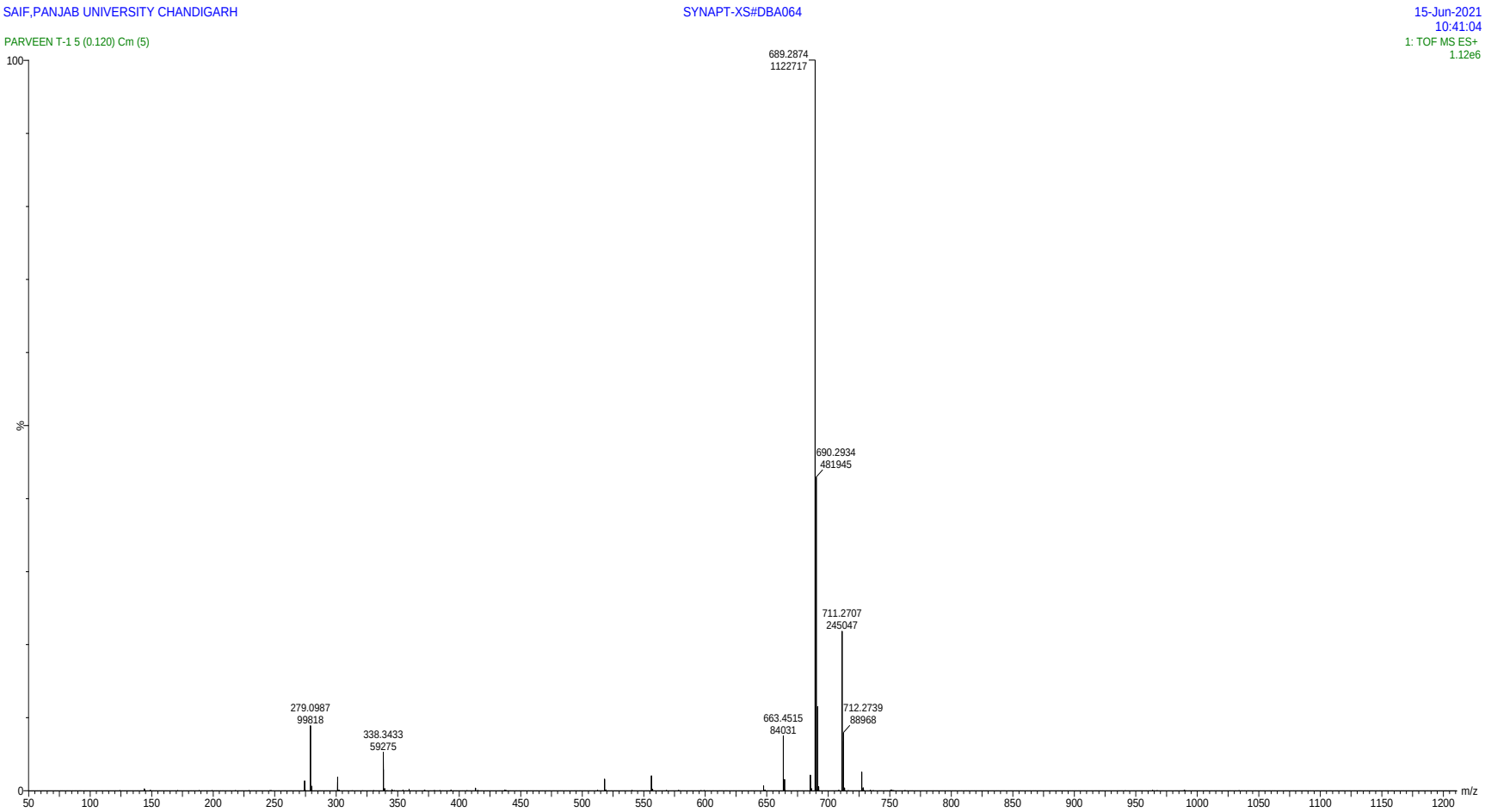

Mass spectrum of 59c

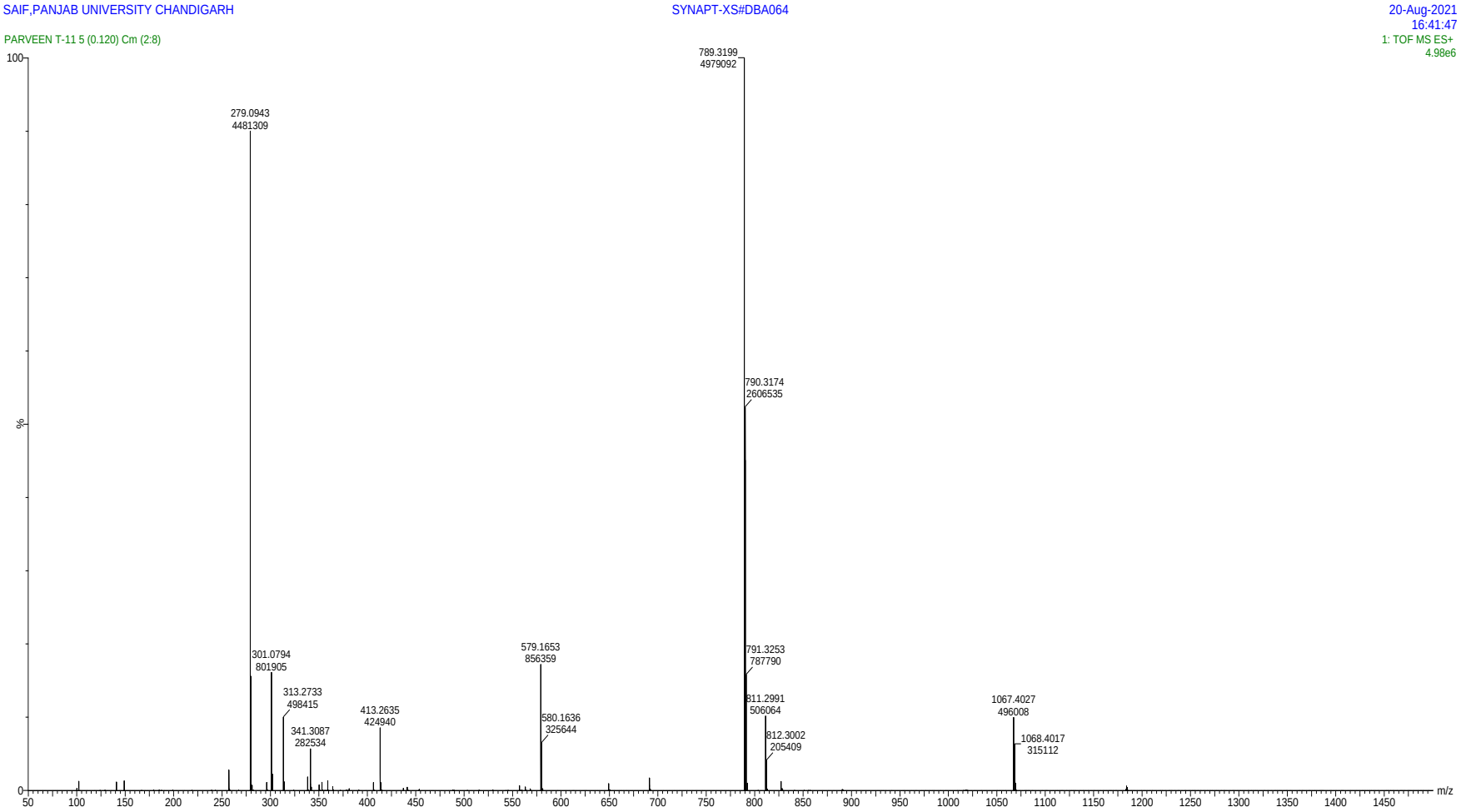

Mass spectrum of 60b

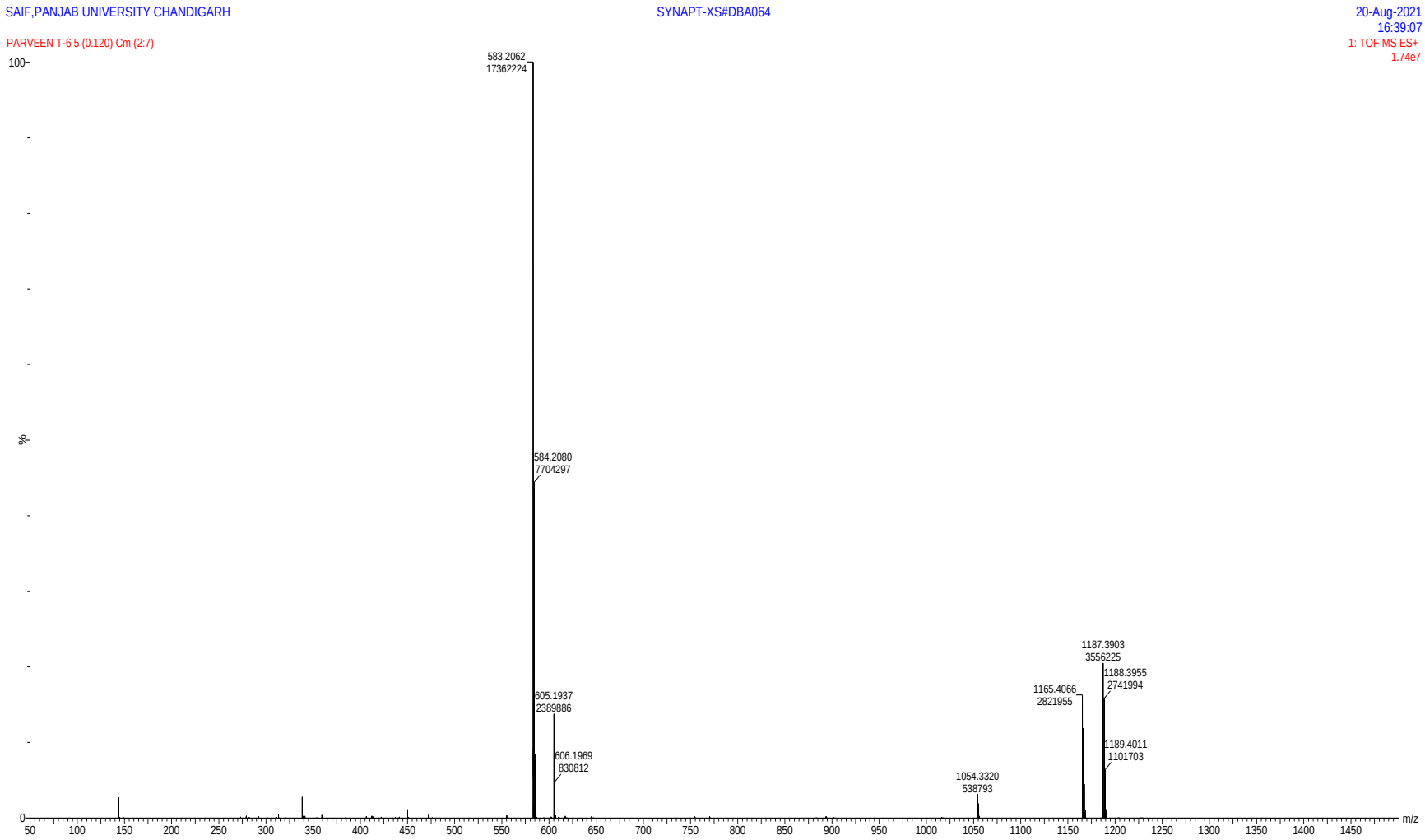

Mass spectrum of 60c

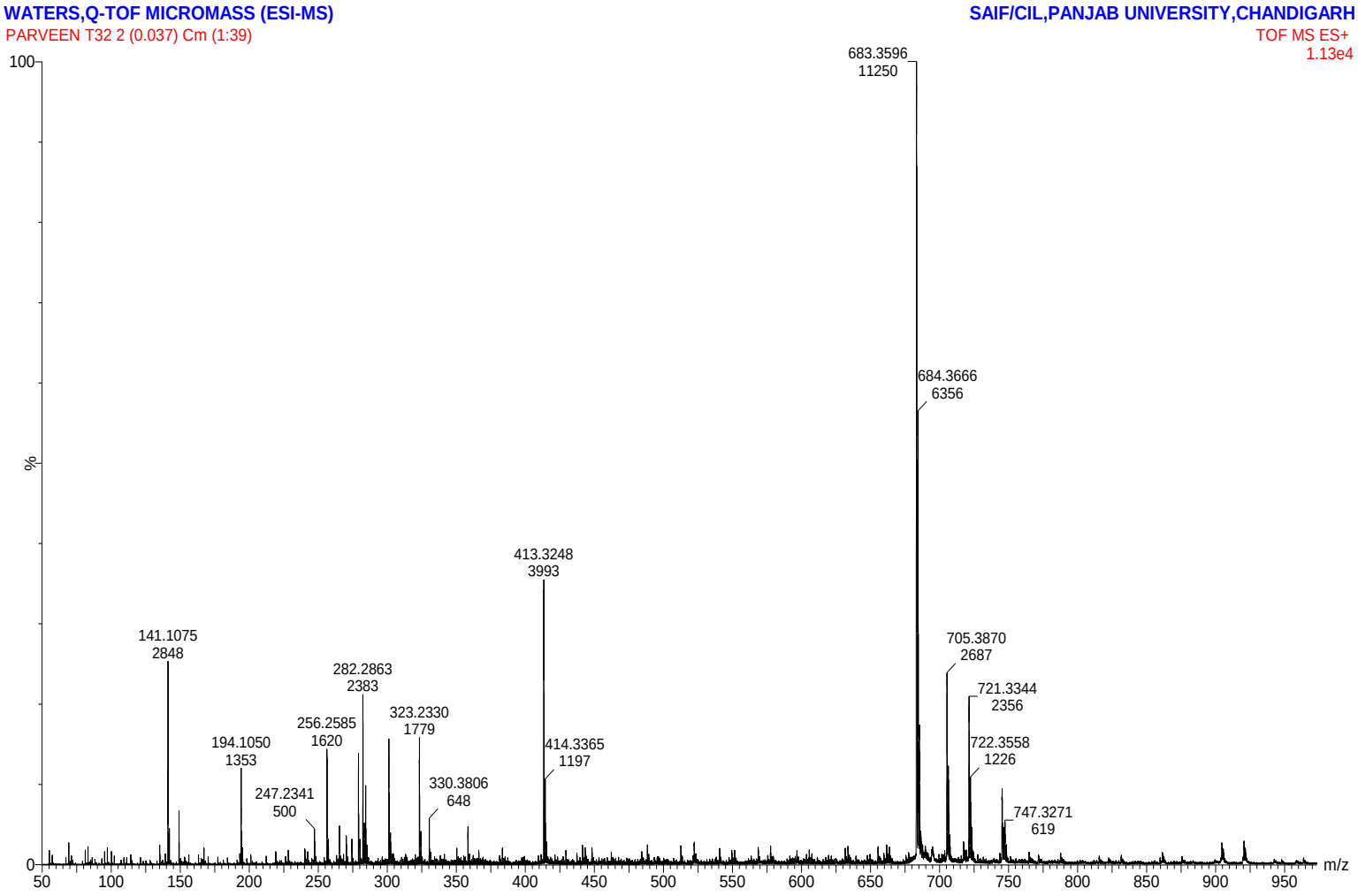

Mass spectrum of 61b

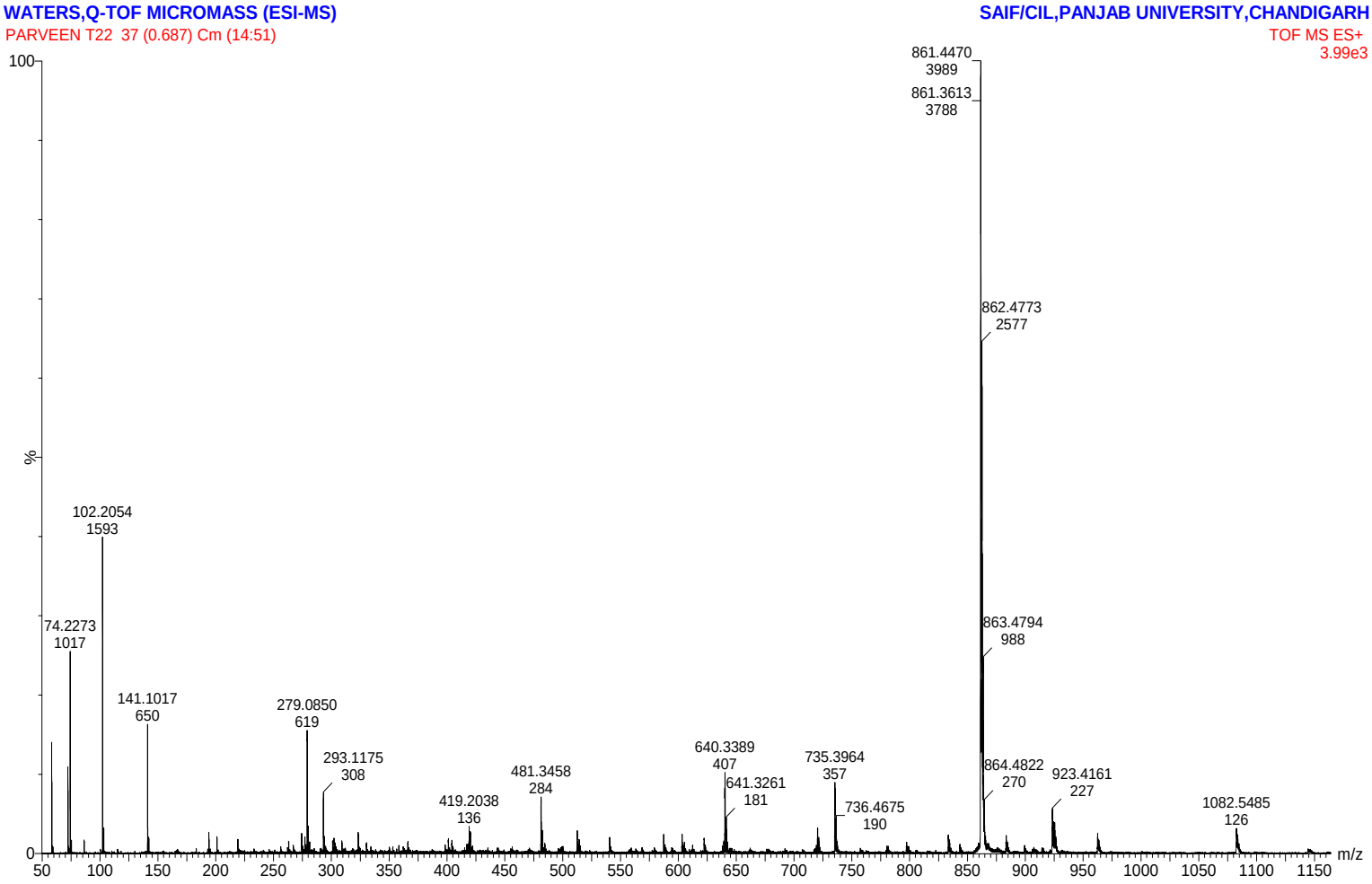

Mass spectrum of 62b

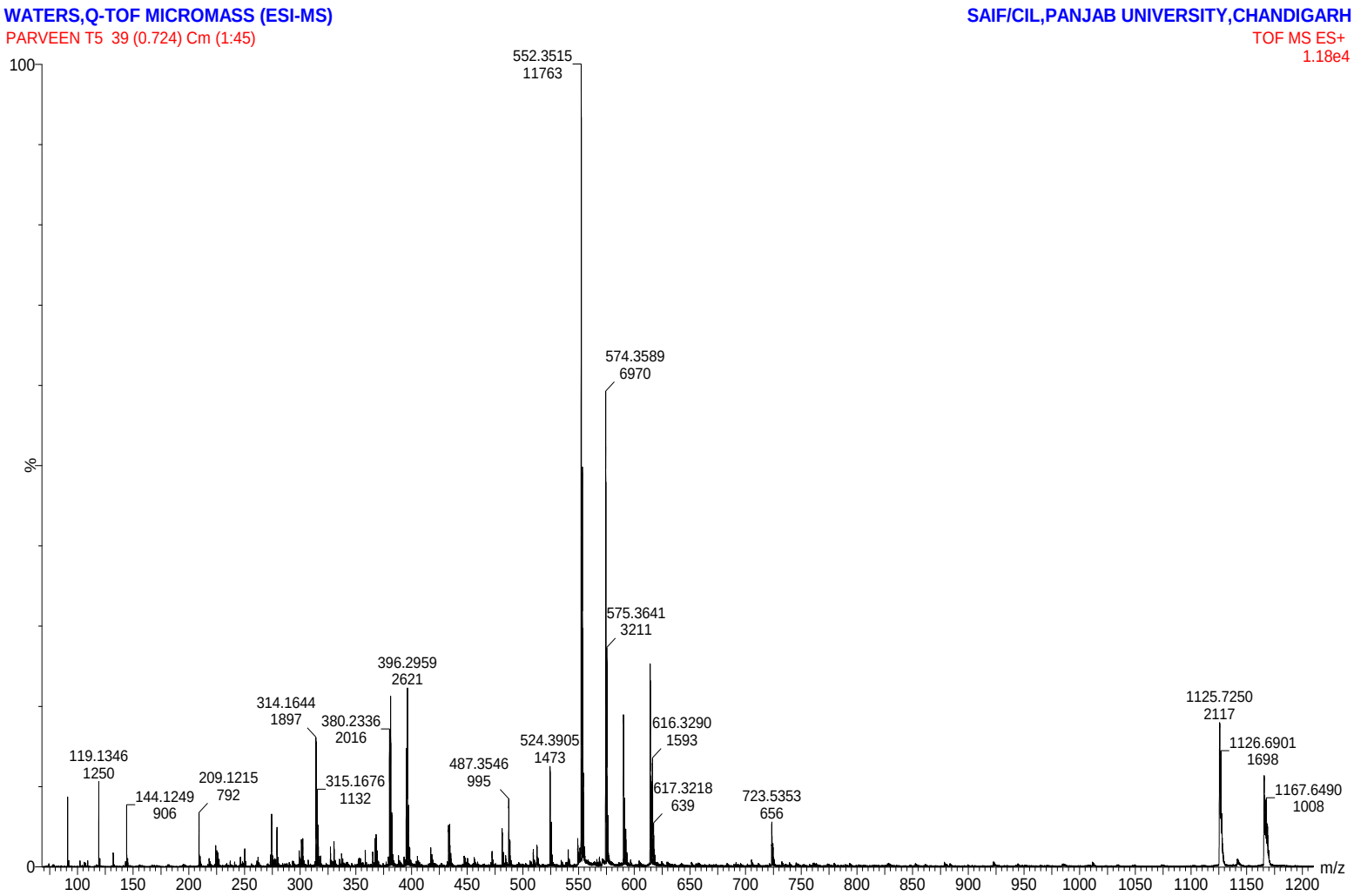

Mass spectrum of 62c

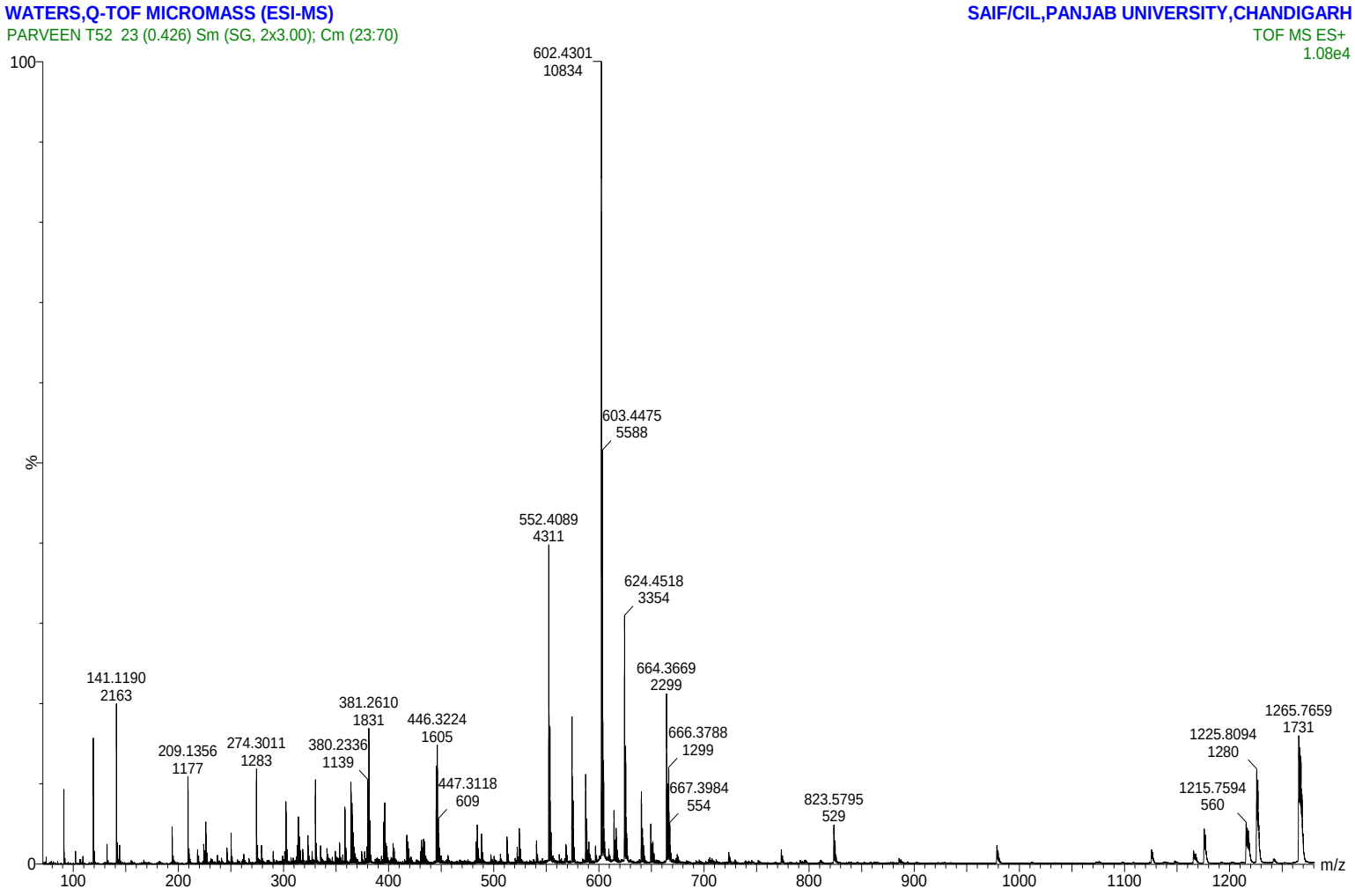

Mass spectrum of 63b

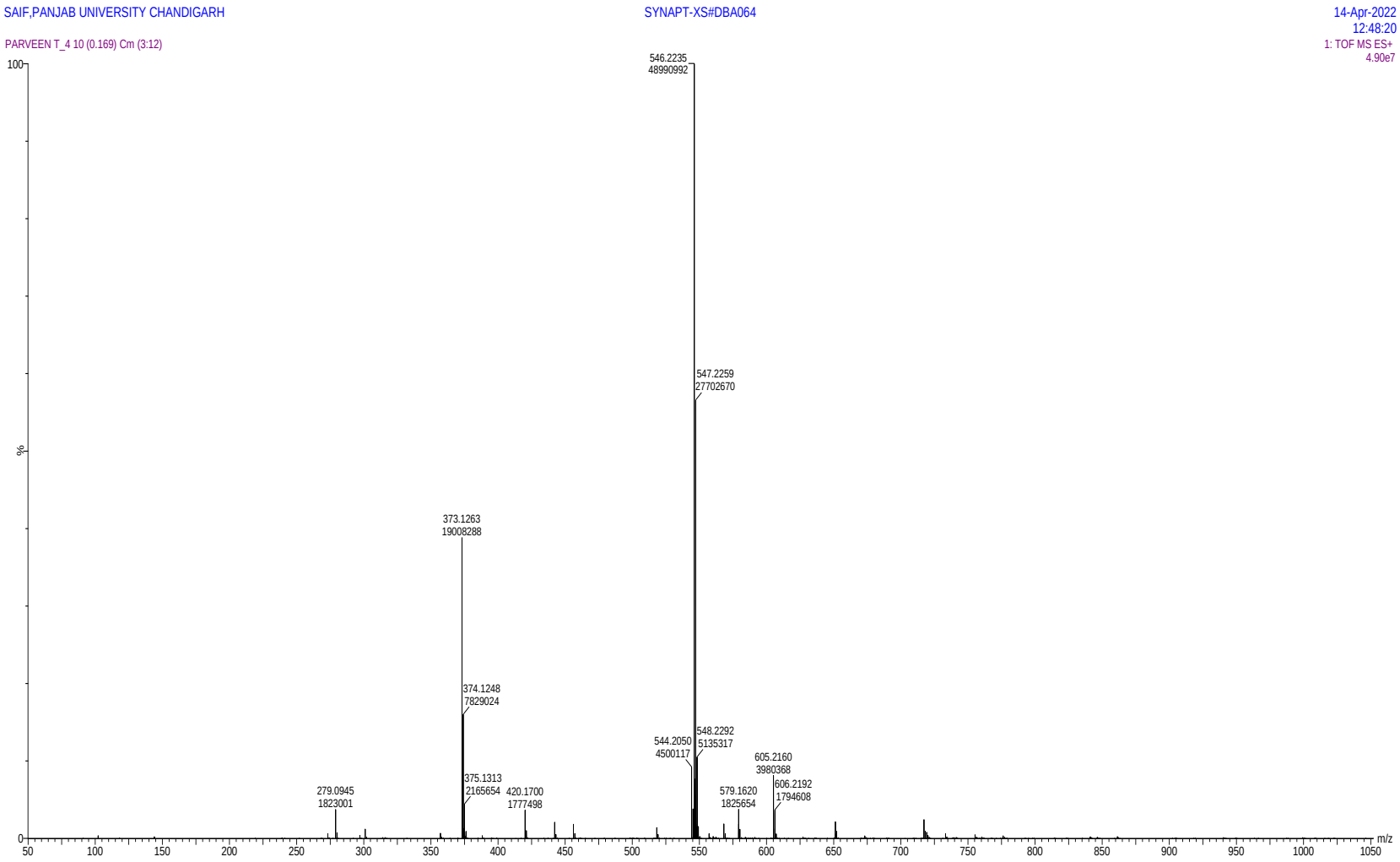

LIST OF PUBLICATIONS

1. **Review article** with title **"Robust and Versatile Cu (I) metal frameworks as potential catalysts for azide-alkyne cycloaddition reactions : Review"**, published in ***Molecular Catalysis Journal-Elsevier (Impact factor 5.062)***, 2021, 504, 111432.
2. **Research article** with title **"Quick CuAAC' Chemistry for Hg(II) and Mn(II) ion sensing via 9H-carbazole derivatives"** published in ***Inorganica Chimica Acta-journal-Elsevier (Impact factor 2.545),*** 2021, 527, 120560.
3. **Research article** with title **"Click generated o-Cresolphthalein linked 1,2,3-triazole derivative for selective Pb(II) ion recognition"** published in ***Molecular structure-journal-Elsevier (Impact factor 3.841),*** 2022, 1251, 131985.
4. **Research article** with title **"Copper (I)-Catalyzed 'Quick Click' generated 1,2,3-Triazole anthraquinone linkers for selective detection of Fe (II) ions"** published in ***Inorganic Chemistry Communications-journal-Elsevier (Impact factor 3.428),*** 2022, 141, 109524.
5. **Research article** with title **"1-Naphtholphthalein appended 1,2,3-triazole via CuAAC: A molecular assembly for selective Co(II) ion recognition"** published in ***Inorganica Chimica Acta-journal-Elsevier (Impact factor 3.118),*** 2023, 551, 121470.
6. **Book chapter** with title **"Functionally modified ionic liquids as green solvents for extraction and removal of toxic metal ions from contaminated water"** published in book titled **"Recent Approaches for Green Chemistry Analysis and Sample Preparation"** by **Springer publications**. DOI:10.1007/978-3-030-96534-1 8
7. **Book chapter** with title **"Applications of Biodegradable Polymers and Plastics"** published in book titled **"Applications of Biodegradable Materials and Plastics"** by ***Wiley-Scrivener,*** **USA publications. https://doi.org/10.1002/9781119905301.ch24**

LIST OF CONFERENCES AND WORKSHOPS

1. **Presented a poster** entitled **"Modifications of Chitosan with different functional groups and their Applications to Adsorption: A Review"** in an International workshop organized by Lovely Professional University, Phagwara from 5th Nov, 2019 to 6th Nov, 2019.
2. **Presented a poster** entitled **"Removal of heavy metal ions, dyes and other organic pollutants from water by adsorption on Chitosan and its composites"** in UGC Sponsored National Seminar on Recent Advances in Chemical Sciences held on 26th Feb, 2020 at Khalsa College Amritsar.
3. **Presented a poster** entitled **"Synthesis of metal ion sensors through CuAAC: An approach to click chemistry"** in an International workshop organized by Lovely Professional University, Phagwara from 25th June, 2021 to 26th June, 2021.
4. **Oral presentation** entitled "**Copper(I) catalyzed azide-alkyne cycloaddition 'CuAAC': "Fast and High yielding" synthesis of Fe (II) ion sensors**" in an International conference organized by Lovely Professional University, Phagwara ***(ICMET-2021)*** from 18th Feb, 2022 to 19th Feb, 2022.
5. **Presented a poster** entitled "**Synthesis of a 1,2,3-triazole linked sensor of Pb (II) ion through copper (I)-catalyzed azide-alkyne cycloaddition reaction**" in a National conference organized by PG Deptt. of Chemistry, Khalsa College, Amritsar ***(RACS-VIII)*** on 11th March, 2022.
6. **Presented a poster** entitled **"1,2,3-Triazole linked Chemosensors via CuAAC: Detection of metal ions"** in an International symposium organized by Deptt. of Chemistry, GNDU Amritsar on 19th March, 2022.
7. **Oral presentation** on topic **'Click' generated 1,2,3-Triazole linked molecular assemblies: Effective metal ion sensors** in an International conference organized by Deptt. of Chemistry, Deshbandhu College, University of Delhi from 8th April, 2022 to 9th April, 2022.

SHORT TERM COURSES

1. Six days Short Term Course on **"Scientific Writing Using Typesetting Software LaTeX"** from 17-10-2020 to 01-11-2020 at HRDC, Lovely Professional University, Phagwara.
2. One week UGC-Sponsored Online Short Term Course on **"Climate Change and Disaster Management"** from 25-03-2021 to 31-03-2021 at HRDC, Guru Nanak Dev University, Amritsar

Certificate No. 225475

LOVELY PROFESSIONAL UNIVERSITY
Transforming Education Transforming India

RAFAS

Certificate of Participation

This is to certify that Prof./Dr./Mr./Ms. **Ms. Parveen Saini**

of **Lovely Professional University**

has given poster presentation on **Synthesis of metal ion sensors through CuAAC : An approach to click chemistry**

in the International Conference on "Recent Advances in Fundamental and Applied Sciences" (RAFAS 2021) held on June 25-26, 2021, organized by School of Chemical Engineering and Physical Sciences, Lovely Faculty of Technology and Sciences, Lovely Professional University, Punjab.

Date of issue : 15-07-2021
Place of issue: Phagwara (India)

Prepared by
(Administrative Officer-Records)

Organizing Secretary
(RAFAS 2021)

Convener
(RAFAS 2021

DIVISION OF RESEARCH AND DEVELOPMENT

[Under the Aegis of Lovely Professional University, Jalandhar-Delhi G.T. Road, Phagwara (Punjab)]

Certificate No.240402

Certificate of Participation

This is to certify that **Ms. Parveen Saini** of **Lovely Professional University, Phagwara, Punjab, India** has presented paper on **Copper(I) catalyzed azide-alkyne cycloaddition 'CuAAC': "Fast and High yielding" synthesis of Fe (II) ion sensors** in the **International Conference on Materials for Emerging Technologies (ICMET-21)** held on February 18-19, 2022, organized by Department of Research Impact and Outcome, Division of Research and Development, Lovely Professional University, Punjab.

Date of Issue: 16-03-2022
Place: Phagwara (Punjab), India

Prepared by
(Administrative Officer-Records)

Dr. Vipul Srivastava
Convener
(ICMET-21)

Dr. Manish Vyas
Organizing Secretary
(ICMET-21)

Dr. Chander Prakash
Co-Chairperson
(ICMET-21)

KHALSA COLLEGE AMRITSAR

Estd. 1892

Estd. 1892

(An Autonomous College)

National Seminar on

RACS-VIII

"Sustainable Chemistry"

(Friday, March 11, 2022)

CERTIFICATE

This is to certify that Dr./Mr./Ms. PARVEEN SAINI of S.D.A.N College, Dinanagar has organised/participated/presented a poster/oral presentation entitled Synthesis of 1,2,3-triazole Linked Sensor of Pb(II) ion through CuAAC Reaction in **National Seminar on Recent Advances in Chemical Sciences (RACS - VIII)** on the theme of **"Sustainable Chemistry"** held on **March 11, 2022** organised by Dunnicliff Chemical Society, Post Graduate Department of Chemistry, Khalsa College Amritsar.

Dr. Randhir Singh	Dr. B.K. Randhawa	Dr. Punita Tiwari	Dr. Mehal Singh
HOD & Coordinator	Co-Coordinator	Organising Secretary	Principal & Patron


Two Days International e-Conference on
Recent Advancements in Chemical Sciences: Health, Environment and Society
(ICRACS - 2022)
8th - 9th April 2022
Certificate
This is to certify that
Parveen Saini , Lovely Professional University, Phagwara Punjab -144411
has delivered an oral presentation in the International e-Conference ICRACS - 2022,
organized by Department of Chemistry, Deshbandhu College, University of Delhi.
Dr Umesh Kumar
(Convener)
Prof. Sushila Singhal
(Convener)
Prof. Rajiv Aggarwal
(Principal)

Department of Chemistry
Guru Nanak Dev University, Amritsar

Certificate of Participation

This is certified that

Parveen Saini

has presented a poster titled

1,2,3-Triazole linked Chemosensors via CuAAC: Detection of metal ions

in one day **International Symposium on "Recent Advances in Self-assembled Materials and Supramolecular Chemistry"** to celebrate the 60th birthday of Prof. Manoj Kumar organized by the Department of Chemistry, GNDU.

19/3/2022

Prof. Sukhprit Singh
Chairperson
ISSAMSUPRA 2022

Dr. Prabhpreet Singh
Organizing Secretary
ISSAMSUPRA 2022

Supported by

ROYAL SOCIETY OF CHEMISTRY WILEY RSC Advances ACS Publications Most Trusted. Most Cited. Most Read.

Certificate ID: 60000007

HUMAN RESOURCE DEVELOPMENT CENTER

[Under the Aegis of Lovely Professional University, Jalandhar-Delhi G.T Road, Phagwara (Punjab)]

Certificate No. 211990

Certificate of Participation

This is to certify that **Ms. Parveen Saini** D/o Sh. Kundan Lal Saini participated in **Short Term Course on Scientific Writing Using Typesetting Software LaTeX** organized by Lovely Professional University w.e.f. **October 17, 2020** to **November 01, 2020** (6 Days) and obtained "**B**" Grade.

Date of Issue : 01-11-2020
Place : Phagwara (Punjab), India

Prepared by	**Checked By**	**Head**
(Administrative Officer-Records)	**Program Coordinator**	**Human Resource Development Center**

e-certificate

Reference No. HRDC/STC: 12 Date 31/03/2021

University Grants Commission
Human Resource Development Centre (HRDC)

GURU NANAK DEV UNIVERSITY, AMRITSAR

UGC-Sponsored Online Short Term Course

This is to certify that Dr./Mr./Ms. Parveen Saini

Designation Asstt. Professor (Chemistry) *at* S.D.A.M. College, Dinanagar, Distt. Gurdaspur, Punjab

affiliated to Guru Nanak Dev University, Amritsar

participated in the ***One Week Online Short Term Course on Climate Change and Disaster Management*** *conducted from 25-03-2021 to 31-03-2021.*

Prof. (Dr.) Adarsh Pal Vig	Prof. Anish Dua	Dr. Puja Dhir	Prof. (Dr.) Jaspal Singh Sandhu
Director	Co-ordinator	Co-ordinator	Vice Chancellor